CDF Study Report
WFI
A Wide Field Imager for Supernovae Surveys and Dark Energy Characterisation

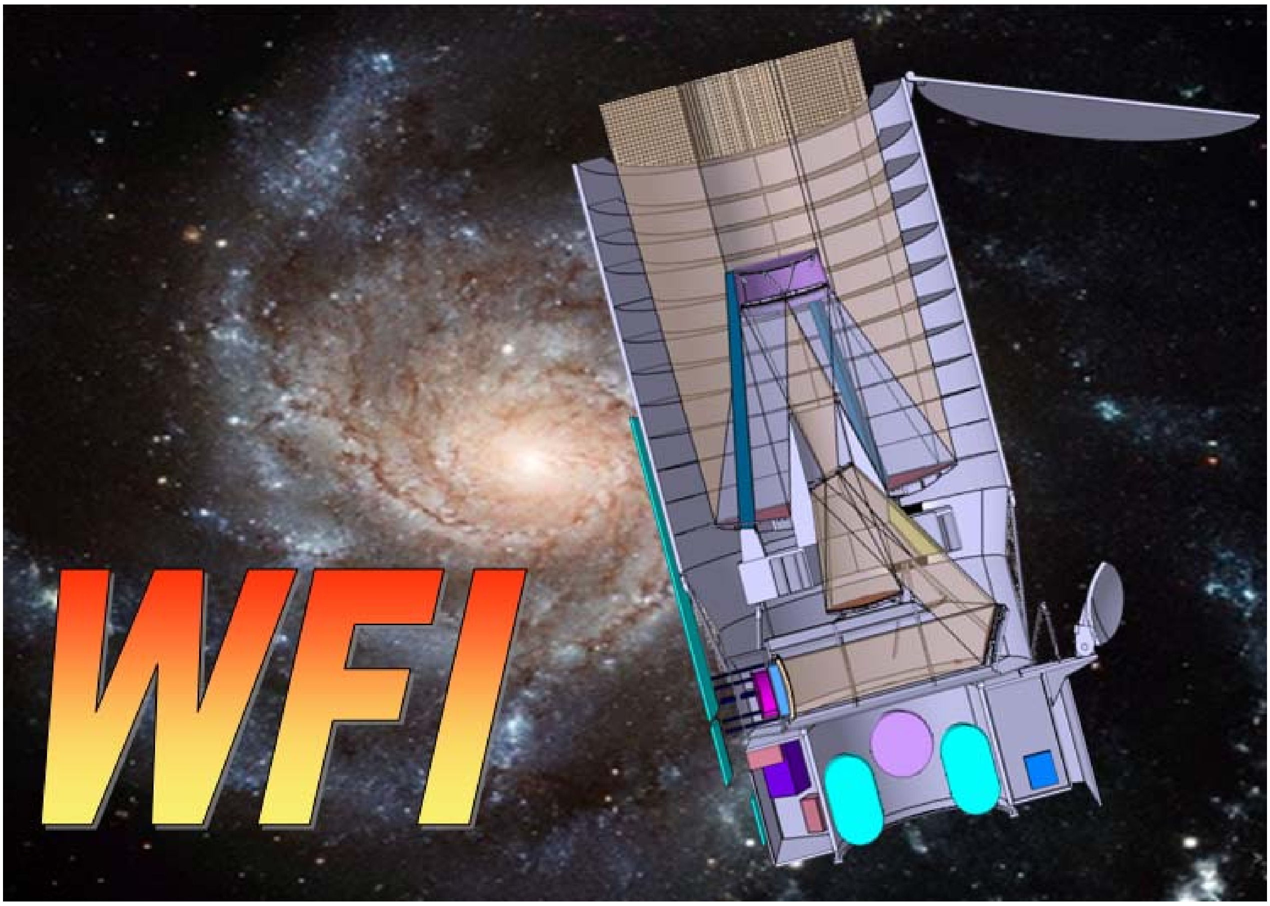

FRONT COVER

CAD Image of the Wide Field Interferometer in orbit with telescope cover open

Further information and/or additional copies of the report can be requested from:

P. Gondoin
ESA/ESTEC/SCI-AM
Postbus 299
2200 AG Noordwijk
The Netherlands
Tel: +31-(0)71-56554486
Fax: +31-(0)71-56554690
philippe.gondoin@esa.int

For further information on the Concurrent Design Facility please contact:

M. Bandecchi
ESA/ESTEC/TEC-SYE
Postbus 299
2200 AG Noordwijk
The Netherlands
Tel: +31-(0)71-5653701
Fax: +31-(0)71-5656024
Massimo.Bandecchi@esa.int

This Page Intentionally Blank

TABLE OF CONTENTS

This Page Intentionally Blank

1 INTRODUCTION

1.1 Background

The ESA Concurrent Design Facility (CDF) was requested and financed by ESA/ESTEC/SCI-AM to carry out a feasibility study for an optical-near-infrared wide field imager (WFI). Such a mission would search for Type Ia supernovae over a given redshift range with optical and near-infrared wavelength coverage.

The overall aim of the mission would be to use supernova observations to model the changing rate of expansion of the universe and to determine the contributions of decelerating and accelerating energies such as the mass density and dark energy density. This model could be constructed using a Hubble diagram (redshift vs. magnitude) populated with supernovae measurements.

This study is the first step in the feasibility assessment of a technology reference mission and a follow-on phase-A industrial study is foreseen for the payload, where most of the technology development is needed.

1.2 Scope

The objectives of the study were to assess the feasibility of an optical-near-infrared wide field imager mission with particular emphasis on the following:

- To assess the reference mission (orbit, payload and service module configuration)
- To perform a preliminary payload design starting from the initial work done by SCI-AM
- To define a reference service module design for the following payload industrial study
- To identify and define interface requirements between the P/L and SVM
- To identify technology development issues
- To analyse mission risk

1.3 Terminology

In this study report, the following system breakdown and associated terminology is used:

The spacecraft is split into:

- Payload Module
- Service Module

The Payload Module includes:

- Telescope; in turn composed of optics proper (i.e. the mirror system), optical support structures, baffle and telescope mechanisms (i.e. refocusing mechanisms and lid)
- Instruments; the Camera (i.e. optical and NIR imager) and the Spectrometer. The Camera includes a Focal Surface Assembly with detectors, support structure, Read-out electronics and Data Handling Unit. The Spectrometer features its own Optics, Detector Plane and Read-out electronics and, for the sake of the present study, uses the Data Handling Unit

of the Camera.
Note: The Data Handling Unit of the Camera is physically located onboard of the Service Module.

- The Fine Guidance Sensor system; this is strictly part of the service module AOCS but physically located on the Camera Focal Surface and therefore associated, in this study, to the Payload Module
- The Payload Thermal Control System composed of two Radiator Assemblies, a cold one for Detector cooling and a warm one for Read-out electronics cooling

The WFI preliminary product tree is presented in Figure 1-1.

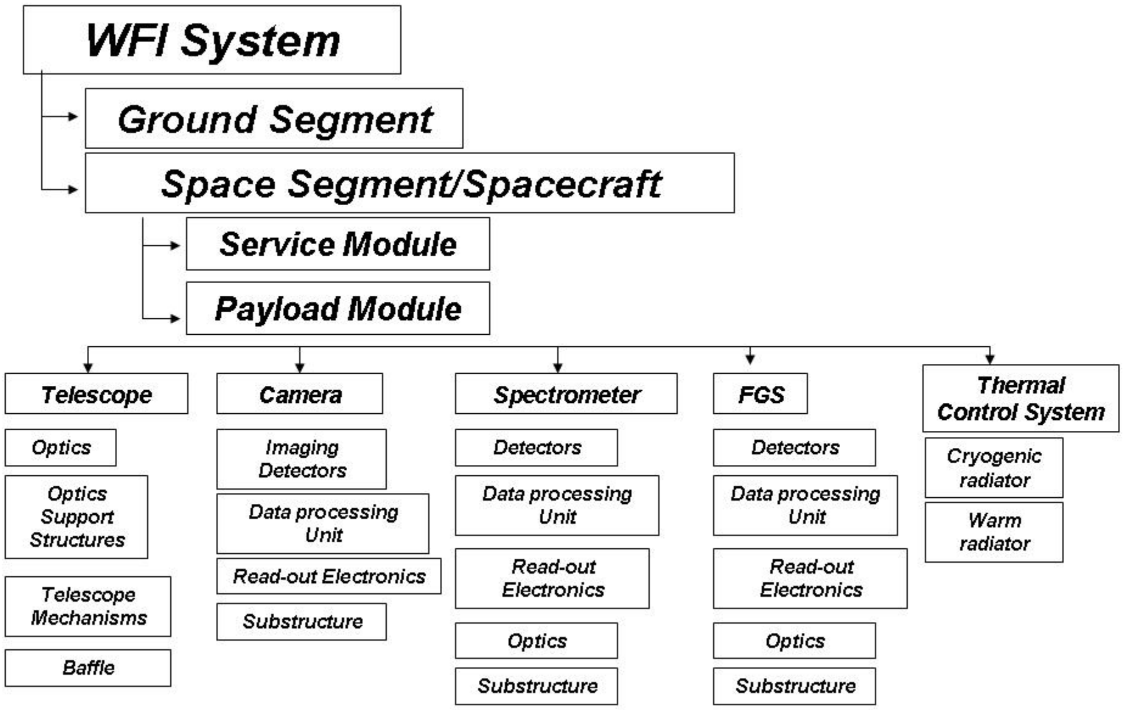

Figure 1-1: WFI Product Tree

1.4 Document Structure

The report is a cut-down (for use as a pdf document) version of the technical report, in that it doesn't contain cost and programmatic data. The layout of this report can be seen in the Table of Contents. The Executive Summary chapter provides an overview of the study; details of each domain addressed in the study are contained in specific chapters.

The costing information is published in a separate document CDF-47(B).

An Interface Requirements Document to identify the interfaces between the Payload Module (PM) and the Service Module (SVM) has been produced as a separate document CDF-47(C).

2 EXECUTIVE SUMMARY

2.1 Study Flow

A feasibility study for an optical-near-infrared wide field imager (WFI) using the ESA Concurrent Design Facility was requested by ESA/ESTEC/SCI-AM. Such a mission would search for Type Ia supernovae over a given redshift range with optical and near-infrared wavelength coverage. The overall aim of the mission would be to use supernova observations to model the changing rate of expansion of the universe and to determine the contributions of decelerating and accelerating energies such as the mass density and dark energy density. This model could be constructed using a Hubble diagram (redshift vs. magnitude) populated with supernovae measurements.

The study began with a kick-off on March 14th 2006 and finished with an Internal Final Presentation on April 11th 2006. It consisted of eight technical half-day sessions of the interdisciplinary study team of ESTEC and ESOC specialists.

The objectives of the WFI study were:

- To assess the reference mission (orbit, payload and service module configuration)
- To perform a preliminary payload design starting from the initial work done by SCI-AM
- To define a reference service module design for the following payload industrial study
- To identify and define interface requirements between the P/L and SVM
- To identify technology development issues
- To analyse mission risk

2.2 Mission Requirements and Design Drivers

The main mission science requirements for the WFI study are listed below:

- Perform wide field imaging of supernovae in multiple filter bands over a wavelength range of 0.3-1.8 microns with I-band diffraction limited optics and a revisit rate of 5 days
- Detect supernovae at magnitude 2.2 below peak luminosity with an SNR ≥ 5
- Measure supernovae spectra near peak luminosity with a resolution of 100 $\lambda/\Delta\lambda$ over a wavelength range of 0.3-1.8 microns
- Measure photometric redshifts and spectra of supernovae host galaxies
- Cover two survey fields, one close to each ecliptic poles within ±20 deg from the pole

General mission constraints are:

- Launch date between 2015 and 2020
- Launch vehicle Soyuz-Fregat 2-1b
- Minimise cost

2.3 Mission and Design Summary

Mission Objective	To detect, identify, and analyse more than 2000 Type 1a supernovae over a redshift range $0.3 < z < 1.8$ in two 10 sq deg survey fields close to the north and south ecliptic poles	
Payload	The instruments: • Camera: visible and NIR detectors, 1 sq deg FoV • Integrated Field Spectrometer (IFS): visible and NIR detectors, resolution 100 $\lambda/\Delta\lambda$ • Fine Guidance Sensor (FGS)	
Launcher	Soyuz-Fregat 2-1b Performance: 2090 kg to L2 direct injection (incl. 1666 ∅ adapter mass)	
Mission	Orbit	L2 near-Halo Lissajous orbit, dimensions 800 000 km X 600000 km, period 6 months
	Launch date	2017
	Mission lifetime	Cruise: 2 months In-orbit, nominal: 3 years In-orbit, extended: 3 years
	ΔV total	34 m/s
	Observation Strategy	5 day cadence over a strip of 10 deg sqr: 4 days imaging, 1 day spectrometry + calibration
Payload Module (PLM)	**Total mass**	1420 kg dry (incl all margins)
	Structure	2.9m height external baffle
	Optics	5-mirror configuration, primary mirror (M1) diameter: 2.15m
	Thermal	Mirrors at 290K, max ΔT M1/M2= 0.5K, between detectors at 150K, passive cooling
	Mechanisms	Refocusing mechanisms for M2, M5
	Instruments	Camera, FGS, and IFS inlet located on same curved focal surface Detectors: visible: p-channel CCDs, IR: HgCdTe (1.8 μm cut-off)

Service Module (SVM)	**Total mass**	490 kg dry, 560 kg wet (incl all margins)
	Structure	Hexagonal box with 1666 ∅ central cylinder
	Propulsion	Hydrazine monopropellant system for mission manoeuvres ΔV, Cold gas or FEEP for AOCS with 500µN thrusters
	AOCS	Startracker for pointing up to 15 arcsec, FGS (on PLM) for fine pointing down to 1.5 arcsec, RPE: 10 mas/2000s
	Data Handling	600 Gbit buffer to store camera data between comms windows
	Power	Solar Array: AsGa TJ cells Batteries: Li-Ion pack
	Comms	Ka-Band 26 GHz, 50 Mbps data rate, 0.7m steerable HGA TC/TM in X band 4 kbps data rate
Operations	**Ground stations**	Cebreros; upgraded for 26GHz
Programmatics	**Phase A start**	2007
	Phase B start	2008
	Launch date	2017
	Model philosophy	STM, EQM, PFM, Dev Model for primary mirror and focal surface array

2.4 Enabling Technologies

Item	Technology status	Required development
SiC primary mirror	Technology available (flight qualified in 2007) for size up to 1.5 m diam monolitic, up to 3.5 m in segments	2.15 m diameter monolitic CVD coated mirror or segmented CVD coated mirror
26 GHz transponder	Available for low data rates (Artemis, TDRSS)	High data rate (50 Mbit/s) transponder
FGS	Conceptual design	5-10 mas pointing accuracy star tracker
Focal plane	large focal plane with n-CCD developed for Gaia	large focal plane with rad hard CCD with low read-out noise

Table 2-1: Enabling technologies required

This Page Intentionally Blank

3 MISSION OBJECTIVES

3.1 Background

3.2 Science Objectives

The mission scientific goal is the measurement of a set of cosmological parameter as in Table 3-1. Type 1a supernovae are used as cosmological measurement tools RD[3].

MG - Overall Mission Goals	
Dark Energy	GOAL: Obtain a 5% measurement of the equation of state of the Dark Energy driving the acceleration of the universe
Mass Density	GOAL: Obtain a 2% measurement of the mass density of the universe
Vacuum Energy Density	GOAL: Obtain a 5% measurement of the vacuum energy density

Table 3-1: Overall science mission goals

More specific requirements for supernova observations then apply (Table 3-2, Table 3-3, Table 3-4). The mission objective for WFI is to detect, identify and analyse a set of over 2000 Type 1a supernovae over a redshift range of 0.3 to 1.8. The survey fields are to be chosen close to the ecliptic poles so as to minimise the zodiacal light noise contribution.

SR - Science Requirements		
SR.BAS - Baseline Science Requirements		
SR.BAS-1	Detect, identify and analyse more than 2000 Type Ia supernovae over a redshift range of 0.3 < z < 1.8	GOAL: Primary Science: Statistical sample is to be approx. 2 orders of magnitude greater than the current published data set of ~42 supernovae
SR.BAS-2	Search for the SN in two fields, one close to each of the ecliptic poles (within 20 deg each side of North/South pole), with each field having a size of approximately 10 sq degrees.	Poles for minimum zodiacal noise. Solar avoidance angle of 70 degrees required.

Table 3-2: Baseline measurement requirements

It is decided to use two types of measurements for supernova observations: imaging and spectrometry. The requirements for imaging measurements are given in (Table 3-3) and those applicable to spectrometry are given in (Table 3-4). These requirements set important parameters such as the wavelength coverage, revisit rate, resolution, and signal-to-noise that in turn determine the payload characteristics and applicable payload requirements.

SR.IMG - Imaging Requirements	
Wide Field Imaging	Perform wide field imaging in multiple filter bands over a wavelength range of 0.3 to 1.8 microns with I-band diffraction-limited optics

SR.IMG - Imaging Requirements	
Luminosity	Derive supernovae peak luminosity to 2% (statistical) or better through multiple measurements over the supernovae light curve
Photometry Data Points	Obtain measurements for at least 10 (peak and off-peak) points along the SN light curve with first detection at average 2.2 magnitudes below peak with SNR>5
Photometry Filters	Measure supernova with broadband filters in six visible light ranges and three infra-red ranges.
Host Galaxy Photometric Redshift	Measure photometric redshift of supernova host galaxy

Table 3-3: Science requirements for imaging

SR.SPM - Spectrometry Requirements	
Spectrometry	Measure supernovae spectra near peak luminosity with a resolution of 100 ($\lambda/\delta\lambda$) over 0.30 to 1.8 microns.
Spectra Light Curve Measurements	Measure spectra for a subset (10%) of supernova with z<0.7 along light curve at TBD points over a wavelength range of 0.30-0.65 microns
Silicon and Sulfur features	Measure the broad (200A) Silicon (6150A rest-frame) and Sulphur (5350A rest-frame) features.
Host Galaxy Spectra	Measure spectra of supernova host galaxy at SN peak brightness (and after SN event if required) over a wavelength range of 0.30-1.8 microns.

Table 3-4: Science requirements for spectrometry

4 MISSION ANALYSIS

The mission analysis work in the context of the CDF study was concerned with the selection of an operational orbit that is consistent with the scientific, payload and communications requirements, the analysis of the launcher performance, transfer strategy, station-keeping cost, orbital geometry and ground station visibility conditions.

4.1 Requirements and Design Drivers

The following requirements and design drivers are relevant to the mission analysis process:

4.1.1 Target Orbit

The baseline orbit has been selected (see 5.2.2) as an orbit around the Earth-Sun L2 point that can be reached with maximized payload mass, i.e., without deep space manoeuvres. Typically this leads to a large-amplitude Lissajous or Halo.

4.1.2 Ground Stations

The ESA ground stations to be regarded in the analysis are:

- Cebreros (Lon: 4.367 deg W, Lat: 40.455 deg N, Alt: 789 m)
- New Norcia (Lon: 116.192 deg E, Lat: 31.048 deg S, Alt: 224 m)
- Maspalomas (Lon: 15.567 deg W, Lat: 27.75 deg N, Alt: 2 m)

4.1.3 Launch Vehicle

The baseline launch vehicle is defined as Soyuz-Fregat 2-1b, launched from Kourou. For this vehicle, a dedicated launch shall be assumed.

4.2 Assumptions and Trade-Offs

4.2.1 Target Orbit

In addition to the baseline large-amplitude Lissajous orbit around the L2 point, a trade-off shall be performed with the following alternatives:

- A reduced-amplitude Lissajous orbit, where the Sun-Spacecraft-Earth angle is constrained to below 15 deg, as for the Gaia mission
- An inclined HEO with a period of several days, as for several current ESA space telescope missions, e.g. Integral
- A heliocentric orbit trailing the Earth, as for the NASA IR space telescope Spitzer.

4.2.2 Launch Vehicle

As a launch alternative, a shared launch with Ariane 5 ECA into GTO using the standard midnight launch window shall be considered.

4.3 Baseline Design

4.3.1 Large-Amplitude Lissajous Orbit Around Lagrange Point L2

The Lagrange point L2 in the Sun-Earth system is one of the locations specific to the three-body problem. Near the L2 point, which is “beyond” the Earth, as seen from the sun, at a distance of around 1.5 million km, the combined gravitational effect of Earth and Sun is such that a body located there will travel around the Sun with a period of one year, so it will maintain approximately the same distance and location relative to the Earth if displayed in a coordinate frame that rotates around the Sun with the Earth. Normally, a spacecraft at a larger distance from the Sun would move more slowly than the Earth, quickly drifting away.

A spacecraft will never be located directly in the L2 point (apart from being physically impracticable, this would also place the spacecraft eternally inside the Earth penumbra). It will orbit around the L2 location on a wide loop with a period of 6 months. Two classes of such “orbits” exist:

- Halo orbits are typically very wide, they trace approximately the same path in the sky as seen from the Earth, and they are eclipse-free.
- Lissajous curves can have large or small amplitudes, they do not trace the same figure over and over again and they may pass through the Earth penumbra cone. Lissajous curves with very large amplitudes may have properties similar to Halos. Typically, reaching a large-amplitude Lissajous curve can be achieved without any DSMs, while reaching a narrow Lissajous requires a DSM, the size of which depends on the amplitude reduction to be performed.

All such orbits require station-keeping. The cost depends on the residual uncertainties in the perturbation model and also on the frequency of the correction manoeuvres. A major source of such uncertainties is the acceleration induced by solar radiation pressure, which cannot be modelled with absolute accuracy. A typical value for the Station-keeping cost is 2 m/s/year. For launch performance and delta-v budget see Table 5-20.

On a low-amplitude Lissajous curve, eclipse avoidance manoeuvres may have to be performed at regular intervals to prevent the trajectory from intersecting the Earth penumbra cone. Additionally, the spacecraft may pass through the Moon penumbra cone, which can reduce the available sunlight by up to about 13%.

4.3.1.1 Operational Orbit

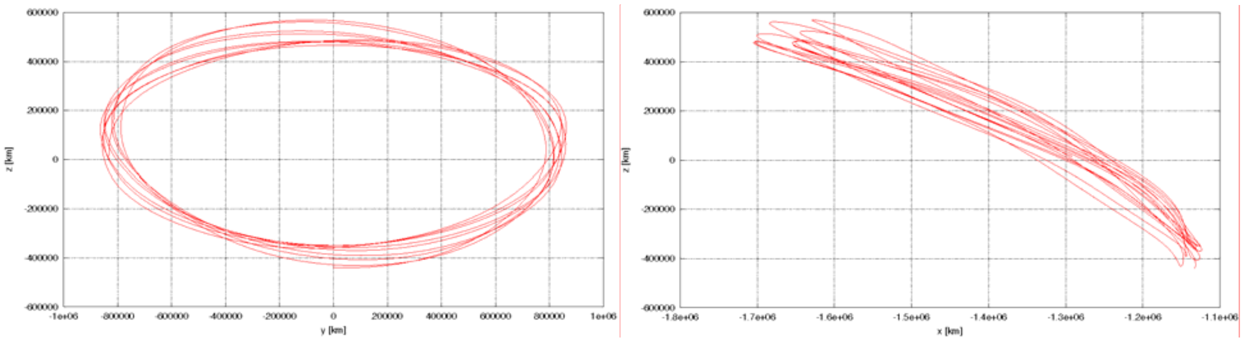

Figure 4-1: y-z (left) and x-z (right) Views of the WFI baseline operational orbit

Figure 4-1 shows the trajectory curve for the operational orbit, in the y-z-view (left hand diagram), as it would appear when looking from the Earth into the anti-sun direction, and in the x-z-view (right-hand diagram), x denoting the anti-sun-axis and z the out-of-ecliptic direction. The figure shows the large excursions of more than 600,000 km and 800,000 km in the z- and y-directions. Also, there is a large variation in the x-direction, which varies between 1.13 million and 1.7 million km. The period on the ellipse-like curve is 6 months.

The large amplitudes in the orbit lead to the variations in Earth range and Sun-Spacecraft-Earth-Angle (SSEA) shown in Figure 4-2. The range varies between 1.2 and 1.8 million km, the SSEA between 16 and 33 deg. The range is an important input for the design of the communications system, the SSEA drives on the telescope baffle design. At no point do eclipse conditions occur.

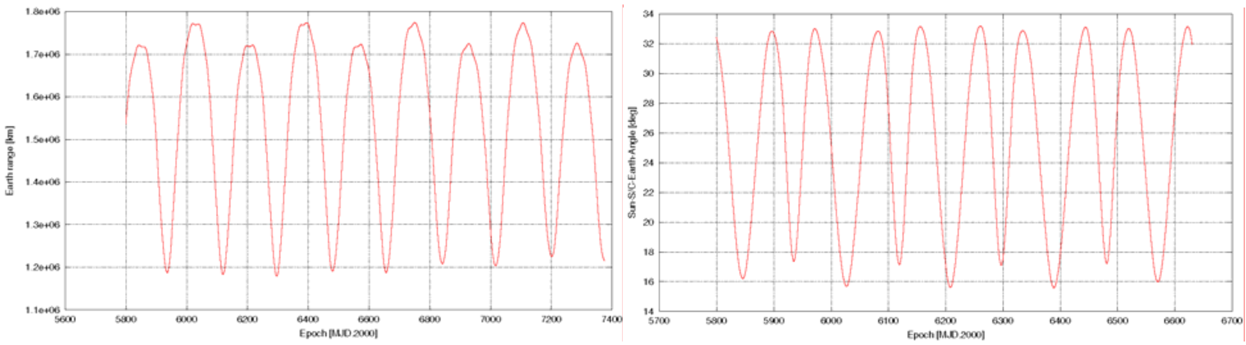

Figure 4-2: Earth Range and SSEA on WFI baseline operational orbit

4.3.1.2 Coverage on the baseline operational orbit

Ground station coverage conditions for the three regarded ground station locations also show a strong variation with time due to the spacecraft motion on the orbit around L2. The period of the variation is 6 months.

Min. el. [deg]	Pass dur. [h]	Cebreros	Maspalomas	New Norcia
5	Minimum	8.3	9.6	9.2
	Mean	11.3	11.3	10.9
	Maximum	13.5	12.6	12.9
10	Minimum	7.2	8.7	8.4
	Mean	10.3	10.5	10.1
	Maximum	12.5	11.8	12.1
20	Minimum	4.7	6.9	6.5
	Mean	8.4	9.0	8.4
	Maximum	10.7	10.3	10.5

Table 4-1: Ground Station coverage on WFI baseline operational orbit

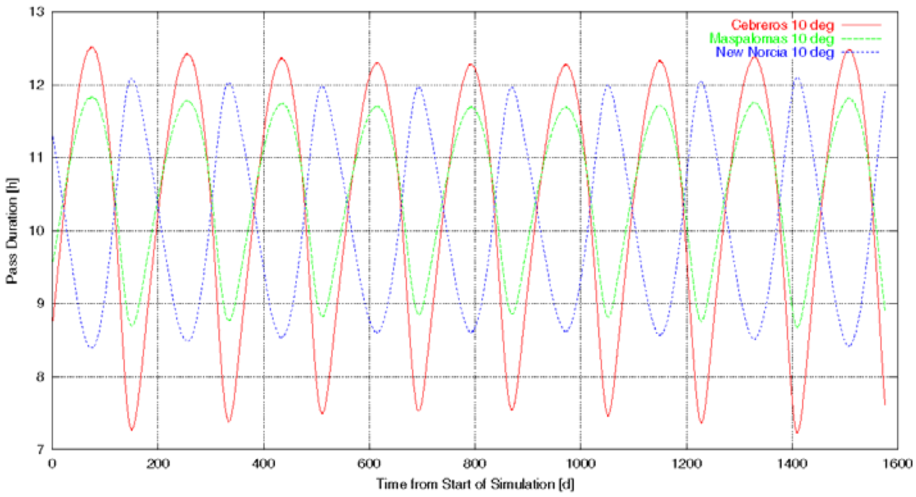

Figure 4-3: Coverage evolution for WFI baseline orbit, 10 deg Min. elevation

The dependency of minimum, mean and maximum duration of the daily coverage passes on the epoch is shown in Table 4-1, which also highlights the influence of the minimum elevation over the local horizon for each ground station location. The most favourable ground station, with the least variations and the highest mean value is Maspalomas, due to its location close to the equator. However, this is also the station with the smallest antenna size.

4.3.1.3 Transfer orbit

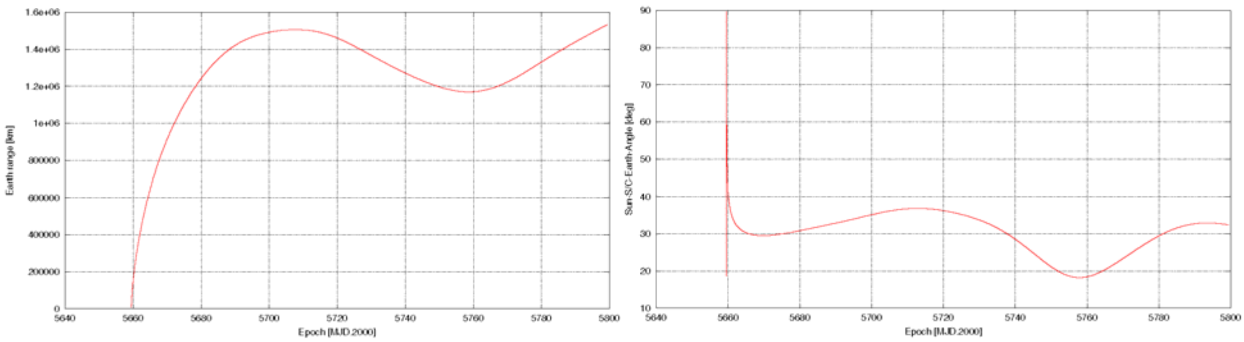

Figure 4-4: Earth range and SSEA for transfer to WFI baseline orbit

There is no clear separation between transfer and operational orbit due to the absence of an insertion manoeuvre. The range increases sharply at first, reaching 1 million km only 11 days after departure from LEO. There are no eclipses and the SSEA remains below 37 deg, only slightly larger than the maximum of 33 deg achieved during the operational orbit. The transfer phase can be seen as over around 40-50 days after departure, but the experiment hardware can be commissioned earlier than that.

4.4 Options

4.4.1 Shared Launch with Ariane 5 ECA into Standard GTO

Should the payload capacity of a dedicated Soyuz-Fregat launch not suffice for the WFI mission, a possible alternative is a shared launch with an Ariane 5 ECA. The most common type of launch for the Ariane 5 family is into GTO, mostly using the midnight launch window. For such a launch, the apogee would be oriented towards the sun direction, which would be useful for launch into the L1 point but not L2. A rotation of argument of perigee would be too expensive or require too long if natural drift is used.

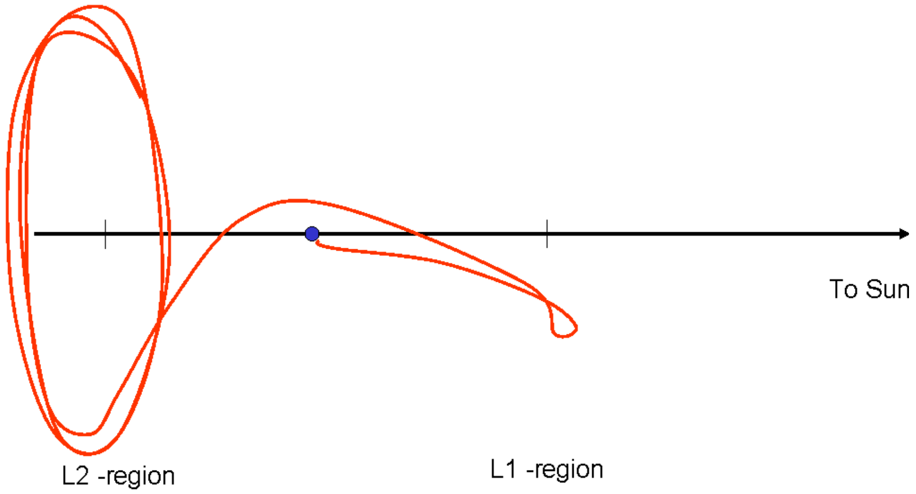

Figure 4-5: Qualitative example of transfer to L2 via L1

However, detailed numerical analysis performed by M. Hechler of ESOC Mission Analysis RD[2] showed that it is possible to reach an orbit around L2 by inserting first into the WSB at L1. The transfer trajectory is very sensitive and requires careful control, but the feasibility has been demonstrated. The impulsive manoeuvre cost is around 755 m/s starting out from GTO and the transfer duration is 100 – 200 days. Typically, the spacecraft moves out to the L1 WSB, then returns to the Earth, performing one or several wide loops, before ending up in an orbit around L2. An example of such a transfer is shown in Figure 4-5.

4.4.2 Reduced-Amplitude Lissajous Orbit Around L2

As described in Section 4.3.1.1, the baseline operational orbit, reachable without DSMs, features large amplitudes and leads to an SSEA of up to 33 deg. Limiting SSEA to less than 15 deg requires a considerable reduction of the amplitudes. The transfer will then incorporate a sizeable DSM with a magnitude of 120-160 m/s, as Gaia analysis has shown RD[1].

Furthermore, for the Gaia mission, eclipse avoidance is required every 6 years. One eclipse avoidance manoeuvre costs 15 m/s. It might be possible to perform the entire WFI mission including extension within an eclipse-free period, if the initial phase can be chosen just right, which will constrain the launch date. Otherwise, 15 m/s have to be budgeted on top of the DSM and the Station-keeping cost.

4.4.3 Inclined HEO

For the choice of the HEO, a series of tradeoffs were made. The higher the orbital period, the better the scientific merit, but the lower the orbital stability and the launcher performance. The lower the inclination, the higher the launcher performance and the more balanced the coverage properties, but the longer the eclipse durations.

The compromise solution found was for a HEO with a period of 3 days and an inclination of 28.5 deg. Up to this inclination, the Soyuz-Fregat performance does not decrease much with respect to a near-equatorial launch. When raising the perigee to an altitude of 9000 km and selecting the initial argument of perigee correctly, orbital stability requiring little or no station-keeping for at least 5 years could be obtained at least for some launch times per day. The first constraint was that the perigee altitude should never decrease below 4000 km.

The second constraint was that the maximum eclipse duration encountered during an assumed 5-year mission should not exceed 2 hours. When applying this constraint and retaining only launch epochs for which orbital stability is guaranteed, there is still a 90-minute launch window every day.

Inclination [deg]	28.5
Perigee and apogee altitudes [km]	9000 x 153,684
Launch orbit [km]	180 x 153,684
Operational orbital period [d]	3
Initial argument of perigee [deg]	240
Final argument of perigee [deg]	300
Perigee raising manoeuvre [m/s]	217
Launch mass w/adapter [kg]	2360
Final mass after perigee raise [kg]	2130

Table 4-2: Summary of orbit properties for WFI HEO Orbit

Table 4-2 summarizes the properties of the HEO orbit as proposed for the WFI case. As can be seen, due to the large perigee raising manoeuvre the actual final spacecraft mass hardly improves with respect to the L2 case.

Due to the chosen argument of perigee, which drifts through 270 deg, northern ground stations have a better view of the apogee and therefore provide favourable link conditions. Nevertheless, daily ground station passes cannot be guaranteed, even for Cebreros.

Figure 4-6 shows the coverage of the celestial vault, here shown in ecliptic longitude and latitude, with minimum viewing angle constraints of 35 and 70 deg with respect to the Earth and Sun limb, respectively. The regions of interest, the ecliptic poles, have near-full coverage; only the ecliptic south pole is slightly penalized due to the choice of argument of perigee.

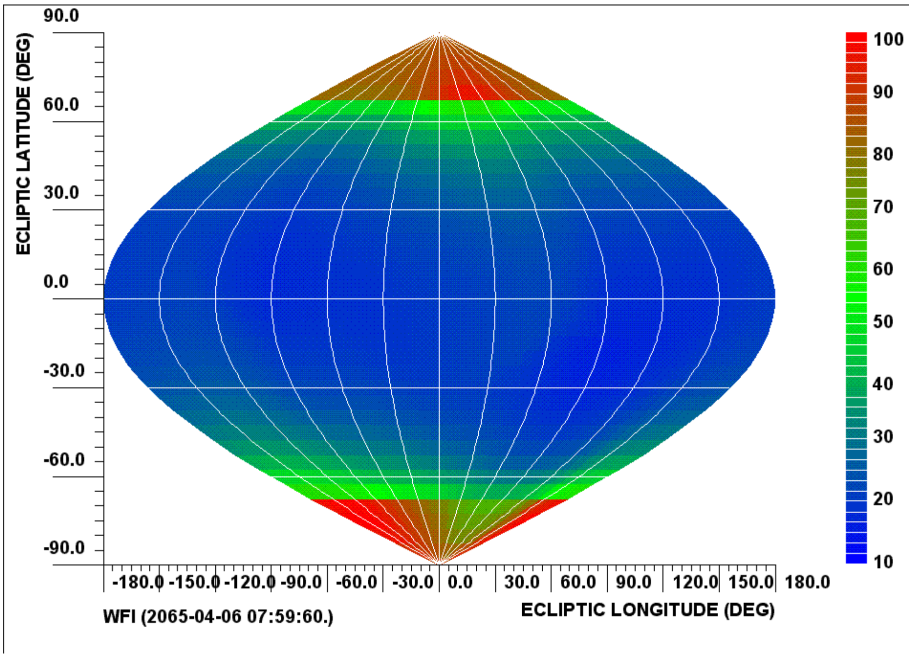

Figure 4-6: Celestial vault coverage quality for HEO Orbit

4.4.4 Trailing Orbit

The NASA IR telescope Spitzer was launched into an Earth trailing orbit, i.e., a heliocentric orbit that slowly drifts away from the Earth but remains at a heliocentric range of approximately 1 AU. Spitzer's drift rate is around 0.1 AU/year.

The way to achieve a drift orbit is to insert the spacecraft into a slightly hyperbolic orbit (C_3 ca. 0.4 km^2/s^2), aiming at the anti-sun direction. The spacecraft will then initially be in the immediate vicinity of the Earth. As the Earth will still exert considerable gravitational perturbations, the spacecraft orbit will gain energy and thus increase. The increase in orbital energy corresponds to an increase in the semi-major axis. The orbit also becomes slightly eccentric, making it loop away from the Earth. The drift rate initially increases strongly, and then becomes quasi-constant.

C_3 for escape [km^2/s^2]	0.4
Earth range [km / AU]	
After 1 year	7.2 million / 0.05
After 2 years	22.9 million / 0.15
After 5 years	76 million / 0.5
Maximum sun range [km / AU]	158 million / 1.06
Minimum sun range [km / AU]	144 million / 0.96
Launch mass w/adapter [kg]	2020 kg

Table 4-3: Properties of trailing orbit

Table 4-3 summarizes the salient characteristics of the trailing orbit. The payload mass is slightly lower than for L2 orbits, and the Earth range is much larger and increases with time. The benefits are:

- The spacecraft never experiences an eclipse pass
- There are no DSMs and no need for station-keeping. Also, it is not necessary to correct the dispersion in the Delta-vee imparted by the Fregat stage. Therefore, the spacecraft does not require an onboard orbit control system. This benefit alone leads to savings that outweigh the slightly lower launch mass.
- In the present analysis, launch in March was assumed. For this launch date, the New Norcia ground station has 12 hours of coverage every day, except for the first two months of the mission, when the daily pass duration is slightly shorter.

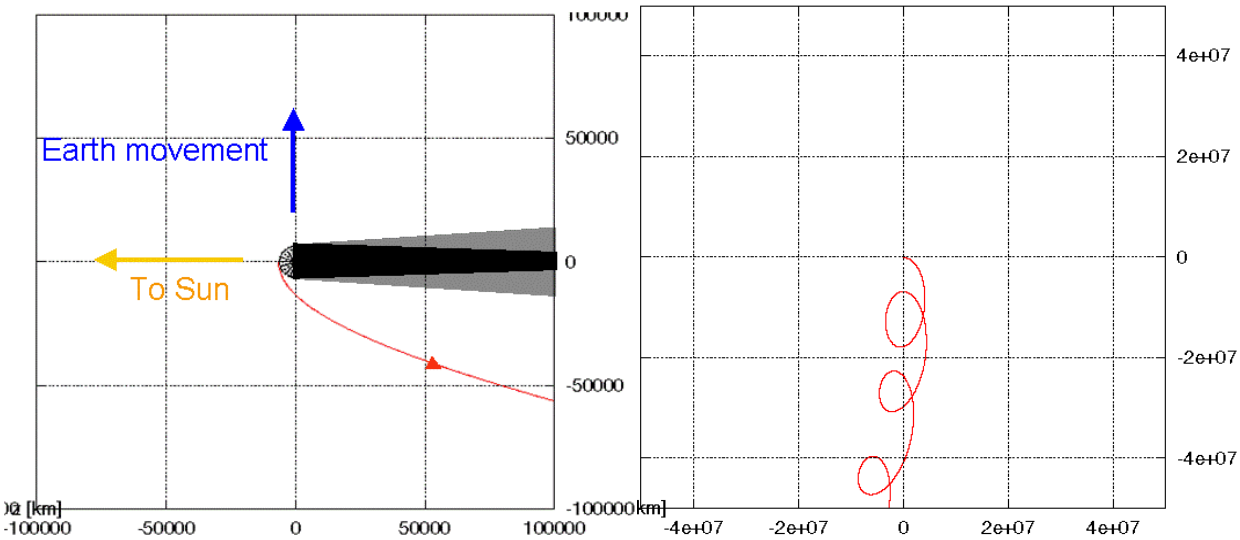

Figure 4-7: Close-up and pan view of trailing orbit trajectory

Figure 4-7 shows a close-up of the trajectory at escape and a panned view of the orbit as it drifts away from the Earth in loops. In both cases, a rotating coordinate frame is chosen, with the Sun constantly in the –x-direction and the Earth moving in the +y-direction. It can be seen how the spacecraft remains well clear of the eclipse cone and how the trajectory evolves with time.

Figure 4-8 shows the Earth and sun distance as function of time for a period of 5 years. Note how the Earth perturbations have a strong initial effect, increasing the drift rate. With time, the drift rate becomes constant.

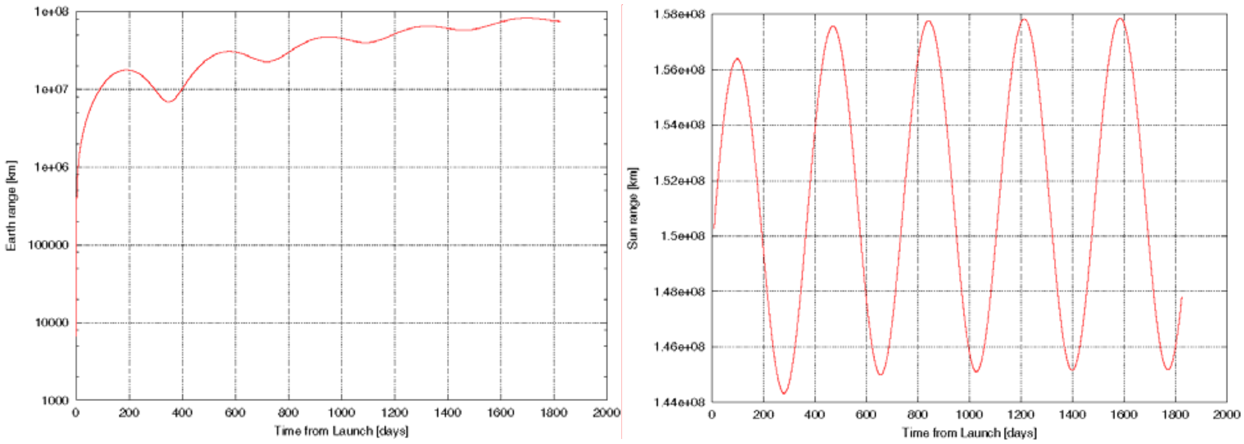

Figure 4-8: Earth and Sun Range on Trailing Orbit

This Page Intentionally Blank

5 SYSTEMS

5.1 System Requirements and Design Drivers

5.1.1 Overall Mission Requirements

The main scientific requirements are reported in Chapter 3. From these requirements a set of payload and mission and system requirements has been derived. This is complemented by programmatic constraints set by the organisation and planning of the ESA Science Programme

The programmatic requirements concern cost and schedule of the mission and determine the subsequent launch vehicle selection and overall technology readiness approach (Table 5-1).

PM – Programmatic Requirements		
PM.SCH Schedule and Budget		
Cost Constrained	The WFI mission cost shall be cost constrained (incl tech dev, launch, ground ops mission+sci).	Cosmic vision programme target (yearly budget of space science directorate approx)
Schedule	WFI shall be launched between 2015 and 2020.	Cosmic Vision programme target 2015-2025, Worst case for tech development and schedule is 2015
Technology Readiness	Only technologies with a TRL of 5 by 2009 (start ph-B) shall be used.	
Launch Vehicle Selection	Launch Vehicle shall be Soyuz-Fregat	To keep within cost limit

Table 5-1: Programmatic requirements

The first science requirements are relevant to the observation strategy (Table 5-2). These specify survey field size and geometry and observation cadence which allow imaging and spectrometry measurements to be made with adequate quality and frequency.

MS – Mission Systems Requirements		
MS.OBS Observation Strategy		
Survey Field Dimensions	Each survey field shall be a strip on the sky of height 1 degree, length 11.833 degrees	Total area of approx 10 sq deg per field after edges discarded
Imaging Scan	Perform imaging over each survey field with steps of 300 arcsec and two dither-exposures per step where each dither-exposure shall be 8x125s (visual band), 1000s (NIR band) in duration	
Revisit Rate	Make repeat photometric measurements over the same area of the sky once every 5 days.	To match SN evolution timescale for low z SN + ability to predict peak luminosity in time
Obs Cadence	The observation cadence shall include 4 days of imaging followed by 1 day of calibration and spectrometry measurements made during the slew back to the start of the scan strip	

Data Downlink	The photometry data shall be downloaded during the 4 days allocated to the imaging scan	To ensure that data is downloaded in time to select target SN for spectrometry measurements
Spectrometer Measurements	For each selected SN target at near-peak luminosity, spectrometry shall be performed on target for exposure time of TBC f(z, band, SNR)	

Table 5-2: Observation strategy requirements

Orbit requirements (Table 5-3) are also derived so as to enable observation of the required survey fields. Given the high frequency of the observation cadence it is also a wish to maximise the uninterrupted observation time. The orbit requirements affect the mission architecture down-selection process described in section 5.3, and the observation strategy baseline described in section 5.3. Furthermore, the nominal mission lifetime is specified as three years which allows adequate time to meet the target of minimum 2000 supernova (detection and follow-up).

MS.LOP Launch and Orbit Parameters		
Orbit	GOAL: The mission orbit should allow uninterrupted observation time	Stable viewing of the survey fields
Orbit-Visibility	The orbit shall allow visibility of north and south ecliptic poles	
Noise	The orbit selection shall minimise the overall straylight noise input into the focal surface	Satisfaction of the SNR>5 req for high redshift supernovae
MS.LIF Design Life		
Mission Lifetime	The WFI nominal operational lifetime shall be 3 years.	For baseline SN measurements, approx 16 months observation time for each pole + commissioning (4 mo)
Extended Mission Lifetime	The WFI extended operational lifetime shall be 3 years.	To be allocated to other science measurements (for example weak lensing). For consumables no margin should be applied.
MS.GSO Ground Station and Operations		
Ground Station Selection	The mission shall be compatible with the ESA DSN	

Table 5-3: Other mission systems requirements

5.1.2 Payload Module Requirements

The telescope requirements (Table 5-4) are primarily designed to ensure adequate image quality according to the baseline imaging requirements of Table 3-3. The wide field of view is also important to ensure sufficient sky coverage and revisit rate. These requirements impose constraints on the design of the optical system, but also influence the design of other subsystems. On-orbit adjustment mechanisms, thermal stability and control, and an external baffle design with adequate straylight rejection are significant drivers for the corresponding sub-system designs.

TR – Telescope Requirements		
TR.OTA – General Optical Telescope Assembly (OTA) Design Requirements		
Aperture	The WFI telescope shall have a collecting area unobscured equivalent to a nominal aperture of 2 metres.	Diffraction limited, wide field
Field of View	The focal surface shall have a nominal 1-degree square field of view with diffraction limited images at 1 micron wavelength.	SN discovery rate, diffraction limited optics
Throughput	TBD	Function of mirror coating
Wavefront Error	The wavefront error shall be kept below 71.4 nm RMS	From Marechal criterion
Delta Wavefront Error	The delta wavefront error shall be kept below 49.4 nm RMS	From Marechal criterion. Delta wavefront error = in-orbit stability of the wavefront error
On-orbit Focusing	The OTA shall be adjustable on-orbit	3 DoF for M2 is sufficient
Alignment Requirements (z)	Delta z between M1 and M2 shall be less than +- 1 um	
Alignment Requirements (theta)	Delta theta between M1 and M2 shall be less than +- 2 urad	
Operational Temperature	The OTA shall be kept at 290K during science measurements	To avoid ground cryogenic testing (cost)
Non-Operational Temperature	The OTA shall be kept within the range of 200-320K during non-operational periods.	
Temperature Difference M1/M2	The delta-T between M1 and M2 shall be lower than 0.5K	
Temperature Variation	The variation of temperature on the surface of each mirror shall remain within a delta-T of 0.3K	
Particulate Contamination	Lower than 200 ppm at EOL inside telescope, on mirrors	From XMM mission
Accommodation	All instruments shall use the output beam from the telescope	Simplest optical train (lower cost for production, testing), optical adjustments to focus image do not detract from performance of other instruments
Straylight level	Straylight contribution to noise shall be at least a factor of 10 less than the zodiacal light contribution	

Table 5-4: Telescope requirements for OTA

The science requirements and telescope requirements play a major role in the instrument specification. Detectors are chosen to satisfy the wavelength coverage and SNR required, and the camera layout is designed to accommodate nine filter bands and a one square degree instrumented field of view. These camera requirements are presented by detector type in (Table 5-5, Table 5-6, Table 5-7). Subsystem designs such as thermal control and configuration are constrained by this set of requirements.

CR – Camera Requirements		
CR.FSA – Focal Surface Assembly Design Requirements		
Filter Wheel	No filter wheel shall be used	Filter wheel would add mechanism complexity

Camera Layout Symmetry	The camera layout shall be symmetric/asymmetric with respect to spacecraft rotations of 90, 180 degrees	Keep FSA on cold side wrt sun, keep solar array pointed to sun, while imaging all areas of sky w all filters
Detector Temperature	The camera detectors on the focal surface shall be kept at 150K	Keep noise low (less than zodiacal light) to get early SN detection, assume CCDs MCTs can operate at same temperature

Table 5-5: Camera requirements for FSA

CR.VIS – Visible Detector (CCD) and Filter Requirements		
Field of View	The field of view occupied by visible detectors shall be 0.5 x 0.5 square degrees	Half of square area on focal surface
CCD Wavelength Coverage	The CCDs shall be sensitive to wavelengths in the range 0.3-1.0 microns	
CCD Radiation Specification	TBD	
CCD Pixel Size	The pixel size of the CCDs shall be 10 um square	
CCD Pixel Count	The detector will be made up of 72 CCDs with each being a 2900x2900 pixel array.	
CCD Read Noise	The average read noise for CCDs shall be below 6 e-	
CCD Read Time	The read time for CCDs shall be <= 21s (4-node readout, 100 kHz)	
CCD Integration time	The integration time for the CCDs shall be approx 125s which corresponds to one sub-frame	Integration time limited by cosmic ray events.
Visual Filter Bands	The CCDs will be covered by filters from 6 different visual bands, centre frequencies TBD	

Table 5-6: Camera requirements for visible detectors (CCDs)

CR.NIR – Near Infra-Red Detector (HgCdTe) and Filter Requirements		
Field of View	The field of view occupied by NIR detectors shall be 0.5 square degrees	Half of square area on focal surface
MCT Wavelength Coverage	The MCTs shall be sensitive to wavelengths in the range 0.9-1.8 microns	
MCT Radiation Specification	TBD	
MCT Pixel Size	The pixel size of the MCTs shall be 20 um square.	
MCT Format	The detector will be made up of 72 MCTs with each being a 1450x1450 pixel array.	
MCT Read Noise	The average read noise for MCTs shall be below 8 e-	
MCT Exposure time	The exposure time for the MCTs shall be 1000s total (one frame) with non-destructive sub-frame readouts every 15.6s.	Min exposure time limited by S/N for first detection
NIR Filter Bands	The MCTs will be covered by filters from 3 different NIR bands, centre frequencies TBD	

Table 5-7: Camera requirements for NIR detectors (MCTs)

The requirements for the camera read-out electronics (Table 5-8) are derived from the exposure times and read-out strategies for the two detector types.

CR.ROE – Read-Out Electronics Requirements		
Readout Frequency CCDs	The CCDs shall be read out at the end of each integration period of 125s (destructive readout).	
Readout Frequency MCTs	The MCTs shall be read out at the end of each period of 15.6s (non-destructive readout) and reset after 1000s.	

Table 5-8: Camera requirements for ROE

The requirements for the Integral Field Spectrometer (IFS) instrument (Table 5-9) and read-out electronics (ROE) (Table 5-10) are derived from science requirements affecting the specific features to be observed and the relevant wavelength coverage as well as the spatial and frequency resolution necessary.

IR – IFS Requirements		
IR.GEN – Integral Field Spectrometer General Requirements		
IFS Field of View	The field of view of the IFS shall be 3x3 arcseconds	
IFS Optical Wavelength Coverage	The IFS optical branch shall be sensitive to wavelengths of 0.3 to 1.0 microns	
IFS NIR Wavelength Coverage	The IFS NIR branch shall be sensitive to wavelengths of 1.0 to 1.8 microns	
IFS Radiation Specification	TBD	
IFS Pixel Size	TBD	
IFS Spatial Resolution	The spatial resolution of the image slicer shall be 0.10 arcseconds per slice.	
IFS Resolution	The IFS resolution shall be better than 100 ($\lambda/\Delta\lambda$) with SNR better than 10	
IFS Magnification	The magnification provided by the IFS optics shall be a factor of 2	
IFS CCD Exposure	The exposure time for the CCDs shall be TBD s total (one frame) with destructive sub-frame readouts every 125s.	
IFS MCT Exposure	The exposure time for the MCTs shall be TBD s total (one frame) with non-destructive sub-frame readouts every 15.6s.	Total exposure time to be calculated as a function of redshift
IFS Format	TBD	
IFS Temperature range	The IFS detectors shall be kept at 150K	

Table 5-9: Spectrometer general requirements

IR.ROE – Read-Out Electronics Requirements		
Readout Frequency CCDs	The CCDs shall be read out at the end of each integration period of 125s (destructive readout).	
Readout Frequency MCTs	The MCTs shall be read out at the end of each period of 15.6s (non-destructive readout) and reset after 1000s.	

Table 5-10: ROE requirements for spectrometer

The payload data handling system (DHS) requirements (Table 5-11) are derived from the instrument architectures as well as the observation strategy requirements. A significant amount of on-board processing is necessary to reduce the science data generation rate to a level which is compatible with possible comms system architectures.

DH – Payload Data Handling Requirements		
DH.GEN – Data Handling System Requirements		
On-board processing	The camera sub-frames shall be processed on board to combine into 1000s frames and remove cosmic ray events	
On-board processing	The payload DHS shall be capable of handling an input data rate of 29 Tbytes raw data in 1000s	8xVIS + 64xNIR = 2bytes* (8*72*2900^2 + 64*72*1450^2) = 29 Tbytes
Compression Factor	The system shall be able to compress the data by a factor of >=1.5	Compressed data per frame = 1.51/compression factor
Buffer size	The size of the buffer for data storage on-board shall be capable of storing 2 frames of data before processing and 24h compressed image frames	
Processing requirements	The processor shall be chosen to meet visible and NIR data processing needs and data compression needs	

Table 5-11: Payload data handling requirements

The fine guidance sensor (FGS) is a critical component of the payload that allows long exposures to be taken without too much degradation in image quality and signal to noise ratio thus satisfying the science requirements. The FGS design is coupled with the spacecraft AOCS design, and the imposed requirements (Table 5-12) are also derived from absolute pointing error (APE) and relative pointing error (RPE) requirements which are further presented in section 8.7.

FR – FGS Requirements		
FR.GEN – Fine Guidance Sensor Requirements		
Accommodation	The FGS shall be located on the focal surface	
Redundancy	The FGS shall be redundant (at least two units)	Fine pointing ability is critical for mission success
FGS Field of View	The FGS field of view shall be 2.2x2.2 arcmin – At least probability 99% of one guide star magnitude <= 16.5 in FoV TBC	
FGS Wavelength Coverage	The FGS shall be sensitive to wavelengths of 0.30 to 1.0 microns	

FGS Radiation Specification	TBD	
FGS Pixel Size	The max pixel size for the FGS shall be 13 micron (down to min of 8 micron)	
FGS Output	The FGS shall provide an output signal to the AOCS control system at min frequency 1 Hz	
FGS Accuracy	The FGS measurement accuracy shall be less than 5 mas	
FR.ROE - Read-Out Electronics Requirements		
Readout Frequency CCDs	The CCDs shall be read out at the end of each integration period of 100ms (destructive readout).	To provide (after filtering) 1 Hz output to AOCS

Table 5-12: FGS requirements

5.1.3 Service Module Requirements

General spacecraft requirements are given in Table 5-13. These are imposed by the launch vehicle selection and constrain the configuration and baffle design in particular, as well as the entire spacecraft structural design.

SC - Spacecraft Requirements		
SC.GEN - Spacecraft General Requirements		
Length	The WFI Total spacecraft length (including telescope, SVM) shall fit within the Soyuz ST fairing - see graphic (less than 5070 mm at max dia.).	“METOP” fairing assumed
Diameter	The WFI Total spacecraft diameter (including telescope, SVM) shall be less than 3800 mm.	
LV Adapter	The Spacecraft shall interface the LV via the 1666 ∅ standard Soyuz Fregat 2.1b adapter	Compatibility with Gaia design
Eigen Frequencies	The WFI spacecraft fundamental frequencies shall be >= 15 Hz lateral and >= 35 Hz longitudinal	

Table 5-13: General spacecraft requirements

Service Module requirements that are direct consequences of the above science and payload requirements are reported below in Table 5-14 to Table 5-17.

SM - Service Module			
SM.GEN - Spacecraft Functional Requirements			
SM.GEN-1	2-Space segment	Obs Strategy	The SVM design shall be such that the observation strategy in MS.OBS may be carried out.
SM.GEN-2	2-Space segment	Mounting	The SVM shall provide a mecahnical interface to the telescope
SM.GEN-3	2-Space segment	Power	The SVM shall provide power to the payload instruments
SM.GEN-4	2-Space segment	Temperature	The SVM shall guarantee a temperature at the mechanical interface with the PM (-10,+20 degC)

Table 5-14: SVM functional requirements

SM.ACS - Spacecraft AOCS Requirements			
SM.ACS-1	2-Space segment	APE	The WFI Absolute Pointing Error shall be less than or equal to 1 arcsec (3 sigma)
SM.ACS-2	2-Space segment	RPE - LOS	The WFI Relative Pointing Error in the Line of Sight between steps shall be less than or equal to 10 milliarcsec (1 sigma) over 2000s, and 40 milliarcsec (3 sigma) over 2000s
SM.ACS-3	2-Space segment	RPE - Around LOS	The WFI Relative Pointing Error around the Line of Sight between steps shall be less than or equal to 1 arcsec (1 sigma) over 2000s, and 4 arcsec (3 sigma) over 2000s
SM.ACS-4	2-Space segment	Settling time	The settling times after AOCS pointing manoeuvres shall be consistent with the given observation strategy

Table 5-15: SVM AOCS requirements

SM.DHS - Spacecraft DHS Requirements			
SM.DHS-1	2-Space segment	Data Storage	The service module mass memory shall provide data storage for P/L compressed data and S/C housekeeping data

Table 5-16: SVM Data handling requirements

SM.COM - Spacecraft Communications Requirements			
SM.COM-1	2-Space segment	Frequency band	The baseline frequency band shall be Ka 26 GHz
SM.COM-2	2-Space segment	Freq band option	GOAL: X-band option using ESA DSN should be considered
SM.COM-3	2-Space segment	Science data-rate	The comms design shall be able to handle a science data rate of 40 Mbps
SM.COM-4	2-Space segment	TM/TC data-rate	The comms design shall be able to handle a TM/TC data rate of 4 kbps

Table 5-17: SVM communication requirements

An overview of the spacecraft margin philosophy is presented in Table 5-18.

SC.MAR - Spacecraft Margin Philosophy		
Link Budget	A 3dB margin shall be applied in calculating the link budget	
System mass margin	A system margin of 20% shall be added to the dry mass which is calculated as a sum of all the components including maturity margin	
Maturity mass margin	Mass margins of 5, 10 or 20% shall be added to unit best mass estimate depending on unit technology maturity.	Specific policy applies for structures and optics
Power system margin	A 20% margin shall be applied at system level to the overall budget	
DeltaV margin	A deltaV margin of 5% shall be added to mission manoeuvres	

SC.MAR - Spacecraft Margin Philosophy	
Propellant margin	A propellant margin of 2% shall be added to propellant calculations for manoeuvres
AOCS impulse	A margin of 100% shall be added to the AOCS total impulse calculation for the nominal mission lifetime

Table 5-18: Spacecraft margin philosophy

5.1.4 Additional Design Requirements

To minimise mission risk, additional margins have been introduced in the spacecraft design:

- All structures and optics units shall have a 20% maturity margin disregarding their maturity level
- The spacecraft shall be sized to accommodate the cold gas (worst case for mass and volume) and the FEEP fine pointing system (worst case for power) to allow a decision to be taken in later phases of the project.
- The spacecraft design shall be capable of accommodating the worst mass and volume optical design options (5-mirror design) to allow a more detailed trade-off to be carried out in later phases of the project.
- A worst-case, maximum data compression factor of 1.5 shall be considered for image processing. This represents the worst case in the design of the communication system and in the definition of the observation strategy.

5.1.5 Discussion of the Requirements and Design Drivers

An analysis of the requirements shows the areas that are most critical for the spacecraft and mission design.

The requirement for imaging high red-shift supernovae with SNR bigger than 5 leads to the need of a large telescope aperture and mass. The main design driver of the mission is to make this compatible with the mass performance limitation of a Soyuz launch, especially taking into account the need of a low noise orbit, away from Earth, which implies lower launch capability.

An additional mission/system design driver is the combination of the required large data volume of the imaging function and the short survey field revisit time. These together, lead to the need for onboard processing and high data rate transmission and rule out the use of conventional X-band communication system. Moreover, science operations and communications shall occur at the same time if the revisit time requirement is to be matched. This implies that the power design shall cope with a higher power demand.

The definition of the observation strategy that fits with the required science operations and the associated spacecraft resources and constraints is the main system design activity. This is described in detail in 5.3.1.

Another consequence of the science requirements is the need for high pointing stability. This requires that an additional micro-thruster assembly be added to the system for fine control and the addition of a Fine Guidance Sensor that needs to be developed.

Finally, high dimensional stability is required to avoid optical misalignment. Therefore, the optical support structures need to be designed for high stiffness and minimum relative thermal dilatation. This limits the choice of materials and requires that generous margins are considered at this stage.

5.2 System Trade-Offs

Several trade-offs were carried out at system level to define the system baseline configuration and design. The most important ones are:

- Trade-off among micro-thruster technologies for fine pointing
- Trade-off fixed versus deployable/steerable solar array
- Trade-off between two alternative optical configurations
- Trade-off among mission orbits.

The first two trade-offs are fully described in 8.1 and 8.4 respectively; the third trade-off is summarised here below.

5.2.1 Telescope Configuration – 4-Mirror vs. 5-Mirror

Two telescope configurations have been considered. The first is a 4-mirror Korsch layout, and the second is a 5-mirror layout. Advantages and disadvantages of each are presented in Table 5-19. The difference between the two configurations is not large; the selected baseline has been the 5-mirror configuration which is a worst case in terms of mass and a best case in terms of science performance. However, as discussed previously, the spacecraft and mission design is such that the 4-mirror configuration can also be accommodated.

		4-mirrors	5-mirrors
total mass		-3%	reference
comfiguration	distance M1-M2	+30%	reference
science performances	IFOV (useful)	-11%	reference
	scanning efficiency	-8%	reference
	optical performances	similar (diffraction limited)	similar (diffraction limited)
manufacturing complexity		Drawback: * complexity due to the size of the primary mirror (2m): CVD coating pb	Drawbacks: * complexity due to the size of the primary mirror (2m): CVD coating pb * curved FPA
AIV complexity		Drawbacks: * 3 power mirrors in 2 axis	Advantage: *3 power mirrors in one axis Drawbacks: * curved FPA * higher sensitivity to misalignment: 5microm for 1% degradation of MTF(compared to 12microm for the 4 mirror concept)

Table 5-19: Comparison between 4- and 5-mirror configurations

5.2.2 Orbit Selection

In summary, the main factors considered for orbit selection were:

- Capability to perform uninterrupted imaging (to fulfill sky strip revisit time req.)
- Coverage of North and South ecliptic poles (to fulfill the survey field req.)
- Soyuz launch capacity and total delta-V

- Downlink capability as combination of ground station visibility from orbit and range
- Low environment disturbances to simplify fine attitude control
- Stable thermal environment to ease detector cooling and cope with stability requirements
- Low straylight from Earth and/or Sun to reduce baffle dimensions and mass

Several orbits were considered and traded according to these parameters (see Table 5-20).

Orbit	Soyuz perfo (kg)	Delta-V req. (m/s)	Science req.s	Optical Noise	Comms	Thermal	AOCS	Notes
L2 halo orbit (800000 km)	2200	32	North and South poles coverage, Uninterrupted imaging possible	High view angle to Earth (>28deg) due to North-South orbit excursion	need to use 26 GHz band to cope with the data rate, 7-hour/day min visibility for ESA DSN GS	Stable environment	Only SRP disturbances	Low delta-V
L2 small Lissajous orbit (400000 km)	2200	142	North and South poles coverage, Uninterrupted imaging possible	Lower view angle to Earth (15 deg) compared to above	need to use 26 GHz band to cope with the data rate, 7-hour/day min visibility for ESA DSN GS	Stable environment	Only SRP disturbances	Baffle design fits into Soyuz fairing but higher propellant mass compared to above
HEO 3-day low inclination	2360	237	South pole coverage implies large Earth view angle, max about 2-day per orbit continuous imaging	Earth disturbance reduces the useful part of the orbit for science or large baffle design	need to use 26 GHz band to cope with the data rate, up to 12-hour visibility of GS	Variable environment (max eclipse 2 hours), need of time for stability after orbit phase close to Earth: reduction of useful part of orbit for science	Only SRP disturbances druing measurement (close to apogee)	No mass gain compared to L2 halo and reduction in science req.s
Earth trailing orbit	2180	0	North and South poles coverage, Uninterrupted imaging possible. After nominal mission (3 yrs) the drift of theS/C from Earth is too high for high data rate measurements	Low view angle to Earth: no orbit North-South excursion	Possibility of using 32 GHz band. 8-h/day visibility of ESA DS GS, max range 20 mil km	Stable environment	Only SRP disturbances	Large HGA and high comms power but simple baffle design and no main propulsion

Table 5-20: Comparison of orbit options for WFI mission

The L2 halo orbit is the best compromise between fulfilment of science requirements and mission mass capability although it would require an update of one of the ESA DSN ground stations to the 26 GHz frequency band. The 800000km radius orbit has a lower total deltaV than the smaller L2 orbit and therefore has been selected as baseline, as long as Earth straylight is acceptable and the baffle size can be limited to Sun rejection. This issue is discussed further in 7.1.

The HEO orbit did not result in a significant increase in launch mass and the reduction in observation time due to Earth proximity at perigee, would lead to a longer revisit time, so this option was not considered further.

The Earth trailing orbit could be very favourable since it would not require a ground station upgrade and it is the one with minimum delta-V requirement. However, after two years the spacecraft to Earth range becomes too large to keep the data rate requirement without a major oversizing of the communication and power subsystems. This option could be reconsidered if the mission data rate could be reduced.

5.2.3 Mission Geometrical Constraints

The selection of the L2 orbit and choice of a fixed solar array have important consequences on the mission and science operations.

To simplify the pointing required for the observation strategy and keep the sun aspect angle to the solar array ≤ 45 deg, the spacecraft design must satisfy two conditions. First, the detector layout shall be symmetric/anti-symmetric with respect to rotations of 90 degrees (see Figure 5-1). Second, the spacecraft shall be rotated by 90 degrees every 3 months as shown in Figure 5-2 such that the detectors always see the sky from an acceptable orientation and the solar panels receive enough sunlight.

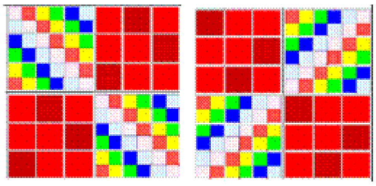

Figure 5-1: Detector layout 0 deg and 90 deg rotation

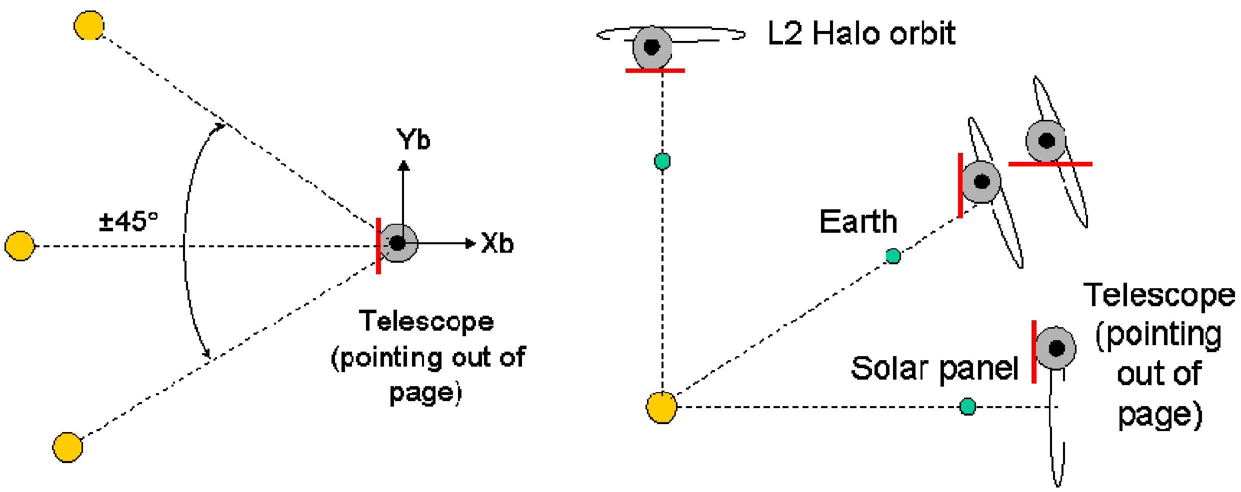

Figure 5-2: Mission geometry over time for L2

The survey field requirement states that each field shall be located within ± 20 degrees of the North or South ecliptic pole. The Sun aspect angle to the axis of the telescope can then be calculated as a combination of the on-ecliptic angle (α=±45 deg) and the tilt angle due to the survey field req. (β= ± 20 deg). This geometry is shown in Figure 5-3.

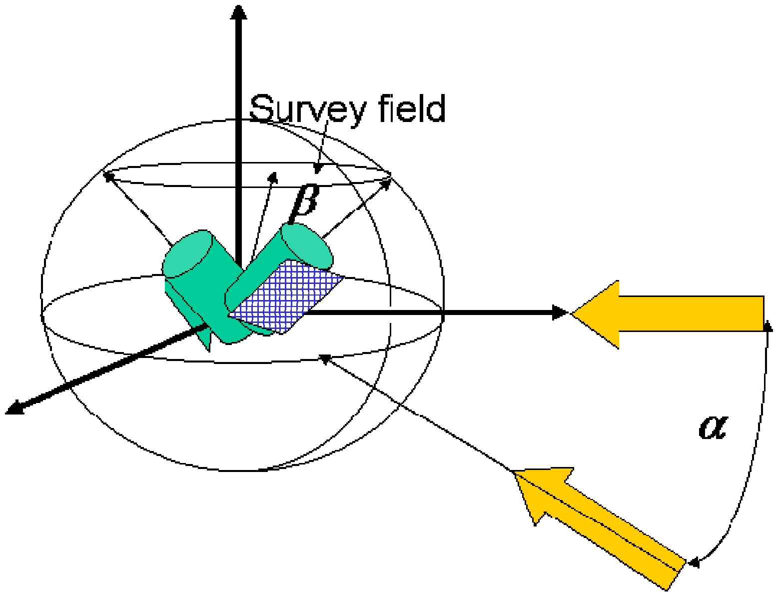

Figure 5-3: Survey field geometry

To minimise the contribution of Earth straylight, the L2 halo orbit insertion is performed so that telescope tilt is maximum when S/C is at its maximum angle from Earth with an off-axis angle of 45 deg. However, the contribution of Earth straylight has been found to be non-critical. The Sun, Earth, Spacecraft geometry for the baseline L2 orbit is shown in Figure 5-4.

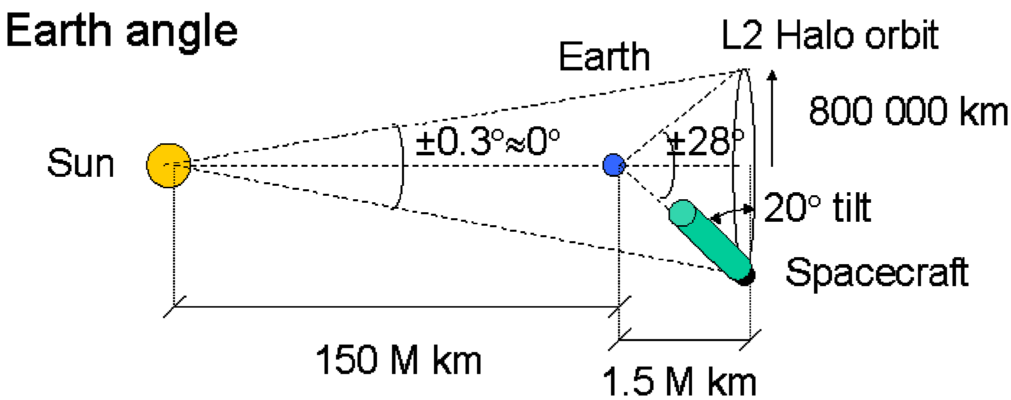

Figure 5-4: Sun, Earth, Spacecraft geometry for L2 orbit

The minimum sun rejection angle for baffle design is 70 degrees, and the minimum Earth angle is 48 degrees as shown in Figure 5-5.

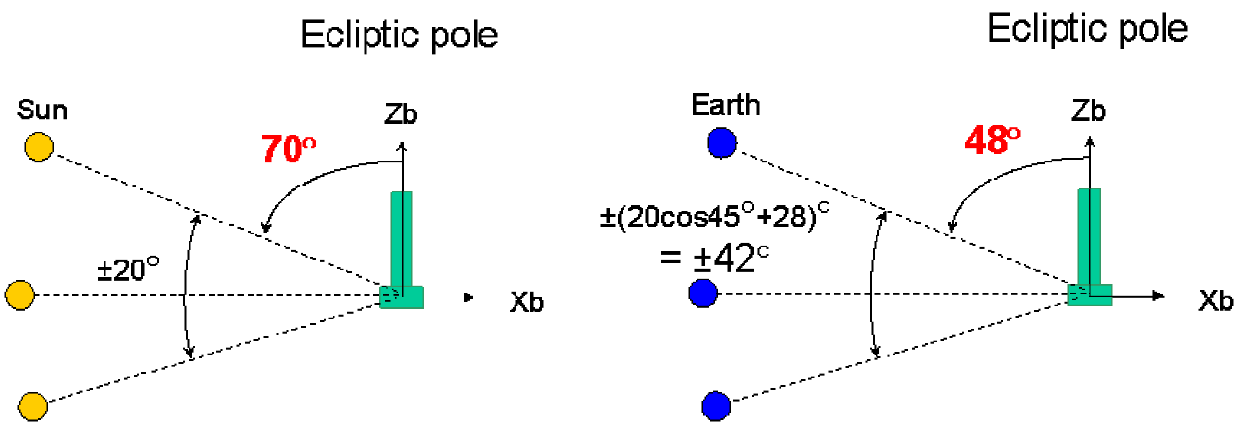

Figure 5-5: Minimum Sun angle and minimum Earth angle

5.3 System Baseline Design

5.3.1 Observation Strategy Implementation

The mission must be able to carry out two types of measurements in order to fulfill the given science requirements. The first type of measurement involves using the camera (visible and NIR detectors) to take photometric images of the entire survey field with a revisit rate of five days. The second type of measurement is carried out using the spectrometer (IFS) to target discovered supernovae at their peak luminosity (i.e. at a certain point in time) within the survey field and within an allocation of one day.

The observation strategy will be the same for each survey field each close to one ecliptic pole, so only one field will be considered here. Every five days, the observation cadence will be repeated thus providing an appropriate revisit rate to satisfy science goals in terms of number of samples during the rise time for low redshift supernovae.

The photometric observations are performed by scanning the survey field of approximately ten square degrees one step at a time. Each step represents a shift of 300 arcsec in the scan direction which corresponds to the length of one visible band filter (see Figure 5-6).

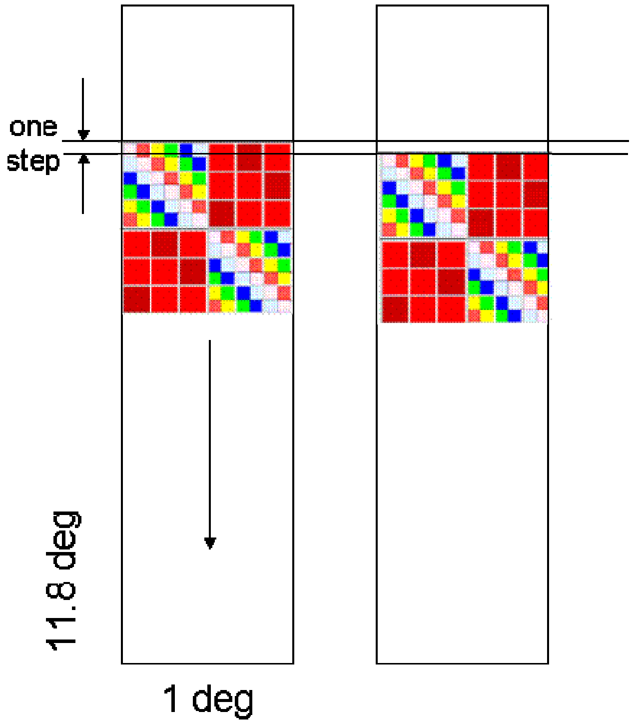

Figure 5-6: Schematic of imaging scan showing step size

The actions to execute a single step are as follows:

1. Take a 1000 second exposure
2. Adjust telescope pointing by n+½ pixels (approx 10”) dithering in each of cross-track direction and scan direction (approx 15” along the diagonal) using micro-thrusters and AOCS system (star-tracker + fine guidance sensor)
3. Take another 1000 second exposure
4. Adjust telescope pointing by -10” in the cross-track direction and 290” in the scan direction

These four actions are repeated for 144 steps along the survey field.

During each 1000s exposure, the CCDs (visible) are read out destructively 8 times, so each of these 8 sub-frames is an image with 125s integration time. The MCTs (NIR) are read out non-destructively 64 times during the 1000s, so each of the 64 sub-frames is a step in the integration, and the final sub-frame is an image with 1000s integration time.

After four days of photometric observations, the fifth day of the observation cadence will be spent making spectrometry measurements. These measurements need to be performed for each identified supernova as it reaches its peak luminosity, and this event will be predicted using previous photometry data points. The observation schedule will be updated to include a sequence of supernovae which are close to their peak luminosity, and during the slew back to the start of the scan strip, the telescope will point to each identified supernova target for a given exposure time (which depends on redshift). Visual and NIR spectra will be taken simultaneously using CCD and MCT detectors.

5.3.2 Observation Strategy Verification

An analysis has been carried out to identify the spacecraft design parameters that make the given observation strategy possible. Such parameters are shown in Table 5-21.

The cadence length of five days is given by the revisit rate required. The pointing time values are calculated for a thrust capability of 500µN. Lower thrust values result in settling times that are too long in the sense that the complete imaging sequence can no longer be completed in the allocated four days from the five day cadence. The compression factor of 1.5 is taken as a conservative estimate, and higher factors may be possible depending on the particular algorithm and image. The spectrometer exposure time is an estimate and will vary depending on the redshift of the target supernova.

CADENCE		
Cadence length	5	d
Number of img steps	144	
Dither exp per img step	2	
IMAGING (IMG)		
Pointing time (dither)	67	s
Pointing time (step)	249	s
Exposure time (Img)	1000	s
SPECTRO (IFS)		
Time required for pointing per target (estimate 2 deg slew)	1088	s
Exposure time (Spectro)	1000	s
DATA		
Compression factor	1.5	
Compressed Frame size IMG (VIS+NIR, 1000s total exposure)	8.00	Gbits
Compressed Frame size IFS (VIS+NIR, 1000s total exposure)	149.68	Mbits
COMMS		
Comms option	Ka-band 26GHz	
Science data rate (max)	40.0	Mbit/s
Comms visibility (max)	4.5	h/d

Table 5-21: Input parameters for observation strategy verification

Given these input values, the required comms duration, science data rate, and the total scan length can be calculated and compared with the available resources. The diagram in Figure 5-7 shows how these parameters are calculated.

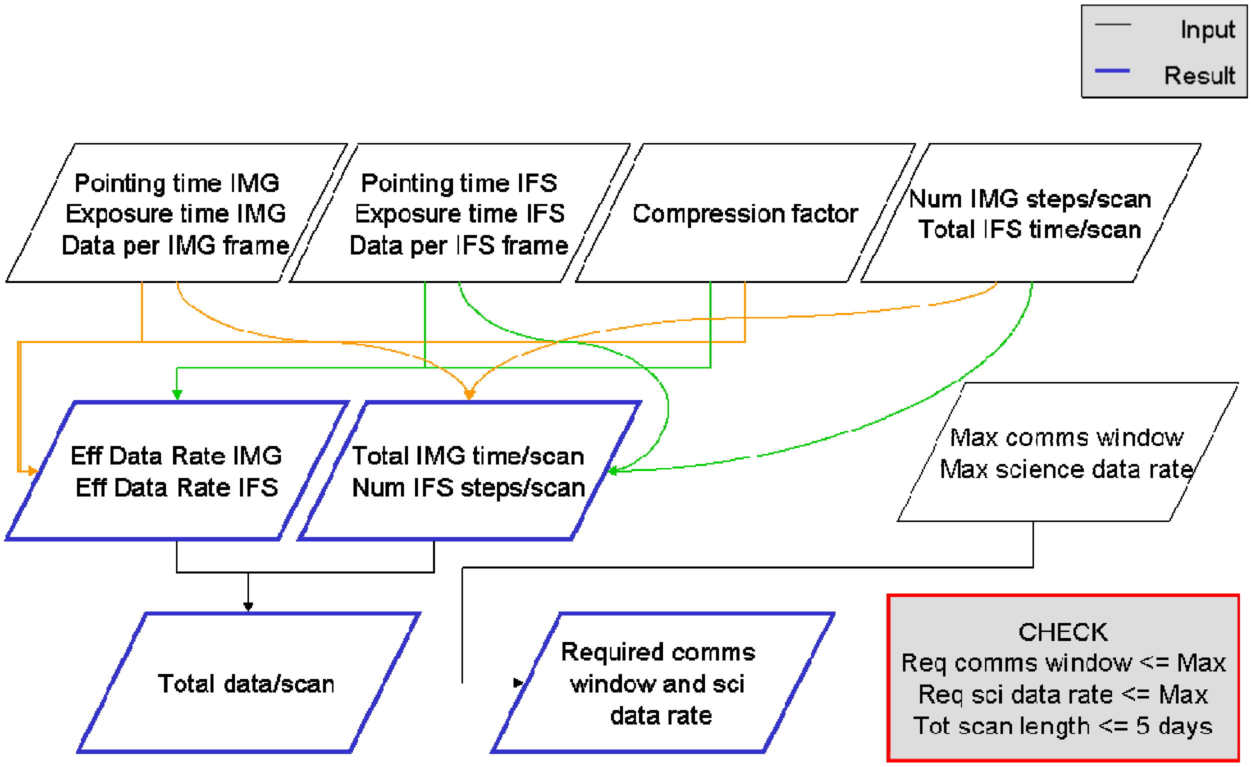

Figure 5-7: Observation strategy verification schematic

The calculated results are shown in Table 5-22. The imaging scan takes 3.86 days, and the spectrometry takes 0.99 days for a total of 4.86 days which is within the available cadence length of 5 days. The total data generated during the imaging scan is 2304 Gbits, and this can be downlinked at a science data rate of 40 Mbps during a comms window of 4 hours per day. These values fit with the maximum available science data rate (40Mbps) and comms window (4.5h/d worst case), so the observation strategy described is feasible, and the thrust level of 500uN provides acceptable pointing times. The strategy implies that comms and science measurements must occur simultaneously.

CALCULATED VALUES		
Eff data rate to output buffer in IMG mode (compressed)	6.91	Mbits/s
Eff data rate to output buffer in IFS mode (compressed)	0.07	Mbits/s
Tot data generated 4 days (compressed)	2304.00	Gbits
Tot data generated last day (compressed)	6.14	Gbits
Science data rate (required)	40.0	Mbit/s
Comms visibility (required)	4.0	h/d
Tot time req for IMG mode complete scan	3.86	d
Number of spectro steps (chosen to make up 24h total)	41	
Total scan length	4.85	d

Table 5-22: Calculated values for observation strategy verification

A back-up option of comms using the X-band was also considered. In this case, the science data rate would be constrained to 3.5 Mbps, due to bandwidth availability and the maximum visibility would be approximately 8 hours. With these constraints, only 25% of the science data could be downlinked, so this option was discarded.

5.3.3 Spacecraft Baseline Design Description

Section 1.3 reports the mission general product tree. The two main elements are the Payload Module and the Service Module. The following interfaces are highlighted:

- For the sake of this study, the baffle is considered part of the Payload Module and is used as support for the payload module thermal radiators
- The payload module interfaces mechanically to the Service module through a 6-point interface on the upper plate of the SVM from which a system of struts goes to the upper structure of the payload optical bench
- There is an electrical interface through the upper plate of the SVM. All power generation and conditioning resides on the SVM
- All data handling units for payload and service module are located inside the SVM. The payload computer and the payload memory which interface on one side to the payload read-out electronics, are connected to the SVM data handling through a redundant MIL 1553 bus and through serial SpaceWire links

5.3.3.1 Payload module design description

The payload module breakdown is reported in section 1.3.

The core unit is the mirror assembly for which the five-mirror optics design is taken as baseline as it is the worst case in terms of mass. The four-mirror Korsch design could be accommodated as a back-up solution with some modifications to the baseline and represents the worst case in terms of volume due to the required increased height of the baffle. A mass budget for the payload module at equipment level is presented in Table 5-23.

Element 1 - WFI Spacecraft						
	nr	Mass (kg) per unit	Total Mass (kg)	Margin (%)	Margin (kg)	Mass (kg) with Margin
Payload Module			**999.38**			**1186.30**
Telescope			**692.77**			**829.42**
STRUCTURE			437.42			524.90
External Baffle (incl. Vanes)	1	152.12	152.12	20.00	30.42	182.54
External Baffle cover	1	20.57	20.57	20.00	4.11	24.69
PLM optical bench	1	100.00	100.00	20.00	20.00	120.00
PLM M2 -support structures	1	40.00	40.00	20.00	8.00	48.00
PLM M3 - support structures	1	15.00	15.00	20.00	3.00	18.00
PLM M1 struts	1	3.00	3.00	20.00	0.60	3.60
PLM M2 struts	1	3.00	3.00	20.00	0.60	3.60
PLM M3 struts	1	3.00	3.00	20.00	0.60	3.60
PLM M4 struts	1	3.00	3.00	20.00	0.60	3.60
PLM M5 struts	1	3.00	3.00	20.00	0.60	3.60
PLM internal baffle (incl. vanes)	1	10.44	10.44	20.00	2.09	12.53
PLM Focal Plane Assembly	0	40.00	0.00	20.00	0.00	0.00
PLM lower optic bay	1	40.00	40.00	20.00	8.00	48.00
Baffle support - pedestal	1	11.00	11.00	20.00	2.20	13.20
Closure panel - lower baffle	6	2.21	13.29	20.00	2.66	15.95
Alu_foil covering internal	0	12.22	0.00	20.00	0.00	0.00
Miscelleaneous (bracket,insert)	1	20.00	20.00	20.00	4.00	24.00

Element 1 - WFI Spacecraft	nr	Mass (kg) per unit	Total Mass (kg)	Margin (%)	Margin (kg)	Mass (kg) with Margin
THERMAL			19.08			20.99
WP on 1/4 on baffle ext. surf.	1	1.06	1.06	10.00	0.11	1.17
20 layers MLI on 3/4 baffle ext. surf.	1	12.45	12.45	10.00	1.25	13.70
2 mil Goldised Kapton (HS and FP rear side and top of baffle ext. surf.)	1	0.31	0.31	10.00	0.03	0.34
Al ring	1	5.26	5.26	10.00	0.53	5.78
MECHANISMS			28.50			34.20
Cover door mechanism	1	3.50	3.50	20.00	0.70	4.20
Refocusing mechanism M2	1	15.00	15.00	20.00	3.00	18.00
Refocusing mechanism M5	1	10.00	10.00	20.00	2.00	12.00
OPTICS			207.78			249.33
M1	1	165.00	165.00	20.00	33.00	198.00
M2	1	21.51	21.51	20.00	4.30	25.81
M3	1	5.25	5.25	20.00	1.05	6.30
M4	1	6.56	6.56	20.00	1.31	7.87
M5	1	9.47	9.47	20.00	1.89	11.36
Camera			**136.33**			**163.60**
INSTRUMENTS			136.33			163.60
Camera detector assembly	1	48.57	48.57	20.00	9.71	58.29
Camera read-out electronics	1	77.76	77.76	20.00	15.55	93.31
Calibration device	1	10.00	10.00	20.00	2.00	12.00
Spectrometer			**30.67**			**36.80**
INSTRUMENTS			30.67			36.80
Spectrometer optics & detectors	1	26.35	26.35	20.00	5.27	31.62
Spectrometer read-out electronics	1	4.32	4.32	20.00	0.86	5.18
Payload DHS			**80.47**			**90.89**
INSTRUMENTS			23.80			28.56
OBDH	1	23.80	23.80	20.00	4.76	28.56
HARNESS			56.67			62.33
Harness PLM	1	56.67	56.67	10.00	5.67	62.33
FGS			**5.30**			**6.36**
AOCS			5.30			6.36
Fine Guidance Sensor	2	2.65	5.30	20.00	1.06	6.36
Payload Thermal Control			**53.85**			**59.23**
THERMAL			53.85			59.23
Black paint on baffle and top int. surf.	1	4.93	4.93	10.00	0.49	5.42
FP Radiator (structure+WP+int. finishing)	1	15.47	15.47	10.00	1.55	17.02
ROE Radiator (structure+WP+int. finishing)	1	2.21	2.21	10.00	0.22	2.43
Graphite Heat Path Bars	1	28.08	28.08	10.00	2.81	30.89
Payload Heaters/Sensors	1	3.15	3.15	10.00	0.32	3.47

Table 5-23: Mass budget for payload module

5.3.3.2 Service module design description

The service module (SVM) design is "Conventional" in the sense that it is similar to previous missions (Herschel-Planck, Gaia, XMM) and uses components with heritage.

Re-use of one of the SVMs used in previous ESA missions was not investigated in detail within this study. Re-use could potentially be considered, in particular for GAIA, but several modifications would be necessary.

Anyway, the Service Module geometry and structure of Gaia could be retained as it fits with the Soyuz fairing and it is compatible with the WFI Payload Module dimensions, interfaces and induced loads. The accommodation and selection of units inside and outside has been changed according to the WFI mission requirements.

The solar array is body mounted on three sides of the hexagonal SVM, and the volume driver is the size of the cold gas and monopropellant tanks. The baseline comms system uses a 26GHz transmitter and a 0.7m diameter steerable HGA. A mass budget for the service module at equipment level is presented in Table 5-24.

Element 1 - WFI Spacecraft	Nr	Mass (kg) per unit	Total Mass (kg)	Margin (%)	Margin (kg)	Mass (kg) with Margin
Service Module			**357.51**			**406.12**
STRUCTURE			139.03			166.84
SVM Central cylinder	1	60.20	60.20	20.00	12.04	72.24
SVM Shear Panel	6	2.88	17.30	20.00	3.46	20.76
SVM External Panel	6	3.25	19.50	20.00	3.90	23.40
SVM Top Floor	1	2.12	2.12	20.00	0.42	2.54
SVM bottom floor	1	2.12	2.12	20.00	0.42	2.54
SVM PLM I/F strut	6	4.87	29.20	20.00	5.84	35.04
Additional Solar Panel	1	8.60	8.60	20.00	1.72	10.32
THERMAL			14.31			15.75
SM Radiator (WP+int. finishing)	1	0.05	0.05	10.00	0.01	0.06
20 layers MLI on SM ext. surf.	1	9.77	9.77	10.00	0.98	10.75
Heat pipes	1	3.00	3.00	10.00	0.30	3.30
Miscellaneous	1	1.00	1.00	10.00	0.10	1.10
SM Heaters/Sensors	1	0.49	0.49	10.00	0.05	0.54
MECHANISMS			12.40			13.07
Antenna Pointing mechanism	1	7.00	7.00	5.00	0.35	7.35
APM electronics	1	4.40	4.40	5.00	0.22	4.62
Holddowns	2	0.50	1.00	10.00	0.10	1.10
COMMS			31.40			35.22
X/X transponder	2	3.80	7.60	5.00	0.38	7.98
X-band SSPA	2	1.10	2.20	5.00	0.11	2.31
26 GHz transmitter	2	2.00	4.00	10.00	0.40	4.40
26 GHz TWTA	2	2.50	5.00	10.00	0.50	5.50
HGA	1	8.00	8.00	20.00	1.60	9.60
LGA	2	0.30	0.60	5.00	0.03	0.63
RFDU	1	4.00	4.00	20.00	0.80	4.80
DATA HANDLING			39.00			44.90
SVM computer	1	19.00	19.00	10.00	1.90	20.90
SVM Mass Memory	1	20.00	20.00	20.00	4.00	24.00
AOCS			12.70			13.34
Star Sensor	3	3.00	9.00	5.00	0.45	9.45
Gyro Assembly	2	1.45	2.90	5.00	0.15	3.05
Sun Sensor	2	0.40	0.80	5.00	0.04	0.84
PROPULSION			54.66			57.87
Monoprop Thrusters	8	0.22	1.76	5.00	0.09	1.85

Element 1 - WFI Spacecraft	Nr	Mass (kg) per unit	Total Mass (kg)	Margin (%)	Margin (kg)	Mass (kg) with Margin
Monoprop Other Dry Mass	1	11.80	11.80	5.00	0.59	12.39
Monoprop Tank	1	8.50	8.50	5.00	0.43	8.93
GAIA Cold Gas Thrusters	12	0.10	1.20	20.00	0.24	1.44
Cold Gas Tank	2	12.70	25.40	5.00	1.27	26.67
Cold Gas Feed System	1	6.00	6.00	10.00	0.60	6.60
POWER			25.67			27.97
Li-Ion Pack (18650HC) Standard AEA	1	5.40	5.40	5.00	0.27	5.67
Solar Array AsGa TJ	1	11.59	11.59	10.00	1.16	12.75
PCDU	1	8.68	8.68	10.00	0.87	9.55
HARNESS			28.33			31.17
Harness SVM	1	28.33	28.33	10.00	2.83	31.17

Table 5-24: Mass budget for service module

5.3.4 Spacecraft Mass Budget

The overall spacecraft mass budget is presented in Table 5-25. The mass drivers are primarily structural. One is the baffle mass which depends on the survey field requirement of +/- 20 deg from each pole, the orbit selection and the telescope aperture. A second driver is the overall telescope structure which depends on the optics design and telescope aperture. Also, the optics subsystem mass is significant, and again this depends mostly on the telescope aperture. It is apparent that reducing the telescope aperture and consequently the telescope diameter could lead to significant mass savings but at the cost of telescope performance.

	Total Mass (kg)	Margin (%)	Margin (kg)	Mass (kg) with Margin
Service Module	**357.51**			**406.12**
Payload Module	**999.38**			**1186.30**
TOTAL DRY	**1356.90**			**1592.42**
System Margin		20.00	317.45	318.48
TOTAL DRY + SYSTEM MARGIN				**1910.90**
Propellant	71.86	2.00	1.44	73.30
Adaptor	90.00	0.00	0.00	90.00
TOTAL WET				**2074.20**
TARGET S/C MASS AT LAUNCH				2090.00
Below mass target by				15.80

Table 5-25: Spacecraft summary mass budget

5.4 System Options

Several options for further mass reduction were also considered. An outline of these options is presented in Table 5-26.

Option	Description	Effect on s/c mass [kg]	Launch margin [kg]
Baseline			16
FEEP	SVM design only based on FEEP rather than compatible also with Cold Gas	-24	40
Smaller SVM	Service Module height reduced by 0.15m (optimal internal volume allocation)	-21	37
Survey field reduction	Survey field reduced to +-10 deg from ecliptic poles as opposed to baseline +-20 deg and baffle design reduced accordingly	-30	46
4-mirror optics	4-mirror Korsch design used rather than 5-mirror baseline	-39	54
Reduced M1 diameter	M1 diameter reduced to 2.0m from 2.15 (baseline) and telescope tube scaled accordingly	-91	107
Lunar flyby	Lunar flyby used to increase Soyuz capacity to L2, additional small dV needed for manoeuvres	+21	165

Table 5-26: Options on the baseline for mass reduction

The survey field reduction to ±10 degrees from ±20 degrees results in a decrease in Sun view angle and baffle height from 2.9m to 2.5m and a corresponding mass savings. The four mirror optics option gives a small mass advantage the baffle height would just fit in the Soyuz fairing since this configuration results in an increased M1-M2 distance. The reduced M1 diameter is a less favourable option than the others since it would mean a reduction in light gathering power of the telescope and thus in image quality. For a significant increase in available launch mass, the final option involving a lunar swingby offers the most potential even if at the cost of a small delta-V increase for navigation corrections. However, a lunar swingby would add considerable risk to the mission and the mission operations are modified and cost would need to be re-examined.

In the end, if additional margin is sought, a combination of the above measures, if not all together, can be envisaged.

5.5 Verification of Signal To Noise Ratio Requirement

The requirement of the optical performances of the camera is to enable the detection at 2.2 magnitude below the peak brightness of the Supernovae with a SNR of 5 at least.

5.5.1 The Model

A model of Signal to Noise Ratio has been initiated in order to assess the optical performances of the mission.

The first step was to set-up the model for the camera up to 1 µm, including the following inputs:

- The implemented source is Supernovae type 1-A simulated as a blackbody with emission and absorption lines, the brightness is simulated in B-band with a redshift.

- The noise taken into account in the model is composed of the electronic and photon noises, the zodiacal light and the straylight; the straylight level is considered as 1/10th of the zodiacal light and with the same spectrum.
- The simulation of the optical chain considers the area of the entrance aperture, the reflectivity of the mirrors as GAIA (silver coated mirrors), the PSF of the optics (function of the wavelength), the filters, the spectral responses like quantum efficiency and performances of the CCD and all the characteristics up to 1 µm.

The model provides the SNR values at different redshifts (z) for different magnitude below the peak brightness and the simulated image in the different bands. No margin has been taken into account in the SNT calculated.

The faintest signals from Supernovae with redshift of 1.7 are situated towards NIR. Therefore, as a second step of modelisation, the NIR part with the MCT detectors of the camera shall be established.

Moreover the optical performance of the spectrometer needs also to be assessed in further activities.

5.5.2 The Camera SNR At 1 µm

This paragraph presents different results of the camera SNR at 1 µm. All the tables use the same convention for the compliance with SNR≥5: the cells in green expresses the compliance and the ones in red the non-compliances. The criterion of 2.2 magnitudes below the peak brightness is not taken into the colour convention.

The SNR calculated for a redshift of 1 for different magnitudes below the peak brightness is presented in Table 5-27.

SNR at z=1 for following Magnitude below the peak brightness:	0	0.5	1	1.5	2	2.2
No band	176.07	108.51	66.59	42.98	27.35	22.25
Band U	4.24	2.56	1.69	1.03	0.63	0.56
Band B	31.03	20.01	12.03	7.75	5.12	4.06
Band V	64.26	40.40	24.62	16.15	9.88	8.14
Band R	122.72	79.36	49.96	31.49	19.59	16.31

Table 5-27: Camera SNR for z=1 and for different magnitudes below the peak brightness

The z=1 redshift supernovae are then detected in:

- Bands V and R up to at least 2.2 magnitude below the peak brightness
- Band B to 2 magnitude below the peak brightness.

The SNR calculated for a redshift of 1.8 for different magnitudes below the peak brightness is presented in Table 5-28.

SNR at z= 1.8 for Magnitude below the peak brightness=	0	0.5	1	1.5	2	2.2
No Band	50.88	30.23	19.24	12.43	8.19	6.28
Band U	0.2	0.13	0.08	0.05	0.03	0.03
Band B	2.87	1.84	1.15	0.72	0.45	0.38
Band V	10.12	6.25	4.01	2.52	1.58	1.34
Band R	37.65	23.91	14.89	9.34	6	5.1

Table 5-28: Camera SNR for z=1.8 and for different magnitudes below the peak brightness

The z=1.8 redshift supernovae are then detected in:

- Band R up to at least 2.2 magnitude below the peak brightness
- Bands V up to 0.5 magnitude below the peak brightness.

The SNR for magnitude of 2.2 below the peak brightness as function of the redshift (z) is presented in Table 5-29.

z	1	1.2	1.4	1.6	1.8
No Band	22.25	16.32	11.76	8.53	6.28
Band U	0.56	0.24	0.11	0.06	0.03
Band B	4.06	2.28	1.27	0.71	0.38
Band V	8.14	5.42	3.35	2.06	1.34
Band R	16.31	12.64	9.38	6.87	5.1

Table 5-29: Camera SNR for different redshifts and for different 2.2 magnitudes below the peak brightness

The supernovae with a redshift up to z=1.2 are detected at 2.2 magnitude below the peak brightness in bands V and R. Only the band R can detect the supernovae at 2.2 magnitude below the peak brightness for a redshift of 1.8.

This result is somehow promising but IR verification could not be performed within the study timeframe. At the issue of this report, it cannot be confirmed yet if the SNR requirement can be fully verified by the present WFI design.

Figure 5-8 provides an example of the image (bright central point) simulated on CCD focal plane for redshift z=1 at magnitude 0 with respect to the supernovae peak brightness. The different squares correspond to the different bands starting with U at the bottom (left when turning the sheet) of the page.

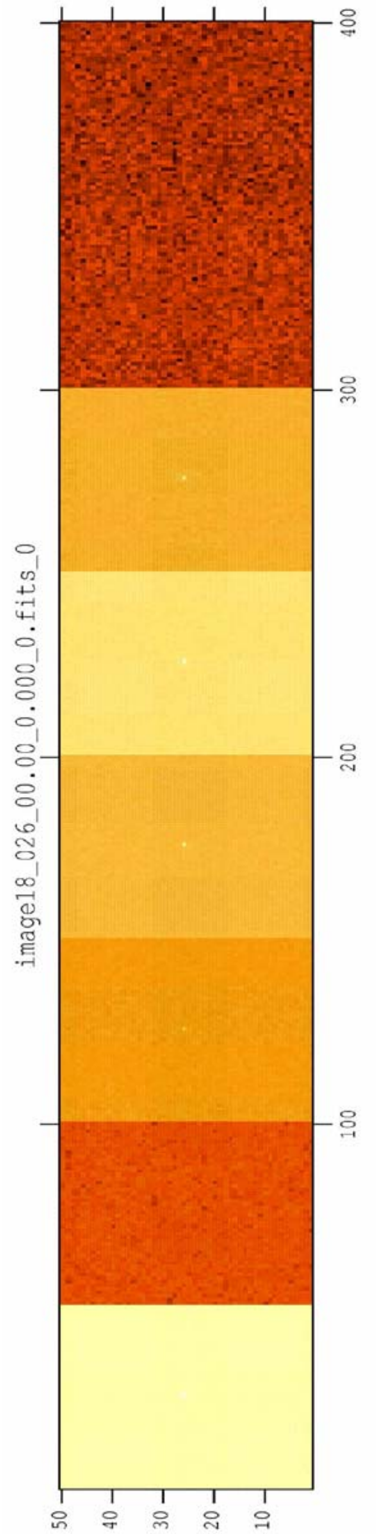

Figure 5-8: Images on CCD focal plane for z=1, magnitude 0 at SNe peak brightness, U-band on the bottom (left)

6 CONFIGURATION

6.1 Requirements and Design Drivers

The configuration has to comply with the following requirements:

- It shall fit in the fairing of the SOYUZ launcher
- It shall accommodate all equipment and instruments
- It shall provide unobstructed field of view for the telescope, sensors, antenna(s), thermal radiators and solar panels
- It shall provide access to install and service components during ground operations.

6.2 Assumptions and Trade-Offs

The initial assumption for the spacecraft is that the telescope (payload) needs to be decoupled from the SVM; hence the spacecraft configuration is divided into two functional parts:

- The Service Module [SVM]
- The Payload Module [PLM], including the 5 mirror telescope. This has been conceived as much as possible as a self-contained system with a reduced number of mechanical and electrical interfaces

6.3 Baseline Design

Figure 6-1 shows the baseline configuration for the WFI spacecraft. The functional division is shown by depicting the SVM and the PLM separately. In orbit these will be connected at the interface.

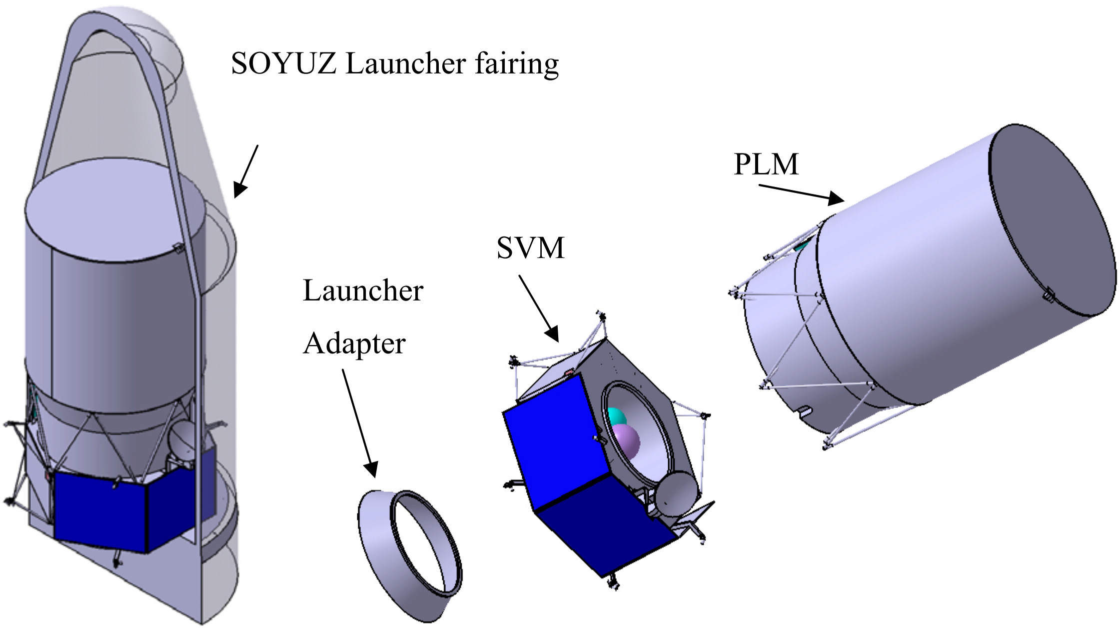

Figure 6-1: WFI baseline configuration

Figure 6-2 shows the configuration of the WFI satellite in orbit. The cover has been opened after launch and the configuration for observation is obtained.

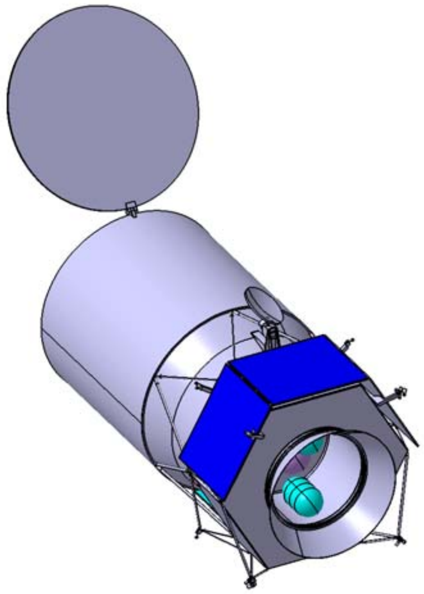

Figure 6-2: WFI In orbit configuration

In Figure 6-3 a cross section is shown with the position of the telescope mirrors inside the spacecraft. On the right is a picture of the mirrors including the actual path of the rays in the optical system to the focal surface.

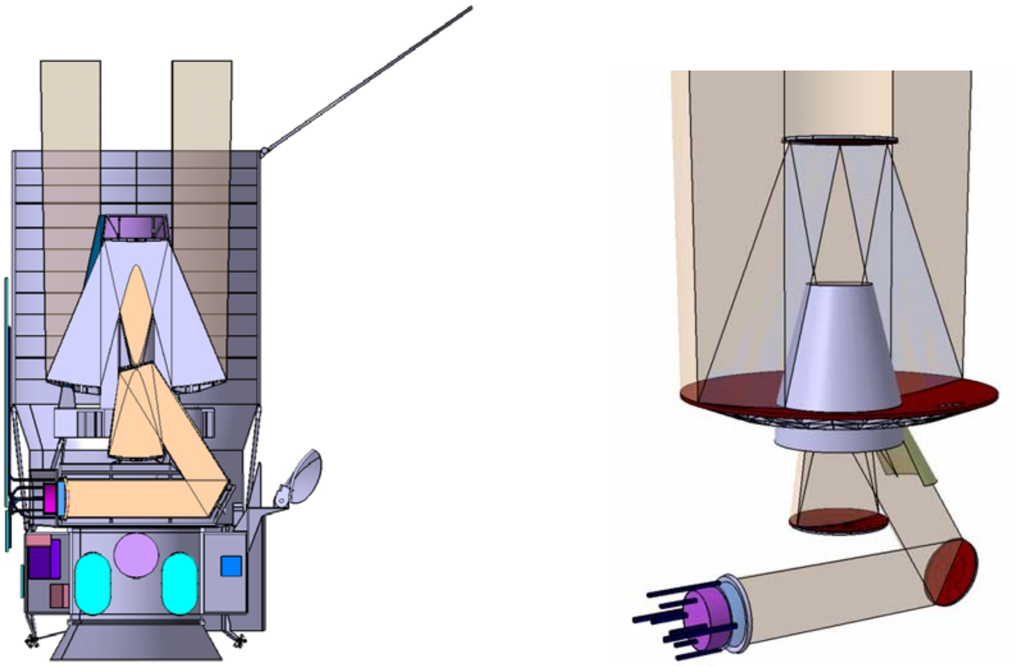

Figure 6-3: Cross section of the spacecraft (including ray-trace of the mirror)

6.3.1 PLM

An external view of the Payload Module [PLM] is shown in Figure 6-4 The Telescope is protected from the sun with a large sun-baffle. During launch the volume of the sun-baffle, containing the telescope, is closed by a lid to protect from contamination.

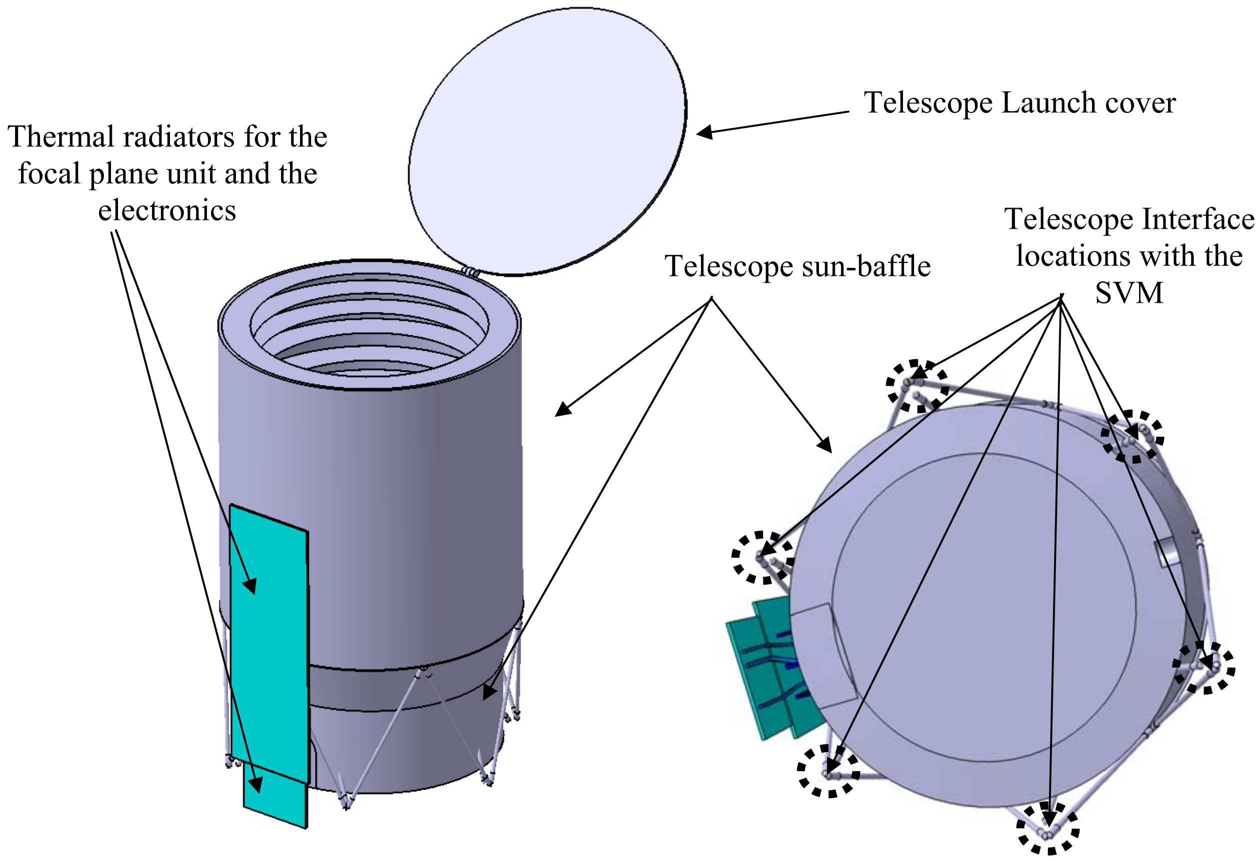

Figure 6-4: PLM external view, interface with SVM

Six interface locations are used to attach the PLM to the SVM. These interfaces are through the brackets which connect the struts from the PLM to the SVM. These struts come from two different major parts of the PLM. Six major struts support the optical bench, which connects all the mirrors and focal plane detector. Twelve smaller struts connect the sun-baffle to the SVM, which effectively decouples the sun-baffle from the optical bench of the telescope.

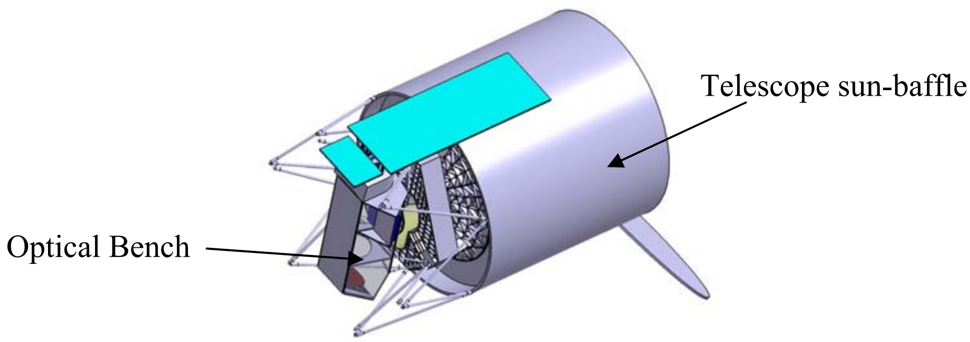

Figure 6-5: Optical bench inside the sun-baffle

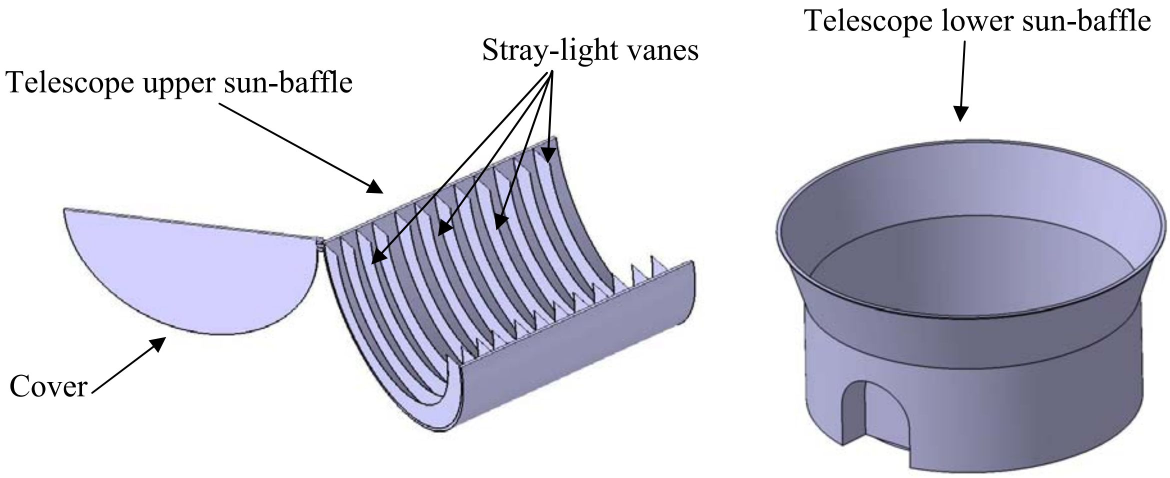

Figure 6-6: Two major parts of the sun-baffle

The sun-baffle consists of two main parts Figure 6-6. The upper sun-baffle, shown in a cut-away view, is a cylindrical shell that contains a series of vanes to reduce stray-light disturbances. The lower sun-baffle is a lightweight frame that covers the third mirror, the fifth mirror and the focal plane instruments.

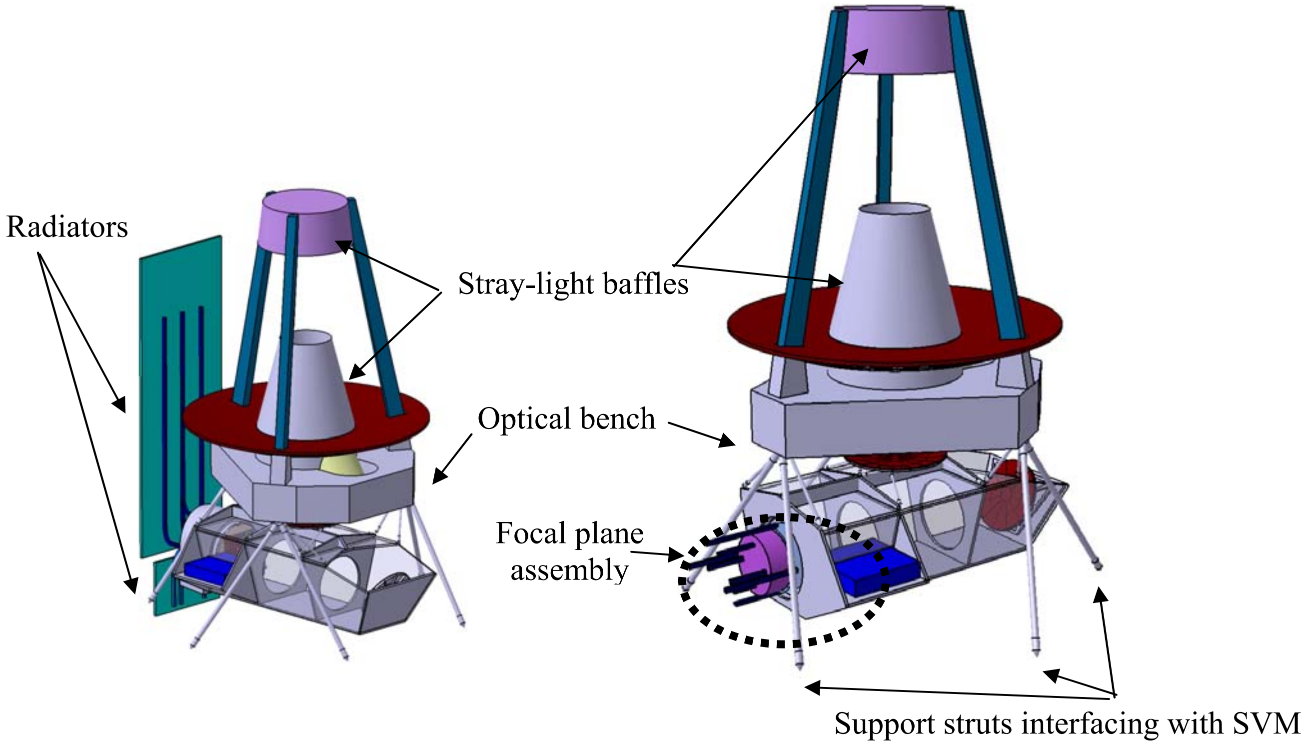

Figure 6-7: Optical bench

Figure 6-7 shows the optical bench for the telescope and mirrors with, and without the thermal radiators for the focal plane assembly. The optical bench is a large structural plate to which all the mirrors and structures interface. The focal plane assembly is shown in more detail in Figure 6-9. Additional internal baffles are shown, which are implemented to minimize the effects of stray-light between the mirrors.

While Figure 6-8 gives the breakdown of the mirrors, focal plane assembly and structure.

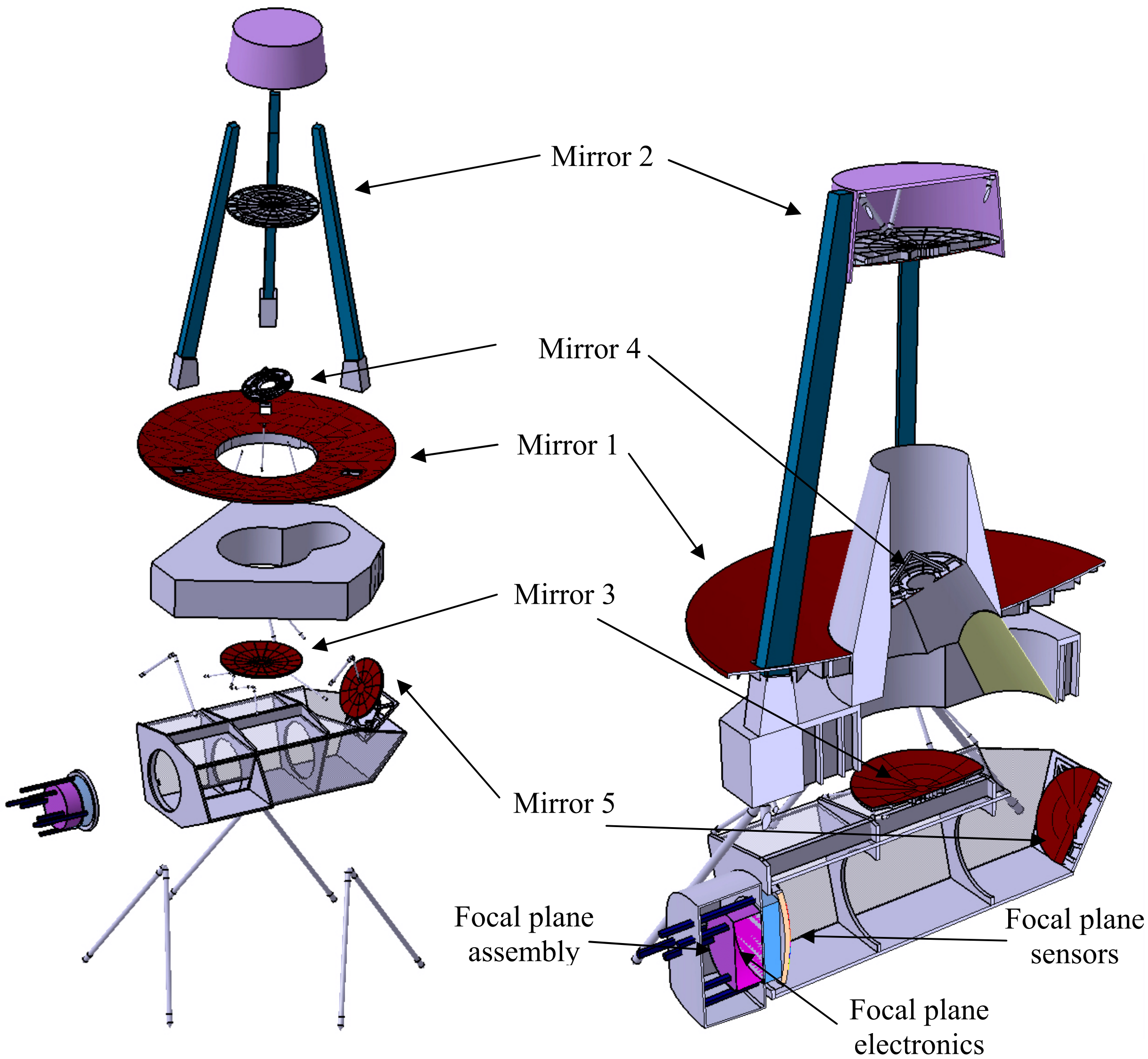

Figure 6-8: Telescope mirror and structure

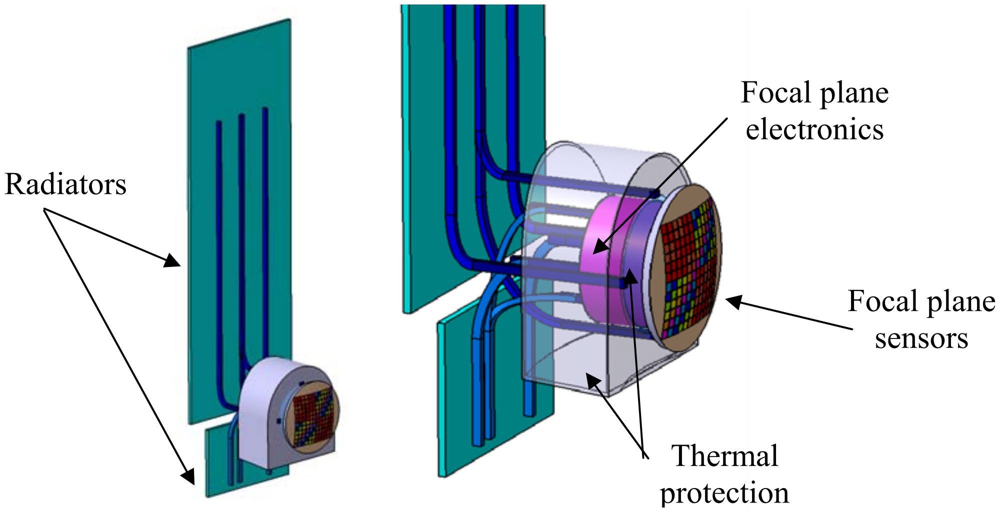

Figure 6-9: Focal plane assembly, electronics, and radiators

6.3.2 SVM

Figure 6-10 shows the SerVice Module, including major sub-systems.

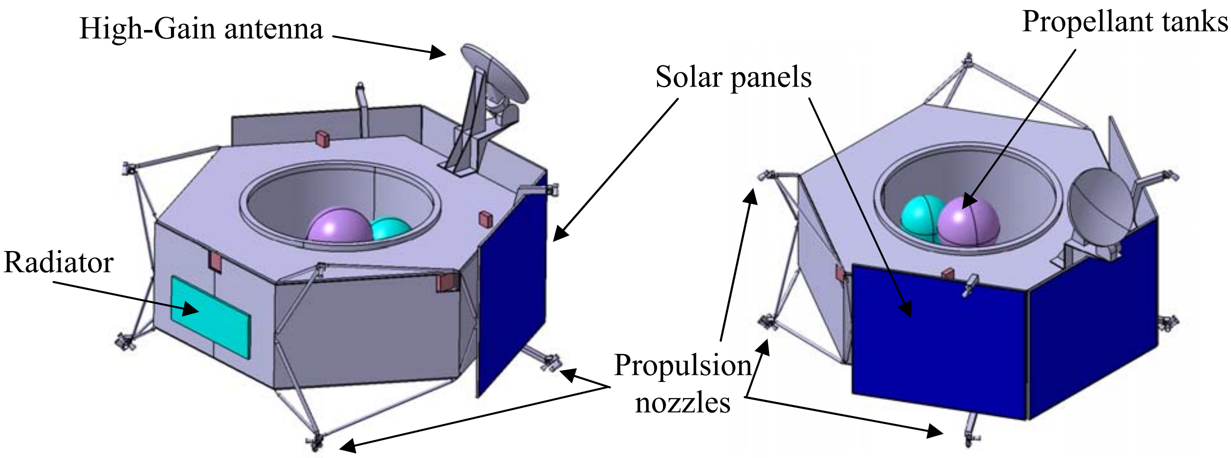

Figure 6-10: Service Module (SVM)

Inside the SVM there is sufficient volume available for all the sub-system units as can be seen in Figure 6-11. This configuration is relevant to the option with cold gas thrusters as this is the most demanding in terms of volume due to the large tanks required. The SVM size and internal structures together with the mechanical interfaces to the PLM are based on the GAIA structure.

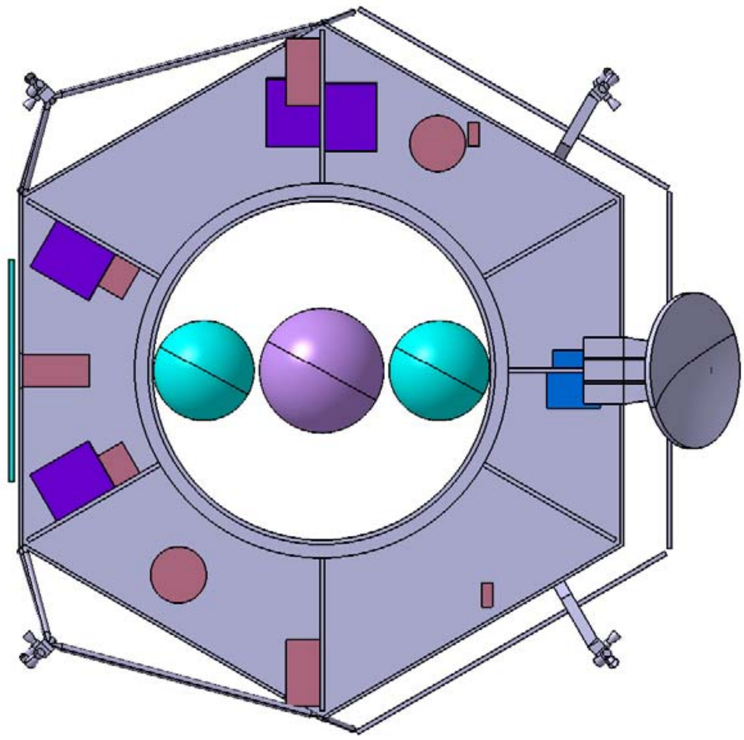

Figure 6-11: SVM top view (top panel removed)

The driver of the configuration is the body mounted solar array which is sized for a power mode with measurement and transmission at the same time. So as not to oversize the SVM dimensions, in particular the height, the solar array has been mounted on dedicated panels slightly detached from the smaller main body.

A further reduction of the SVM height is possible taking into account that some internal volume is unused.

6.4 Overall Dimensions

The overall dimensions of the WFI spacecraft are shown in Figure 6-12. From the interface with the launcher the height to the top of the sun-baffle cover (closed for launch) is 5.79 meters. The maximum width comes from the SVM (Solar panels), which measures 3.255 meters.

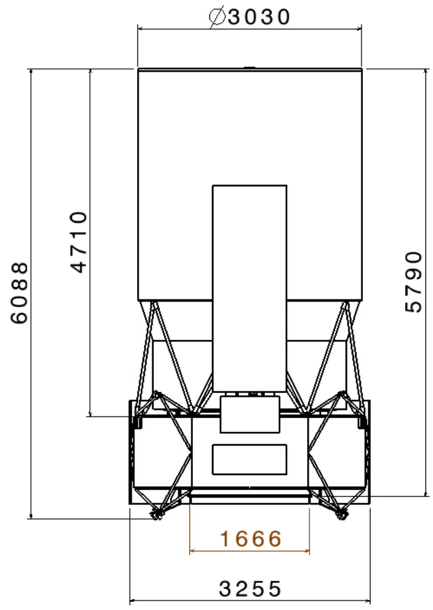

Figure 6-12: Overall dimension WFI spacecraft

6.4.1 PLM Dimensions

Figure 6-13 shows the main dimensions of the PLM. The height is measured at 4.63 meters, and the diameter is 3.03 meters.

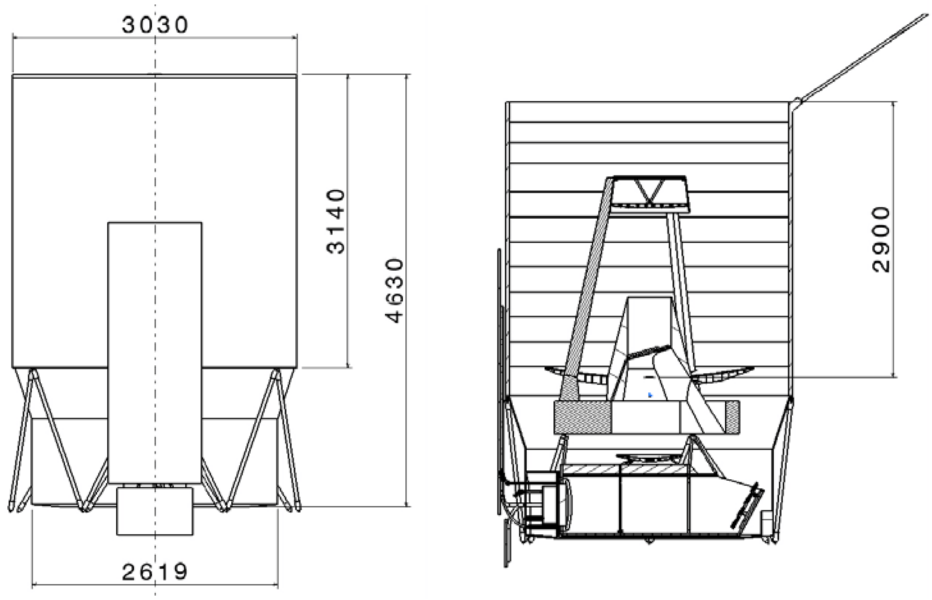

Figure 6-13: PLM dimensions

The cross-section view shows the distance between the entrance aperture and the top of the sun-baffle, which is 2.9 meters.

6.4.2 SVM Dimensions

Figure 6-14 shows the dimensions of the SVM. The main body of the SVM is a hexagon shape structure with dimensions of 2.715 x 3.135 meters and a height of 1.15 meters inspired to the main structure of the GAIA SVM. When considering the solar panels and other external parts, the overall envelope is 2.975 x 3.255 meters with a height of 1.743 meters. The High-Gain antenna has a height above the top platform of the primary structure of 1.012 meters in stowed position.

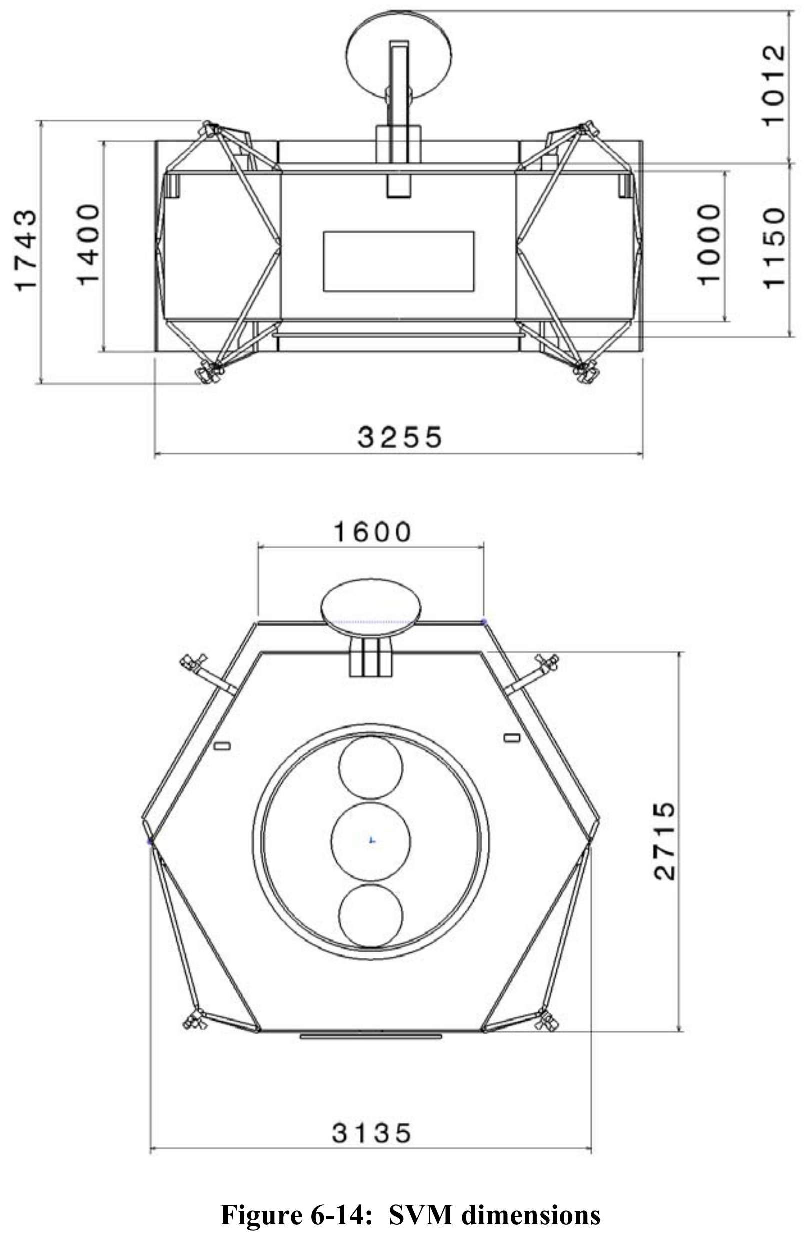

Figure 6-14: SVM dimensions

7 PAYLOAD MODULE

The content of the following chapter represents the design of the different elements of the Payload Module grouped by discipline.

Because of this arrangement, the baffle design is described under Optics, although this element belongs to the Service Module Structures.

Conversely the FGS design (part of the payload) is described under the AOCS section of the Service Module chapter.

7.1 Optics

7.1.1 Requirements and Design Drivers

Table 7-1 shows a list of the optical parameters and values.

Parameters		Value
Field Of View (FOV)		Equivalent to 1 deg^2
Focal length		20 m
Equivalent un-obscured pupil diameter		2 m
Imaging quality		Diffraction limited @1micron
Spectral Range	Visible	350nm-1000nm
	Infrared (IR)	1000nm-1800nm
Filters		Red-shifted B-band filters: 6 for the visible 3 for the IR

Table 7-1: List of optical parameters and values

The filters are placed directly on the focal surface of the telescope. Those filters with their underlying detectors are the photometric instrument ("camera").

Table 7-2 summarises the analysis of the requirements that leads to important option reduction.

Basically, the large FoV and the image quality requirements drive the optical configuration towards a multi-mirror design (at least 3 powered mirrors).

Design drivers	Consequences
Large FOV	• Off-axis configuration reflectors are excluded • One or two mirrors configuration are excluded
Pupil dimensions (2 meters)	• In front (refractive) compensators are excluded
Large spectral bandwidth	• Dioptric components are excluded : • Optical configurations using dioptric field flatteners or compensators are excluded
Limited overall dimensions	• Use of reflectors and plane mirrors to bend the optical path
Image quality diffraction limited @1 microns over all the FOV	• One or two mirrors configurations are excluded

Table 7-2: List of design drivers and consequences

7.1.2 Telescope Trade-Off

Due to the above design drivers in Table 7-2, configurations with one or two powered mirrors only are excluded as the achievable image quality does not fulfil the requirements.

Two different concepts for the telescope are proposed. Both have an intermediary image between the secondary and the tertiary reflector and the exit pupil of the system is easily accessible.

The first solution is a re-scaling of the original design proposed by D.Korsch (RD[12]). The second solution is original and requires some additional work on the mechanical structure.

7.1.2.1 Trade-off criteria

The following trade-off criteria were applied:

- *Focal surface complexity*: The sensors pattern shall respect the following constraints:
  - Each point in the FOV will be imaged on every filters (visible and IR) during the scanning
  - All detectors shall be implemented on the focal surface
  - No filter wheel shall be used
- *Mass*: the reflector mass is estimated assuming a 50 kg/m^2 surface density except for the primary mirror, for which the mass density is 51.5 kg/m^2. Those values assume light weight SiC reflectors
- *Reflectors manufacturing*: Two criteria are defined. The first is the sagital departure of the surface from the best fit sphere during manufacturing. The second is the slope departure of the surface from the best fit sphere
- *Overall volume*: The volume of the telescope will be determined and compared with the Fregat's fairing dimensions
- *Mechanical structure*: The complexity of manufacturing and integration of the telescope structure will drive the choice of the optical concept
- *Straylight baffling*
- *Sensitivity to alignment*: The sensitivity to alignment drives the design of the mechanical structure of the payload
- *Scanning efficiency*: The scanning duration for the two telescope options (see Chapter 5)

7.1.3 Option 1: 4 Mirror Configuration

7.1.3.1 Optical layout

The optical layout of option 1 is as shown in Figure 7-1 and Table 7-3, Table 7-4.

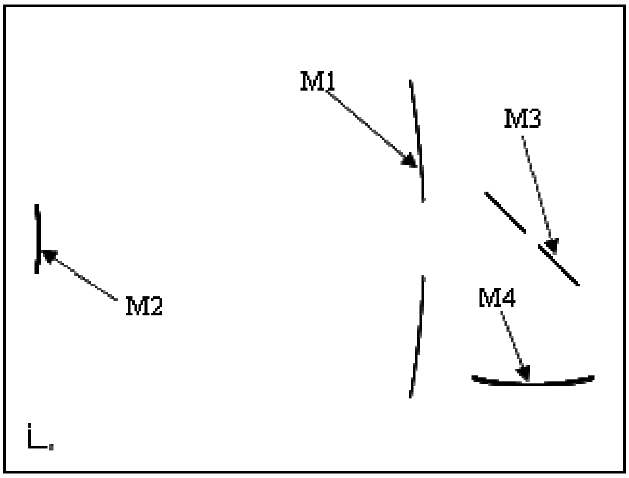

Figure 7-1: Numbering of reflectors

		M1	M2	M3	M4
Radius of curvature (mm)		5812.64 cc	1212.53 cx	Infinity	1511.74 cc
Aspheric definition	K	-0.9759565	-1.878873	0	-0.5648871
	A	0	0	0	0
	B	0	0	0	0
	C	0	0	0	0
	D	0	0	0	0
Useful optical Dimensions (mm)		∅2000	∅409.34	820×580	∅790.18
Comments		Obscuration is 23.5%		Obscuration is 200×150 mm^2 diameter	

Table 7-3: Definition of reflectors

Distances (mm)				Tilt X (degrees)
M1-M2	M2-M3	M3-M4	M4-Focal surface	M3
2412.81	3096.81	903.19	1723.33	45

Table 7-4: Relative position of reflectors

The distances and tilt M_i-M_{i+1} are expressed wrt the local frame of M_i.

The aspheric surfaces are defined as described in Figure 7-2

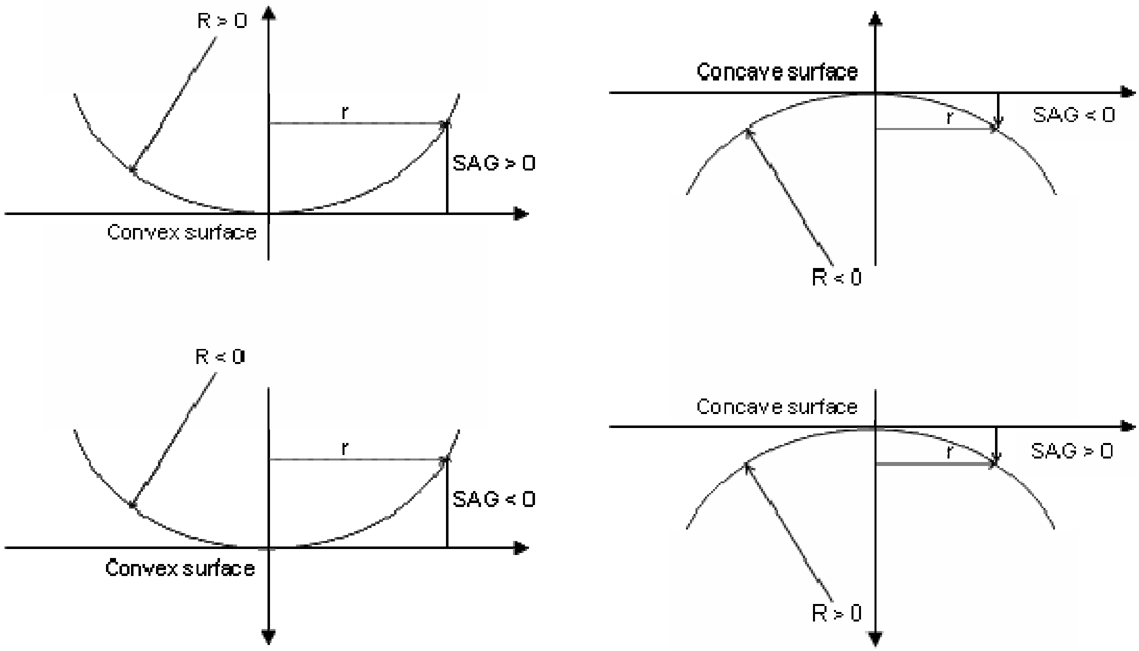

Figure 7-2: Sign convention in Zemax

The definition used is the one defined by the software ZEMAX. The convention for the signs is explained in Figure 7-2. The equation of an even aspheric surface is the following:

$$SAG = \frac{r^2}{R \times \left[1 + \sqrt{1 - (1+k) \times \left(\frac{r}{R} \right)^2} \right]} + Ar^2 + Br^4 + Cr^6 + Dr^8$$

The SAG is defined for a surface with its vertex at the origin. R is the radius of curvature of the surface, k the conic constant and A, B, C, D the generalised coefficients of aspherisation.

Figure 7-3 shows the light path through the optical layout for Option 1.

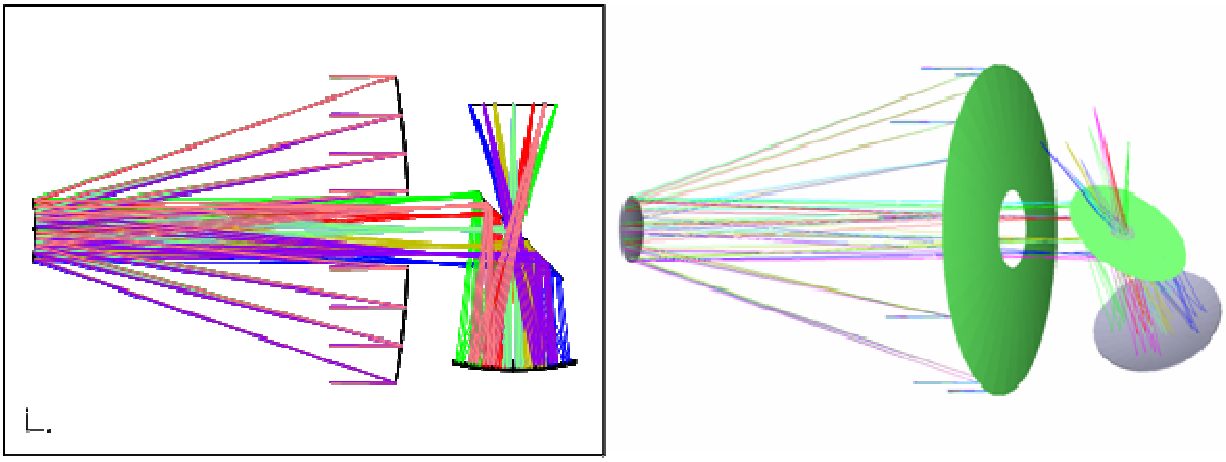

Figure 7-3: Schematic of optical layout for Option 1

The main advantages are:

- An easily accessible intermediary image
- An accessible exit pupil
- A flat focal surface

The stray light baffling can be easily done with a field stop placed at the intermediary image plane. Furthermore, since the folding mirror is placed on the exit pupil, only the rays within the field of view of the telescope can reach the focal surface.

The main drawbacks are:

- A large tertiary mirror
- An annular field of view
- A large M1 – M2 distance (long telescope)

All the data dealing with the reflectors position (tilt, decentres) and distances are given in the local reference frame.

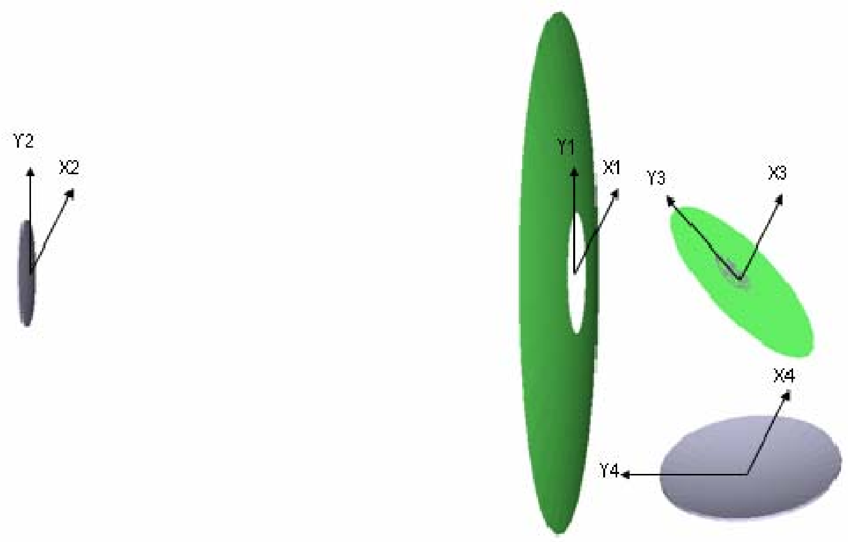

Figure 7-4: Description of the local coordinates for all reflectors

The axis Y3 is tilted by 45 degrees wrt to Y2 around X3.

7.1.3.2 Optical characteristics

Option 1 has the following FoV performance:

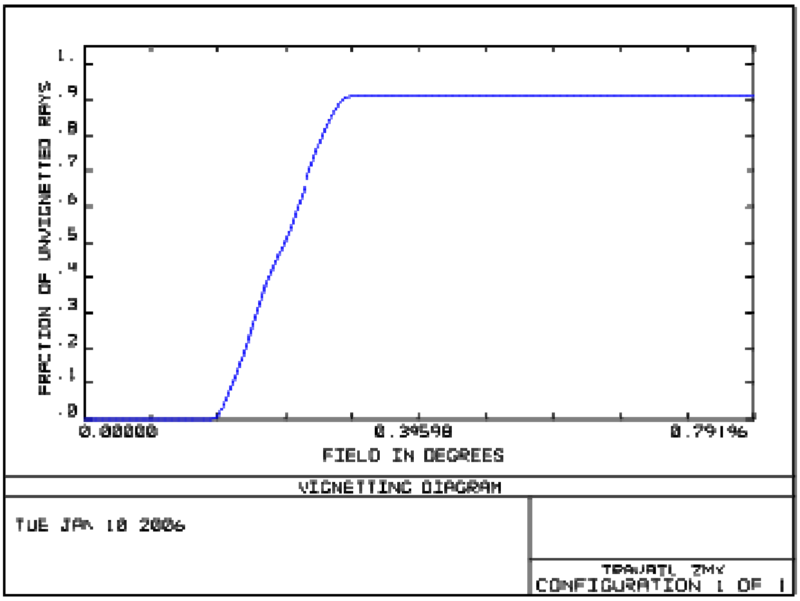

Figure 7-5: Vignetting of the FOV

As shown in Figure 7-5, the minimum vignetting is obtained for an angle of 0.317 degrees corresponding to a diameter of 110.66 mm on the focal plane.

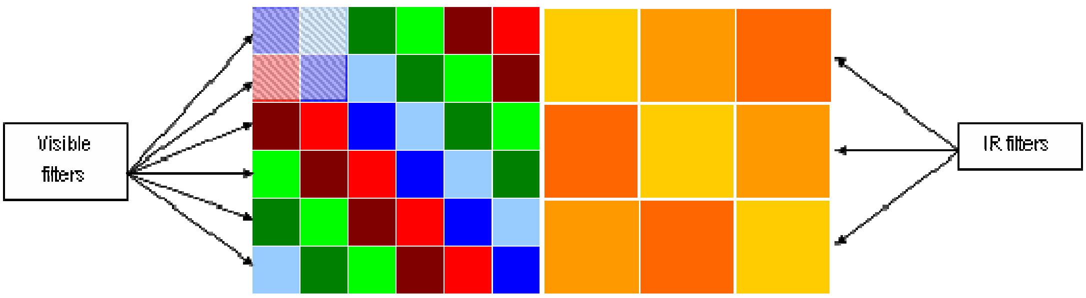

Figure 7-6: Geometry of the two photometric channels

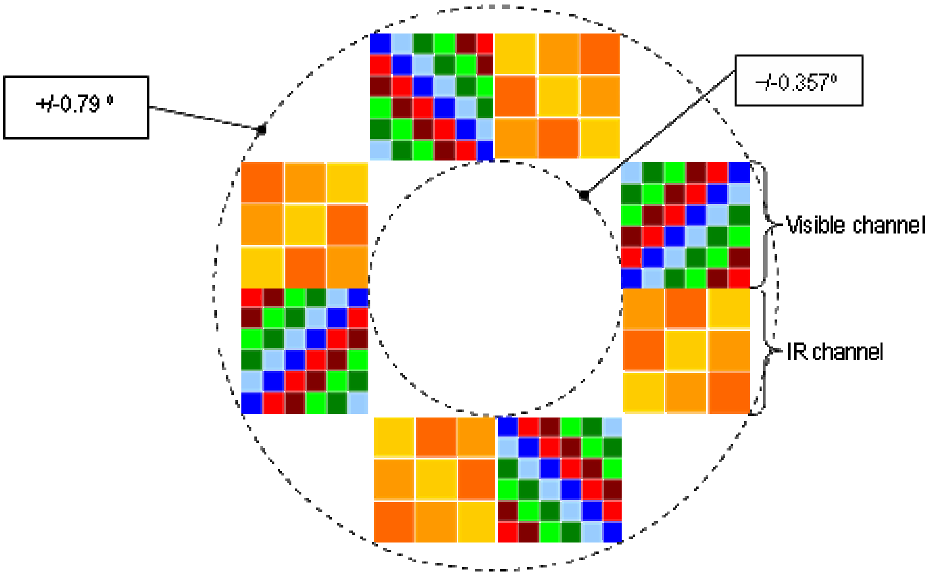

Figure 7-7: Filters pattern on the telescope focal surface

The pattern of the sensors Figure 7-6 and Figure 7-7 on the focal plane is driven by the shape of the FOV. Since the FOV is annular, the detectors cannot cover the entire FOV. On an annulus four distinct rectangular areas can be used without overlapping (see Figure 7-7).

To avoid filters with large dimensions, each area will include visible and IR channel (see Figure 7-6).

The angular area equivalent covered by the 4 areas described above is given by:

$$Area = \frac{8}{5} \times FOV^2$$

The necessary FOV in order to cover a 1 deg^2 area is then ±0.791 degrees. The FOV actually used is an annulus between 0.36 and 0.791 degrees.

7.1.3.3 Image quality

Figure 7-8 and Figure 7-9 are related to the image quality of option 1.

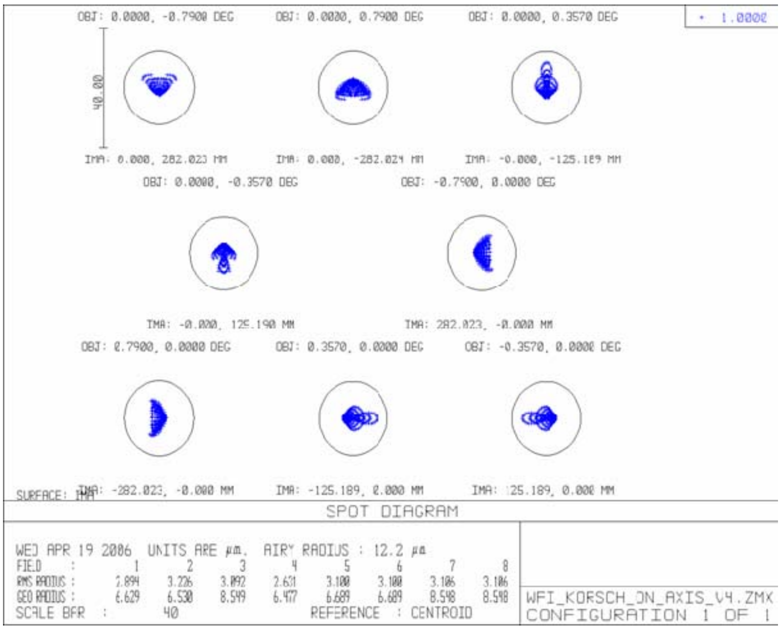

Figure 7-8: Spot diagram over the whole FOV

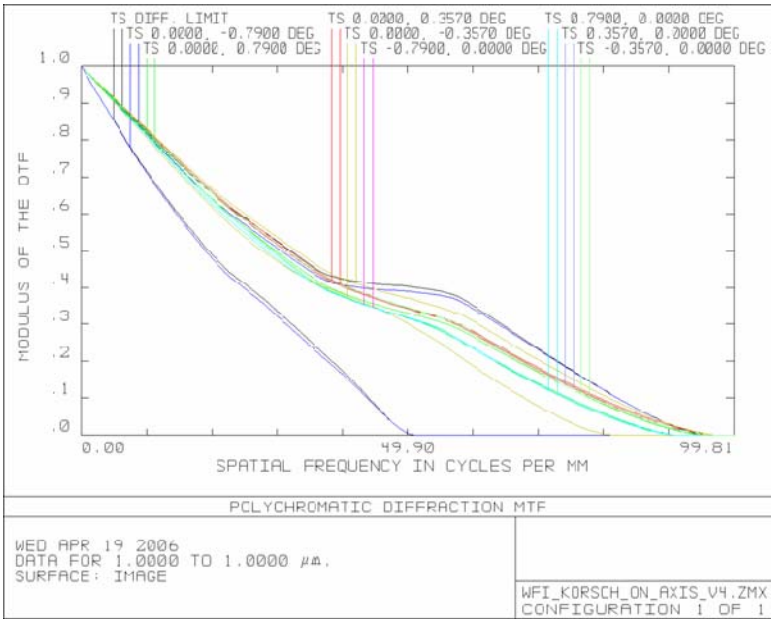

Figure 7-9: MTF

The Airy disk diameter is shown on the spot diagram. The nominal system is limited by diffraction at λ=1 micron over the entire FOV.

The maximum distortion is 2.3% at the edge of the FOV.

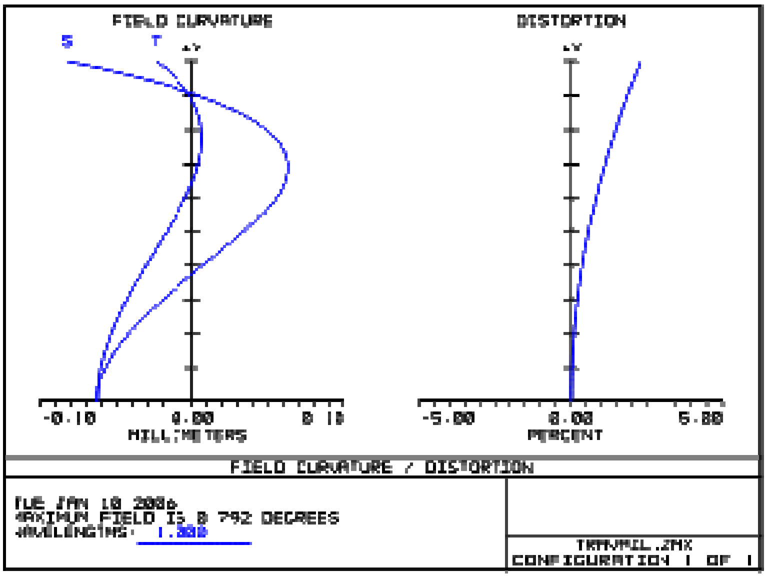

Figure 7-10: Distortion over the focal surface

The optimised focal length is 20 000 mm.

The focal surface is plane. The image plane is a 534 mm radius circle.

7.1.3.4 Mass

The mirror mass is calculated is performed assuming that all the reflectors are made of SiC.

	Dimensions (mm)	**Obscuration (mm)**	**Area (m^2)**	**Weight (kg)**
M1	∅2000	∅469	2.98	153.5
M2	∅409.34	0	0.131	6.55
M3	820×580	200×150	0.35	17.5
M4	∅757.66	0	0.454	22.7
			Total =	**200.22**

Table 7-5: Reflectors mass budget

7.1.3.5 Alignment sensitivity

Table 7-6 shows the tolerances obtained for a change of 10% in the WFE wrt to the nominal theoretical performances.

The configuration is sensitive to distance change between the elements but also to shape change of the powered reflectors (M1, M2, M4). Refocusing capabilities has to be foreseen on M2. Indeed the distance M1-M2 is one of the most sensitive parameter.

Min	Max	Units	
			Reflectors shape
-1.46E-03	1.03E-03	Millimeters	M1
-1.57E-03	2.23E-03	Millimeters	M2
-2.00E+00	2.00E+00	Fringes	M3
-9.09E-03	1.28E-02	Millimeters	M4
			Reflectors Z position
-5.16E-04	7.32E-04	Millimeters	M1
-4.98E-04	7.07E-04	Millimeters	M2
-1.43E-02	1.02E-02	Millimeters	M3
-8.97E-03	1.26E-02	Millimeters	M4
-3.32E-02	2.35E-02	Millimeters	Focal plane
			Reflectors decenters and tilt
			M1
-8.82E-03	8.82E-03	Millimeters	Dec X
-8.82E-03	8.82E-03	Millimeters	Dec Y
-1.69E-04	1.69E-04	Degrees	Tilt X
-1.69E-04	1.69E-04	Degrees	Tilt Y
			M2
-8.90E-03	8.90E-03	Millimeters	Dec X
-8.90E-03	8.90E-03	Millimeters	Dec Y
-6.60E-04	6.60E-04	Degrees	Tilt X
-6.60E-04	6.60E-04	Degrees	Tilt Y
			M3
-1.52E-03	1.52E-03	Degrees	Tilt X
-2.15E-03	2.15E-03	Degrees	Tilt Y
			M4
-1.49E-01	1.49E-01	Millimeters	Dec X
-1.49E-01	1.49E-01	Millimeters	Dec Y
-2.85E-03	2.85E-03	Degrees	Tilt X
-2.85E-03	2.85E-03	Degrees	Tilt Y
			Focal surface
-5.00E-01	5.00E-01	Millimeters	Dec X
-5.00E-01	5.00E-01	Millimeters	Dec Y
-1.13E-02	1.13E-02	Degrees	Tilt X
-1.13E-02	1.13E-02	Degrees	Tilt Y

Table 7-6: Sensitivity table

7.1.4 Option 2: 5 Mirror Configuration

7.1.4.1 Optical layout

Figure 7-11 gives the reflector numbering and Table 7-7 and Table 7-8 gives the definition and relative positions of the reflectors.

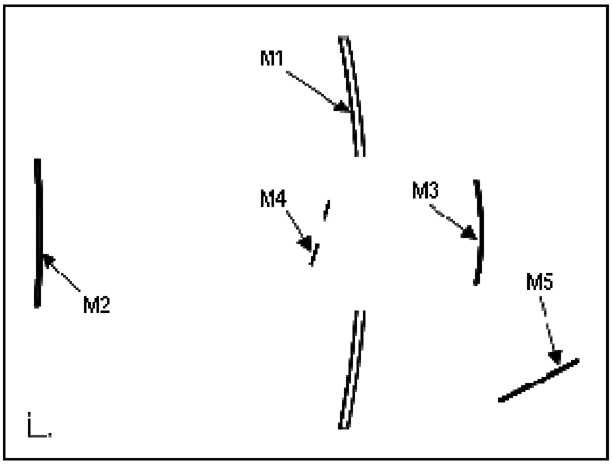

Figure 7-11: Reflectors numbering

		M1	M2	M3	M4	M5
Radius of curvature (mm)		5398.672 cc	4460.866 cx	1497.542 cc	Infinity	Infinity
Aspheric definition	K	-0.792278	0	0	0	0
	A	0	-3.009853e-10	-6.135674e-4	0	0
	B	5.810543e-14	1.466381e-11	-4.44745e-11	0	0
	C	0	-3.676956e-18	-9.172888e-18	0	0
	D	0	1.322922e-24	0	0	0
Useful optical Diameter (mm)		∅2200	∅814	∅694	Semi-major axis = 220 Semi-minor axis = 211	Semi-major axis = 262 Semi-minor axis = 230
Comments		Obscuration ∅880mm			Obscuration: Semi-major axis = 71mm Semi-minor axis = 66mm	

Table 7-7: Definition of reflectors

Distances (mm)					Tilt X (degrees)	
M1-M2	M2-M3	M3-M4	M4-M5	M5-Focal surface	M4	M5
1787.76591	2639.511	1101.745	1887.626	1820.611	16	29

Table 7-8: Relative position of reflectors

The distances M_i-M_{i+1} are expressed wrt the local frame of M_i.

The tilts of Mi are expressed wrt the local frame of M_{i-1}.

Figure 7-12 shows the light path through the optical layout for option 2.

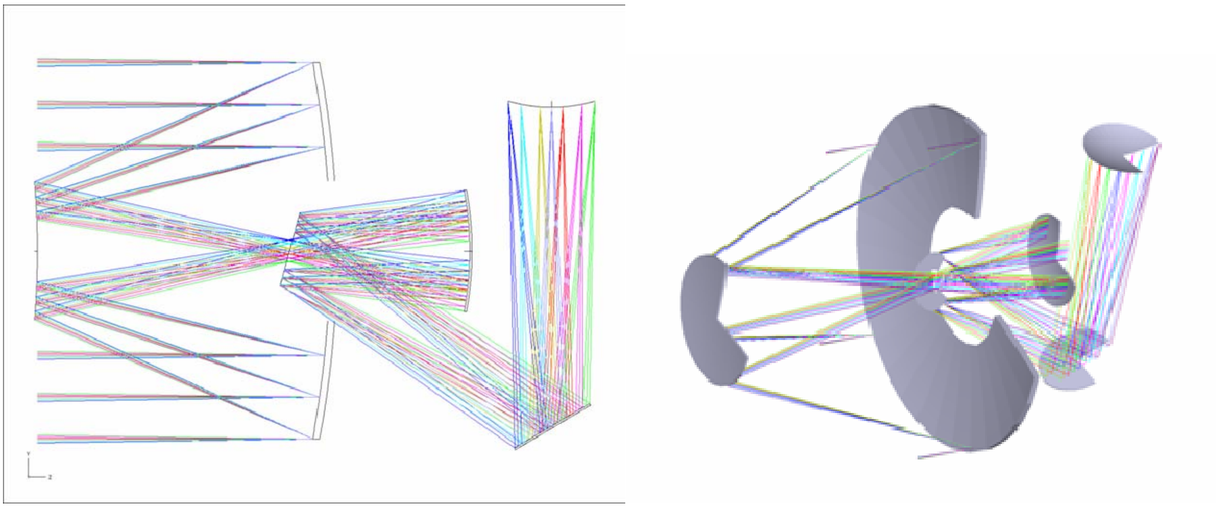

Figure 7-12: Option 2 configuration layout

The originality of this solution lies in the position of the image pupil: on the intermediary image plane. The exit pupil is also the field stop of the telescope.

The main assets are:

- An unobscured field of view
- An easily accessible intermediary image
- An easily accessible intermediary image pupil

The main drawbacks are:

- A large obscuration of the primary reflector. To obtain an area equivalent to a 2m entrance pupil, the primary needs to be oversized.
- A large secondary reflector
- A curved focal surface

All the data dealing with the reflectors position (tilt, decentres) and distances are given in the local reference frame.

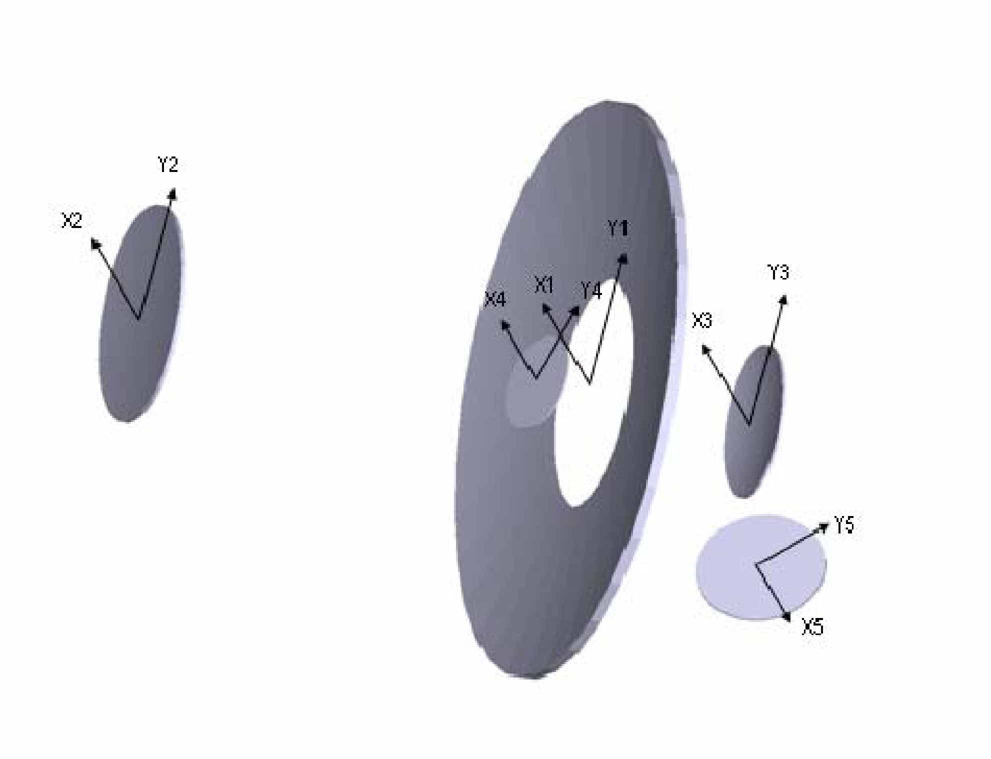

Figure 7-13: Local coordinates system overview

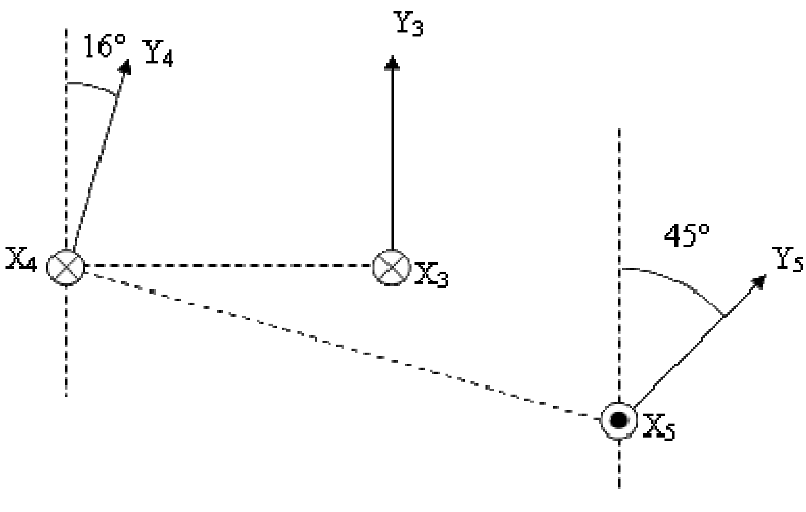

Figure 7-14: Tilt of M4 and M5 local referential

7.1.4.2 Optical characteristics

The field of view and detector architecture is shown in Figure 7-15.

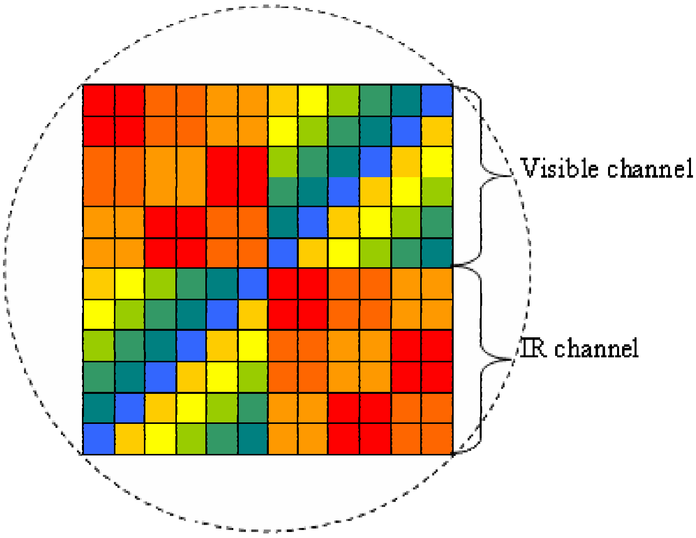

Figure 7-15: FOV and detector architecture

In this configuration, the FOV is not vignetted and the entire focal surface can be covered by filters.

The equivalent angular area is then given by:

$$Area = 2 \times FOV^2$$

A FOV = ±0.75 degrees is enough to fulfil the requirement of 1 deg^2 with margins.

The Visible channel is composed of 2x6x6 = 72 filters. The IR channel is composed of 2x6x6 = 72 filters. All the filters have the same size and a single detector underlies one filter.

This architecture ensures redundancy of data in the IR channel in one single scanning.

7.1.4.3 Image quality

Figure 7-16 and Figure 7-17 are related to the image quality of option 2.

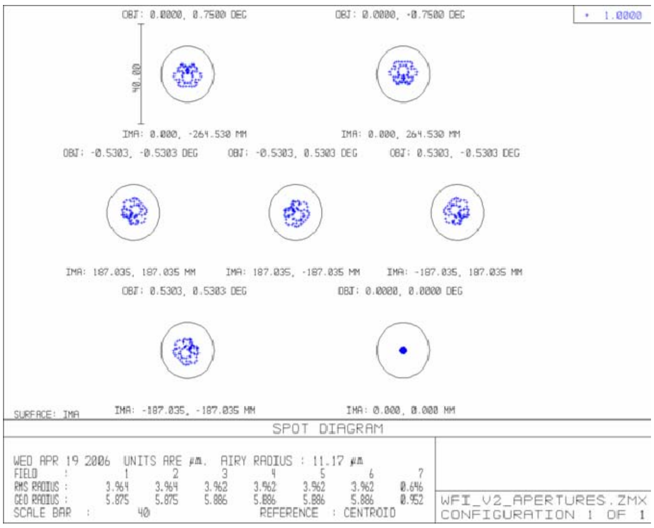

Figure 7-16: Spot diagram for option 2 over the entire FOV = ±0.75 degrees

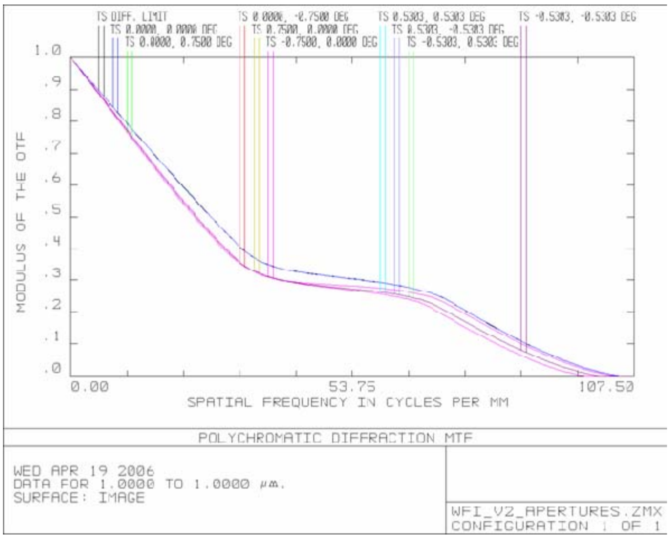

Figure 7-17: MTF for option 2

The Airy disk diameter is shown on Figure 7-16. The nominal system is limited by diffraction at λ=1 micron over the entire FOV.

Figure 7-18 shows the distortion for option 2.

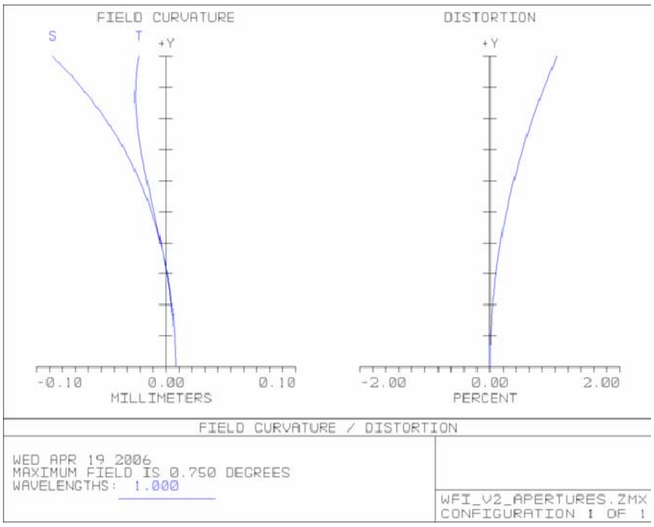

Figure 7-18: Field curvature and distortion – Option 2

The distortion is 1.03% at the edge of the FOV = ±0.75 degrees.

The focal length is 20 000mm.

The optimum focal surface is convex wrt the incident light and has the following characteristics:

- Radius of curvature : 962.349 mm
- Conic constant : -1.735079

7.1.4.4 Mass

The weight calculation is performed assuming that the reflectors are made of SiC.

	Dimensions (mm)	Obscuration (mm)	Area (m^2)	Weight (kg)
M1	∅2150	∅880	3.201	165
M2	∅814	0	0.43	21.5
M3	∅694	0	0.105	5.25
M4	½ major axis = 220 ½ minor axis = 211	½ major axis = 71 ½ minor axis = 66	0.131	6.55
M5	½ major axis = 262 ½ minor axis = 230	0	0.189	9.45
			Total =	**207.75**

Table 7-9: Reflectors mass budget

7.1.4.5 Alignment sensitivity

Table 7-10 shows the tolerances obtained for a change of 10% in the WFE wrt to the nominal theoretical performances.

The configuration is sensitive to distance change between the elements but also to shape change of the powered reflectors (M1, M2, M4). Refocusing capabilities has to be foreseen on M2. Indeed the distance M1-M2 is one of the most sensitive parameter.

Min	Max	Units	Comments
			MIRRORS SHAPE TOLERANCES
-1.13E-03	7.15E-04	Millimeters	M1
-4.21E-03	6.57E-03	Millimeters	M2
-1.46E-03	9.02E-04	Millimeters	M3
-5.48E-02	3.41E-02	Fringes	M4
-1.42E-01	2.28E-01	Fringes	M5
			Reflectors Z position
-3.58E-04	5.64E-04	Millimeters	M1
-2.64E-04	4.16E-04	Millimeters	M2
-1.51E-03	9.58E-04	Millimeters	M3
-9.76E-03	1.56E-02	Millimeters	M4
-1.71E-02	1.07E-02	Millimeters	M5
-1.88E-02	3.01E-02	Millimeters	Focal surface
			M1 POSITION TOLERANCES
-5.81E-03	5.82E-03	Millimeters	Dec X
-5.81E-03	5.82E-03	Millimeters	Dec Y
-1.14E-04	1.14E-04	Degrees	Tilt X
-1.14E-04	1.14E-04	Degrees	Tilt Y
			M2 POSITION TOLERANCES
-7.95E-03	7.95E-03	Millimeters	Dec X
-7.95E-03	7.95E-03	Millimeters	Dec Y
-1.99E-04	1.99E-04	Degrees	Tilt X
-1.99E-04	1.99E-04	Degrees	Tilt Y
			M3 POSITION TOLERANCES
-2.15E-02	2.15E-02	Millimeters	Dec X
-2.15E-02	2.15E-02	Millimeters	Dec Y
-9.82E-04	9.82E-04	Degrees	Tilt X
-9.82E-04	9.82E-04	Degrees	Tilt Y
			M4 POSITION TOLERANCES
-1.08E-03	1.08E-03	Degrees	Tilt X
-1.08E-03	1.08E-03	Degrees	Tilt Y
			M5 POSITION TOLERANCES
-1.80E-03	1.80E-03	Degrees	Tilt X
-2.05E-03	2.05E-03	Degrees	Tilt Y
			FOCAL SURFACE POSITION TOLERANCES
-1.78E-01	1.78E-01	Millimeters	Dec X
-1.78E-01	1.78E-01	Millimeters	Dec Y
-1.00E-02	1.00E-02	Degrees	Tilt X
-1.00E-02	1.00E-02	Degrees	Tilt Y

Table 7-10: Sensitivity table

7.1.5 Optical Payload Configuration Trade-Off

A trade-off between the two options has been performed. The results of the trade-off are reported in the Systems Chapter. Here only the scanning efficiency is described in detail. The selected baseline is option two.

7.1.5.1 Scanning duration

To assess the scanning duration for both options, consider the time spent in each configuration to scan a 10 degrees long stripe in the sky. This time length is directly linked to the scanning duration of one IR filter and also to the telescope FOV expressed in degrees.

The parameters for both configurations are as follows:

	Scanning duration (T)	Scanning duration for a single IR filter (t)	IR filter FOV (α)	Telescope FOV (FOV)	Number of sub-frames per filter (N)	Scanning velocity (V)
Option 1	$T_1 = \left(\frac{10}{FOV_1} \times 3\sqrt{5} + 12\right) \times t_1$	t1	$\alpha_1 = \frac{FOV_1}{3\sqrt{5}}$	FOV_1	$N_1 = \frac{t_1}{\tau}$	$V_1 = \frac{\alpha_1}{t_1}$
Option 2	$T_2 = \left(\frac{60}{FOV_2\sqrt{2}} + 6\right) \times t_2$	t2	$\alpha_2 = \frac{FOV_2}{6}\sqrt{2}$	FOV_2	$N_2 = \frac{t_2}{\tau}$	$V_2 = \frac{\alpha_2}{t_2}$

Table 7-11: Parameters for scanning duration for both options

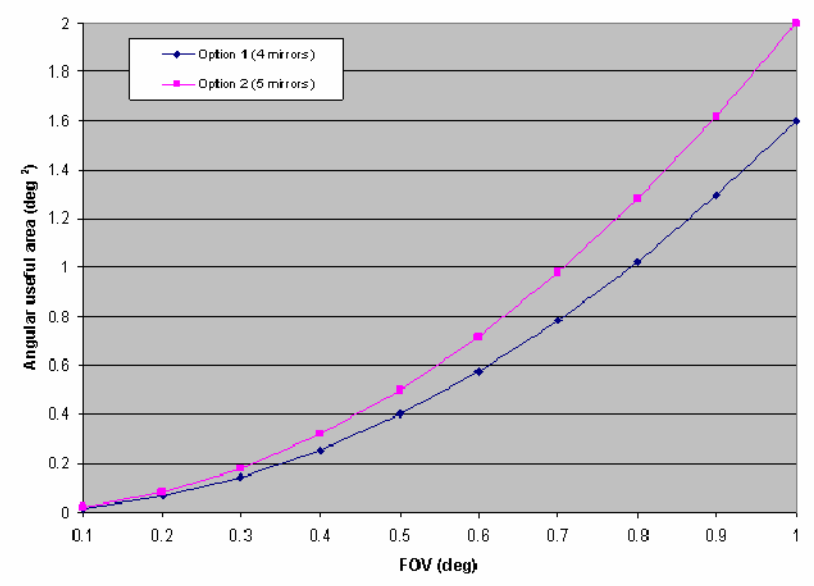

Figure 7-19: Angular area versus FOV for both configurations

Figure 7-19 shows that the requirement of 1 deg^2 can not be met at the same time for both configurations with the same FOV. In option 1 the minimum FOV is ±0.79 degrees, in option 2 the minimum FOV is ±0.71 degrees.

In that case we have: $T_1/T_2 = 1.472 \times t_1/t_2$. Thus the scanning duration will be the same in both configuration only if $t_1/t_2 = 0.679$.

Three different cases have been analysed:

1. same scanning velocity for both configurations
2. same number of sub-frames for both configurations
3. same scanning duration for both configurations

7.1.5.1.1 Equal scanning velocity for both options

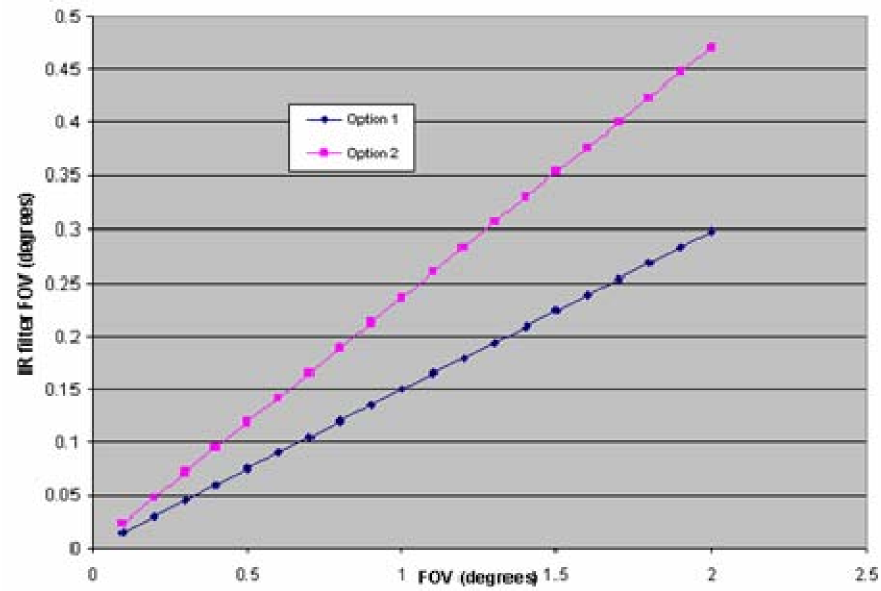

Figure 7-20: IR filter FOV versus telescope FOV

The angle α covered by a single filter (visible or IR) is smaller in option 1 than in option 2. The Figure 7-20 shows the FOV of one IR filter wrt to the telescope FOV.

If one considers that in both configurations the scanning velocity V is the same, the ratio t_1/t_2 is equal to $\alpha_1/\alpha_2 = 0.7$ with the values $FOV_1 = \pm 0.79$ degrees and $FOV_2 = \pm 0.71$ degrees.

Thus $T_1/T_2 = 1.03$. Option 1 is then almost equivalent to option 2 in terms of scanning duration but the number of images per filter (or sub-frames) is lower. The ratio of sub-frames number is $N_1/N_2 = \alpha_1/\alpha_2 = 0.7$. Since the Signal to Noise Ratio (SNR) changes as $\sqrt{N}$, the detection of faint objects with option 1 will be less efficient than in option 2: $SNR_1/SNR_2 = 0.84$.

7.1.5.1.2 Equal number of sub-frames in both options

A same number of sub-frames imply the same efficiency of detection for both options.

We assume that the time required for the acquisition of one sub-frame is the same in both options. In that case $t_1/t_2 = 1$ thus $T_1/T_2 = 1.472$.

The scanning duration in option 2 is lower than in option 1 with the same data quality.

7.1.5.1.3 Equal scanning duration

If we have $T_1/T_2 = 1$, then $t_1/t_2 = N_1/N_2 = 0.679$. The SNR ratio is then $SNR_1/SNR_2 = 0.82$.

In the case that $T_1/T_2 < 1$, we have $SNR_1/SNR_2 < 0.82$. Thus the minimum loss in terms of SNR wrt option 2 is 18%.

7.1.5.1.4 Conclusion

The scanning duration in option 1 can be lower than in option 2 but at the cost of detection efficiency of fainter objects. While, for the same detection capabilities, option 2 is clearly the most efficient configuration since the 10 degrees long stripe is scanned in a shorter time length. The actual gain in terms of scanning duration of option 2 wrt option 1 is:

$$\left.\begin{array}{l} FOV_1 = \pm 0.79 \text{ degrees} \\ FOV_2 = \pm 0.75 \text{ degrees} \end{array}\right\} \Rightarrow \frac{T_2}{T_1} = 0.65 \text{ thus } 35\% \text{ of gain}$$

7.1.5.2 Baffle length

As the distance M1-M2 is longer in option 1, this will require a longer baffle. This has a direct impact on the accommodation in the launcher fairing. The baffle in option 2 will be 0.6 meter shorter than in option 1 which is quite important in view of the limited space in the Soyuz-Fregat fairing.

As this trade-off may be re-opened in future project phases, in the present study the overall design has been such that both configurations can be accommodated.

7.1.6 Baseline Design

7.1.6.1 Secondary mirror compensation capabilities

As shown above, compensation capabilities are needed. A study on the best strategy has shown that the most efficient way to compensate for any perturbation of the imaging quality is refocusing of M2 combined with tilts around the axis Y_2 and X_2.

7.1.6.2 Reflectors

7.1.6.2.1 Geometry

Hereafter only the reflectors aperture geometry will be described.

The aperture values are given in the local coordinates of the reflector.

- M1

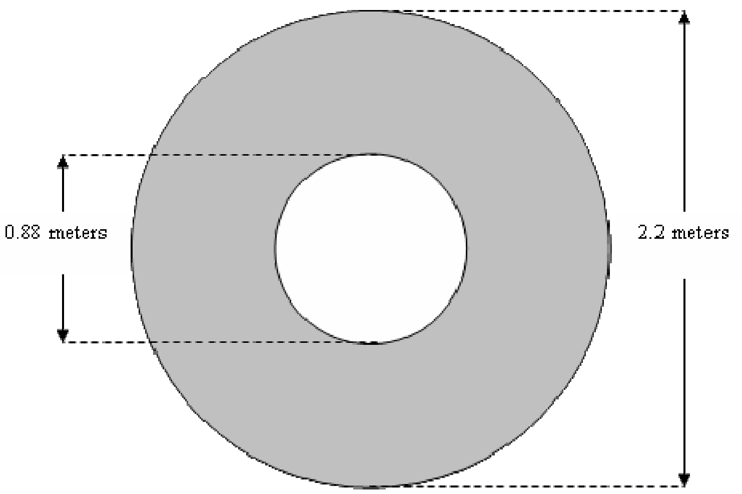

Figure 7-21: M1 apertures

The useful optical aperture is 2.185 meters which gives a collecting area equivalent to a 2m unobscured aperture.

- M2

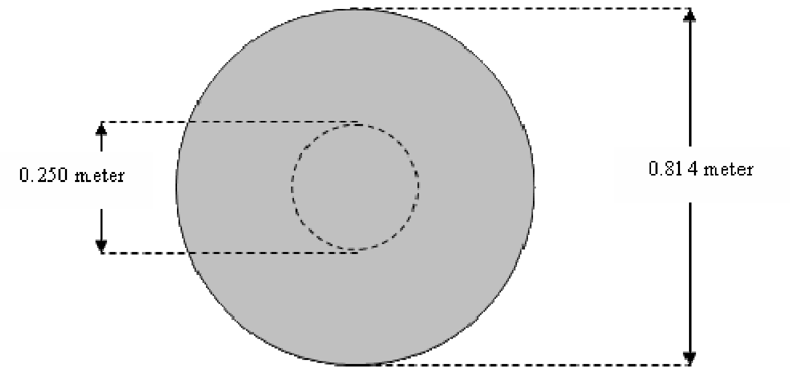

Figure 7-22: M2 aperture

The useful optical aperture is an annulus whose outer diameter is 0.790 meter and inner diameter is 0.250 meter.

- M3

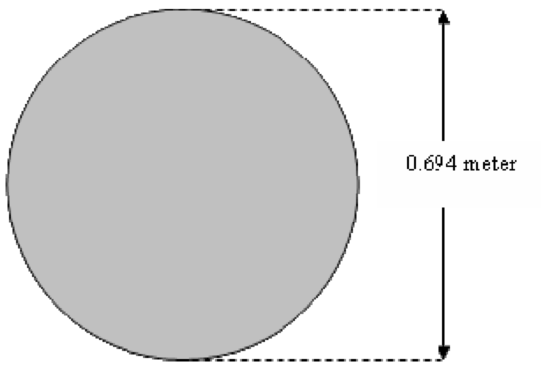

Figure 7-23: M3 aperture

The useful optical aperture has a diameter of 0.690 meter.

- M4

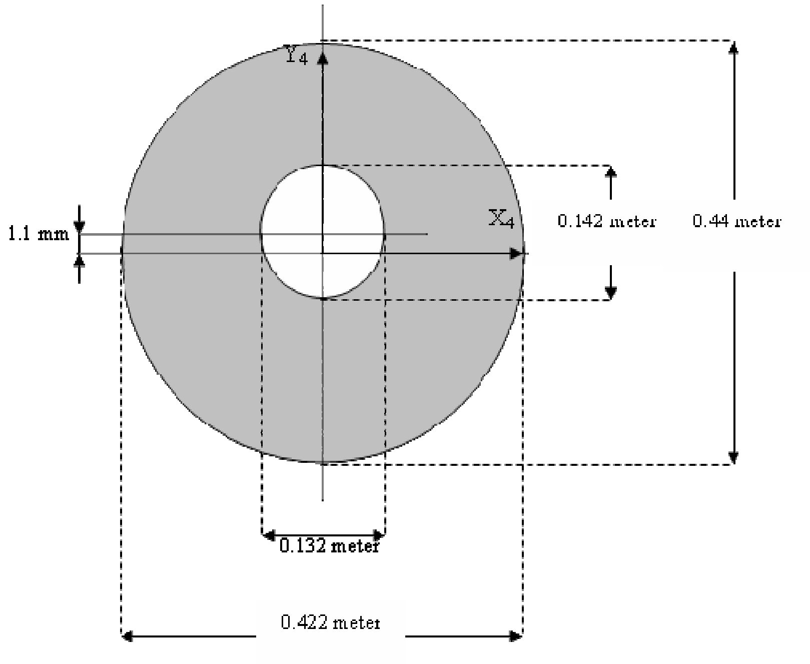

Figure 7-24: M4 aperture

The clear aperture of the mirror is elliptic. The dimensions of the major and minor axis are indicated in Figure 7-24. The central obscuration is also elliptic and shifted wrt the centre of the clear aperture towards the Y_4+ direction.

The given values do not include margins. For the obscuration dimensions, the margins must be coherent with the tolerances in tilt and decentring for M4.

- M5

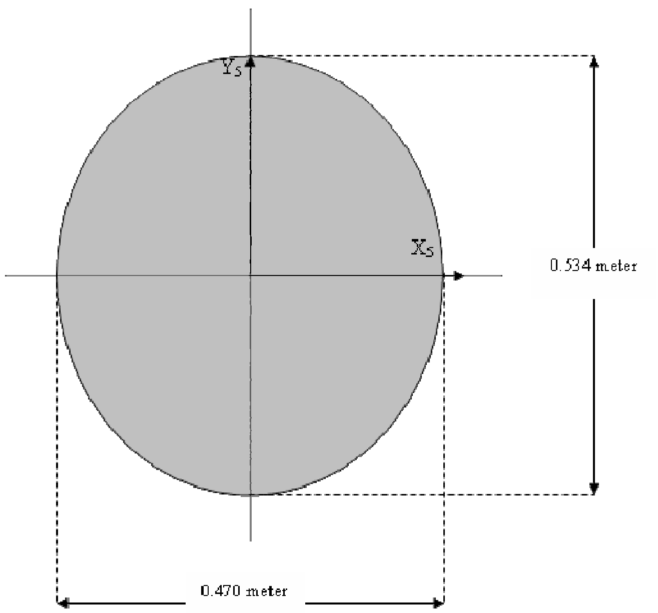

Figure 7-25: M5 aperture

The useful optical aperture is an ellipse whose major axis is 0.524 meter and minor axis is 0.460 meter.

7.1.6.3 Material

The reflectors will be in lightweight SiC. An alternative in Zerodur was assessed for the primary mirror but the estimated mass for such reflector, based on the mass density of the SOFIA primary mirror (RD[15]) is about 400 kg.

7.1.6.4 Coatings

In the considered wavelength range the most efficient coating is the Silver-multilayer coating. It presents a reflectivity of 87% to 98% in the spectral range 400 nm to 3000 nm (RD[17]).

Its main drawback is the high probability of degradation in presence of humid atmosphere. For long term storage the reflectors will need to be stored in low humidity conditions.

7.1.6.5 Performances

7.1.6.5.1 Nominal theoretical performances

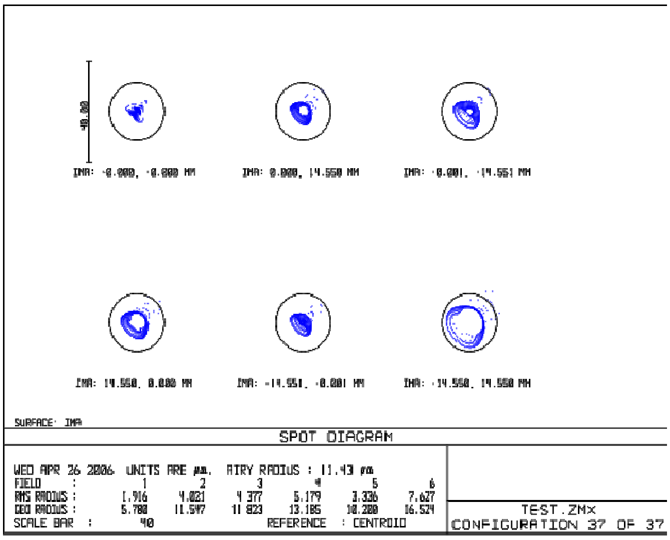

Figure 7-26: Spots diagram over the area of the detector located at the edge of the FOV

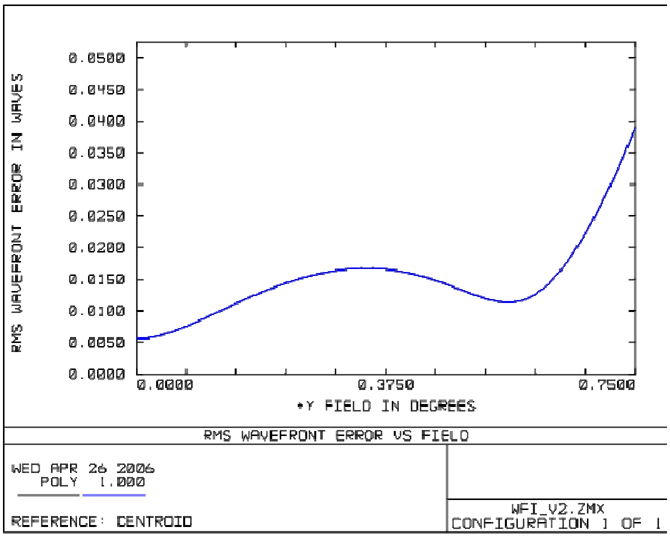

Figure 7-27: Nominal WFE variation with the FOV

Figure 7-26, considers a detector located at the edge of the telescope FOV. The image quality is the one obtained at the edges and at the furthest corner from the centre of the telescope FOV.

The nominal theoretical WFE averaged over the FOV is 22 nm RMS.

7.1.6.5.2 WFE degradation due to tolerances

The main contributors to WFE degradation are:

- Assembly of the telescope structure
- Manufacturing of reflectors
- Mount
- Launch perturbations
- Stability due to thermal variations
- Compensation accuracy
- Gravity release

The Strehl ratio is given by $S = e^{-(2\pi \times \sigma_{RMS})^2}$, with σ_{RMS} being the WFE RMS.

The WFE and ΔWFE are defined by:

$$\begin{cases} WFE_{RMS} = WFE_{theoretical} + \Delta WFE_{RMS} \\ \Delta WFE_{RMS}^2 = \Delta WFE_{assembly}^2 + \Delta WFE_{mount}^2 + \Delta WFE_{manufacturing}^2 + \Delta WFE_{stability}^2 + 2 \times \Delta WFE_{accuracy}^2 + \Delta WFE_{launch}^2 + \Delta WFE_{gravity}^2 \end{cases}$$

The term ΔWFE defines the degradation from the nominal WFE due to the contributors previously listed.

The calculated WFE is averaged over all the field of view with a 1-σ probability.

The Marechal's criterion states that optical systems with a RMS WFE lower than λ/14 can be considered as diffraction limited. Thus the maximum ΔWFE allowed wrt the nominal WFE is 49.4 nm RMS.

7.1.6.5.3 WFE breakdown

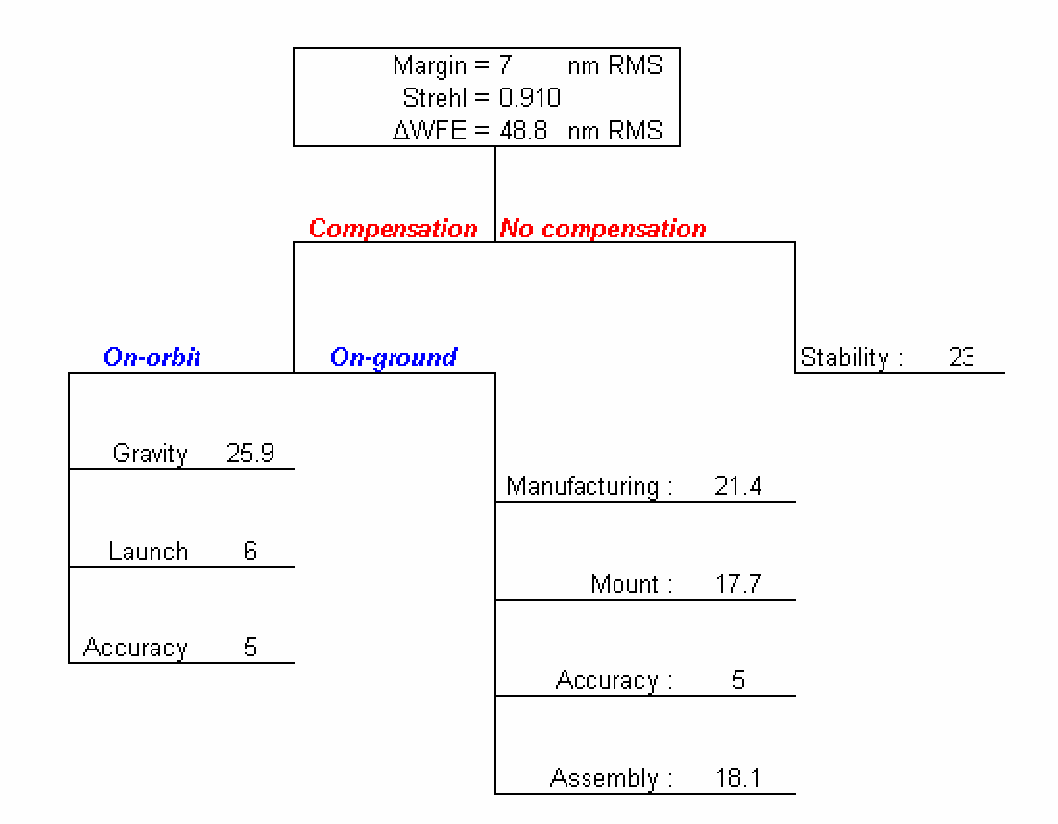

Figure 7-28: WFE breakdown

Figure 7-28 shows the apportioning of the WFE error amongst different contributors.

The compensation is assumed to be performed with 3 (on-orbit) or 5 (on-ground) degrees of freedom of M2.

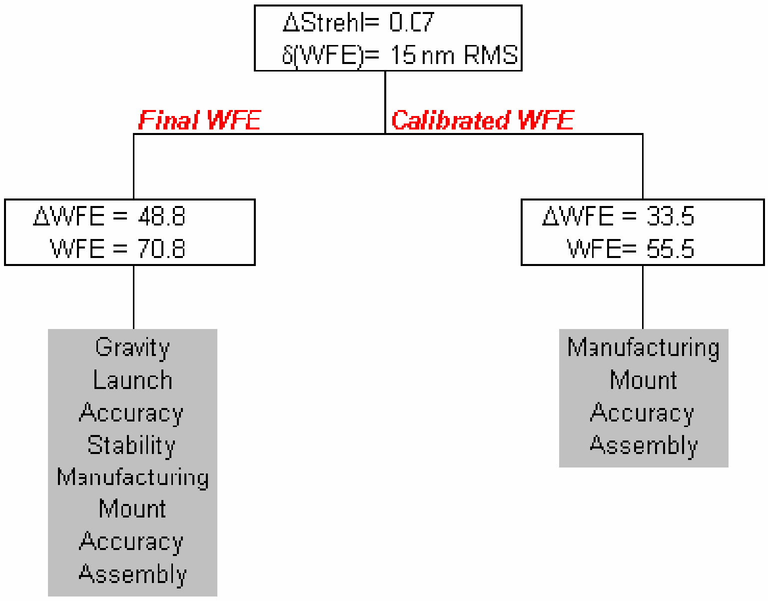

Figure 7-29: Strehl ratio difference between final WFE and calibrated WFE

The WFE on-ground is assumed to be calibrated. Consequently the allowable change in the encircled energy is linked to the $\Delta Strehl = Strehl_{Final} - Strehl_{Calibrated}$. According to the criteria defined above, the maximum allowable ΔStrehl is 0.07.

7.1.6.6 Realignment requirements

7.1.6.6.1 On-orbit

For correction on-orbit, a 3 DoF mechanism on M2 is required.

The degrees of freedom are:

- Translation along the Z_2 axis
- Tilts around X_2 and Y_2

	ΔZ (µm)	**θ_X (mrad)**	**θ_Y (mrad)**
Stroke	±350 (TBC)	±0.175	±0.175
Accuracy	±1	±0.01	±0.01

Table 7-12: Stroke and accuracy for on-orbit correction

7.1.6.6.2 On-ground

For correction on-ground, a 5 DoF mechanism on M2 is required.

The degrees of freedom are:

- Translation along the X_2, Y_2, Z_2 axis

- Tilts around X_2 and Y_2

	ΔZ (mm)	ΔX (mm)	ΔY (mm)	θ_X (mrad)	θ_Y (mrad)
Stroke	±2 (TBC)	±2 (TBC)	±2 (TBC)	±1 (TBC)	±1 (TBC)
Accuracy	±0.001	TBD	TBD	±0.01	±0.01

Table 7-13: Stroke and accuracy for on-ground correction

The accuracy for $\Delta Z, \theta_X, \theta_Y$ detailed in Table 7-13 needs to be achieved by the M2 mechanism. The large strokes can be achieved with a 5 DoF independent platform holding the M2 reflector during the telescope assembly. The displacements accuracy of this platform will be compliant with the positioning tolerances of M2 during assembly and with the M2 correction mechanism strokes.

7.1.6.6.3 Temperature

The following thermal requirements hold in order to minimise the contribution of thermal distortion.

	Temperature gradient between reflectors	Reflectors temperature error wrt the operational temperature
ΔT (K)	±0.5	±0.3

Table 7-14: Temperature gradient and reflector temperature error

7.1.6.7 Straylight baffling and analysis

7.1.6.7.1 Straylight sources and associated requirements

The major sources of concern are Sun, Earth and Moon. Straylight shall not limit the observation of the faintest objects, i.e. straylight shall be lower than the zodiacal background which is the dominant straylight source within the field of view. The zodiacal background is equivalent to m_v=32 (m_v=28 in V band). Based on a collection area of the telescope of 2.15m in diameter and an obscuration of 800mm, focussing of a point source on 2x2 pixels (20x20μm^2), a homogeneous straylight distribution on the focal surface and positioning of the S/C in orbit around L2 the following requirements can be derived:

source	attenuation required
Moon	$5\ 10^6$
Earth	$9\ 10^7$
Sun	$4\ 10^{13}$

Only straylight outside the field of view is considered in the analysis.

7.1.6.7.2 Baffle design

The telescope will need two baffles: an outer cylindrical baffle around M1 and M2 and an inner baffle around the hole in M1 allowing only light from M2 to propagate further in the system. The outer baffle can be designed as single or double stage baffle, the latter providing a higher straylight suppression. However, a double stage baffle is not compatible with the available fairing volume of a Soyuz Fregat. Consequently, an analysis was performed to assess whether a single stage baffle provides sufficient straylight shielding. Some improvements could still be made to the single baffle geometry e. g. in the baffle entrance region thereby improving in particular the Sun attenuation.

The inner baffle is a design compatible with the beam envelope and it complements the outer baffle by preventing low order scatter into the region beyond the M1 hole.

Two specific designs were actually assessed: 1). a baffle designed for Sun and Earth (small L2 halo orbit: 400.000km) and 2). a baffle designed for Sun only.

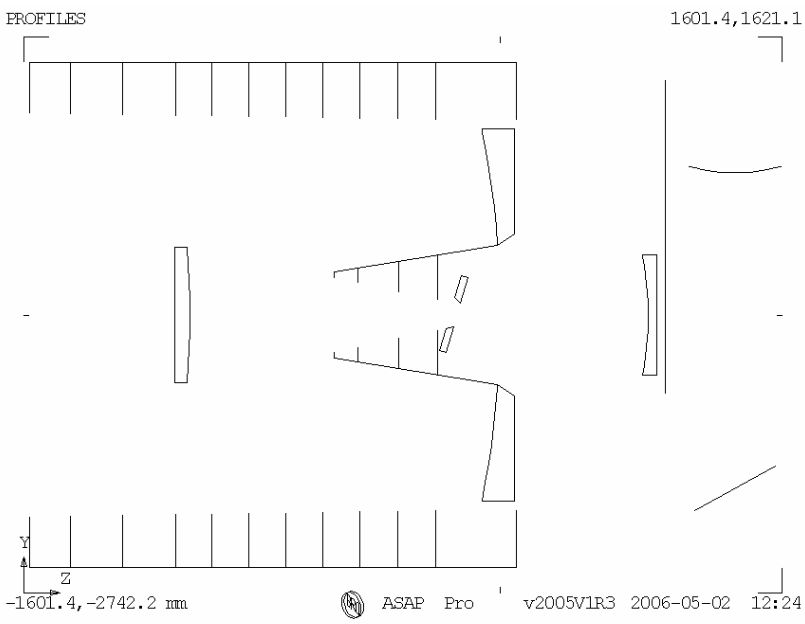

Figure 7-30: Baffle vane layout

7.1.6.7.3 Model

The straylight model contains the geometry of the outer baffle and the inner baffle but no effort is made to implement the M2 support (tripod) and mounting structures of the mirrors. The vanes are 1mm thick. The vane tips are not considered sharpened.

All non-optical surfaces are defined as lambertian scatterers with a 5% diffuse reflectivity. The BSDF of the mirrors represents a well polished mirror and results in a total integrated scatter (TIS) of 0.125%.

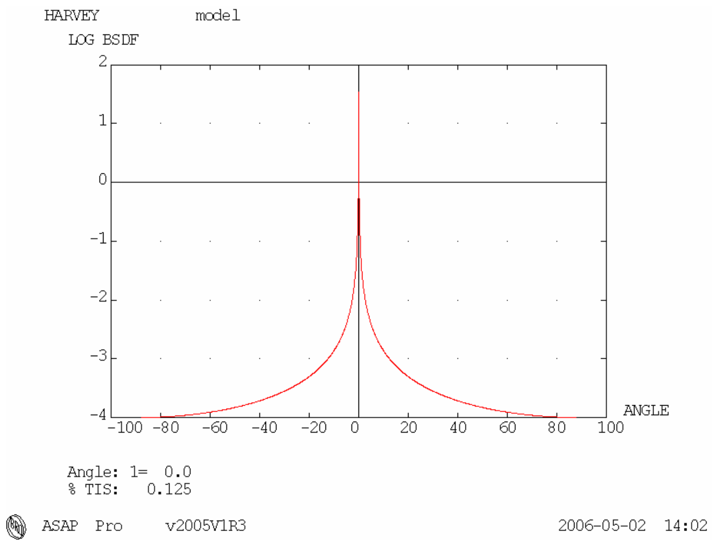

Figure 7-31: BSDF of the mirrors

The model does not consider any scatter mechanisms in the area behind the M1 since they are not expected to contribute significantly. This also implies that all structural elements present in this area are considered to be perfectly absorbing.

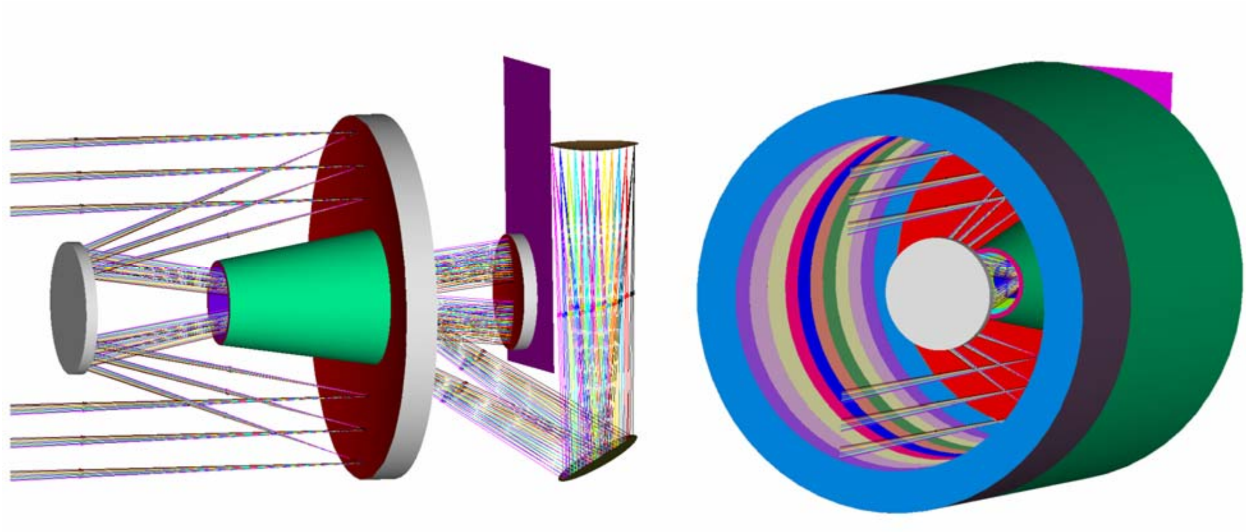

Figure 7-32: 3D view of inner and outer baffle

7.1.6.7.4 Results

Four major scatter paths carrying more than 80% of the flux to the focal surface were identified:

1. Double scatter in entrance area of baffle and subsequent scatter on M1 or M2

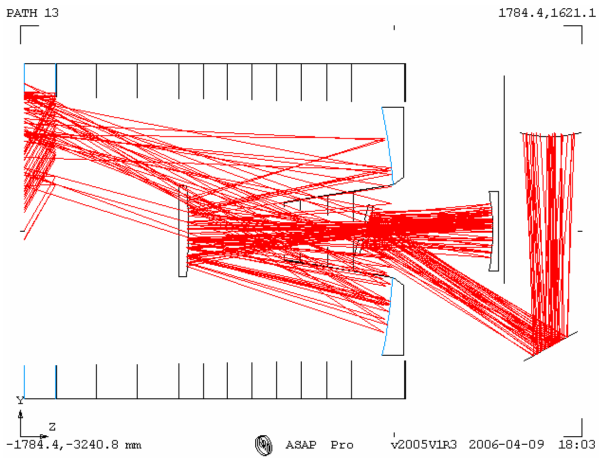

2. Scatter on one of the vane tips and subsequent scatter on M1 or M2

3. Double scatter in entrance area of baffle and subsequently at structural elements around the rim of M1. This path is caused by pupil aberrations and oversizing of M4 with respect to M1.

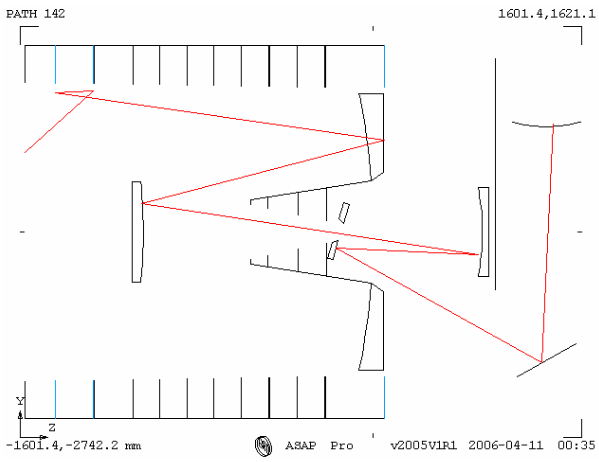

4. Scatter in entrance area of the baffle, the front vane of the inner baffle and the M2

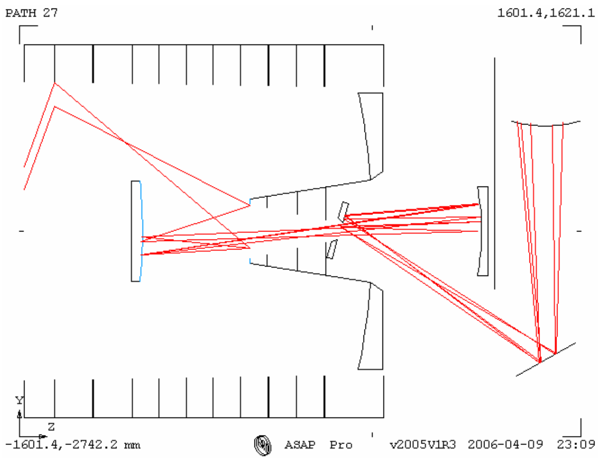

The total straylight attenuation is shown in Table 7-15 calculated with an uncertainty of an order of magnitude

	70º baffle (Sun case design)	60º baffle (Earth case design for small orbit)	requirement
Earth (large orbit)	10^{11}	-	$9 \cdot 10^{7}$
Earth (small orbit)	10^{12}	10^{13}	$9 \cdot 10^{7}$
Sun	10^{13}	10^{13}	$4 \cdot 10^{13}$

Table 7-15: Total straylight attenuation

A single stage baffle seems just compatible with the straylight requirements, therefore this is the solution retained in the present study. The most critical source is the Sun; Earth and Moon do not drive the baffle design and can be allowed to shine into the baffle beyond M2.

The baffle design under investigations allows for several design optimizations in order to gain some margin with respect to the sun case requirement such as reshaping of the baffle entrance to improve Sun rejection, implementation of sharp vane tips, application of a high performance black coating on the baffles (TIS < 5%) and possibly a relocation of the telescope pupil to M4. The marginal performance with respect to the Sun also implies that mirror roughness and contamination need to be well controlled since they directly impact the straylight suppression of the entire telescope.

7.1.7 Technology Assessment

7.1.7.1 Primary mirror manufacturing and integration

Monolithic SiC parts of up to 1.5x1.0 m can be manufactured by sintering and larger sizes can be obtained by non reactive brazing techniques (RD[18]). This process has been successfully used on several space projects such as the 1.5-m diameter parabola of the Aladin telescope and the 3.5-m diameter Herschel primary mirror. In these mirrors the fairly porous SiC bulk material causes large straylight levels. For the two previously mentioned projects this is not of importance: Herschel operates in the far infra-red and straylight due to thermal emission is dominant and the Aladin telescope is a pure 'photon collector', i.e. straylight presents a loss in collection efficiency but is otherwise of no concern.

The situation is different for WFI that requires imaging quality in the VIS and NIR with low straylight. SiC mirrors for this type of application ultimately need to be produced with a dense cladding layer that can be polished to the required roughness of less than 1nm. However, Europe has no current facilities to apply this layer on a mirror of this size (closest mirror at the limit of facility dimension: GAIA Primary 1.5x0.75 m^2).

The following technologies (to be developed) in order of increasing criticality could be envisaged in order to enable the manufacturing of the WFI primary mirror:

1. Application of an ICVI SiC cladding after pre-polishing of the mirror since the achievable cladding layer thickness is low
2. Set-up of a sufficiently large facility with the CVD process of Schunk
3. Application of the CVD cladding layer before the brazing of the individual mirror segments

The assembly of the SiC reflectors with the telescope structure is also an issue. According to RD[18] two assembling techniques have been developed, qualified and also successfully used in space telescopes: (a) bolting SiC-SiC or SiC-metal with metallic bolts, (b) gluing SiC-SiC or SiC-metal with epoxy material. Those techniques have to be validated wrt to requirements of telescope working in the visible and near infrared.

7.2 Instruments

7.2.1 Introduction

To achieve the mission scientific goals, the following instrument reference suite has been assumed:

- Camera which includes two photometers : one for the visible bandwidth and one for the Near Infrared (NIR) bandwidth
- Integral Field Spectroscopy (IFS), is an imaging spectrometer which provides a spectrum simultaneously for each spatial sample of an extended two dimensional field.

Both instruments use a part of the field of view of the telescope.

7.2.2 Requirements

Table 7-16 to Table 7-18 report the instrument main requirements and characteristics.

Parameters		**Value**
FOV		1 deg^2
Spectral range		350 nm-1000 nm
Sensor	Pitch	10 μm
	Plate scale	0.10 arcsec/pixel
	Type	High-Resistivity P-channel CCD's
	Temperature	140 K
Filters		6 bands

Table 7-16: Camera – visible photometer requirements

Parameters		**Value**
FOV		1 deg^2
Spectral range		1000 nm-1800 nm
Sensor	Pitch	20 μm
	Plate scale	0.20 arcsec/pixel
	Type	HgCdTe detector (1.8 um cut-off)
	Temperature	140 K
Filters		3 bands

Table 7-17: Camera – infrared photometer requirements

Parameters		Value
FOV		3x3 $arcsec^2$
Spectral range	Visible channel	350 nm- 1000 nm
	IR channel	1000 nm-1800 nm
Sensor type	Visible channel	High-Resistivity P-channel CCD's
	IR channel	HgCdTe detector (1.8 um cut-off)
Spectral resolution		100
Plate scale	Visible channel	0.1 arcsec/pixel
	IR channel	
Spatial resolution		0.1 arcsec/slice

Table 7-18: Integral field spectrometer requirements

7.2.3 Camera Focal Surface Array Concept

7.2.3.1 Filters definition

The central wavelength and bandwidth of each filter is determined as a scaled redshift of the B-band rest frame defined in the UBVRI Johnson photometric system. The definition of the B-band rest frame can be found in RD[10]. The scaling is the one used in the SNAP programme (RD[11]).

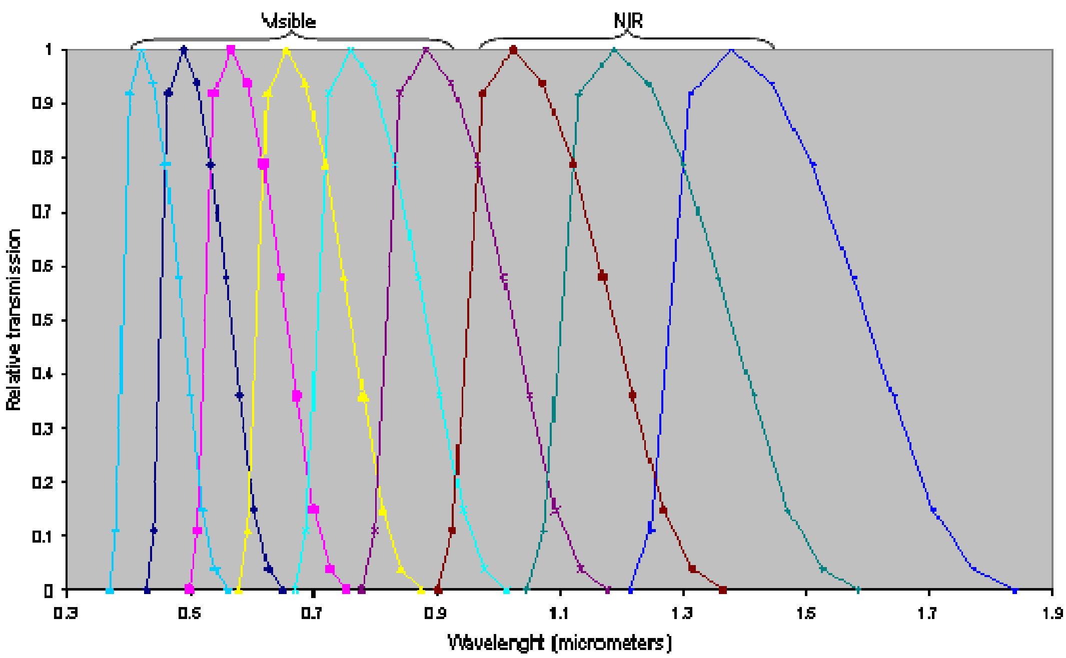

Figure 7-33 : Relative transmission of the set of filters

Filter		Peak transmission wavelength (μm)	Bandwidth @half maximum (μm)
Visible channel	1	0.4200	0.100
	2	0.4872	0.116
	3	0.5652	0.135
	4	0.6555	0.156
	5	0.7605	0.181
	6	0.8821	0.210
NIR channel	7	1.0233	0.244
	8	1.1870	0.283
	9	1.3769	0.328

Table 7-19 : Peak wavelength and bandwidth of the filters shown in Figure 7-33

7.2.3.2 Camera detectors pattern

The size of the detectors is 29.1×29.1 mm^2. For the visible channel the pixel size is 10μm while for the NIR channel the pixel size is 20μm.

Each channel is constituted by 72 detectors divided in two groups of 6×6.

Each row and column of the FSA has 12 detectors, 6 for the visible photometer and 6 for the NIR photometer.

In the visible channel, each filter covers one detector. In the NIR channel, each spectral bandwidth is covered by four adjacent detectors ensuring data redundancy when scanning along one row or column.

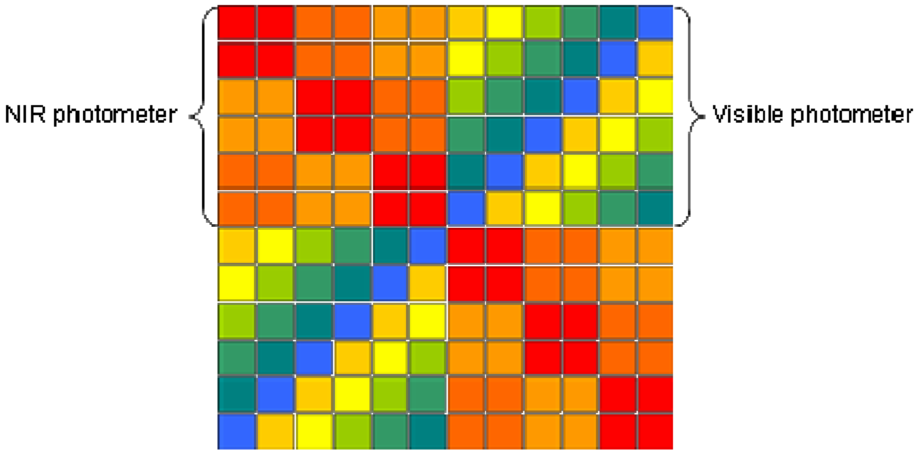

Figure 7-34: Detectors pattern on the telescope focal surface

The telescope focal surface is aspheric with a radius of curvature of R = 962.35 mm and the conic constant is k = -1.7350. This surface can be accurately reproduced with a structure in SiC or in metal on which the detectors will be mounted.

Due to the curvature, the spacing between the detectors is not constant over the FOV. The current gap width is assumed to be around 2 mm which is consistent with the present technology capabilities. The lay-out of the detectors needs to be refined when more information is available about the mechanical interface of the detectors. At that stage, the lay-out should also be optimized with respect to the distortion of the telescope in order to minimize the data loss due to the gaps. The current detector arrangement is optimized for minimum defocus over each individual detector.

7.2.4 IFS Optical Concept Description

In contrast to scanning spectrometers, IFS crams the full three-dimensional data in a single exposure on the detector.

An IFS is made of two successive stages:

1. The spatial stage whose function is to reformat the field of view (Integral Field Unit or IFU).
2. The spectral stage whose function is to disperse and focus the light on the detector (Spectrometer).

The spatial stage is the most critical part. There are currently three types of IFU: lenslet units, fibres unit and slicers unit. They differ in the spatial arrangement of the elements.

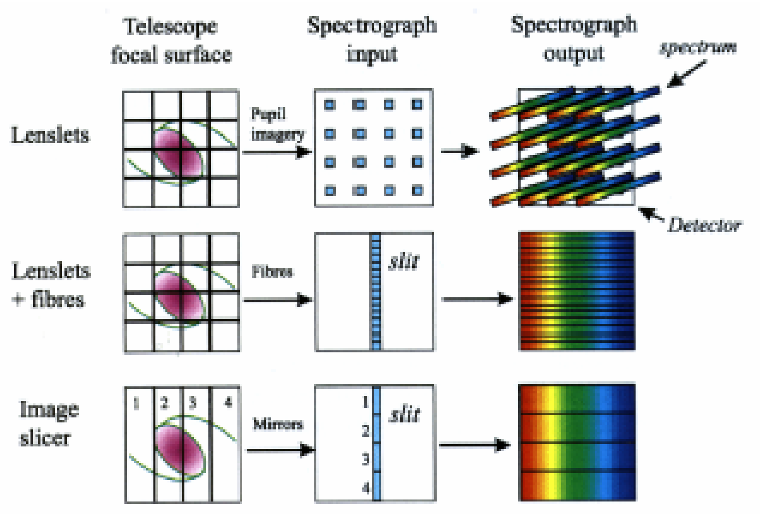

Figure 7-35 : Principles of the main types of IFS

IFU using MEMS is also a candidate (RD[6]).

7.2.4.1 Lenslets IFU

This type of spectrometer uses an array of lenses to sample the field of view. The light intercepted by each lenslet is focused in a spot called the micropupil which is an image of the telescope pupil. Micropupils are then dispersed by the spectrograph in a conventional manner. The ratio of the lenslet diameter to the micropupil diameter must be large (typically 50). It is this demagnification that saves space on the detector to store the spectral dimension. A slight rotation between the dispersion direction and the microlens array orientation avoids spectral overlap in one dimension. In the other dimension, a wide-band interference filter limits the spectral range to a finite length to prevent overlap. The lenslet size is typically of the order of mm which does not generally match the sampling scale at the telescope focal plane. An enlarger, preceding the lens array, is thus added to adapt the spatial sampling to the expected spatial resolution. The total packing efficiency on the detector is limited by the need to separate each spectrum from its neighbours as neighbouring pixels do not share the same wavelength.

The dispersion of the micro pupils is done only in one spatial direction. To avoid overlapping of the spectra, the array of lenslets is rotated around the optical axis wrt the detector.

The throughput of this type of IFS is generally good: square or hexagonal lenslet shapes provide a 100% covering efficiency and the lenslet can be made of glass and coated. A drawback is that a significant fraction of spectra is truncated if spectra are too long; in practice, the maximum spectral length should be less than 25% of the detector format in the dispersion direction to minimize this effect. Also, because of the small size of the micro pupils, the spatial resolution of such apparatus is quite low.

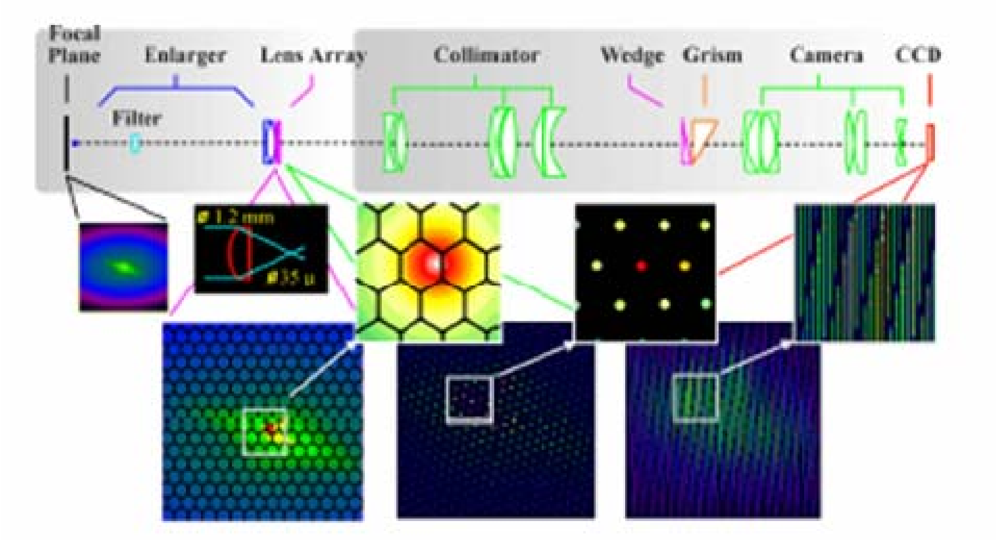

Figure 7-36: Layout of the IFS OSIRIS using lenslets

7.2.4.2 Fibre IFU

Fibre IFUs use optical fibres arranged in a close-packed bundle at the telescope focal plane and then reformatted into a pseudo-slit, which is then fed into the spectrograph. This presents an advantage compared with lenslet IFUs in the sense that the spectra can be as long as the detector format allows. On the other hand, fibre IFUs suffer from a lower efficiency owing to limited packing efficiency at the entrance (generally less than 75% owing to geometrical stages. loss and cladding) and focal ratio degradation. The latter is due to diffusion by imperfections within the fibre and diameter variation along it. This effect introduces some light loss and becomes more important with large f numbers. This constrains the designs of the spectrograph and the spatial stage. Fibre IFUs need to be calibrated carefully to control the fibre-to-fibre point spread function and transmission variations.

Adding lenses in front of the fibres helps to increase the packing efficiency and to solve the problem of focal ratio degradation. Each lenslet forms an image of the telescope pupil at the entrance of each fibre in the bundle. At the output, a linear array of lenslets forms a pseudoslit fed to the spectrograph.

The throughput is limited by the coupling between the microlenses and the fibres. In theory, the coupling efficiency is about 40%.

7.2.4.3 Slicer IFU

The slicer IFUs use mirrors in the telescope focal plane to cut the field of view into a number of strips which are then rearranged into a one-dimensional long strip. The slicer is composed of two sets of mirrors: the first set slices the field of view in a number of strips and reflects them into different directions while the second set rearranges the strips and aligns them into one continuous long strip. Slicer IFUs are comparable with fibre IFUs in terms of spectral coverage, but they are more efficient in terms of packing efficiency as the spatial sampling is continuous along each strip. The tilt of each sub-mirror produces a defocus between the two edges of each slice. This defocus translates into losses in spatial resolution and throughput. This gives a practical limit to the maximum number of slices that can be accommodated by such an IFU as defocus increases with the number of slices. To avoid any loss by diffraction, the slices shall be larger than the diameter of the Airy disk on the slices.

7.2.4.4 MEMS IFU

MEMS can be used in two different methods: as a scanning device or as a field selector. In the case of a scanning device, MEMS can perform the field selection by dividing the field in multi sub-pupils that can be imaged independently through scanning on a single spectrometer. Since the whole field is not use at one measurement this instrument would fall in the scanning spectrometer category and not IFS. However, MEMS can be very compact and scanned over high speeds making their selection only dependent on the scientific requirements. Another possible implementation of MEMS is as a shutter device. In this approach the MEMS can be used as a two dimensional reconfigurable field selector device such as a mirror array or as a micro shutter array. In this case, the instrument would operate more like a Multi Object Spectrometer, where the MEMS perform the task of selecting specific targets in the telescope field of view. Several strategies to avoid overlapping of object in the detector can be implemented. This could provide some simplification on the overall optical design but is again dependent of the scientific objectives for the instrument. Clear disadvantages of using MEMS are the use of movable parts that are subject to failure and require power and active control.

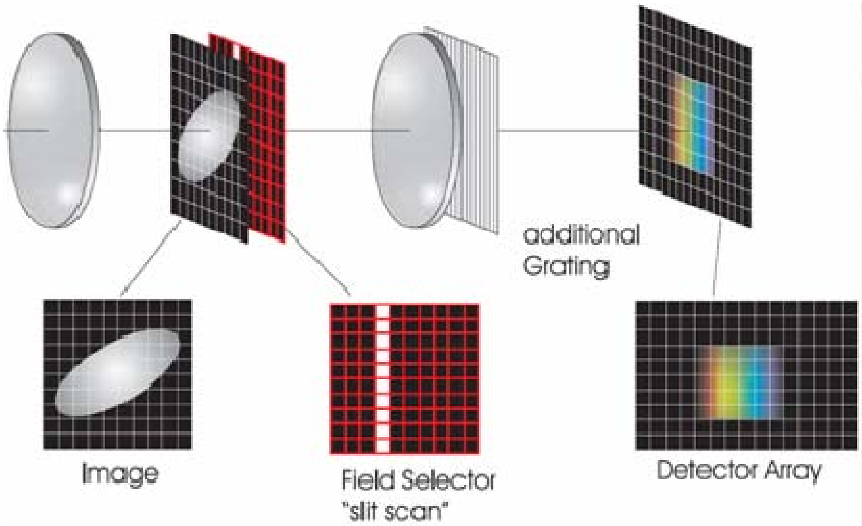

Figure 7-37: Example of MEMS IFU

7.2.4.5 IFU type trade-off matrix

Table 7-20 shows the IFU trade-off matrix.

Criteria	Value (0 – 5)				Comments
	Lenslet array	Fibre bundle	Mirror slicer	MEMS	
Spatial resolution	3	2	5	5	
Spectral resolution	3	5	5	4	
Transmission	4	1	5	5	
Broadband operation	2	3	5	5	
Manufacturability	4	5	3	3	
Compactness	4	5	3	4	
Structural complexity	4	4	3	4	
Alignment sensitivity	3	4	3	4	
FOV sampling	3	5	5	2	
Failure risk	5	5	5	1	
Average	3.5	3.9	4.2	3.7	No weighting coefficients are applied

Table 7-20: IFU trade-off Matrix

The average note of the fibre bundle IFU and the one using mirror slicer are close, but when comparing their respective spatial resolution and transmission, the image slicer is the best solution. This is the baseline of the present study.

MEMS are for now disregarded because of the low maturity.

7.2.5 IFS Layout

Figure 7-38 shows the IFS basic layout.

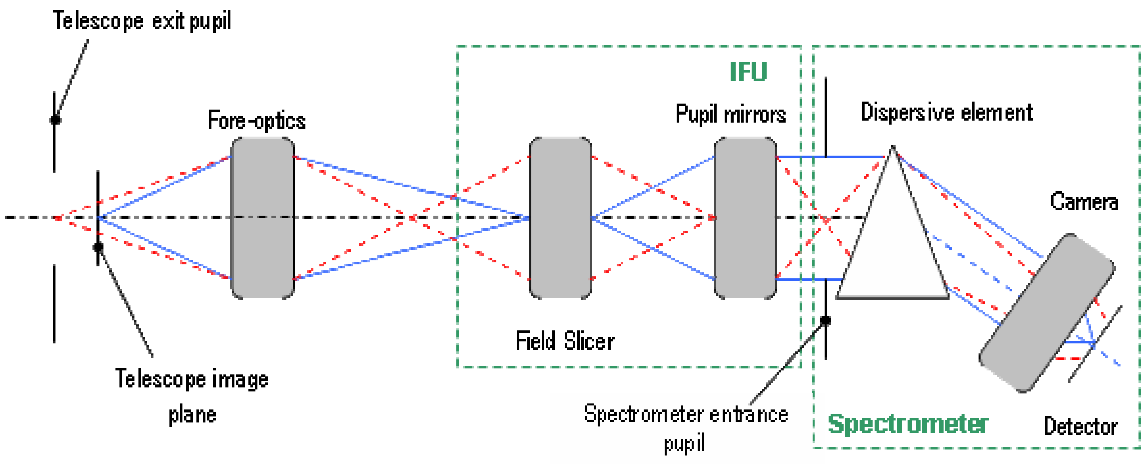

Figure 7-38: IFS basic layout

The following elements are identified:

- *Fore-optics*: This set of optics adapts the size of the image in the telescope to the slicer size. It may also correct for the telescope residual aberrations if needed.
- *Field slicer*: Spatially separates images of the telescope exit pupil. There is one pupil image per slice. The pupil is imaged on the pupil mirrors.
- *Pupil mirrors*: A set of small mirrors performing the arrangement of the different pupils on one single slit. This slit is the slit of the spectrograph. The light beam is collimated at the exit of the pupil mirror set.
- *Dispersive element*: The dispersive element can be either a prism or a diffraction grating each solution having its advantages and drawbacks.
- *Camera*: This system focuses on the detector the light coming from the dispersive element.

This basic layout does not include the dichroic beam splitter necessary to split the beam according to the spectral bandwidth channel (visible and NIR). Such beamsplitter will be placed in the plane of the spectrometer entrance pupil where the beam is collimated. Consequently, two prisms will be necessary, one for each channel.

The IFS field of view (FOV) is extracted from the telescope focal surface. A pick-up mirror is placed close to the focal surface

7.2.6 IFS Design Drivers

7.2.6.1 Field slicer

The specification for the spatial resolution is 0.1 arcsec/slice. This gives a number of slices of 3/0.1= 30 slices for the field slicer. Furthermore, the FOV of the spectrometer is equivalent to a $290\times290\ \mu m^2$ area on the focal surface of the telescope. Such a dimension is too small to implement a field slicer; consequently a magnification stage (or fore-optics) is necessary before the slicer.

The losses of light due to diffraction are limited if each individual slice has a width larger than the Airy disk (RD[7]). This criterion gives the maximum magnification of the fore-optics for a given slice dimension.

The relations between the magnification and the number of slices are the following:

- *Airy disk diameter on the slice*: $\lambda N'$, with N' the working F/number in the image space of the magnification stage and λ the wavelength.
- *Magnification*: $M = N'/N = l_{min}/(\lambda N)$, with l_{min} the minimum slice width, N the working F/number of the telescope (N=10).
- *Number maximum of slices* : $S_{max} = M\times 290/l_{min} = 290/(\lambda N)$

For the NIR channel, the maximum number of slices is 16 while it is 29 for the visible channel. Consequently, if we use a single image slicer with 30 slices, the NIR channel will suffer stray light due to diffraction.

The number of slices also drives the magnification of the fore-optics system.

In the presented layout, the slices will be powered mirrors.

7.2.6.2 IFS detectors

In the telescope focal surface, the resolution is 0.1 arcsec/pixel (Visible channel) and 0.2 arcsec/pixel (Infrared channel) which corresponds to a resolution of 10 arcsec/mm for both channels. While for the spectrometer, the resolution is 0.1 arcsec/pixel with $20\times 20\ \mu m^2$ pixels, thus a spatial resolution of 5 arcsec/mm. The magnification of the overall optical system is then M=2.

For both channels, the number of pixels is fixed by the required spatial and spectral resolution and by the number of slices in the image slicer. More generally the number of pixels is given by:

- In the spectral direction: $N_{spectral} = 2 \times R \times (\lambda_{max}-\lambda_{min})/\lambda_{min}$, with λ_{max} and λ_{min} the maximum and minimum wavelength of the considered spectral bandwidth, R the spectral resolution. The minimum bandwidth defined by $\Delta\lambda=\lambda min/R$ is then sampled by two pixels.
- In the spatial direction: $N_{spatial} = (3/0.1) \times S$, with S the number of slices of the image slicer. The spatial resolution is 0.1 arcsec/pixel.

<table>
<tr><th></th><th></th><th>NIR</th><th>Visible</th></tr>
<tr><td rowspan="3">Direction</td><td>Spectral</td><td>160</td><td>372</td></tr>
<tr><td rowspan="2">Spatial</td><td colspan="2">900 (30 slices)</td></tr>
<tr><td colspan="2">450 (15 slices)</td></tr>
</table>

Table 7-21 : Number of pixels in each direction on the IFS detectors

7.2.7 Baseline Design

7.2.7.1 Fore-optics

The magnification of this stage of the IFS is G=50. Furthermore this stage should bring correction for the telescope aberrations in the considered FOV. Thus the fore-optics assembly will include at least two powered mirrors and at least one pick-up mirror located close to the telescope focal surface.

The pick-up mirror has a diameter of about 1 mm (image size of about 0.3 mm). Two positions are possible for the pick-up mirror: at the centre of the focal surface or on the sides outside the area occupied by the FSA.

At the sides, the free space allows an easy positioning of the pick-up mirror. The drawback is that the telescope pupil will be tilted wrt the spectrometer pupil adding pupil aberrations in addition to the astigmatism due to the curvature of the focal surface. A better image quality can be obtained with the mirror placed at the centre of the focal surface. In that case the mirror mounting is problematic due to the lack of free-space in this area.

The first described position is thus chosen as baseline since it is the more realistic. Furthermore this configuration enhances the modularity of the payload.

7.2.7.2 Field slicer

The number of slices of the image slicer is 30 as a baseline in order to fulfil the 0.1 arcsec/slice requirement.

The individual slice size is 17mm length and 1mm width.

Studies show that the slice mirrors surface roughness has a tremendous impact on the IFS throughput. This roughness shall be lower than 2nm over the entire slices surface. The typical roughness for diamond turned aluminium surfaces is 10nm while the standard roughness for polished glass surfaces is 0.7nm. Clearly, slice mirrors in glass is the choice to be taken. To obtain a thermally stable system, material like Zerodur or ULE can be chosen.

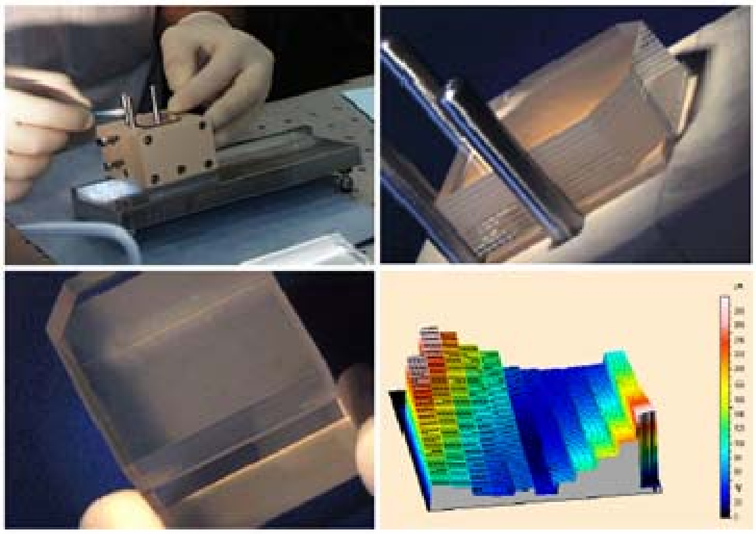

Figure 7-39: Field slicer developed in the context of SNAP mission

The slice mirrors can be flat or curved depending on the desired pupil imaging. In the baseline, curved mirrors are preferred since this configuration allows shorter distances (RD[4]) between the field slicer and the pupil mirrors and thus improves the compactness of the IFS.

7.2.7.3 Pupil mirrors

The pupil mirrors are powered reflecting surfaces. The function of the pupil mirrors is to collimate the beam coming from each slices of the field slicer. This stage re-arranges the pupil's image along a single direction and imaged them onto the spectrometer entrance pupil.

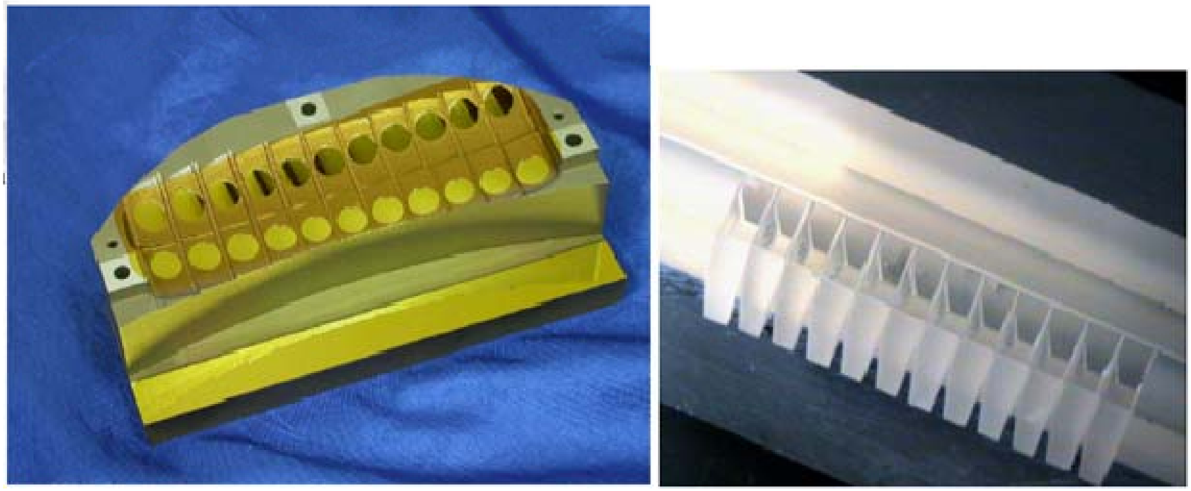

Figure 7-40: Examples of pupil mirrors

The figure on the left shows a pupil mirrors array in aluminium, on the right an array in glass.

The pupil mirrors array will have small mirrors (one for each slice) which individual diameter will be of about 5mm (averaged value with margins deduced from values found in literature).

The pupil mirrors array shall be in Zerodur or ULE in order to have an assembly insensitive to temperature changes and with a good polishing quality.

7.2.7.4 Dispersive element

The spectral dispersion can be performed either with diffraction grating or prisms. Each channel will have its own dispersive element.

7.2.7.5 Camera

This stage focuses the light after the dispersive element. Its magnification will be such that the spatial resolution on the detectors on both channels will be 0.1 arcsec/pixel. Each channel will have its own camera.

7.2.8 Options

The choice made of 30 slices in the field slicer in order to fulfil the requirements may lead to strong straylight which in turn may degrade the performances of the spectrometer. Three options are possible in that case:

1. Use a single field slicer for both channels with 15 slices

2. Use a different field slicer for each channel: 15 slices for the NIR channel and 30 slices for the visible channel. We assume here that the fore-optics system is the same for both channels, the impact will be on the slices width (1mm in the NIR and 0.5mm in the visible).
3. Use a different field slicer for each channel: 15 slices for the NIR channel and 30 slices for the visible channel. The fore-optics are also different for both channels. The magnification will be 50 for the NIR and 100 for the visible.

In the first case, the resolution per slice will be the same for both channels: 0.2 arcsec/slice.

In the second and third case, the resolution per slice will be different: 0.2 arcsec/slice in the NIR channel and 0.1 arcsec/slice in the visible. Furthermore this may induce an increase in the volume and mass of the spectrometer.

The third option shall be disregarded since it implies a higher degree of complexity and also a higher increase of mass and volume that in the other options.

7.2.9 Calibration System

In order to achieve 2% of accuracy on the brightness level of the Supernovae, the overall VIS and NIR imagers and spectrometer need to be calibrated.

The calibration shall be performed over the large wavelength range from 380nm-1800nm and over a large range of magnitude, from 16 to 29. This is very demanding, especially considering that the standard stars are bright, the engineering targets faint, the spectral energy distribution of Supernovae different than the ones of the stars and high accuracy requires lots of energy at all wavelength. Therefore, a specific activity on the calibration strategy shall be performed during further activities.

For the aim of this study, the SNAP calibration device (RD[19]) has been taken into account. It is composed of a shutter, calibration lamps and focus star lamps (see Figure 7-41).

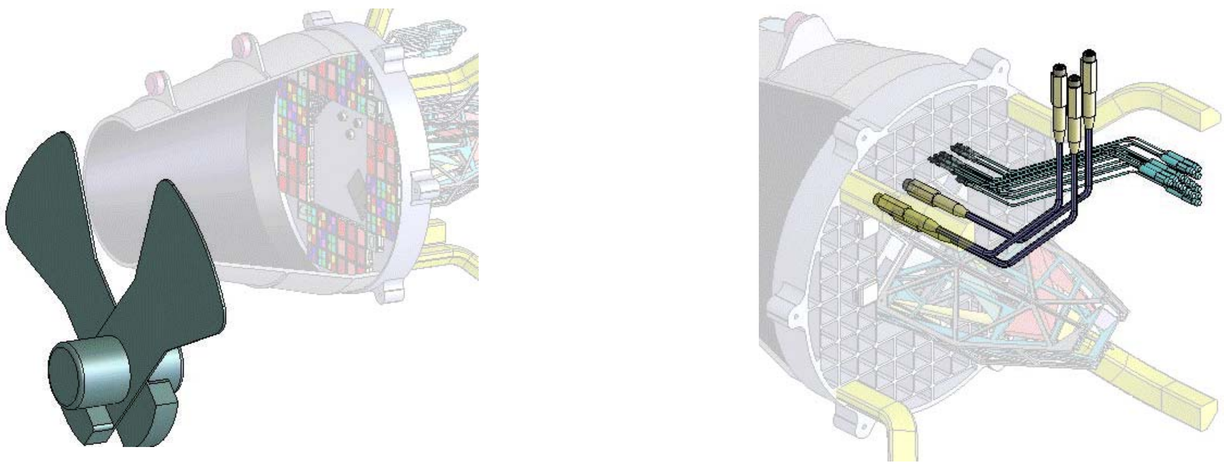

Figure 7-41: SNAP calibration device, the shutter, the calibration lamps and focus star lamps (RD[19])

A mass of = 12 kg including margin has been allocated based on the SNAP device (7.5 kg for the shutter).

7.3 Mechanisms

The following mechanisms are required onboard the Payload Module:

- Refocusing mechanism for secondary mirror M2

7.3.1 Re-focussing Mechanism Requirements

In the current 5 mirror constellations refocusing can be done most effectively with the secondary mirror M2. The mirror diameter is 814 mm and the mass ± 21.5 kg.

On ground the mirror shall be adjustable in 5 DoF:

- In plane ± 2 mm accuracy ± 1 µm
- Focus ± 0.5 mm accuracy ± 1 µm
- Rotation(2) ± 2mrad accuracy ± 10 µrad

In orbit the M2 mirror shall be adjustable in 3 DoF:

- Focus ±150 µm accuracy ± 1 µm
- Tilt (2) ± 2mrad accuracy ± 10 µrad

7.3.2 Assumptions and Trade-Offs

The approach, which has been followed to identify the conceptual design for the WFI mechanisms, is to use as far as possible qualified, off-the-shelf equipment, in order to reduce cost, procurement time and development risks. In case no qualified equipment is available the starting point for the development will be similar already qualified parts.

7.3.3 Baseline Design

7.3.3.1 Re-focusing mechanism

The 5 d.o.f refocusing mechanism currently under development for GAIA mission fulfils the in orbit functional (stroke and accuracy) requirements. A picture of this mechanism is given below.

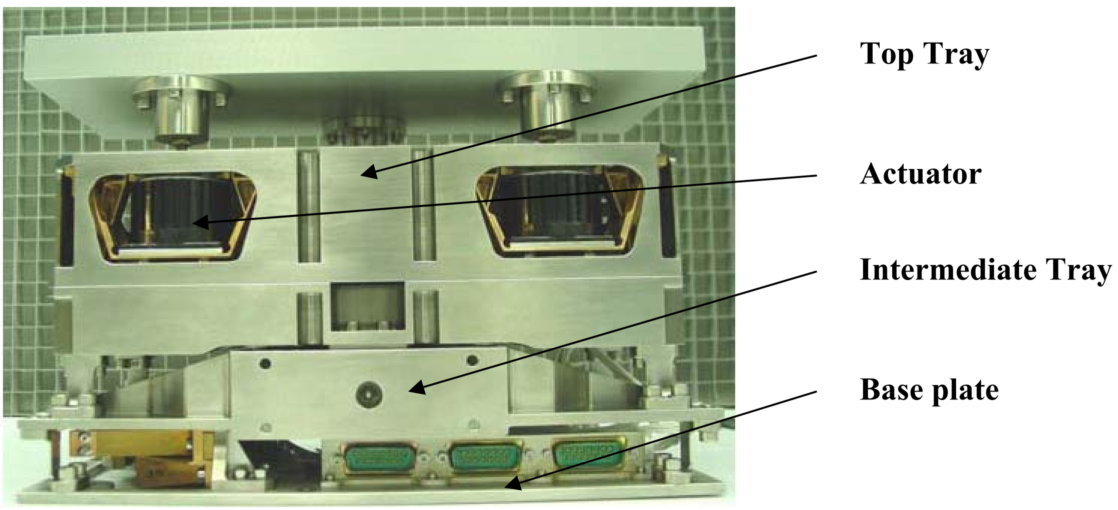

Figure 7-42: GAIA Secondary mirror mechanism

The overall configuration consists of:

- Base plate (INVAR)
- Intermediate tray (Ti6AL4V) attached to base plate with four flexible blades in Y direction (in plane)
- Top tray (Ti6AL4V) attached to in intermediate tray with four flexible blades in X direction (in Plane)
- 5 actuators, 2 in plane and 3 out of plane , see also Figure 7-43

and is designed for:

- Small envelope (110 x 260 x 130 mm^3)
- Operational temperature of 120 K
- Capability to withstand launch loads without hold down and release mechanism

Figure 7-43: GAIA actuator

The actuator is based on a structural reduction and consists of:

- CuBe support structure for a stepper motor
- Permanent magnet stepper motor drives a spindle
- Vespel SP3 nut where the spindle is threaded
- CuBe symmetrical flexure structure provides the reduction ratio by a lever arm
- 2 micro switches.

The mechanism can however not fulfil the following requirements:

- Support to mirror mass of 21.5 kg, the mechanism is designed for a small mirror of about 1.3 kg.
- On ground adjustability requirements (stroke 0.5-2 mm).

The WFI mirror size (814 mm) requires a larger envelope to properly support the mirror.

To adapt the GAIA design to the WFI requirements seems only possible for the in-orbit performance, i.e. improvement of the holding load (load during launch). The improvement of the stroke of the actuator is not possible without a complete redesign of the mechanism.

Possible alternative solutions:

- Option 1:
  - On ground
    - Adjustment done manually (oversized holes and shims)
  - In orbit:
    - - Modified GAIA design (3 DoF.)
- Option 2:
  - On ground:
    - Course adjustment done manually
    - Fine adjustment done with adjustment mechanism, which could consist of: Adjustment screw with spherical head (out of plane movement) Sliding plate (in plane movement) Locking bolt nut and pins
  - In orbit:
    - - Modified GAIA design (3 DoF.)
- Option 3:
  - Dedicated mechanism for on ground as well as in orbit adjustment.

These options have to be studied and assessed in the next phase of the project

7.3.4 List of Equipment

WFI		MASS [kg]			
Unit Name	**Quantity**	Mass per quantity excl. margin	Maturity Level	Margin	Total Mass incl. margin
Click on button above to **insert new unit**					
Refocusing mechanism M2	1	15.0	To be developed	20	18.0
Refocusing mechanism M5	1	10.0	To be developed	20	12.0
Click on button below to insert new unit		0.0	To be developed	20	0.0

Table 7-22: Equipment list

7.4 Structures

7.4.1 Requirements and Design Drivers

The most important functional requirements for the payload structures are:

- To support all the optical elements of the payload to the required tolerance and stability
- To guarantee the required light optical path without obstruction, shadowing, etc.
- To provide internal baffling
- To support the camera focal plane assembly and the IFS
- To provide interface points to the SVM

The required mounting tolerances and stabilities are reported in Chapter 7.1. The most stringent stability requirement is relevant to the distance M1/M2 that shall be kept within an error of 2.5 μm during science operations.

As the spacecraft total mass has a hard limit in the launch mass capability of Soyuz into L2, minimisation of structure mass shall be one of the main drivers of the design.

7.4.2 Assumptions and Trade-Offs

The verification of compliance to thermo-structural stability requirements will require a complex analysis that was outside the scope of this study. In order to reduce the effect of CTE mismatch due to different materials, the whole structural path between M1 and M2 has been designed with the same material of the mirrors: SiC. It is assumed that this, together with sizing for high stiffness, should guarantee the fulfilment of the stability requirement provided the telescope internal temperature gradient can be kept below a certain threshold (see section 7.6)

7.4.3 Baseline Design

Figure 7-44 shows all the components of the payload structure subsystem.

The large M1 mirror is supported in three points by the so called optical bench, a thick, stiff, monolitic SiC plate with a central hole. This is connected to the M2 support structure via three large beams that go through the mirror and join to its supports.

The M2 mirror hangs within a SiC conical structure by means of struts.

The optical bench also supports the internal baffle, a conical CFRP structure that hosts the M4 mirror.

The optical bench is directly connected to the upper plate of the SVM via a set of 12 struts.

Attached to the optical bench is the lower optical bay, a CFRP box structure hosting the remaining mirrors, the focal plane assembly and the IFS. The optical bay is decoupled from the SVM.

Secondary structures, also part of the payload module, are the external baffle and the lower enclosure, a lightweight structure with the function of sealing the gap between the external baffle and the SVM.

The external baffle is a thin aluminium cylindrical structure with vanes on the inside. The dimensioning of the baffle has been based on the XMM one, but no specific FE analysis has been carried out. This is an important point to be taken into account during next phase, as the external baffle is the most massive element.

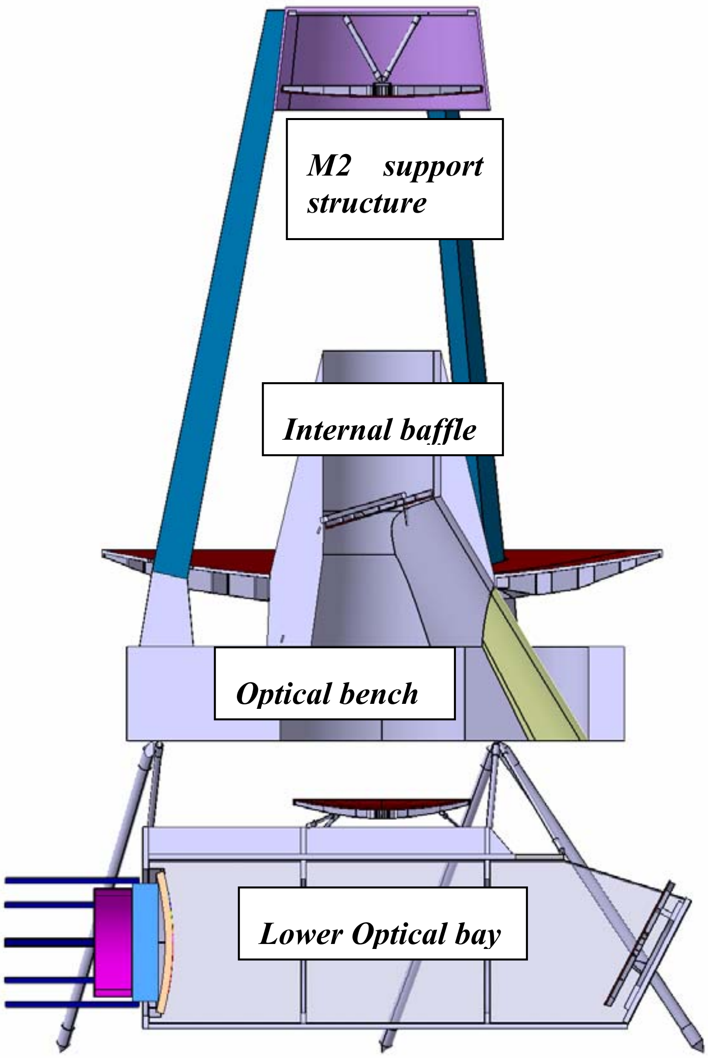

Figure 7-44: Payload structures components

Figure 7-45 below shows details of the payload structure. In particular the mounting of the IFS onto the optical bay is depicted

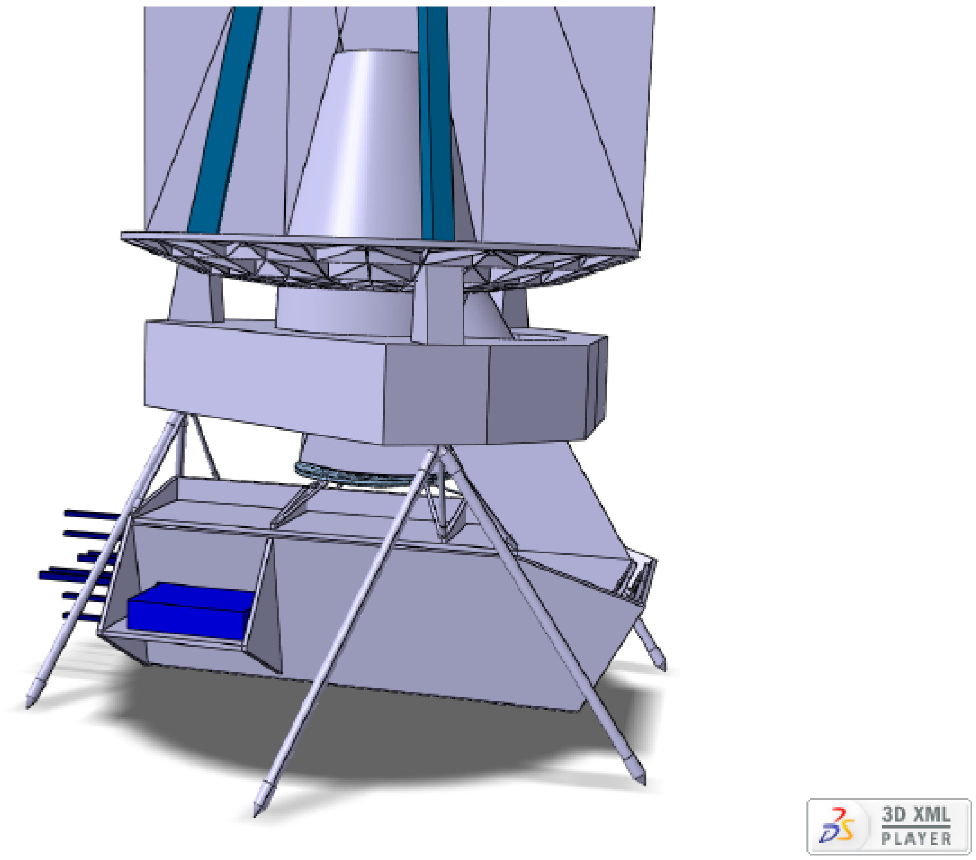

Figure 7-45: Detail of the lower optical bay

7.4.4 List of Equipment

Table 7-23 shows a list of the equipment associated with the payload module structures.

Item	Nr.	M_struct [kg]	Material	Maturity	Unit Margin [%]	Unit mass with margin [kg] [kg]
EXAMPLE	2	9.49		Modification	10	10.44
PLM optical bench	1	100.00	SiC	New dev.	20	120.00
PLM M2 -support structures	1	40.00	SiC	New dev.	20	48.00
PLM M3 - support structures	1	15.00	M55J Laminate	New dev.	20	18.00
PLM M1 struts	1	3.00	INVAR	New dev.	20	3.60
PLM M2 struts	1	3.00	INVAR	New dev.	20	3.60
PLM M3 struts	1	3.00	INVAR	New dev.	20	3.60
PLM M4 struts	1	3.00	INVAR	New dev.	20	3.60
PLM M5 struts	1	3.00	INVAR	New dev.	20	3.60
PLM internal baffle (incl. vanes)	1	10.44	sandwich	New dev.	20	12.53
PLM Focal Plane Assembly	0	40.00	M55J Laminate	New dev.	20	48.00
PLM lower optic bay	1	40.00	M55J Laminate	New dev.	20	48.00
Baffle support - pedestal	1	11.00	M55J Laminate	New dev.	20	13.20
Closure panel - lower baffle	6	2.21	sandwich	New dev.	20	2.66
Additional Solar Panel	1	8.60	sandwich	New dev.	20	10.32
Alu_foil covering internal	0	12.22	ALUMINUM	New dev.	20	14.67
Miscelleaneous (bracket,insert)	1	20.00		New dev.	20	24.00
		0.05		New dev.	20	0.05
		0.05		New dev.	20	0.05
22		**597.43**			**20.0**	**716.92**

Table 7-23: List of equipment

7.5 Data Handling

7.5.1 Functional Requirements

The main functional requirements of Payload Data Handling are:

- To acquire and store scientific data received from payload instruments via high-speed links
- To provide enough processing capability for the requested on-board data processing and data compression
- To playback the processed data to the SVM Mass memory
- To receive macro commands from SVM and to perform command & monitoring functions of the Payload Instruments.

The selection of the technologies and the architecture is driven by three main factors:

- Technology Readiness Level 5 should be achieved by 2009
- The Payload Data Handling shall be tolerant to any single point failure
- The cost shall be kept at a minimum. The main trade-off criteria should therefore be cost and technology maturity.

7.5.2 Data Handling Requirements

WFI observations will be split-up into 1000s exposure frames. Several intermediate read-outs will be needed to reject cosmic rays events and to achieve low noise performance. Since it will be impossible to send to the ground station all the intermediate read-outs a substantial on-board data processing and data compression will be needed.

During a 1000s exposure frame, Visible and NIR imagers will generate about 232 Gbits of raw data at an average data rate of about 232 Mbps. This large amount of data shall be stored and processed by the payload computer. Data acquisition of a frame and data processing of the previous one will be performed at the same time so it shall be possible to store two complete 1000s data frames (464 Gbits).

The algorithms to correct image pixels affected by cosmic rays impact are preliminary, so a precise figure of the processing requirements can not be given. Analysis on draft code (RD[21]) give an estimation of about 780 MOPS including 100% margin.

The lossless compression of corrected images is performed using the RICE algorithm (RD[22]). Preliminary evaluation of the processing requirements has been performed using a software model of the RICE algorithm running in a LEON3 processor simulator (RD[23]). The amount of data to be compressed every 1000s frame is about 12.2 Gbits and it requires about 430 MOPS.

The total processing requirement for cosmic ray removal and compression is therefore about 1200 MOPS.

7.5.3 Assumptions and Trade-Offs

7.5.3.1 Processor technology

The state of the art in Europe is the AT697 processor based on LEON2 IP core (RD[24]). The performance is 86 MIPS (Dhryston 2.1) and 23 MFLOPS (whetstone). The use of this processor is excluded for WFI project since it would require the design of complex multiprocessor architectures with large impact on mass, power consumption and cost.

The successor of LEON2 is LEON3 processor developed by Gaisler Research. A LEON3 multiprocessor implementation called GINA (RD[25]) is under development and first flight prototypes are expected for 2009.

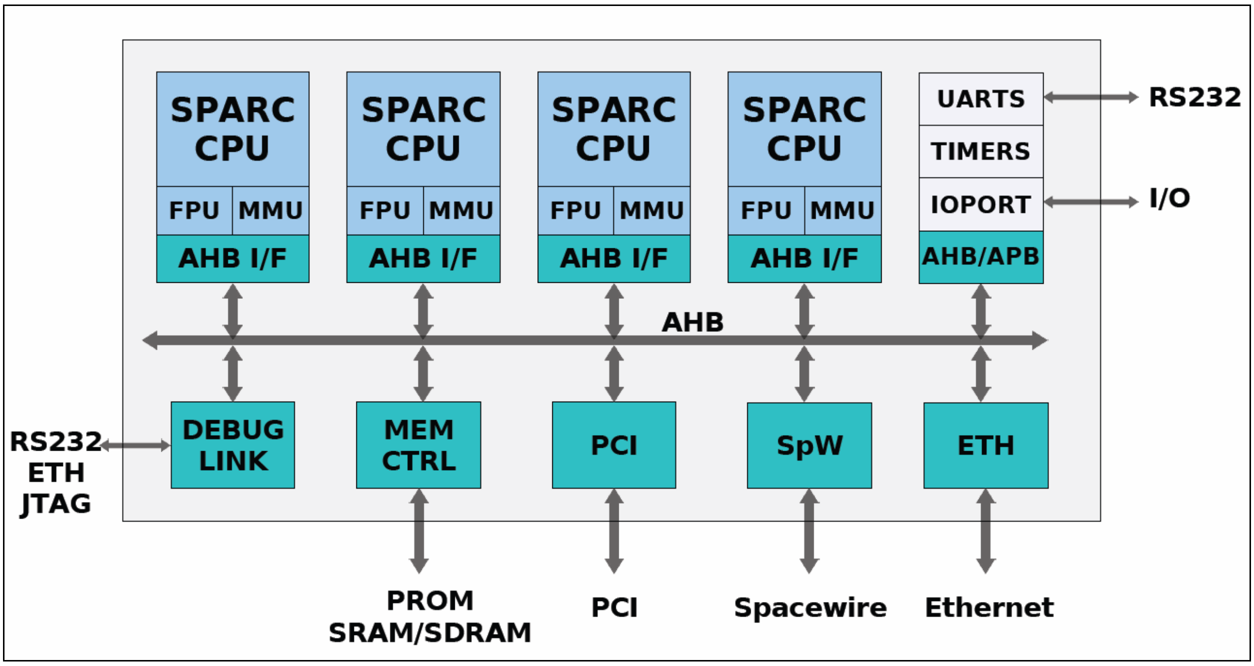

Figure 7-46: GINA processor block diagram

The GINA processor will consist of 4 LEON3 processor cores and a set of other IP cores such as PCI, SpaceWire and CAN. The peak performances expected are 900 MIPS and 900 MFLOPS. WFI Payload Computer would requires the use of two devices working in parallel or the implementation of part of the software algorithms in hardware, for example by using a dedicated coprocessor for data compression.

The use of GINA processor in WFI is a viable solution but uncertainty remains in the development schedule mainly relating to the CMOS technology for flight devices. For the time being this has been considered only as backup for WFI and its use may be reconsidered during the following phases of the project. Anyway, the difference in required resources (especially power) is minor.

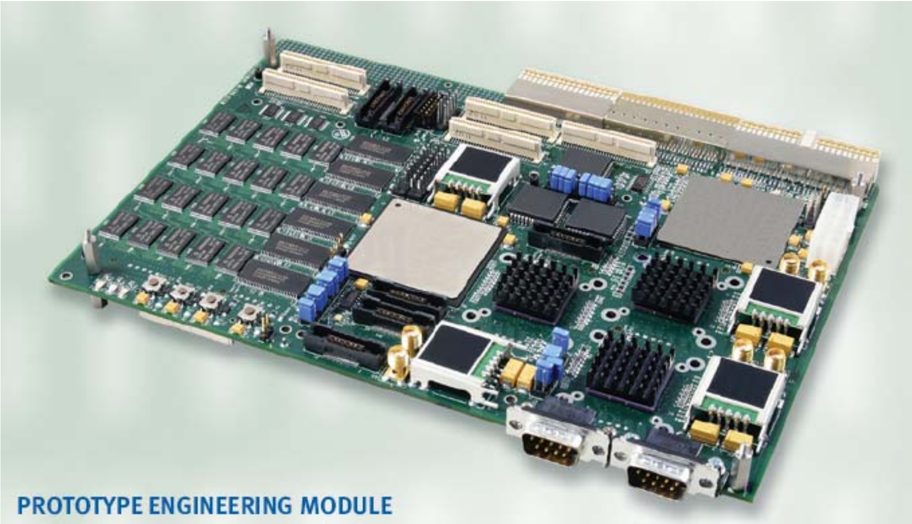

Figure 7-47: SCS750 processor board

The state of the art in the US for space processor board is the SCS750 from Maxwell. The board is based on PowerPC750 processor in triple modular redundant configuration and provides 1800 MIPS peak performance. This board has been selected for the GAIA payload. This option may impose some possible procurement restrictions (ITAR).

The SCS750 board has been selected as a baseline for this study due to its maturity.

7.5.3.2 Fast serial link

SpaceWire is the ESA standard for high speed serial link and it is a consolidated technology.

A number of SpaceWire IP cores and devices are already available. Besides, a SpaceWire Router ASIC design providing 8 SpaceWire input/output ports is close to completion.

SpaceWire is assumed as the baseline for high speed links in WFI. The maximum transmit rate of each link (200 Mbps) will size the number of connections needed.

In the following phases of the project new high speed links technologies, such as the SpaceFibre, could be assessed in order to reach higher rate per link and reduce harness mass.

7.5.3.3 Mass memory

Mass memory design greatly depends on the technology of the memory devices used. The state of the art are 256 Gbits or 512 Gbits devices but the technology is progressing fast and more dense memory devices for space use are expected in future. For WFI the baseline selected is based on memory modules similar to the ones used in Cryosat.

7.5.4 Baseline Design

The payload data handling is composed of the Payload Processor and the Payload Mass Memory, implemented in two different boxes and physically located inside the Service Module to simplify the Payload Module configuration and thermal control. The payload data handling architecture is shown in Figure 7-48.

7.5.4.1 Payload mass memory

The Payload Mass memory is composed of the following boards:

- 2 User Interface Modules (UIM) in cold redundancy
- 5 Memory Modules (MM)
- 2 Power Distribution Modules (PDM) in cold redundancy

The Mass Memory is controlled and managed by the Payload Computer.

7.5.4.1.1 User Interface Module

The UIM is in charge of:

- Receiving the data generated by the Payload instruments via SpaceWire links
- Receiving commands from Payload Processor
- Controlling and commanding each Memory Module
- Routing the input data to the Memory Modules
- Routing the output data from Memory Modules to the Payload Processor

The average data rate from instruments is about 300 Mbps including SpaceWire protocol overhead. The data transfer from Instruments is achieved by three SpaceWire links operating in parallel and simultaneously.

Commands from Payload Modules are received via a UART.

7.5.4.1.2 Memory Modules

Four Memory Modules 128 Gbits each are used for data storage. In order to have an EoL capacity of 465 Gbits, an additional spare Memory Module is used in case one complete Memory Module fails.

Each Memory Module is self standing and can be independently powered, operated and commanded.

7.5.4.2 Payload computer

The payload computer is composed of two sets (nominal and redundant) of three PCBs:

- SCS750 Processor Module (PM)
- Interface Module (IM)
- Power Distribution Module (PDM)

The two sets operate in cold redundancy, that is only one PM, one IM and one PDM are operating at the same time.

7.5.4.2.1 Processor Module

The PM acts as supervisor of the payload instruments by:

- Receiving and decoding macro commands for the instruments from SVM.
- Performing the processing (cosmic rays removal algorithms and data compression algorithm) on visible and NIR data.
- Controlling the payload mass memory.

The PM is based on the SCS750 computer board designed by Maxwell. The board includes 8 Mbytes of EEPROM for program storage and up to 256 Mbytes of protected SDRAM for program execution and for temporary data storage.

The data interface with the SVM is achieved via a redundant MIL-STD-1553 bus interface with Remote Terminal capabilities. The PM is interfaced to the IM via 32-bit cPCI bus. The board include a DMA controller that allows fast transactions between the cPCI bus and the SDRAM without loading the processor.

7.5.4.2.2 Interface Module

IM is under control of the PM and is in charge of:

- Triggering commands to the instruments and acquiring instruments status
- Acquiring data from Payload Mass Memory
- Sending compressed data to SVM Mass Memory.

The IM is interfaced to the PM via cPCI bus. The data interface with the Payload Mass Memory and the SVM Mass Memory is achieved via SpaceWire links.

One SpaceWire link is used for data transfer with Payload Mass Memory and one SpaceWire link with SVM Mass Memory.

7.5.4.2.3 Power Distribution Module

The PDM is in charge to generate all necessary voltages for the PM and IM electronics to operate. The PDM is connected to SVM power supply lines to provide power supply or to inhibit the operation of the PDM.

The selection of which set of boards (either nominal or redundant) is to be used is based on the presence of power supply at the PDM power input.

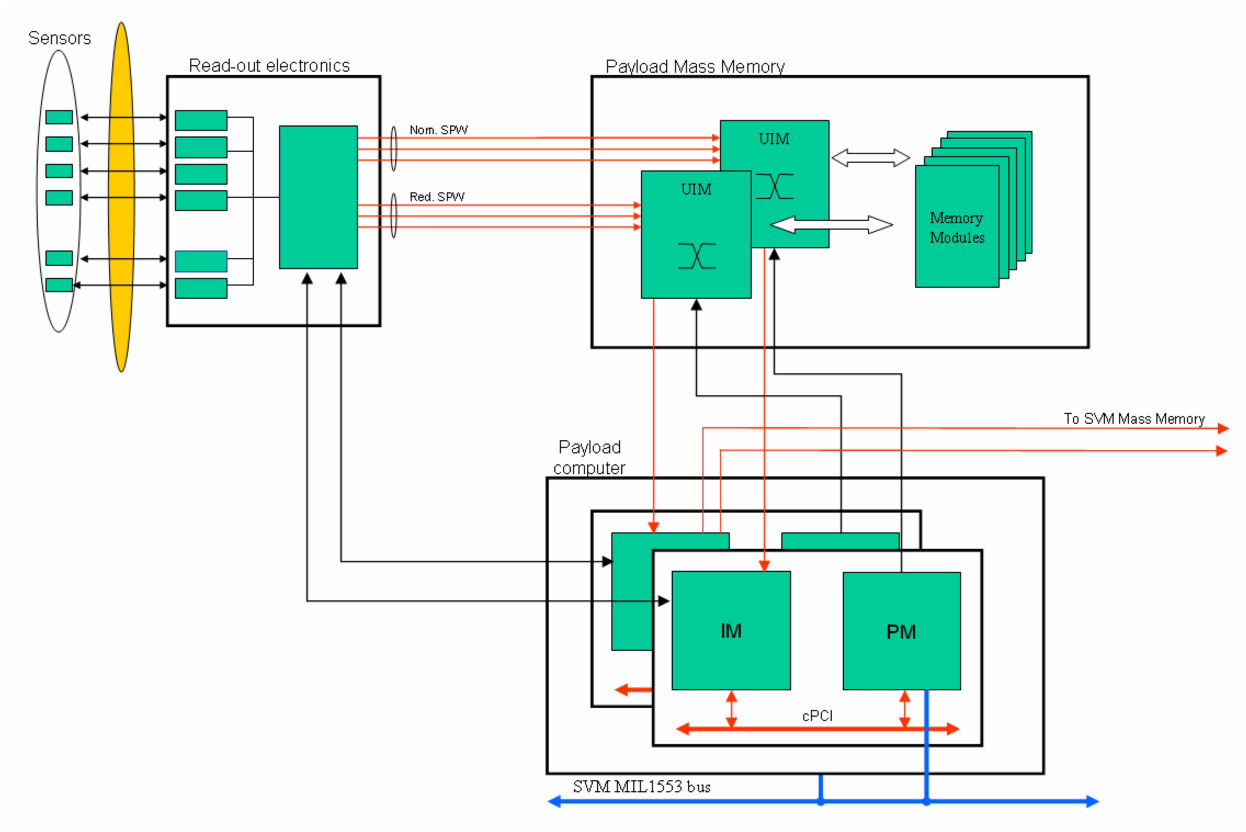

Figure 7-48: Payload Data handling block diagram

7.5.5 Budgets

Element 1	WFI Spacecraft		MASS [kg]			
Unit	Unit Name Click on button above to insert new unit	Quantity	Mass per quantity excl. margin	Maturity Level	Margin	Total Mass incl. margin
3	Payload Computer	1	6.1	To be modified	10	6.7
4	Payload Mass Memory	1	9.5	To be modified	10	10.4
SUBSYSTEM TOTAL		2	15.6		10.0	17.1

Table 7-24: Payload Data handling mass budget

Element 1	WFI Spacecraft		
Unit	Unit Name Click on button above to insert new unit	Quantity	Ppeak
3	Payload Computer	1	27.0
4	Payload Mass Memory	1	21.0
SUBSYSTEM TOTAL		2	48.0

Table 7-25: Payload Data Handling power consumption

7.6 Thermal

7.6.1 Requirements and Design Drivers

The TC shall keep all the equipments within their temperature ranges and, in particular for some of them, satisfy temperature stability requirements. For the payload the TC shall:

- Keep the focal plane where CCD and NIR are mounted at 150 K (-123.15 C) during measurement
- Keep the read-out electronics close to the focal plane at room temperature when operating and at least at -10 C when non operating (e.g. during transfer)
- Limit temperature gradients on the baffle to ease satisfaction of stability requirements
- Keep the mirror system at room temperature during measurement in order to avoid expensive cryogenic qualification testing on ground
- Maintain the mirror M1 and M2 within a difference in temperature of 0.8 K. This latter requirement is derived from the wavefront stability requirement and the associated maximum displacement M1/M2 with the assumption that the mirrors and the relevant support structures are all made of C/SiC to minimise difference in dilation coefficient.

7.6.2 Assumptions

The following inputs have been used for the design:

- Solar flux in Halo orbit =:> 1300/1340 W/m2
- Thermo-optical properties as in Table 7-26

	alpha	epsilon
Goldised Kapton	0.30	0.02
White Paint	0.29	0.90
Black Paint	0.95	0.90
M1/M2	0.49	0.04
CCD&NIR (as Si-cell)	/	0.83

Table 7-26: Thermal properties of TC materials

Values of power dissipations vs. modes were assumed as follows:

Focal Plane Power Consumption per Mode	
Focal Plane Mode 1 total Pon	0
Focal Plane Mode 2 total Pon	0
Focal Plane Mode 3 total Pon	0
Focal Plane Mode 4 total Pon	0
Focal Plane Mode 5 total Pon	0
Focal Plane Mode 6 total Pon	14.688
Focal Plane Mode 7 total Pon	0.408
Focal Plane Mode 8 total Pon	-
Focal Plane Mode 9 total Pon	0
Read Out Electronics Power Consumption per Mode	
Read Out Electronics Mode 1 total Pon	0
Read Out Electronics Mode 2 total Pon	0
Read Out Electronics Mode 3 total Pon	0
Read Out Electronics Mode 4 total Pon	0
Read Out Electronics Mode 5 total Pon	0
Read Out Electronics Mode 6 total Pon	163.266199
Read Out Electronics Mode 7 total Pon	50.22961664
Read Out Electronics Mode 8 total Pon	-
Read Out Electronics Mode 9 total Pon	0

Table 7-27: Power dissipations vs modes

Where mode 6 refers to imaging and mode 7 to spectrometry (see 8.6). The design approach to fulfil the requirement on operational temperature and stability for the optical assembly has been:

- Design the baffle so that it is at a temperature between 20 and 35 degrees depending on the sun aspect angle with respect to the z and x axes of the telescope
- Design the baffle so that its surface temperature is as uniform as possible
- Control the maximum required temperature difference among optical elements by means of heaters commanded by the thermisters.

7.6.3 Baseline Design

7.6.3.1 Baffle design

The baffle is made of Al honeycomb to ease manufacturing of vanes. Sts finishing is:

- Internally black painted due to optics requirements
- White painted on ¼ of the external surface
- MLI covered (20 layers with Goldised Kapton external layer) on ¾ of the external surface to limit the heat loss due to radiation to deep space
- Provided with a set of Aluminium rings for a total equivalent length of L = 20 cm and Thickness = 1 mm to increase radial conductivity and uniform temperature.

MODE	TITLE
1	Launch Mode
2	Initialisation Mode
3	Cruise Mode
4	Stand By Mode
5	100 deg Slew Mode
6	Imaging Mode
7	Spectrometry Mode
9	Safe Mode

Table 7-28: List of Modes

Table 7-29 shows the baffle temperature in the different cases and modes:

MODE	Sun in the baffle		Sun not in the baffle	
	Sun at 0 deg	Sun at 45 deg	Sun at 0 deg	Sun at 45 deg
1 (TC is off)	NA	NA	NA	NA
2	NA	NA	13.37 C	-6.96 C
3	NA	NA	13.37 C	-6.96 C
4	19.49 C	6.42 C	-15.97 C	-35.80 C
5	19.46 C	6.41 C	-16.00 C	-35.26 C
6	19.46 C	7.39 C	-15.50 C	-35.46 C
7	19.47 C	6.41 C	-15.94 C	-35.44 C
9	19.47 C	6.40 C	-15.97 C	-35.80 C

Table 7-29: Baffle temperature vs. cases and modes

Note: A definition of the modes is given in Table 7-28

7.6.3.2 Mirror design

The mirrors (SiC) have α=0.49 ε=0.04 and have heating power installed to remain at room temperature (about 22 C assumed).

In Table 7-29, the required heating powers for M1 and M2 in all modes and for different sun aspect angles. They correspond to a temperature of 20/20.5°C.

MODE	Sun in the baffle		Sun not in the baffle	
	Sun at 0 deg	Sun at 45 deg	Sun at 0 deg	Sun at 45 deg
1 (TC is off)	NA	NA	0.00 W	0.00 W
2	NA	NA	14.69 W	37.44 W
3	NA	NA	14.69 W	37.44 W
4	21.19 W	39.39 W	64.35 W	81.25 W
5	21.19 W	38.74 W	64.35 W	81.25 W
6	21.19 W	38.74 W	63.70 W	81.25 W
7	21.19 W	38.87 W	64.35 W	81.25 W
9	21.19 W	38.74 W	64.35 W	81.25 W

Table 7-30: Heating power allocated to mirrors vs modes and cases

Sun at 0 deg means that it is perfectly in front of the quarter of the baffle which is white painted.

The case named "Sun in the baffle" corresponds to when the telescope axis is tilted 20 degrees towards the Sun direction; "Sun not in the baffle" is when the telescope axis is perpendicular to the Sun direction.

The table does not take into account when the baffle axis is rotated 20 deg. away from the Sun; this represents the coldest case. However the heating power values are very close to the case "Sun not in the baffle and at 45 deg".

The values listed include 30% margin for heating power allocation also to M3 and M4.

7.6.3.3 Focal Plane and Read-out electronics design

Figure 7-49 shows a schematic of the thermal coupling between the focal surface that needs to be kept below 150 K and the read-out electronics. Since this latter needs to stay close to the detectors to reduce noise, some form of shielding is needed. The thermal decoupling is realised as follows:

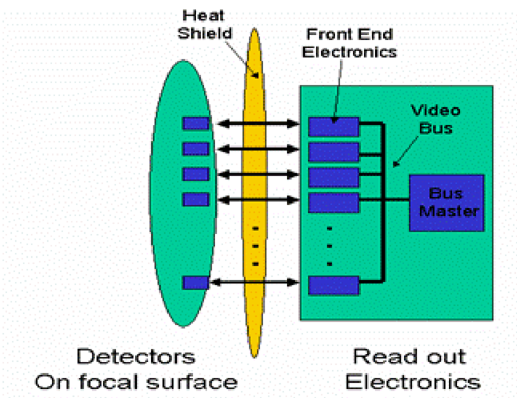

Figure 7-49: FS and ROE schematic

- The surface rear side is Goldised Kapton finished and independently connected to a 2.8 m^2 cold radiator by 4 graphite bars with a section area of 6e-3 m^2
- The read-out electronics are enclosed in a Goldised Kapton finished MLI tent and connected to a 0.4 m^2 independent warm radiator by 4 graphite bars with a section area of 6e-3 m^2
- In between there is a shield made of MLI for radiative decoupling (Goldised Kapton);
- Radiators are white painted on the space pointing side and Goldised Kapton finished on the other side
- The radiator configuration is shown in Figure 6-9

7.6.4 List of Equipment

The thermal units related to the payload are marked respect to the ones related to the service module in Table 7-30.

Element 1	WFI Spacecraft		MASS [kg]			
Unit	Unit Name Click on button above to **insert new unit**	Quantity	Mass per quantity excl. margin	Maturity Level	Margin	Total Mass incl. margin
1	Black paint on baffle and top int. surf.	1	4.93	To be modified	10	5.42
2	WP on 1/4 on baffle ext. surf.	1	1.06	To be modified	10	1.17
3	20 layers MLI on 3/4 baffle ext. surf.	1	14.17	To be modified	10	15.59
4	FP Radiator (structure+WP+int. finishing)	1	15.47	To be modified	10	17.02
5	ROE Radiator (structure+WP+int. finishing)	1	2.21	To be modified	10	2.43
6	2 mil Goldised Kapton (HS and FP rear side and top of baffle ext. surf.)	1	0.31	To be modified	10	0.34
7	Graphite Heat Path Bars	1	28.08	To be modified	10	30.89
8	Al ring	1	5.26	To be modified	10	5.78
9	Payload Heaters/Sensors	1	3.15	To be modified	10	3.47
10	SM Radiator (WP+int. finishing)	1	0.05	To be modified	10	0.06
11	20 layers MLI on SM ext. surf.	1	9.77	To be modified	10	10.75
12	Heat pipes	1	3.00	To be modified	10	3.30
13	Miscellaneous	1	1.00	To be modified	10	1.10
14	SM Heaters/Sensors	1	0.49	To be modified	10	0.54
-	Click on button below to insert new unit		0.00	To be developed	20	0.00
	SUBSYSTEM TOTAL	**14**	**88.96**		**10.0**	**97.86**

Table 7-31: Mass breakdown of thermal control system

The accuracy of standard temperature sensors is about ±0.3 C and temperature dependant as shown in Figure 7-50:

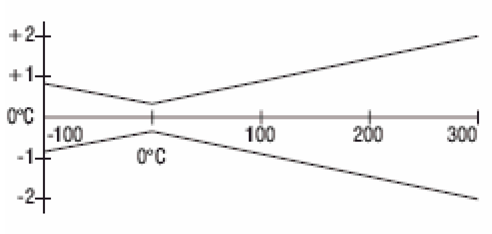

Figure 7-50: Dependence of standard sensor accuracy on temperature

The value of ±0.3 C can be calibrated at the desired temperature. However, the accuracy can go up to ±1 C depending on the type of control electronics.

There are platinum sensors with accuracy of ±0.1 C but very accurate electronics may need to be developed and space qualified.

8 SERVICE MODULE

The content of the following chapter represents the design of the different elements of the Service Module grouped by discipline.

Because of this arrangement, the FGS design (part of the payload) is described under the AOCS section of the Service Module chapter.

Conversely the baffle design is described under Optics, although this element belongs to the Service Module Structures.

8.1 Propulsion

8.1.1 Requirements and Design Drivers

The main functional requirements of the propulsion system are:

- To correct launcher dispersions/navigation errors (ΔV_{TOT} = 21 m/s including margin)
- To perform orbit maintenance (ΔV = 2 m/s per year for 6 years)
- to perform slew manoeuvres according to the observation strategy (see 5.3.1)
- Micro-control during imaging and spectrometry.

These latter two requirements call for the need of a very low thrust level (40 mN, see AOCS 8.7). Such a level of thrust would imply unacceptably long times to perform the navigation correction manoeuvres, therefore a second propulsion system is required.

Due to the low ΔV for manoeuvres, a monopropellant system has been selected as a second system.

8.1.2 Monopropellant System Design

8 CHT 5N-Hydrazine thrusters have been chosen. Their characteristics are shown in Figure 8-1.

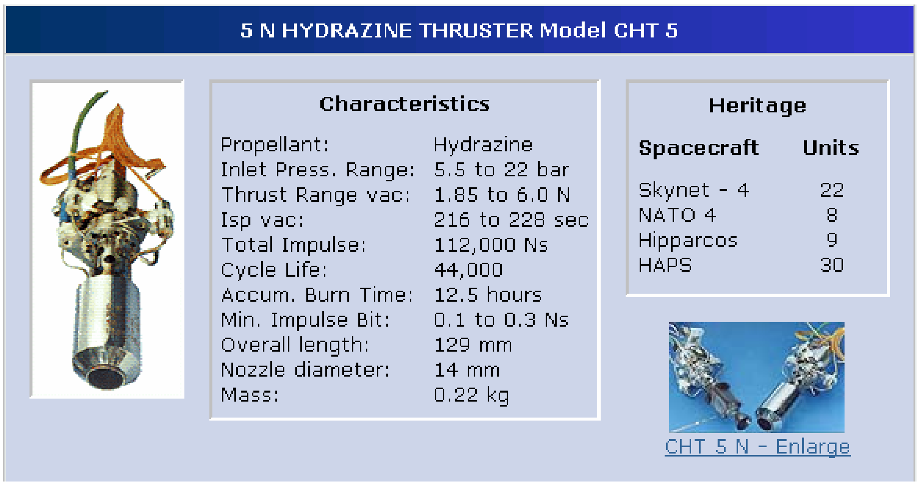

Figure 8-1: 5N-Hydrazine thrusters

The total propellant mass required is 33 kg. The total system wet mass is 55.2 kg

1 XMM tank may be used. A scheme of a possible feed system is shown in Figure 8-2.

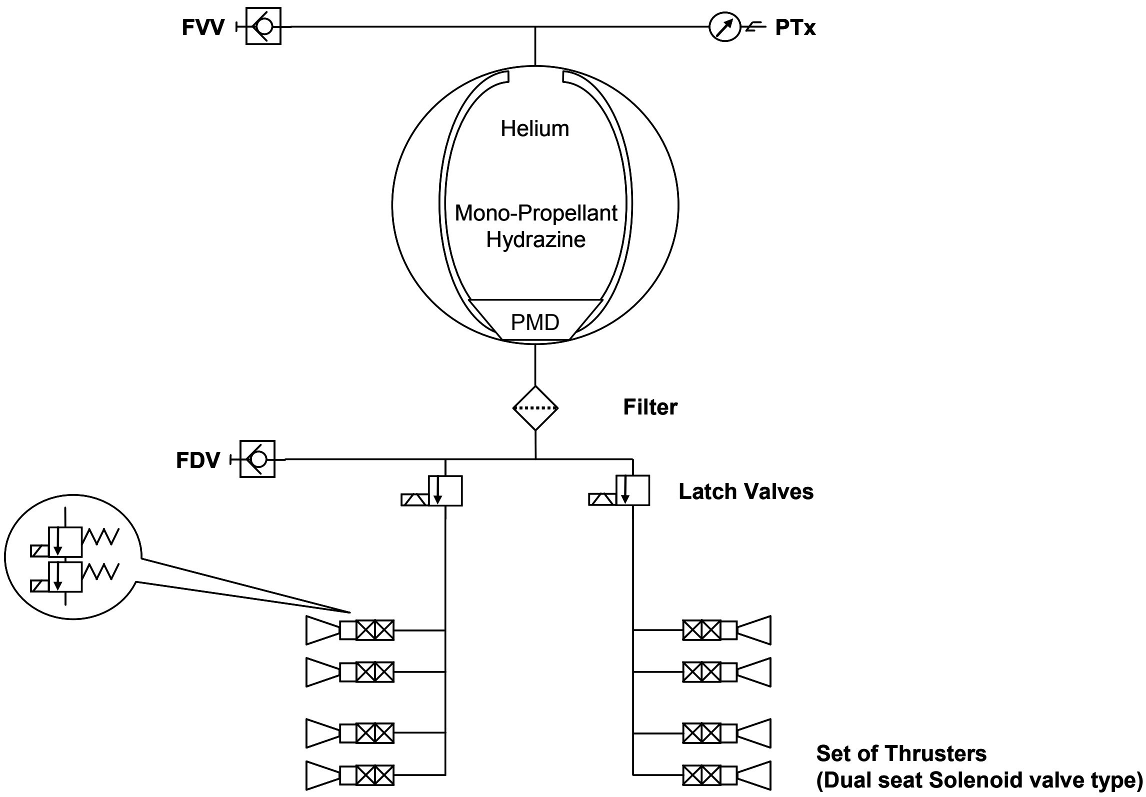

Figure 8-2: Monopropellant system architecture

The maximum power consumption for each Hydrazine valve is in the order of 13.5 W (36V input). The total power required will depend on how many thrusters would be used simultaneously.

8.1.3 Micro-Thrusters System Design

The following requirements drive the selection of the micro-thrust propulsion system to be used:

- Itot = 27098 Ns (see AOCS 8.7)
- 12 thrusters required for slew, scan, roll and dithering manoeuvres (full redundancy)
- Thrust range of 40 µN-500 µN (see AOCS 8.7)
- Thrust resolution of 40 µN (see AOCS 8.7)
- 4 thrusters out of the 12 required to provide thrust in the range 10 µN-100 µN for SRP (resolution of 1.5 µN)
- TRL 5 in 2009 for each component

A description of the candidate micro-thrusters follows:

8.1.3.1 WFI cold gas thrusters system

Three different cold gas thrusters are candidate for WFI mission:

- MAROTTA Micro Cold Gas, EM (Mk.2)
- BRADFORD Micro Cold Gas, EM
- ALENIA Micro Cold Gas, EM

The **MAROTTA** micro cold thruster (EM) is under development. Characterisations test campaigns have been conducted at MAROTTA UK and ESTEC-EPL. Environmental (vibration, shock, thermal cycling) and life testing (10 million open / close cycles) have already been performed on MK1.

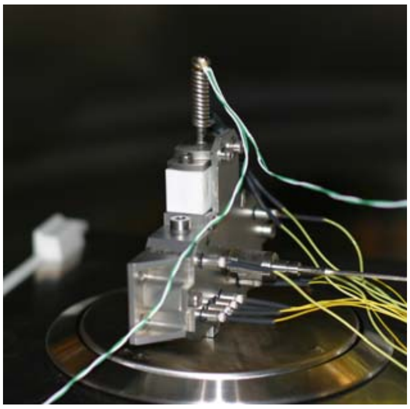

Figure 8-3: MAROTTA Micro Cold Gas MK.1

The performances of the MAROTTA micro cold gas thruster MK1 are shown Figure 8-4.

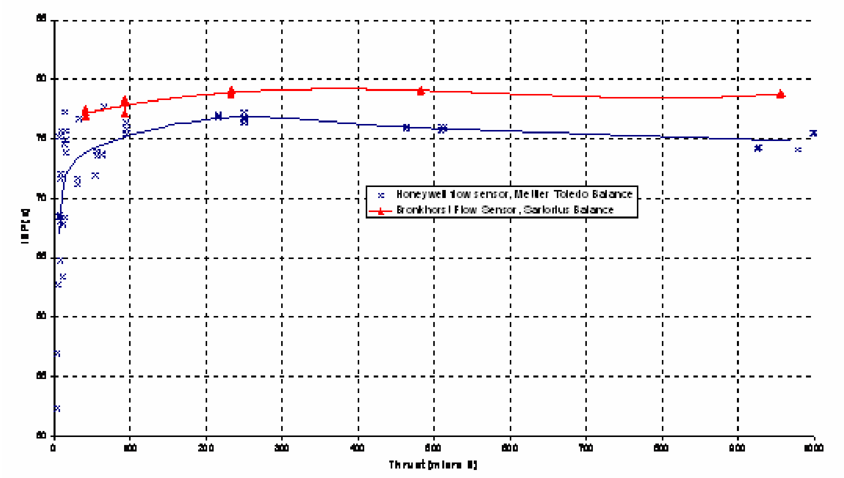

Figure 8-4: MAROTTA Micro Cold Gas performance.

For the **BRADFORD** micro cold gas thruster the solenoid valve has already been qualified for the GOCE mission. Characterisations test campaigns have already been performed at Bradford Engineering and ESTEC-EPL.

Figure 8-5: Bradford Micro Cold Gas

The performances of the BRADFORD micro cold gas thruster are shown in Figure 8-6.

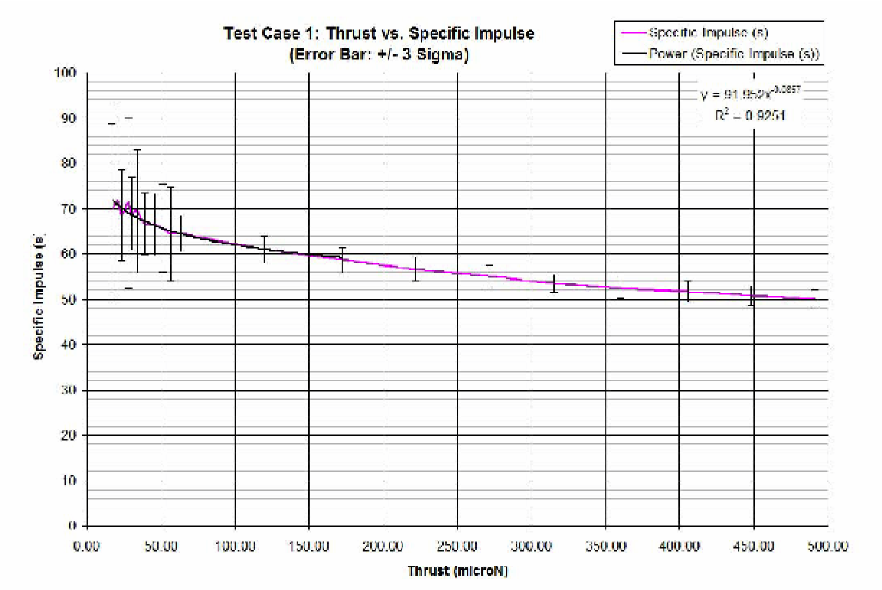

Figure 8-6: BRADFORD Micro Cold Gas performances

Concerning the **ALENIA** micro cold gas thruster to date several different BBs / EMs have been manufactured. The thruster has been extensively tested (environmental testing inclusive).

Figure 8-7: Alenia Micro Cold Gas

8.1.3.2 FEEP thrusters system

Today two different FEEP systems are candidate for Mission: ALTA 150 μN-FEEP and ARC FEEP

The FEEP 150μN sub-system is made up by self-contained thruster clusters (EPSA).

Each EPSA includes:

- 4 Thruster assemblies (including thruster unit, propellant tank and 80 g of propellant)
- 1 Power Processing and Control Unit (PPCU)
- 2 Neutralizers (NA), one active and one cold redundant

Figure 8-8 FEEP-150μN TA

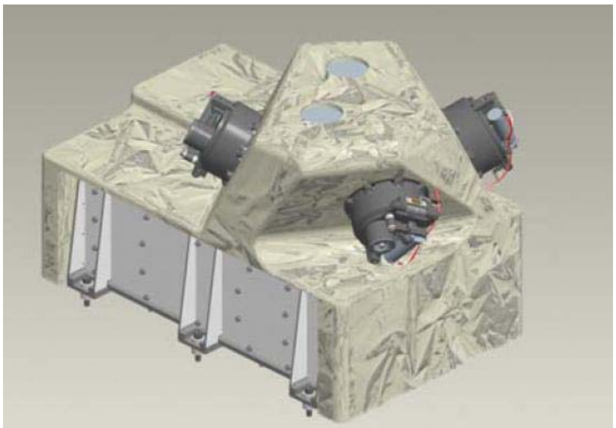

Figure 8-9 MICROSCOPE FEEP-150μN EPSA

The performances of the FEEP-150 thruster are listed in Table 8-1.

Performance	Units
Thrust Range	0.1-250 µN
Thrust Direction	In-plane divergence _ 15° Out-of-plane divergence _ 40°
Thrust Noise	For 10^{-4} [Hz] < f < 10^{-1} [Hz]Log(PSD) = 0.01 · (0.1 / f) [µN^2/Hz] For 10^{-1} [Hz] < f < 1 [Hz]Log(PSD) = 0.01[µN^2/Hz]
Thrust resolution	0.1 µN for T<100 µN 0.3 µN for T>100 µN
Total Impulse	3100 Ns
Specific Impulse	5400-5900-6400s @ 150 µN with - 4,-3,-2kV 6900-7400-7850s @ 30 µN with - 4 ,-3,-2kV
Specific Power	57-61-64 W/mN @ 150 µN with -4,-3, -2kV 53-57-60 W/mN @ 30 µN with - 4,-3, -2kV
Average consumption of Power	53.4 W (3 thrusters ON, 150 µN each + 1 neutralizer) 25.3 W (3 thrusters ON, 30 µN each + 1 neutralizer)

Table 8-1: FEEP-150µN performances

The ARC thruster consists of an Indium Liquid-Metal-Ion-Source with a sharp needle protruding out of a propellant reservoir tank. This reservoir is heated to above 156.6 °C to melt the Indium. If a sufficiently high electric field is applied between the needle and an extractor electrode, a so-called Taylor cone is formed and ions are directly pulled out of the liquid metal surface at the tip of the needle. These ions are accelerated out by the same electric field that created them.

The IN FEEP sub-system includes 4 clusters with:

- 16 In-FEEP needle each one with an Indium reservoir of 14 g
- Integrated pre-resistor for single power supply operation
- 1 Power supply
- Neutralizer

Figure 8-10: ARC In-FEEP cluster

The performances of the in-FEEP are listed in Table 8-2.

	Demonstrated
Thrust Range	0.1- 200 µN (16 emitters)
Thrust Resolution	< 0.3 µN
Specific Impulse	1600-8000 s
Beam Divergence	30°
Total Impulse	175 Ns
Thrust Noise	< 0.1 µN/Hz$^{0.5}$

Table 8-2: In-FEEP performances

8.1.3.3 GIESSEN University RIT- 4 GIE

The mini Radiofrequency Ion Thruster Assembly (RITA) will consist of the following units:

- 4 RIT 4 Thruster and neutralizer
- 1 Flow Control Unit (FCU)
- 1 Radio Frequency Generator (RFG)
- 1 Power Supply and Control Unit (PSCU)

Figure 8-11: GIESSEN University RIT 4 GIE

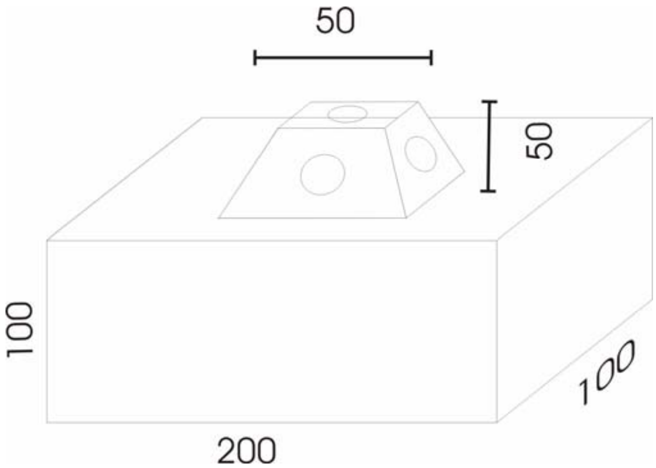

Figure 8-12 GIESSEN RIT 4 GIE System Assembly

The performances of the RIT 4 GIE Thruster are listed in Table 8-3. A GSTP activity will confirm the performances and reach TRL5 in 2007.

	Demonstrated
Thrust	20-100µN 100µN–2mN
Thrust Noise	$<1\ \mu N/Hz^{1/2}$ TBC
Specific Impulse	2000-3500s
Flow Rate	0.006mg/s
Mass Efficiency	Up to 84% Down to 26% @ lowest thrust level

Table 8-3: RIT 4 GIE performances

A preliminary test characterization of the thruster has been performed in ESTEC, ESA Propulsion Laboratory.

Preliminary test have also been performed at 500µN demonstrating an ISP of 2000s and a power consumption of 25 W.

An alternative mini-ion thruster is the one manufactured by QinetiQ scaling down the T5 thruster. As no experimental performance data is available to date, for the QinetiQ thruster, the GIESSEN RIT has been taken as reference.

Initially, in addition to the mentioned options, the following alternatives were investigated.

- Monopropellant + GOCE cold gas thrusters systems
- Monopropellant + mini HET system

- All GAIA cold gas system
- All FEEP thrusters system
- All mini GIE system

All these options were quickly discarded because they were non-compliant with the given requirements.

8.1.4 Trade-Off

Three propulsion system combinations have been identified as eligible baseline:

- Monopropellant system + cold gas thrusters system (same as for GAIA)
- Monopropellant system + FEEP thrusters system as in LISA Pathfinder
- Monopropellant system + Mini GIE (Giessen University or QinetiQ)

All of them comply in principle with the thrust and minimum technology readiness level requirements.

The trade-off among the proposed systems has been based on:

- Mass
- Tank volume
- Power required
- Technology readiness level and flight qualification by the launch date of WFI

The following table reports the main parameters used for comparison in the case of the cold gas and the FEEP systems.

	GAIA Cold Gas		FEEP	
		Note		Note
Dry mass (kg)	32.6		38.5	
Propellant mass (kg)	40.25		1.5	propellant is inside the thrusters
Power required (W)	35		120	
Volume req. (l)	210	2 tanks	NA	
Propellant type	N2		Cs	
Tested lifetime (h)	18000		9000	
TRL	5		5	

Table 8-4: Thrusters trade-off summary

The FEEP system is the lightest and does not require large volume for tank. However, it consumes a significant amount of power during operation. In addition, due to the use of Cesium as propellant there is a (low) risk of contamination.

Overall, both systems could be foreseen for this mission. The final choice is left for future design phases. The WFI mission design presently cannot accommodate both systems being sized for the worst case among the two in terms of mass, volume and power.

In the following sections the different options are described in detail.

8.1.4.1 Monopropellant + GAIA cold gas thrusters system

The system includes:

- 12 Thrusters
- 2 tanks. The dimensions of each tank are in the order of Ø 424 mm x 752 mm.
- A feed system

The maximum amount of propellant considered is 40.2 kg (including margin of 2%).

The total DRY mass allocated for the 'monopropellant + GAIA cold gas thrusters system' (worst case of the three options suggested as baseline) can be found in Table 8-5.

Element 1	WFI Spacecraft		MASS [kg]				
Unit	Unit Name Click on button above to **insert new unit**	Quantity	Mass per quantity excl. margin	Maturity Level	cell name	Margin	Total Mass incl. margin
1	Monoprop Thrusters	8	0.2	Fully developed	e1_unit1_margin	5	1.8
2	Monoprop Other Dry Mass	1	11.8	Fully developed	e1_unit2_margin	5	12.4
3	Monoprop Tank XMM	1	8.5	Fully developed	e1_unit3_margin	5	8.9
4	GAIA Cold Gas Thrusters	12	0.1	To be developed	e1_unit4_margin	20	1.4
5	Cold Gas Tank	2	12.7	Fully developed	e1_unit5_margin	5	26.7
6	Cold Gas Feed System	1	6.0	To be modified	e1_unit6_margin	10	6.6
-	Click on button below to insert new unit		0.0	To be developed	Do not use	20	0.0
SUBSYSTEM TOTAL		**6**	**54.7**		e1_ss_tot_margin	**5.9**	**57.9**

Table 8-5: "Monopropellant + GAIA Cold Gas Thrusters" DRY Mass budget

A total propellant mass of 40.2 kg is estimated for the GAIA cold gas thrusters system.

A total system WET mass of 128 kg is estimated for the entire "monopropellant + GAIA cold gas thrusters" system.

A scheme of a possible feed system is shown in Figure 8-13.

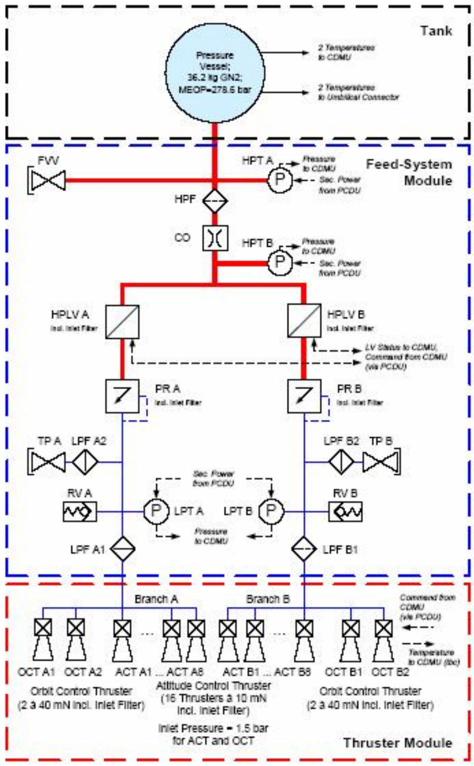

Figure 8-13: Cold gas feed system example

8.1.4.2 Monopropellant + LISA PF FEEP thrusters system (ALTA, ARC)

The system includes:

- 16 FEEP thrusters required to satisfy thrust range requirements (LISA PF and GAIA thrust requirements are in the range of 1µN-250µN). Four LISA PF EPSA will be used.

A total wet mass of 40 kg is estimated for the LISA PF FEEP thrusters system.

The consumption of power (worst case of the three options suggested as baseline) comply with the system budget.

Mode 5 Power Consumption (on)	120.000	W
Mode 5 Power Consumption (stby)	70.000	W
Mode 5 Duty Cycle	20.000	%
Mode 6 Power Consumption (on)	120.000	W
Mode 6 Power Consumption (stby)	70.000	W
Mode 6 Duty Cycle	20.000	%
Mode 7 Power Consumption (on)	120.000	W
Mode 7 Power Consumption (stby)	70.000	W
Mode 7 Duty Cycle	20.000	%

Table 8-6: LISA PF FEEP Thrusters System Power Budget

Particular care has to be taken for the positioning of the EPSA on the S/C to avoid possible contamination issue.

8.1.4.3 Monopropellant + Mini GIE system (GIESSEN University, QinetiQ)

The system includes:

- 12 mini GIE thrusters (for the Giessen University System 3 Thruster Assembly are considered)
- 1 tank
- 2 Flow control units for each TA (Giessen University system)
- Harness and piping

Differential Mode Operation is required by the Giessen University system to comply with SRP thrust range (Itot = 27098 Ns + 170292 Ns).

A total wet mass of 40 kg is estimated for the mini GIE system.

The system complies with the TRL requirement. A GSTP contract for the design, development and test of a mini ion engine system is foreseen starting in 2006 to reach TRL 5 in 2007.

8.1.5 Options

Other options have been considered during the trade off analysis on the propulsion technologies eligible for WFI mission:

- Monopropellant + GOCE Cold Gas Thrusters System: option discarded because of the thrust throttling requirements
- Monopropellant + ALTA Mini HET System: option discarded because of thrust range requirements and resolution requirements
- All Gaia Cold Gas System: option discarded because of mass/volume constraint
- All Lisa PF FEEP Thrusters System (ALTA FEEP or ARC FEEP): option discarded because of time required for launcher dispersion and orbit maintenance
- All Mini GIE System (Giessen University or Qinetiq): option discarded because of time required for launcher dispersion and orbit maintenance

8.2 Mechanisms

The following mechanisms are required onboard the Service Module:

- Antenna pointing mechanism for High Gain Antenna (HGA)
- Baffle cover hold down and deployment mechanism

8.2.1 HGA Pointing Mechanism

The Antenna Pointing Mechanism (APM) shall be used to point the antenna towards the Earth during operational phase. In particular, the APM shall be able to deploy and trim the High Gain Antenna around two axes with:

- Azimuth: ± 60 °
- Elevation: ± 35 °

Two hold down and release mechanisms will be required, together with the APM to stow the antenna of 0.7-metre diameter during launch. The deployment is foreseen during the initialization mode.

For the above mentioned functions, the foreseen HGA mechanisms are:

- 1 two-axis pointing mechanism with associated electronics
- 2 hold-down and release mechanisms

8.2.2 Cover Door Hold-Down and Deployment Mechanism

The main function of the cover door is to protect the telescope optics during ground testing and launch against contamination. The cover door needs to be held-down during launch against the baffle and must be deployed in-orbit. After deployment the door shall be fixed in open position, and re-closing is not required. The cover door is ± 3.0 metre diameter.

8.2.3 Assumptions and Trade-Offs

The approach which has been followed to identify the conceptual design for the WFI mechanisms is to use as far as possible qualified, off-the-shelf equipment, in order to reduce cost, procurement time and development risks. In case no qualified equipment is available the starting point for the development will be similar already qualified parts.

8.2.4 Baseline Design

8.2.4.1 Antenna pointing mechanism

Baseline for the design will be the Rosetta 2 axis pointing mechanism. It is mainly composed out of two identical rotary actuators powered and controlled by a dedicated electronics (APME). The two actuators are oriented 90° to each other and have the following rotational ranges, azimuth (space craft axis) ±170º and elevation (spacecraft axis) ±150º. The antenna pointing is carried out by a stepper motor with an integrated planetary gear, an anti-backlash pinion and a main gear with a reduction of 2600. The absolute position is measured with a 16 bits optical encoder. Integrated into the APM are rotary joints for the routing of the wave-guides and the coaxial cable as well as cable wraps for a stress free routing of the electrical harness.

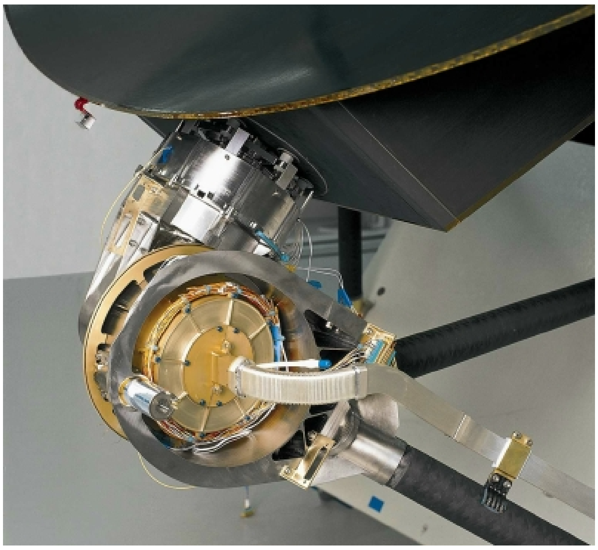

Figure 8-14: 2-Axis Pointing mechanism used for Rosetta

The pointing accuracy of the mechanism is 0.01º, the total accuracy is also linked to the design of the brackets under thermal behaviour and can be a factor 2 or 3 of the actuator capability.

The antenna pointing mechanism will deploy the antenna to its required operational position. No additional device is required, and the deployment can be achieved within a few minutes after release of the hold-down points.

Two standard hold-down and release points will be used to stow the antenna and the pointing mechanism together on the spacecraft during launch in order to provide adequate stiffness and strength. Each hold-down point will be based on a pyro or similar release device to initiate the separation.

8.2.4.2 Cover door hold-down and deployment mechanism

To minimize its complexity i.e. number of mechanisms, the baseline cover concept consists of one single door protecting the aperture.

The main elements of the cover door are:

- Single cover door
- Deployment mechanism
- Hold-down and release system
- Additional hold-down point if necessary.

8.2.4.2.1 Cover Door

To protect the optics against contamination the COROT concept has shown that it is sufficient to cover the aperture fully without a gas tight closure of the baffle. The door has a rim which overlaps the baffle over a certain distance (20 mm) to ensure full protection against contamination. A gap between the baffle and the door rim ensures proper venting of the baffle. The cover door itself will be made of CFRP sandwich structure.

8.2.4.2.2 Deployment Mechanism

The baseline design solution for the cover door is a deployment mechanism based on springs. To overcome the high deployment shocks, which are the main disadvantage of a spring driven deployment, the springs are integrated in a regulated deployment mechanism. This is a cost effective fully qualified concept for deployment of appendages. Its main function is to regulate the deployment and minimize the shock at the end of deployment. The deployment regulator is based on a low melting metal alloy installed in a cavity between two parts that can rotate with respect to each other when that low melting alloy allows it. Figure 8-15 below shows the two main components of the deployment regulator.

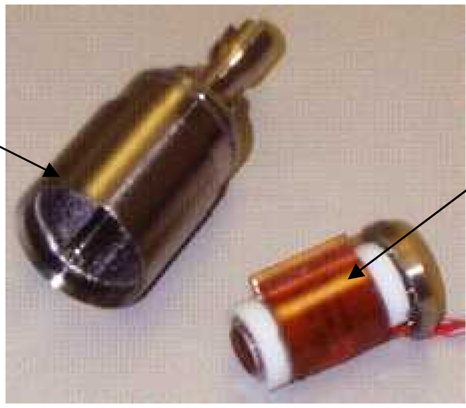

Figure 8-15: Cover deployment regulator main components

In Figure 8-16 the complete mechanism including springs and hinge are shown. For the cover door mechanism it is recommended to use one hinge with spring and regulator and one hinge with spring and without regulator. Modification of the basic hinge design is most likely required to fit the mechanism within the small available envelope. Integration of the hinges in one bracket is a possible solution to minimize the size.

Deployment regulator main characteristics are the following ones:

- Compact <Ø 39x70 mm
- Low mass < 240 grams, including hinges 2.5 kg
- Peak maximum input torque:20 Nm
- Continuous maximum input torque: 14 Nm
- Power: selectable from 10 W to 20 W (depending on the required deployment time
- Deployment time adjustable from 1.5 minutes at +60°C and 20 W to 45 minutes at -40°C and 10 W (for 180°)
- Shock at the end of deployment, angular velocity (at 180°) 0.5 °/sec to 3 °/sec
- Temperature range:
  - Operational from -40°C to +65°C
  - Non operational from -100°C to +100°C
- Mechanical qualification environmental test:
  - Sin vibration: 20 g

- Random vibration 20.5 g_{RMS}
- Quasi static: 20 g

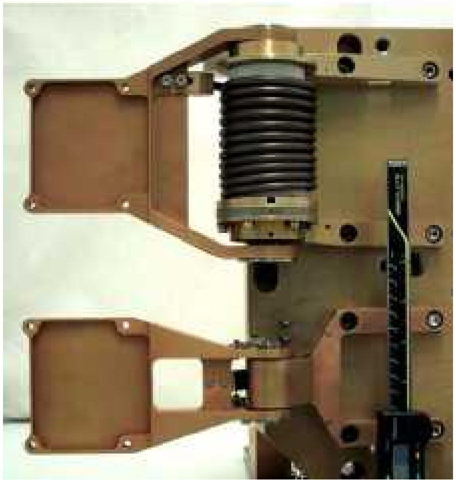

Figure 8-16: Cover deployment mechanism (active and passive hinge)

8.2.4.2.3 Hold down and release system

A simple and reliable solution for the hold down and release of the cover door is the concept used for the COROT mission, presented in the picture below.

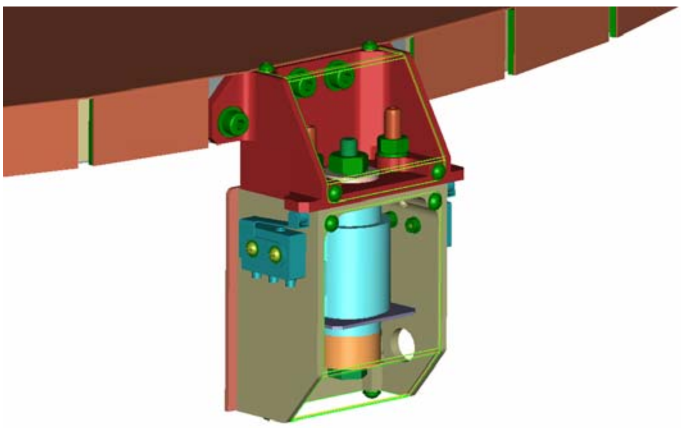

Figure 8-17: **COROT holdown and release device**

The Frangibolt actuator comprises a cylinder of Nitinol (Nickel-Titanium) SMA and a specially designed (integrated) heater (28 Vdc, 80 W). A redundant heater is implemented in the actuator. By heating, the SMA cylinder elongates to fracture a bolt element thereby achieving deployment of the cover. At minimum temperature (-65°C) and minimum voltage of 21.5 Vdc the Frangibolt will actuate in 250 seconds. The total displacement is about 1mm and the bolt fractures at 0.5 mm. At normal voltage (28 Vdc) and –60°C the Frangibolt actuates in 150 seconds.

Figure 8-18 below shows the cross section of a typical Frangibolt joint assembly.

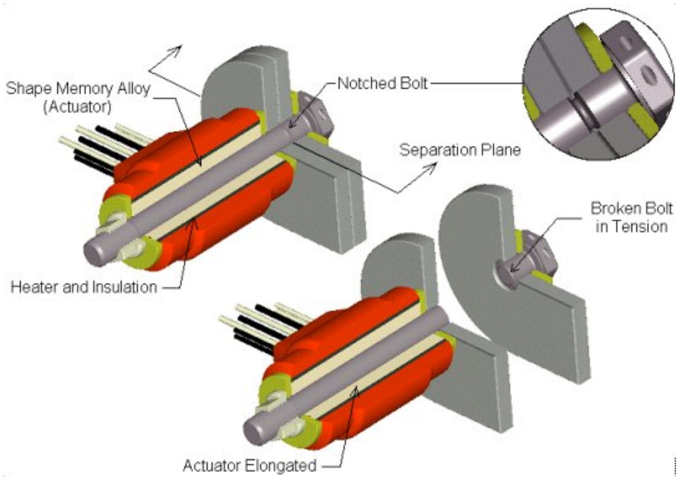

Figure 8-18: Frangibolt

When fully deployed the cover is latched on the external side of the baffle to reduce disturbances to be compensated by the attitude control system. This mechanism has not been assessed in detail in this study.

8.2.5 List of Equipment

Table 8-7 shows the list of equipment associated with the Service Module mechanisms.

WFI		MASS [kg]			
Unit Name	**Quantity**	Mass per quantity excl. margin	Maturity Level	Margin	Total Mass incl. margin
Click on button above to **insert new unit**					
Cover door mechanism	1	3.5	To be developed	20	4.2
Antenna Pointing mechanism	1	7.0	Fully developed	5	7.4
APM electronics	1	4.4	Fully developed	5	4.6
Holddowns	2	0.5	To be modified	10	1.1
	0	0.0	To be developed	20	0.0

Table 8-7: List of equipment - mechanisms

8.3 Structures

8.3.1 Requirements and Design Drivers

- To guarantee the necessary spacecraft strength to survive all phases of mission lifetime (in particular the most critical: e.g. the launch) without failures
- To keep the structural stiffness within certain limits to guarantee the operational functionality of the overall system and avoid coupled resonant responses
- The structure mass shall be minimised
- Simple load path
- Provide support and containment for spacecraft units, equipment
- Provides mechanical support between Launch Vehicle (LV) and Payload Module
- Provides mechanical support to the Stray light baffle/cover/radiator assembly
- To prevent dynamic coupling of the spacecraft with fundamental modes of the LV, the Service Module should be designed with a structural stiffness which ensures that the fundamental frequencies of the spacecraft when hard-mounted at the interface are as follows:
  - in the lateral axis: $\geq$ 15 Hz
  - in the longitudinal axis: $\geq$ 35 Hz
- To accommodate a body mounted solar array of about 6 m^2 on surface (non-projected)
- To accommodate the 0.7 m 2 DoF HGA.

8.3.1.1 Design drivers

- Use of off-the shelf 1666-SF adapter of SOYUZ FREGAT incl. 1666H (EADS-CASA) separation system with a mass of 90 kg
- Payload Module misalignment requirements
- Dimension and mass of the Payload Module and the associated baffle.

8.3.2 Assumptions and Trade-Offs

An analysis of the Service Module structure requirements has shown that the GAIA SM structure could be used as a reference. The GAIA design taken as reference is as from the system level reassessment study of 2002. It is assumed that the same LV adapter will be used. Structural thicknesses have been recalculated for the WFI case. It should be checked at later stages of the project if the same layout could be baselined.

8.3.3 Baseline Design

Primary structure is broken down as follows:

- Central cylinder for axial loads
- Shear panel for axial loads
- Top panel for lateral loads
- SVM – PLM interface struts

The secondary structure includes:

- External baffle (incl. Cover)
- SVM external panels
- All SVM structures are made of Al sandwich with CFRP skins
- Baffle structure is in Al to minimise outgassing, increase conductivity (to achieve uniform temperatures) and simplify vanes attachment.

The interface with the PLM is based on six bipods in V-shape. The PLM ends of the rods are all connected together at the level of the optical bench.

8.3.4 Finite Element Analysis

A simplified FE analysis was performed to verify the structural layout. Figure 8-19 shows the finite element mesh of the Service Module.

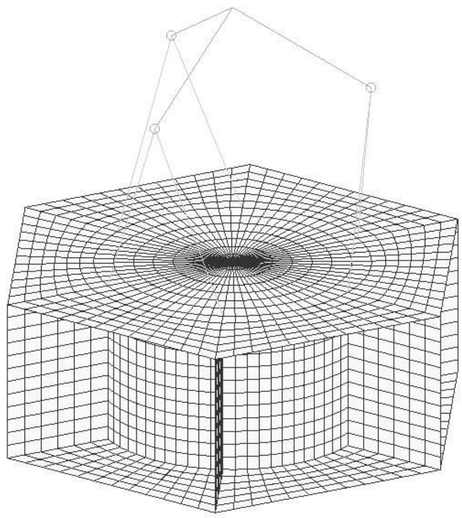

Figure 8-19: FE mesh of SVM

The following structural design was assumed for the analysis. The baffle was not considered.

	Facesheet	**core**
Central cylinder	CFRP - 3 mm	30 mm
Shear Panel	CFRP - 1 mm	20 mm
Top panel	CFRP - 0.5 mm	10 mm
Bottom Panel	CFRP - 0.5 mm	10 mm
External Panel	CFRP - 0.5 mm	10 mm
Struts	M55J laminate r=50mm, t=10mm	
PLM (lumped mass)	Connected via RBE2 element in FEM on 1.66 m above SVM	
Results: first lateral frequency: 36.7 Hz > 15 HZ req		

Table 8-8: Properties used in the FE analysis

Table 8-8 reports the results of the analysis showing ample margin with respect to the first lateral frequency.

MODAL EFFECTIVE MASS FRACTION

MODE NO.	FREQUENCY	X FRACTION	Y FRACTION	Z FRACTION	comments
1	36.70	0.000	0.845	0.000	1st lateral Y-mode
2	36.70	0.845	0.000	0.000	1st lateral X-mode
3	95.59	0.000	0.000	0.869	1st axial Z-mode
4	149.25	0.000	0.000	0.000	
5	150.12	0.000	0.000	0.000	
6	150.12	0.000	0.000	0.000	
7	151.92	0.008	0.000	0.000	
8	151.92	0.000	0.008	0.000	
9	153.16	0.000	0.000	0.000	
10	166.03	0.000	0.000	0.009	

Table 8-9: Modal Effective Mass Fraction

Extending the analysis to take into account the baffle still leads to first lateral frequency >15 Hz but the baffle vanes will need local reinforcements/thickening.

8.3.5 List of Equipment and Budget

Item	Nr.	M_struct [kg]	Material	Maturity	Unit Margin [%]	Unit mass with margin [kg]
EXAMPLE	2	9.49		Modification	10	10.44
SVM Central cylinder	1	60.20	sandwich	New dev.	20	72.24
SVM Shear Panel	6	2.88	sandwich	New dev.	20	3.46
SVM External Panel	6	3.25	sandwich	New dev.	20	3.90
SVM Top Floor	1	2.12	sandwich	New dev.	20	2.54
SVM bottom floor	1	2.12	sandwich	New dev.	20	2.54
SVM PLM I/F strut	6	4.87	M55J Laminate	New dev.	20	5.84
External Baffle (incl. Vanes)	1	173.10	sandwich	New dev.	20	207.72
External Baffle cover	1	20.57	sandwich	New dev.	20	24.69

Table 8-10: Structures equipment list

8.4 Power

8.4.1 Requirements and Design Drivers

The main functional requirements of the SVM power subsystem are listed below:

- The SVM power subsystem shall supply power to all the onboard equipments (payload and platform units) for the whole mission duration
- The SVM power subsystem shall have individual switching capabilities
- The SVM power subsystem shall include individual protections in order to isolate a failure and to avoid its propagation to other units
- The SVM power subsystem shall also have an interface with an EGSE for testing and with the launcher for the launch campaign

The selection of the technologies and the overall power system architecture is driven by the following additional requirements:

- The Technology Readiness Level 5 should be achieved by 2009
- The SVM Power system shall be sized for a nominal mission lifetime of three years with an extension of three years
- The SVM Power system shall be tolerant to single point failure
- The spacecraft position and attitude are constrained by the instrument operations requirements:
  - Spacecraft placed on a L2 orbit with the telescope axis pointing to the normal to the ecliptic plane by +/-20deg.
  - The spacecraft rotates by 90 degrees around the telescope axis every 3 months to keep the Sun aspect angle within the -45/+45 deg range (see Figure 8-20)
  - A power system margin of 20% shall be taken into account in the design of the EPS.

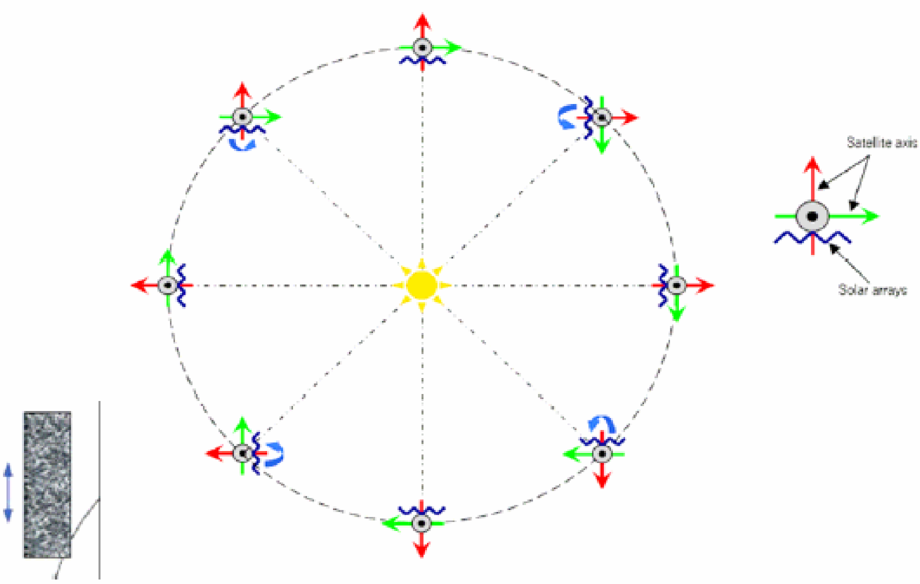

Figure 8-20: Spacecraft position and attitude

8.4.2 Power Requirements

The mission timeline has been divided in eight different functional modes that might be sizing for the power subsystem Table 8-11.

After the completion of the LEOP phase, the spacecraft will never have to cope with sun-occulted phases.

For each phase and each onboard unit, a power profile has been considered consisting of two levels of power consumption (for instance the ON and Standby status) with an associated duty cycle.

Those profiles have been first summed-up for each subsystem and then reported in Table 8-11.

Mode			Thermal	AOCS	Comms	Propulsion	DHS	Mech	Camera detector assembly	Spectrometer optics & detectors	Camera read-out electronics	Spectrometer read-out electronics	OBDH	Harness (excl. PSS)	TOTAL CONSUMPTION	Average Power
Launch Mode		Pon	0 W	0 W	97 W	0 W	35 W	0 W	0 W	0 W	0 W	0 W	0 W	3 W	135 W	
		Pstdby	0 W	0 W	10 W	0 W	35 W	0 W	0 W	0 W	0 W	0 W	0 W	1 W	46 W	
		Duty Cycle	0 %	0 %	0 %	0 %	0 %	0 %	0 %	0 %	0 %	0 %	0 %		0%	
Tref	60 min	Total Wh	0 Wh	0 Wh	10 Wh	0 Wh	35 Wh	0 Wh	0 Wh	0 Wh	0 Wh	0 Wh	0 Wh	1 Wh	46 Wh	46 W
Initialisation Mode		Pon	205 W	6 W	97 W	0 W	35 W	0 W	0 W	0 W	0 W	0 W	0 W	7 W	350 W	
		Pstdby	0 W	6 W	10 W	0 W	35 W	0 W	0 W	0 W	0 W	0 W	0 W	1 W	261 W	
		Duty Cycle	100 %	0 %	4 %	0 %	0 %	0 %	0 %	0 %	0 %	0 %	0 %		4%	
Tref	60 min	Total Wh	205 Wh	6 Wh	13 Wh	0 Wh	35 Wh	0 Wh	0 Wh	0 Wh	0 Wh	0 Wh	0 Wh	5 Wh	265 Wh	265 W
Cruise Mode		Pon	205 W	6 W	97 W	0 W	35 W	0 W	0 W	0 W	0 W	0 W	0 W	7 W	350 W	
		Pstdby	0 W	6 W	10 W	0 W	35 W	0 W	0 W	0 W	0 W	0 W	0 W	1 W	261 W	
		Duty Cycle	100 %	0 %	4 %	0 %	0 %	0 %	0 %	0 %	0 %	0 %	0 %		4%	
Tref	1440 min	Total Wh	4931 Wh	137 Wh	317 Wh	0 Wh	840 Wh	0 Wh	0 Wh	0 Wh	0 Wh	0 Wh	0 Wh	124 Wh	6349 Wh	265 W
Stand By		Pon	260 W	6 W	97 W	0 W	35 W	0 W	0 W	0 W	0 W	0 W	0 W	8 W	406 W	
		Pstdby	0 W	6 W	10 W	0 W	35 W	0 W	0 W	0 W	0 W	0 W	0 W	1 W	317 W	
		Duty Cycle	100 %	0 %	4 %	0 %	0 %	0 %	0 %	0 %	0 %	0 %	0 %		4%	
Tref	1440 min	Total Wh	6246 Wh	137 Wh	317 Wh	0 Wh	840 Wh	0 Wh	0 Wh	0 Wh	0 Wh	0 Wh	0 Wh	151 Wh	7690 Wh	320 W
180 deg Slew		Pon	225 W	6 W	97 W	120 W	35 W	0 W	0 W	0 W	0 W	0 W	0 W	10 W	493 W	
		Pstdby	0 W	6 W	10 W	70 W	35 W	0 W	0 W	0 W	0 W	0 W	0 W	2 W	353 W	
		Duty Cycle	100 %	0 %	4 %	20 %	0 %	0 %	0 %	0 %	0 %	0 %	0 %		10%	
Tref	150 min	Total Wh	563 Wh	14 Wh	33 Wh	200 Wh	88 Wh	0 Wh	0 Wh	0 Wh	0 Wh	0 Wh	0 Wh	18 Wh	916 Wh	366 W
Imaging Mode		Pon	105 W	31 W	65 W	120 W	35 W	0 W	15 W	0 W	240 W	0 W	47 W	13 W	671 W	
		Pstdby	0 W	31 W	0 W	70 W	35 W	0 W	0 W	0 W	99 W	0 W	0 W	5 W	527 W	
		Duty Cycle	100 %	0 %	100 %	100 %	0 %	0 %	100 %	0 %	0 %	0 %	100 %		0%	
Tref	5760 min	Total Wh	10104 Wh	2995 Wh	6240 Wh	11520 Wh	3360 Wh	0 Wh	1410 Wh	0 Wh	9472 Wh	0 Wh	4512 Wh	992 Wh	50606 Wh	527 W
Spectrometry Mode		Pon	175 W	20 W	65 W	120 W	35 W	0 W	0 W	0 W	0 W	7 W	47 W	9 W	479 W	
		Pstdby	0 W	20 W	0 W	70 W	35 W	0 W	0 W	0 W	0 W	3 W	0 W	3 W	424 W	
		Duty Cycle	100 %	0 %	100 %	20 %	0 %	0 %	0 %	100 %	0 %	12 %	100 %		19%	
Tref	1440 min	Total Wh	4206 Wh	480 Wh	1560 Wh	1920 Wh	840 Wh	0 Wh	0 Wh	10 Wh	0 Wh	78 Wh	1128 Wh	204 Wh	10426 Wh	434 W
Safe Mode		Pon	260 W	6 W	97 W	0 W	35 W	0 W	0 W	0 W	0 W	0 W	0 W	8 W	406 W	
		Pstdby	0 W	6 W	10 W	0 W	35 W	0 W	0 W	0 W	0 W	0 W	0 W	1 W	317 W	
		Duty Cycle	100 %	0 %	18 %	0 %	0 %	0 %	0 %	0 %	0 %	0 %	0 %		18%	
Tref	60 min	Total Wh	260 Wh	6 Wh	26 Wh	0 Wh	35 Wh	0 Wh	0 Wh	0 Wh	0 Wh	0 Wh	0 Wh	7 Wh	333 Wh	333 W

Table 8-11: Power Budget

According to this table, the sizing mode in terms of energy and maximum power is the imaging mode. This mode will last nominally several days without interruptions. Therefore, the SVM power subsystem will be sized to fulfil the power level required during this phase which includes a data transmission sequence with Earth. Figure 8-21 shows the power profile during the imaging mode.

During imaging mode, the Camera read-out electronics has a high pulse profile, pulsing 15.6 sec every 125 seconds. After 1000 seconds, the scanning stops for 67 seconds (respectively 249 seconds after 2000 seconds); a power increase is then observed in the propulsion subsystem corresponding to the re-orientation of the spacecraft for the next scanning period.

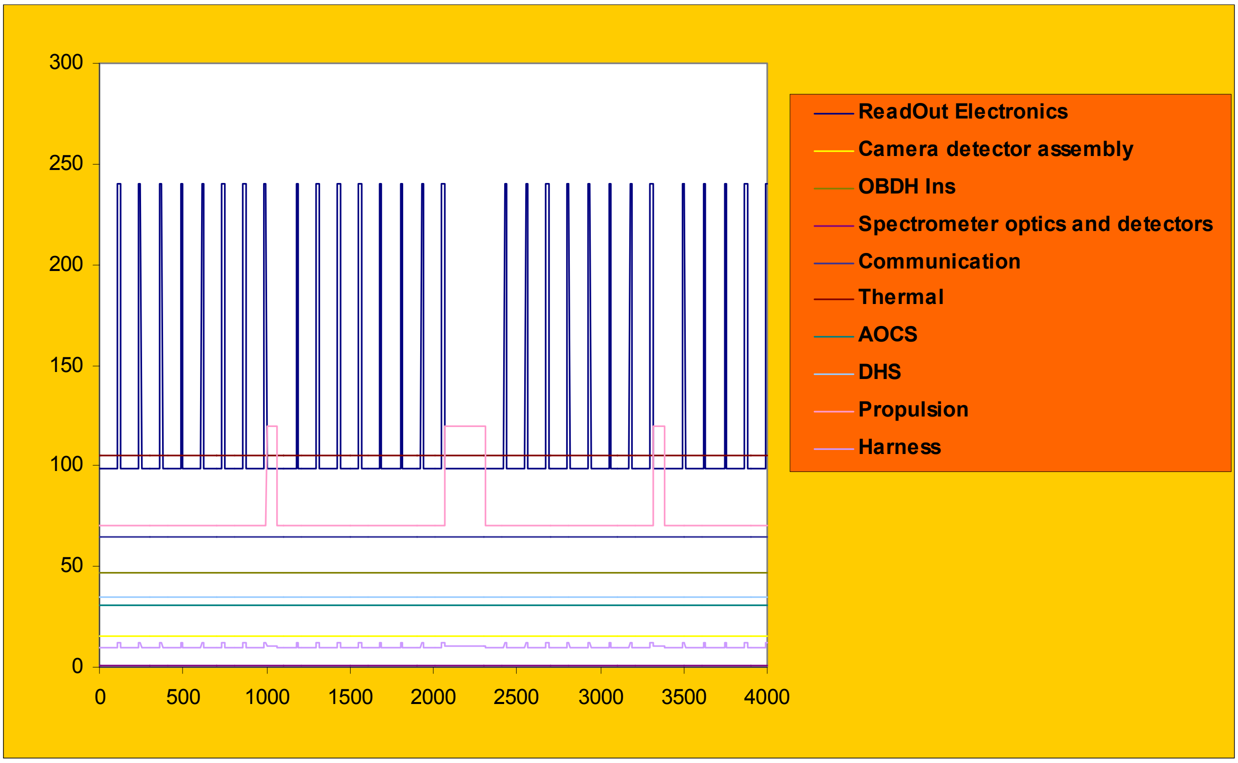

Figure 8-21: Power Profile during Imaging Mode

8.4.3 Assumptions and Trade-Offs

8.4.3.1 Power source technology

The power bus requirements and the constant good sun illumination conditions justify the selection of photovoltaic cells as the source of power for the whole spacecraft.

To simplify attitude control, a design with body-mounted cells is preferred to deployable panels. The reduction in performance due to higher solar cell temperature is counterbalanced by the mass saved by the lack of deployable mechanisms (hinges, springs, hold-down mechanisms….) and the structure.

Mounting cells on the telescope itself would generate additional complexity in thermal control. The AIT phase is also expected to be impacted by adding bus functions in the instrument module itself.

Hence, only a limited external area is available for body mounted photovoltaic cells: the external surface of the SVM. To overcome this limitation, high efficiency cells have been selected. AsGa

TJ cells with an efficiency of 28% in AM0 (25°C) conditions are currently in qualifications. According to the solar cells development technology roadmap, 30% can be confidently assumed to be reached in the timeframe of WFI.

The power generated by the solar array is computed accounting for the various losses (e.g. micrometeorites, mismatches, pointing error, radiations, thermal, coverglasses). Due to possible high sun inclinations conditions, the power generated is calculated according to Figure 8-22.

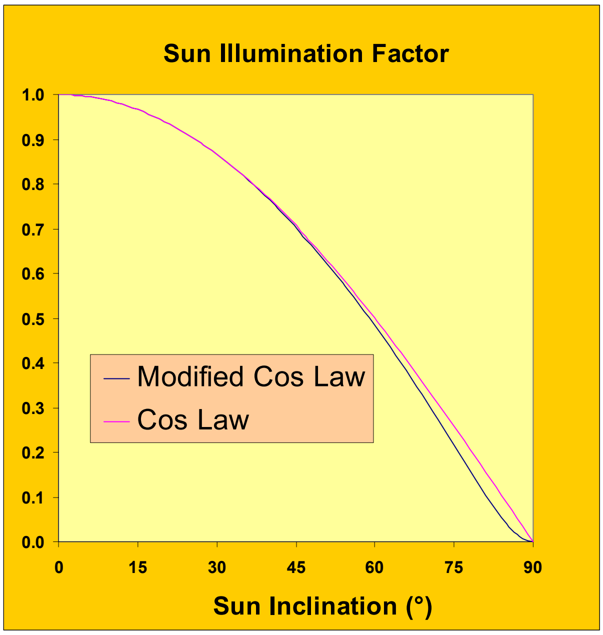

Figure 8-22: Modified Cosinus Law considered for solar cells power generation computation

8.4.3.2 Energy storage technology

An energy storage module is required to complete the power generated by the photovoltaic array for:

- The Launch and Initialisation phase
- The Safe mode (when the attitude of the spacecraft might be temporary lost)
- For supplying the pulse power required by the read out electronics
- For supplying the bus power during manoeuvring phases of the spacecraft (e.g. slew) when enough power generation is not guaranteed by the solar array.

The battery will be accommodated inside the Service Module and will only be deeply discharged a limited number of times.

The battery cells 18650HC performances are considered for sizing the energy storage module. These cells are commercial products already space qualified for various space missions (Venus Express, Mars Express, Cryosat…).

In order to comply with the single point failure tolerance requirement, a provision of 5% additional cells is considered in the battery design.

8.4.3.3 Power architecture selection

The most critical driver for power conditioning is the SA power transmission in Science Mode. Indeed, a conditioning with a good power transmission rate can cope with fewer cells and therefore will require less area on the external sides of the SM.

The other main criteria's highlighted are also:

- The total PCU mass
- The voltage quality delivered to the users
- The cost limitation (reuse of techno/concepts preferred).

According to these design drivers, the solar array is controlled by a shunt regulator rather than an MPPT system.

• Use of Serial Shunt Regulator	• Use of MPPT
– Lightest solution – Low power loss (<5%)	– Constant power loss (5-10%) – More flexibility in solar cells organizations – Optimal solution when the power is critical for a wide range of SA exposure conditions (e.g.: illumination, temperature) – Tolerance to a SPF means either: – Important Solar Array increase – Additional (heavy) MPPT modules in backup

Table 8-12: Trade between SA regulation by means of serial shunt modules or MPPT converters

The four most common power conditioning systems relying on SA shunt modules are listed in Figure 8-23:

- S3R Regulated: The bus is fully regulated but requires mass demanding BCR and BDR units.
- Hybrid Bus: Both a fully regulated and a non regulated bus are available for the onboard units. BDR units are needed to maintain the regulated bus when the solar array is not sufficiently illuminated.
- S4R Regulated: Same as S3R with the exception that the recharge of the battery is done via non used sections of the shunt module.
- S3R Unregulated: The lightest design. Indeed, no battery regulators are implemented and the bus is directly connected to the battery output. The mass benefit is counterbalanced by the loss of efficiency in the dedicated DC/DC converters supplying the units due to a wider input voltage range.

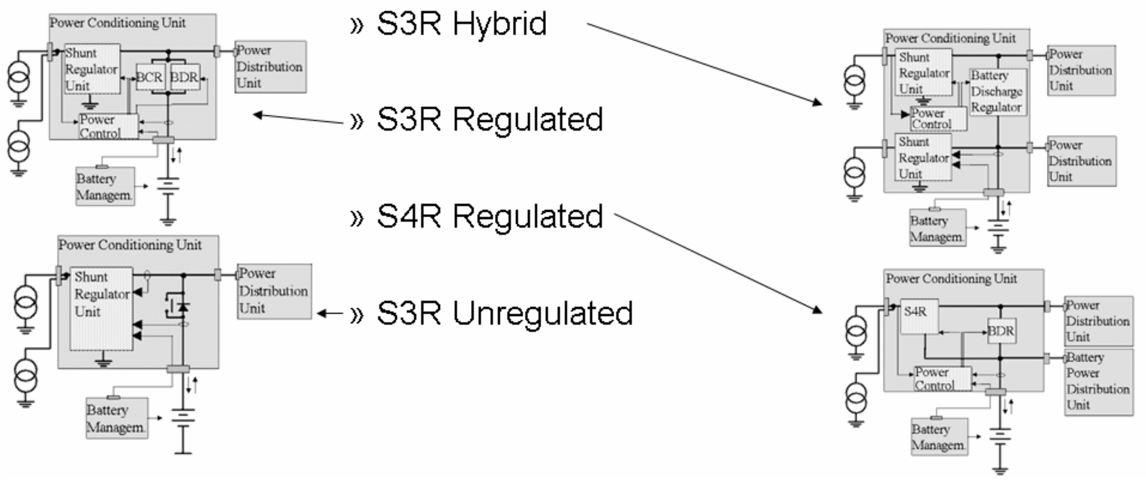

Figure 8-23: Topologies considered based on SA shunt regulation principle

According to the trade results (Table 8-13), the S4R Regulated architecture is the most advantageous topology for the need of the mission.

Factor		S3R Regulated	Hybrid Bus	S4R Regulated Bus	S3R Unregulated
3	*Mass*	0	1	1	2
2	*Voltage Range Science Mode*	2	2	2	1
1	*Voltage Range Non Science Mode*	2	2	2	0
3	*Efficiency (Science Mode)*	2	1	2	2
	Total	12	12	15	14

Table 8-13: EPS Architecture Trade Results

8.4.4 Baseline Design

8.4.4.1 Battery

The proposed battery module is composed of 105 Sony/AEA 18650HC cells assembled in 15 strings of 7 cells, including one extra string for redundancy purpose.

227 mm x 227 mm x 88 mm are the dimensions computed for such a battery module.

The nominal DOD reached during the LEOP phase is expected to be 73%. In case of failure of one cell, the battery discharge can rise up to 78%.

8.4.4.2 Solar Array

The body mounted cells are the drivers for the selection of the shape of the Service Module. In the operational mode, the spacecraft will have to cope with the following attitudes towards the sun:

- ± 45°in the ecliptic plane
- ± 20° with respect to the telescope axis in the plane horizontal to the ecliptic.

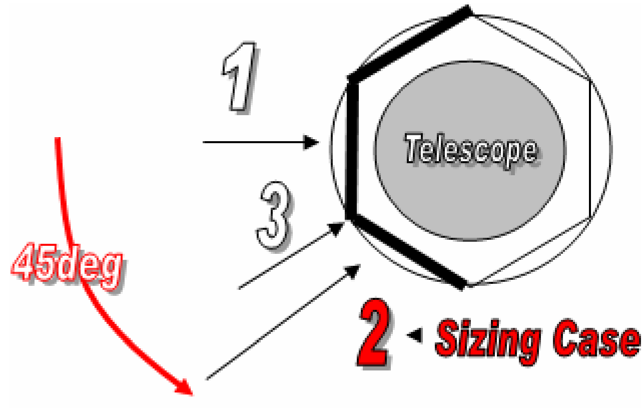

Figure 8-24: WFI Solar Array configuration

Different polygonal shapes for the service module have been traded considering the following factors: photovoltaic generation in all operational attitudes, SM internal clearance available for the onboard units, accommodation of the antennas, mass and complexity of the structure.

A hexagonal shape with solar cells mounted on three adjacent sides is a configuration optimising all these aspects.

A cylindrical shape has not been selected due to the fact that AsGa cells require a planar surface because of their limited bending capability. Furthermore, for onboard units this does not lead to good use of the internal volume.

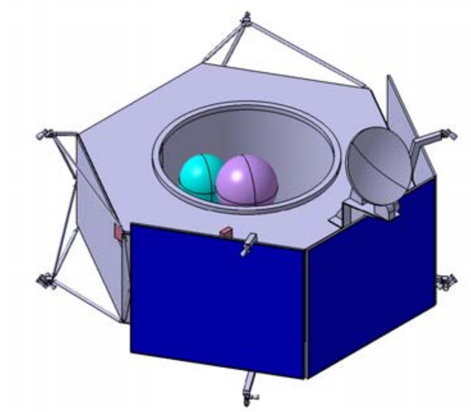

Figure 8-25: WFI Solar Array

The three solar panels mounted on the hexagonally shaped SM generate a good level of power in all attitude operational configurations. The computed identified worst case occurs near a 90° telescope reorientation manoeuvre when the sun inclination reaches 45° degrees and the S/C is tilted by 20° for scanning purpose (Figure 8-24). In this configuration, compared to a perfectly pointing single solar array and neglecting the thermal condition changes, still 52% of power is extracted from the solar cells.

Thermal analysis showed that the solar cells remain under 98 °C.

Compiling all these parameters with the expected degradation figures, a total area of $6.2m^2$ is required for the accommodation of the three panels in line with the Launcher fairing constraint.

8.4.4.3 PCDU

The Power and Conversion Distribution Unit (PCDU) is estimated to require a total of 11 boards. The current proposed PCDU is able to supply up to 48 5A range LCLs or 96 1.5A range LCLs outputs.

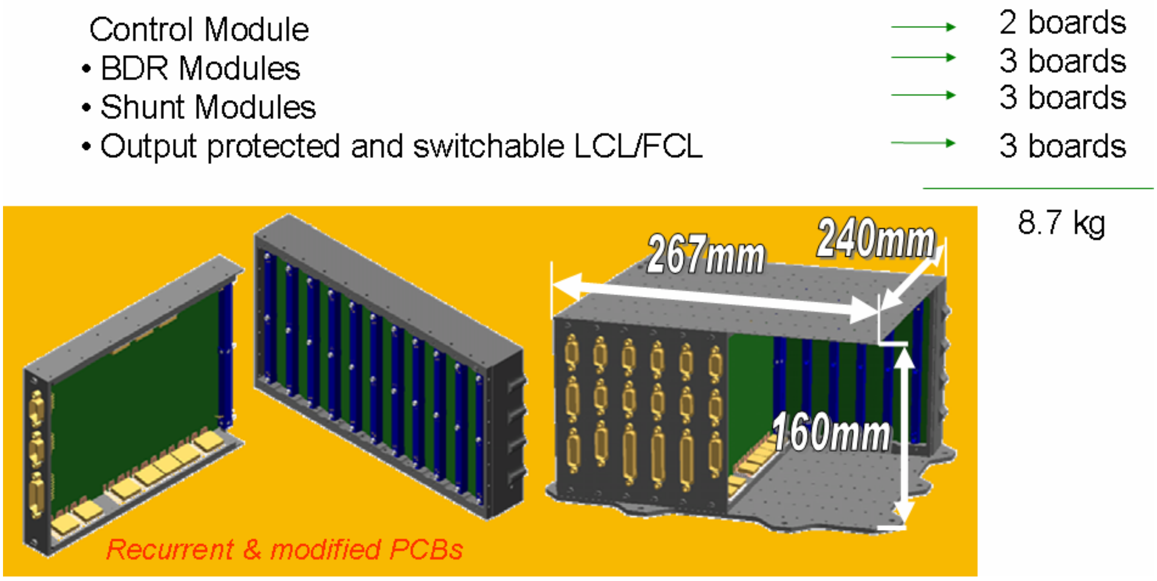

Figure 8-26: PCDU Module Description

8.4.4.4 Simulations results

The graphs of Figure 8-27 corresponds to the time simulation of the Imaging Mode where the following parameters are displayed (computed without the 20% system margin):

- the battery voltage
- the current voltage
- the battery depth of discharge
- the power required on the bus

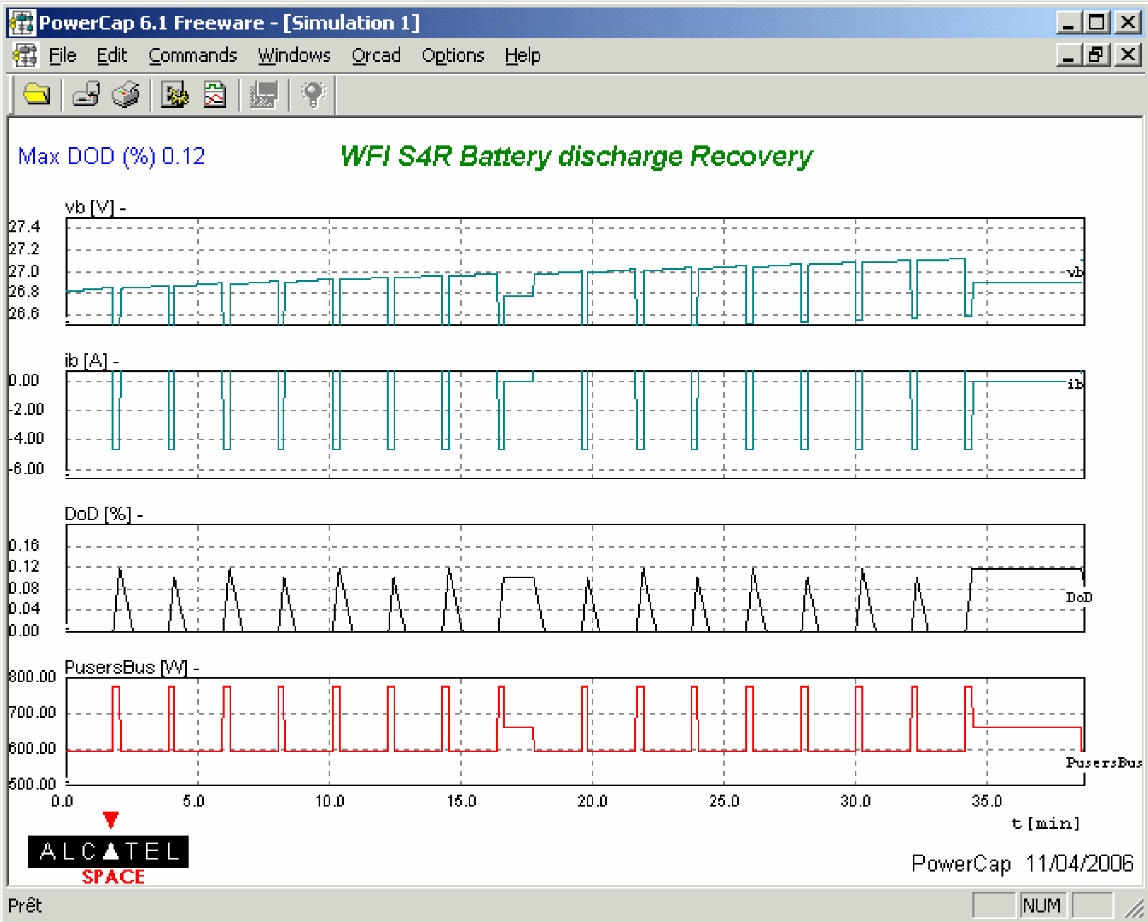

Figure 8-27: Design verification by simulation with the Powercap tool – DoD = Depth of Discharge

The simulation starts with a battery partially discharged. Concerning the voltage evolution, despite the pulses of the read out electronics the battery is nonetheless progressively recharging.

To supply these pulses, less than 0.12% of the total capacity is used.

8.4.5 List of Equipment

Table 8-14 gives a list of the power system equipment including masses and margins.

Element 1	WFI Spacecraft		MASS [kg]			
Unit	Unit Name Click on button above to insert **new unit**	Quantity	Mass per quantity excl. margin	Maturity Level	Margin	Total Mass incl. margin
1	Li-Ion Pack (18650HC) Standard A	1	5.4	Fully developed	5	5.7
2	Solar Array AsGa TJ	1	11.6	To be modified	10	12.8
3	PCDU	1	8.7	To be modified	10	9.5
4				Fully developed	5	0.0
5				Fully developed	5	0.0
-	Click on button below to insert new unit		0.0	To be developed	20	0.0
SUBSYSTEM TOTAL		**3**	**25.7**		**8.9**	**28.0**

Table 8-14: Power System: List of Equipment

The computation of 11.6 kg for the solar array does not include any support as this is already listed in the structure mass budget. Coverglass, adhesive, internal harness and diodes mass contributions are added to the mass of the bare solar cells.

8.4.6 Options: Deployed Solar Array

In order to validate the design choice, a solution relying on a deployed wing, mounted on a 1-axis SADM mechanisms, has been briefly assessed.

A 1-axis SADM will only compensate for the 90° sun drift. Indeed, the 20° inclination of the telescope to scan the whole required sky solid angle can not be compensated for.

Due to all the additional elements required by this type of solar array, despite the power solar panel surface required (3.4 m^2), the mass impact compared to the baseline design is over 18 kg.

In addition, as illustrated on Figure 8-28 other factors independent from the solar cells are justifying the rejection of the option: e.g. AOCS, clearance required for the stowed SA, reliability of the SA deployment mechanisms.

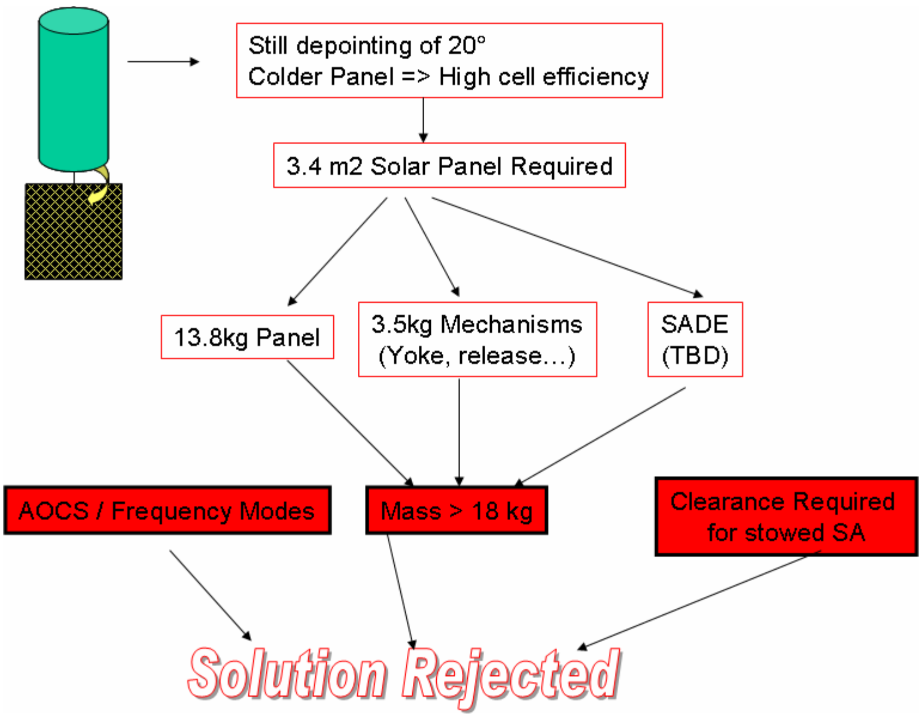

Figure 8-28: Optional Design with deployable SA

8.5 Telecommunications

8.5.1 Requirements and Design Drivers

- The TT&C subsystem shall provide two-way ranging and Doppler capabilities
- A high-rate science data downlink capable of 40 Mbps shall be provided
- To minimise the impact on science observations and power demand, daily contact time with groundstation should be limited to 4h
- Data rates for the telecommand uplink and housekeeping telemetry downlink shall be at least 4 kbps
- Omni directional capability for safety and LEOP shall be provided
- The TT&C subsystem shall show full redundancy except for the high gain antenna
- The maximum operational orbit distance is 1.6 million km
- Earth-pointing is not guaranteed during the whole mission
- Launch date in the 2015 – 2020 timeframe
- Minimum 4 hour communication window available with Cebreros Ground Station.

8.5.2 Assumptions and Trade-Offs

8.5.2.1 Frequency band selection

The occupied bandwidth in the band allocated to Category A Space Research missions (i.e. X-band 8450-8500 MHz) is limited to a maximum of 10 MHz. The maximum transmitted symbol rate in a system implementing GMSK modulation can be calculated as 11.6 Msps. In order to have some margin, **maximum symbol rate of 10Msps** is recommended.

The maximum information bit-rate in X-band, assuming that the maximum occupied bandwidth is available, can be calculated depending on the coding scheme selected.

The bandwidth limitation in the 8450 – 8500 MHz band imposes a maximum data downlink rate of about 6.54 Mbps. This does not meet the above downlink data rate requirements.

This analysis is based on current standard and supported modulation and coding formats. In the future, more spectral efficient modulation schemes (e.g. 8- or 16-APSK) might be available, allowing the transmission of more information within the 10 MHz bandwidth. For 8-PSK assuming a roll-off factor of 0.5, the spectral efficiency is (theoretically) increased a factor 3/2, allowing maximum 9.7 Mbps inside the 10 MHz band (assuming the same code rate). However, this comes at the price of a higher EIRP: for 8-PSK, about 2 dB more EIRP is required (to be delivered by 60% more transmitted RF power or an antenna with a 1.3 times larger diameter). For 16-APSK, about 13 Mbps could be fit into the 10 MHz band, but here at the expense of 4 dB more EIRP (over GMSK). As a conclusion, even with these schemes, reaching the required 40 Mbps in a 10 MHz band is not likely. Also, it is noted that these modulations schemes are currently not supported by ESA groundstation network.

In order to comply with the requirement for the WFI mission, a move to a higher frequency band is necessary. In particular, the Ka-band 25.5 – 27 GHz band (commonly called the ‘26 GHz band’) which has been allocated to Space Research and Earth Exploration Satellites Services, is considered to be the best candidate for the WFI mission.

The Ka-band 33.8 – 32.3 GHz frequency bands although an attractive candidate is strictly reserved for Deep Space, (defined to be beyond L2 by standards).

In conclusion, the selected frequency band for the high-rate science data downlink is the 25.5 – 27 GHz band. For the telecommand and housekeeping telemetry links, the normal X-bands are retained (7190 – 7235 MHz for uplink and 8450 – 8500 MHz for downlink).

8.5.2.2 Ground station selection

Possible ESA groundstations include: New Norcia (Australia) and Cebreros (Spain) which both host a large 35-meter diameter antenna.

At present, the ESA ground station network does not support reception of the 26 GHz frequency. Nevertheless, it is reasonable to assume that the Cebreros 35-meter groundstation will be upgraded to support the 26 GHz band should the WFI project make the explicit request and be willing to contribute financially. Also the third ESA 35m Groundstation, which is expected to be built along the American longitude and scheduled to be operational in 2011, is supposed to support reception at 26 GHz or at least could be easily upgraded to do so.

The visibility of the Cebreros G/S from the selected orbit is adequate and throughout the mission, daily passes with varying duration are guaranteed. Assuming a minimum elevation angle of 10 deg, mean pass duration of about 10h is obtained. Considering the minimum elevation angle of20 deg, the mean pass duration decreases to about 8.5h, this is still considered largely sufficient to comply with the science data return requirements.

In conclusion, the 35-meter Cebreros G/S is selected as the baseline.

Figure 8-29: Cebreros 35-meter ground station

8.5.3 Baseline Design

Figure 8-30 pictures the overall TT&C concept. It is based on a one-way, high rate downlink in the 25.5 – 27 GHz band for science payload telemetry and a two-way, low rate link in the X-band for TC, HK TM and navigation. Both the X-band and Ka-band links are from/to the Cebreros ground station.

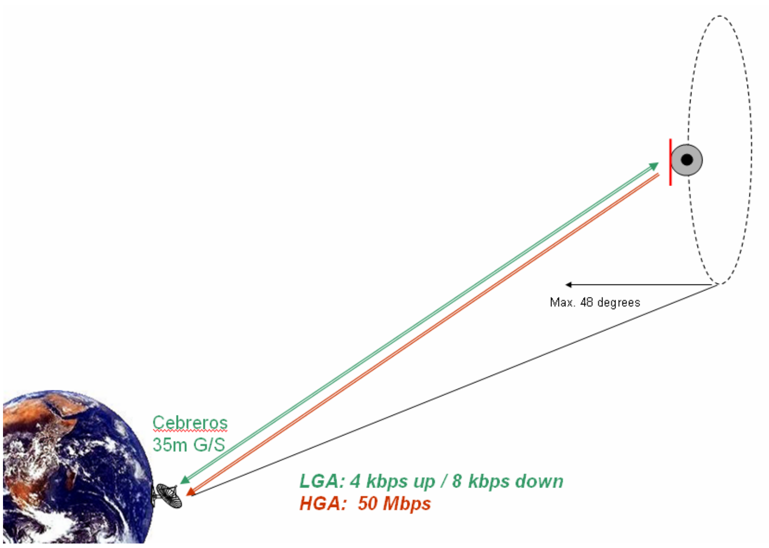

Figure 8-30: Overall TT&C concept

The maximum Earth visibility angle from the selected L2 orbit is 48 deg.

8.5.3.1 On-board TT&C subsystem

The on-board TT&C subsystem is based on:

- Two redundant X-band transponders for receiving telecommands, sending housekeeping telemetry and supporting two-way ranging and Doppler measurements.
- Two redundant 26 GHz telemetry transmitter for sending science payload telemetry
- Two redundant 26 GHz band TWTA’s
- One steerable HGA with dual feed X/26 GHz
- Two omni-directional LGA’s
- Radio Frequency Distribution Unit (RFDU)

The architecture of the on-board TT&C subsystem is shown in Figure 8-31:

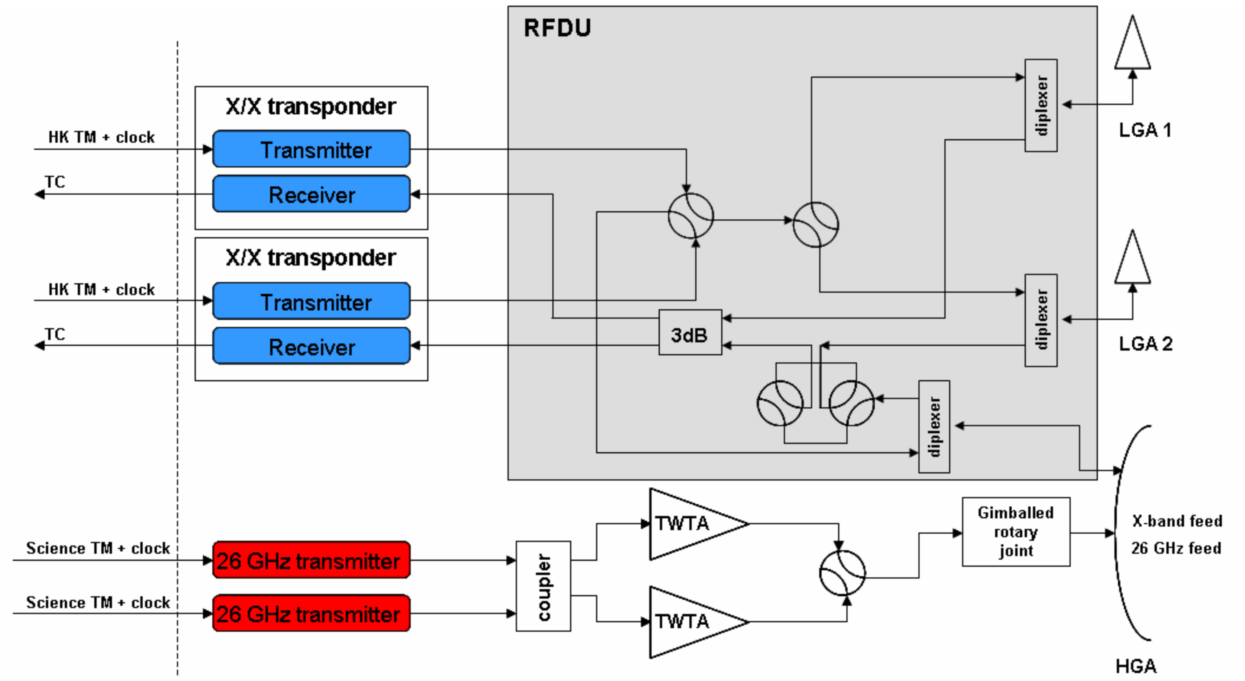

Figure 8-31: Architecture of on-board TT&C subsystem

The high rate science payload telemetry downlink is almost completely decoupled from the classical TT&C function, which is mainly provided by the two redundant X-band transponders. The downlink at 26 GHz is only available via a steerable HGA. The X-band up- and downlinks are available via the two LGA's which provide quasi omni-directional coverage during the LEOP phase and in emergency or safe mode situations. Although not strictly needed, it is pointed out that this architecture also allows the X-band links via the HGA.

8.5.4 Link Budget

8.5.4.1 Modulation and coding

The selected modulation schemes have been chosen from ECSS standard RD[38] considering that this is a CCSDS category-A mission. The used modulation schemes are:

- Telecommand uplink: NRZ/PSK/PM (sine), modulation index 1.0
- Housekeeping telemetry downlink: NRZ/PSK/PM (sine), modulation index 1.25
- Science payload telemetry downlink: SRRC-OQPSK with roll-off 0.5.

Note however that at present, no recommended modulation and coding schemes exist for the baseline 26 GHz band. Nevertheless, it is assumed that for this band as well, the standardisation bodies will likely recommend a modulation scheme which imposes efficient use of the available bandwidth, such as GMSK or SRRC-OQPSK. Since digital implementation of GMSK at 40 Mbps might be difficult, SRRC-OQPSK with roll-off = 0.5 has been selected as the baseline modulation scheme for the science payload telemetry downlink.

For downlink telemetry, the coding scheme selected is the CCSDS standard Convolutional-Reed Solomon concatenated code with interleaving depth I = 5 (see RD[39]). This coding scheme is compatible with the ESA ground network and guarantees a Frame Error Rate of 10^{-5} at Eb/N0 = 2.8 dB. More efficient coding schemes such as Turbo codes are possible candidates as well but as there is currently no commitment on future ground station support and the data rate to be supported is rather high, the current standard coding scheme is selected as baseline.

	TC uplink	HK TM downlink	Payload TM Downlink
Modulation	PCM/PSK/PM (sine)	PCM/PSK/PM (sine)	SRRC-OQPSK, roll-off = 0.5
Forward Error Coding	-	(CC(1/2,7),RS(255,223)) with I = 5	(CC(1/2,7),RS(255,223)) with I = 5
Link quality	BER $\leq 10^{-5}$	FER $\leq 10^{-5}$	FER $\leq 10^{-5}$
Synchronisation	ASM	ASM	ASM

Table 8-15: Selected modulation and coding scheme

The performance characteristics of the selected combination of modulation and coding scheme are summarised in the table below.

Modulation	Coding	Required Eb/No
SRRC-OQPSK with roll-off = 0.5	(255, 223) R-S and basic convolutional rate 1/2	2.8 dB

Table 8-16: Performance characteristic of modulation/coding scheme

8.5.4.2 Groundstation characteristics

The main characteristics of the Cebreros G/S in X-band are:

Transmission		Reception	
Frequency band	**EIRP**	**Frequency band**	**Effective G/T @ 20° elevation**
7190 - 7235 MHz	107 dBW	8400-8500 MHz	50.8 dB/K

Table 8-17: Characteristics of Cebreros groundstation in X-band

The reception characteristics at 26 GHz frequency are currently not known and are estimated for this study.

Reception	
Frequency band	**Effective G/T @ 20° elevation**
25.5 – 27 GHz MHz	53.7 dB/K

Table 8-18: Estimated Cebreros G/T at 26 GHz

8.5.4.3 Atmospheric attenuation

The figure below shows the total (including rain) atmospheric attenuation at 26 GHz.

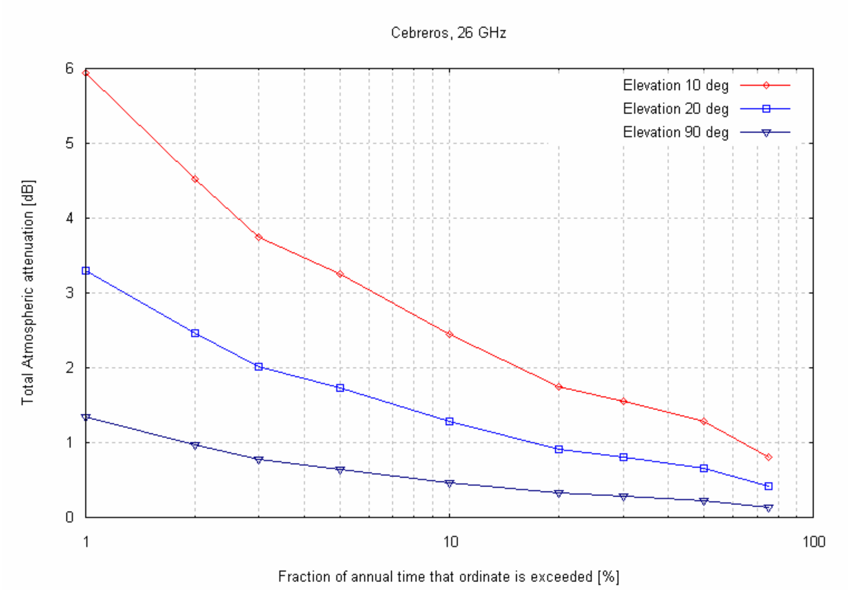

Figure 8-32: Simulated atmospheric attenuation at 26 GHZ

The atmospheric attenuation taken into account is 3.5 dB, corresponding to 20 degrees elevation and 99 % availability. If however 90 % availability is acceptable, an additional gain of about 2 dB can be appreciated.

8.5.4.4 Science payload downlink budget summary

Table 8-19 gives the summary link budget based on a data-rate of 50 Mbps. Assuming an overhead of 20 % due to packet headers/tails, attached synchronisation markers and re-transmissions, this means an effective data rate of 40 Mbps available for science return. Assuming daily communication with the ground station during 4hours is available; this leads to an *overall science return of 576 Gbit/day*.

Input	Value	Comment
Spacecraft EIRP	54.16 dBW	
Path loss	- 244.93 dB	1.6 million km
Atmospheric & Ionospheric loss	- 4.00 dB	3.5 atmospheric and 0.5 ionospheric
Groundstation G/T	53.47 dB/K	35-m Cebreros including pointing losses
Demodulator losses	- 1.00 dB	Assumption
Data-rate	76.99 dBHz	50 Mbps
EbN0	8.81 dB	
Required EbN0	2.8 dB	FER < 10^{-5}, standard ESA coding
Link margin	6.01 dB	Conservative value

Table 8-19: Science payload downlink budget

8.5.4.5 On-board transmit parameters

The spacecraft EIRP is to be provided by the combined effort of the transmitted RF power and the antenna gain and includes any losses in the transmit chain as well as pointing losses. The figure below shows the relation resulting in an EIRP = 54.16 dB (relevant to 50 Mbps) where 1 dB pointing and 1.48 dB transmit losses have been taken into account.

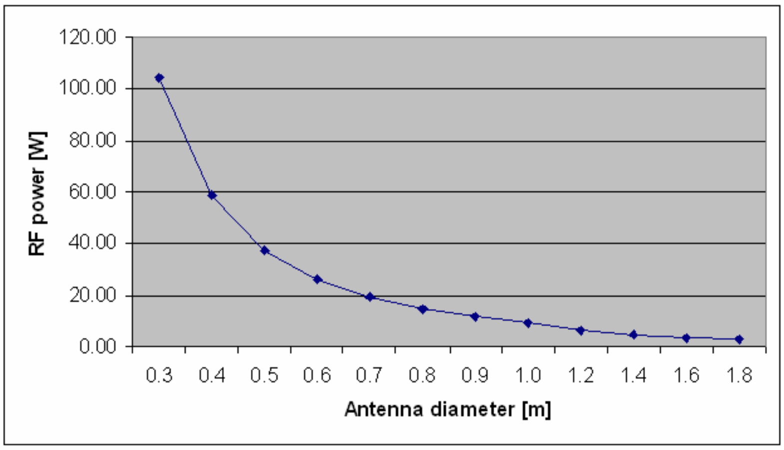

Figure 8-33: Relation between RF power and antenna size for EIRP = 54.16 dB

A rather large 0.7m dish antenna and 20 W RF power is selected as baseline.

Input	Value	Comment
RF Power	13.01 dBW	20 W RF power at amplifier output
Total transmit losses	-1.48 dB	
Antenna gain	43.63 dB	0.7 m dish with 65% efficiency
Pointing losses	-1.00 dB	Pointing accuracy > 0.3 deg
EIRP	54.16 dB	

Table 8-20: Ka-band transmit chain characteristics

8.5.4.6 TC/HK TM link budgets summary

The tables below give the summary link budget for the TC and HK TM links based on a data-rate of 4 kbps in the uplink and 8 kbps in the downlink. These values are considered more than sufficient to serve the needs of WFI.

Input	Value	Comment
G/S EIRP	99 dBW	Cebreros
Path loss	- 233.71 dB	1.6 million km
Atmospheric loss	- 1.0 dB	

Input	Value	Comment
Spacecraft Rx antenna gain	1 dB	At +- 60 from boresight
Total Rx losses	- 6.5 dB	
Spacecraft G/T	- 34.92 dB/K	
Modulation losses	- 4.12 dB	Modulation index 1.0, no ranging
Implementation losses	- 1.5 dB	Assumption
Data-rate	36.02 dBHz	4 kbps
EbN0	16.21 dB	
Required EbN0	9.6 dB	BER < 10^{-5}, no coding
Link margin	6.61 dB	> 3 dB

Table 8-21: Telecommand uplink budget

Input	Value	Comment
Spacecraft Tx power	7 dBW	5 W
Total Tx circuit losses	-3 dB	Conservative value
Spacecraft antenna gain	2 dB	At +- 60 from boresight
Path loss	- 235.11 dB	1.6 million km
Atmospheric loss	- 1.0 dB	
Groundstation G/T	50.85 dB/K	35-m Cebreros including pointing losses
Modulation losses	- 2.83 dB	Modulation index 1.25, no ranging
Demodulator losses	- 0.6 dB	Assumption
Data-rate	39.03 dBHz	8 kbps
EbN0	6.67 dB	
Required EbN0	2.8 dB	FER < 10^{-5}, standard ESA coding
Link margin	3.97 dB	> 3 dB

Table 8-22: Housekeeping telemetry downlink budget

Both link budgets show a comfortable margin > 3 dB. The tables above show the link budgets in absence of a ranging signal. It has been verified that also in the presence of a ranging signal, the link margin in both up- and downlink stays > 3 dB (for ranging modulation indices 0.7 and 0.5 in up and down respectively).

8.5.5 List of Equipment

8.5.5.1 Mass and power breakdown

Total mass with margin is 35.2 kg; in addition RF harness mass is estimated at 2 kg.

Element 1	WFI Spacecraft		MASS [kg]			
Unit	Unit Name Click on button above to **insert new unit**	Quantity	Mass per quantity excl. margin	Maturity Level	Margin	Total Mass incl. margin
1	X/X transponder	2.00	3.80	Fully developed	5	8.0
2	X-band SSPA	2.00	1.10	Fully developed	5	2.3
3	26 GHz transmitter	2.00	2.00	To be modified	10	4.4
4	26 GHz TWTA	2.00	2.50	To be modified	10	5.5
5	HGA	1.00	8.00	To be developed	20	9.6
6	LGA	2.00	0.30	Fully developed	5	0.6
7	RFDU	1.00	4.00	To be developed	20	4.8
8				To be developed	20	0.0
-			0.0	To be developed	20	0.0
SUBSYSTEM TOTAL		7	31.4		12.2	35.2

Figure 8-34: TT&C subsystem mass breakdown

Total power consumption during the 4 hours daily communications slots with the groundstation is 85 W. During normal TT&C, power consumption is limited to 55 W. The two X-band receivers are always ON which leads to a constant power consumption of 20 W.

Unit	Receive only	TT&C transmit &receive	Science data transmit	Comment
X-band TRSP1	10 W	25 W	10 W	From H/P
X-band TRSP2	10 W	10 W	10 W	
SSPA1	-	20 W	-	25% efficiency
SSPA2	-	-	-	
26 GHz Transmitter1	-	-	25 W	
26 GHZ Transmitter2	-	-	-	
26 GHz TWTA1	-	-	40 W	50% efficiency
26 GHz TWTA2	-	-		
Total	20 W	55 W	85 W	

Table 8-23: TT&C subsystem power breakdown

8.5.6 Options

8.5.6.1 Use of X-band

As an alternative to the baseline 26 GHz Ka-band, selecting the X-band for science payload data return would give increased ground station support as both New Norcia and Cebreros support X-band. Selecting X-band would also allow the re-use of the GAIA TT&C subsystem.

However, using the X-band would reduce the science data return by a factor of ten when sticking to current standard coding and modulation schemes. Even with increased downlink time and higher power consumption, the science data return would still be reduced by 80%. Aiming at higher order modulation schemes, 8-PSK could bring down this reduction to a factor of about 6.7

and with 16-APSK, only 5 times less science data is possible. Note however that moving to higher order modulations entails other issues such as increased sensibility to channel non-linearities (filtering, amplifier, phase noise,...) and higher required transmit power. In addition, these modulations schemes are currently not supported by ESA groundstation network. For these reasons, the use of the X-band is discarded.

8.5.6.2 Turbo-coding

Turbo-coding is not baselined because:

- Turbo codes are currently not supported by the ESA G/S network
- It adds complexity to the S/C.

Nevertheless, should the ESA DSN be upgraded in the near future to support Turbo-codes, the WFI mission should benefit from this and implement them on-board to save mass and/or power consumption.

8.5.6.3 Phased-array antenna

Instead of relying on a steerable dish antenna, another possibility is to have a phased-array antenna. The big advantage in this case is that there are no moving parts which can create vibrations and disturb the science measurements. Nevertheless, little technology heritage can be reused from GAIA and embarking a 26 GHz phased-array antenna on WFI would require a new development due to the new frequency band and very high EIRP (about 20 dB more than GAIA). For this reason, the phased-array antenna option was discarded in this study.

8.5.7 Technology Developments for the 26 GHz Band

As the 25.5 – 27 GHz band is fairly 'new', limited heritage is available. Nevertheless, as this band is also allocated to Earth Exploration Services and to (return) space-to-space inter-satellite links, Space Research missions such as WFI could benefit from developments that are made or are ongoing for these other types of missions. In particular:

- Earth Exploration Satellites are expected to move to 26 GHz in the coming years (cfr. GMES). As their data-rate requirements are far higher than is requested for WFI (about factor 10 higher), WFI could benefit from transmitter developments in this area. In this respect, high-rate transmitters prototypes are currently being developed in Europe e.g. at Tesat-Spacecom
- Some heritage in Europe in amplifiers working around 26 GHz is available from inter-satellite links such as Envisat – Artemis and Columbus – Artemis. As an example, Tesat-Spacecom developed a 53W TWTA in the frame of the Columbus project.
- Outside Europe, there is the NASA space network of TDRS satellites that has capability to send/receive in the 23 and 26 GHz bands. Also the NASDA ADEOS-II and the Japanese module of the ISS have the capability to communicate with Artemis in 26 GHz. Finally, also the James Webb Space Telescope baselines a high-rate data downlink at 26 GHz

In conclusion, developments for the on-board 26GHz equipment for WFI would be mainly 'delta'-developments, apart from the upgrade of the 35-meter Cebreros groundstation; although this cost as well might be shared with other Space Research missions that intend to move to the 26 GHz band in the coming years.

8.6 Data Handling

8.6.1 Requirements and Design Drivers

The following requirements drive the design of the SVM Data Handling:

- **Attitude & orbit**: SVM DH shall support the attitude control of the WFI Spacecraft during all mission phases.
- **Telecommands**: SVM DH shall include a central TC handler that receives all ground telecommands, analyses the packets and forwards them to the final destination. DH shall handle both the telecommands directed to the SVM and to the WFI Payload.
- **Telemetry**: SVM DH shall collect Housekeeping TM data of WFI spacecraft including payload, generates TM packets and route them to different virtual channels on the downlink to earth or to different packet stores in the mass memory. Essential TM cyclically stored without software intervention is also included.
- **Thermal control**: SVM DH shall be in charge to keep the spacecraft temperature inside definite limits by reading thermal sensors and controlling heaters.
- **On-board time**: SVM DH shall maintain a time reference whose value will be acquired and inserted into telemetry packets or distributed to the spacecraft units requiring it.
- **On-board storage**: The SVM DH shall provide sufficient onboard data storage capability, to store Housekeeping and compressed scientific data when adequate communications with ground is not possible.
- **Failure detection and recovery**: SVM DH shall include functions to monitor and reporting the WFI Spacecraft health status, functions to reconfigure faulty elements and functions for restoring the Spacecraft to a nominal state or to a safe state depending on the mission phase.
- **Autonomy**: The WFI spacecraft shall perform autonomously nominal operations when ground intervention is not possible. The WFI spacecraft shall remain safe for a period of at least three days, without ground intervention.

As for the payload Data Handling, the selection of the technologies and the architecture is driven by three main factors:

- The Technology Readiness Level 5 should be achieved by 2009
- The SVM Data Handling shall be tolerant to any single point failure
- The cost shall be kept at a minimum.

8.6.2 Assumptions and Trade-Offs

Typically the DH design provides an external redundant serial bus (MIL 1553 or CAN Bus) to provide an efficient means of communications for the control and monitoring of the principal platform and payload equipments. Platform or payload units can be also provided with dedicated RS422 serial links.

For the purpose of this design it has been assumed that the majority of connections will be via MIL STD 1553 bus. A more detailed trade-off between serial bus and dedicated point to point connections shall be performed during the next phase of the project.

8.6.3 Baseline Design

Two different boxes comprise the SVM data handling: the Mass Memory and the On Board Computer (OBC). The selected overall architecture is shown in Figure 8-35.

8.6.3.1 SVM Mass memory

The SVM Mass memory shall acquire, via high-speed links and store, the stream of compressed data from the Payload Computer.

The MM shall be conceived to simultaneously record data and to playback the stored data in formatted CCSDS standard to the transponder assembly.

The amount of data to be compressed by the Payload Computer every 1000s frame is about 12.2 Gbits. Assuming a compression factor of 1.5 (RD[22]) the MM input data rate is about 8.2 Mbps. Assuming a worst case of 24 hours communication outage, the storage requirement is about 700 Gbits.

The MM design is derived from Cryosat. Six Memory Modules 128 Gbits each are used for data storage. To have an EoL capacity of 700 Gbits an additional spare Memory Module is used in case one complete Memory Module fails. Each Memory Module is self standing and can be independently powered, operated and commanded.

The data interface with the SVM OBC is achieved via a redundant MIL-STD-1553 bus interface with Remote Terminal capabilities. One redundant SpaceWire link is used for data transfer with the Payload and one SpaceWire link connects the Telemetry Formatter to the Transponder.

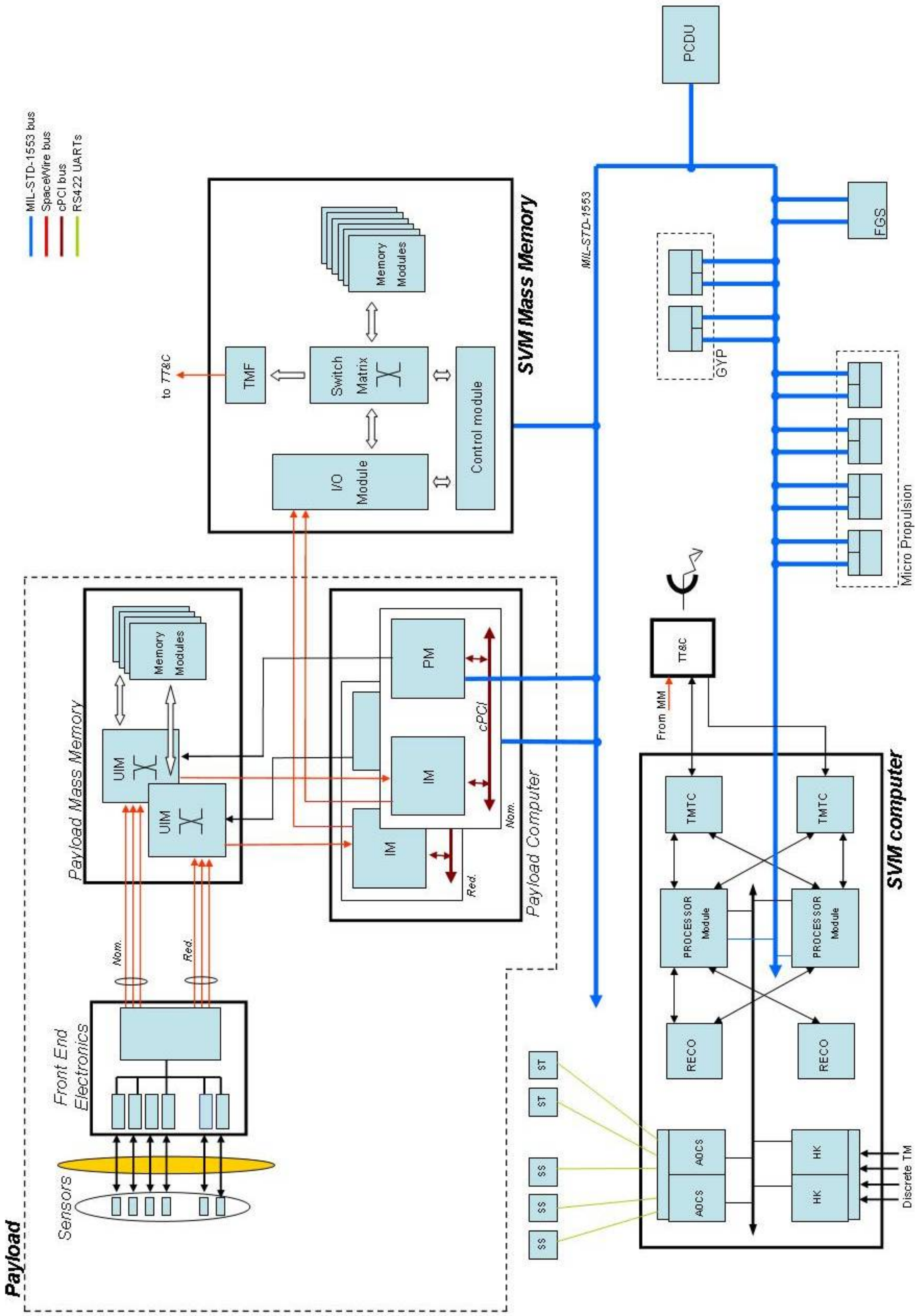

Figure 8-35: WFI Data handling overall block diagram

8.6.4 SVM OBC

There are a number of established suppliers of On-Board Computer (OBC) units, all of which offer internally redundant and fault tolerant designs. Each supplier has adopted generally similar internal unit architectures, based on core processor functions plus modular memory and external interface functions. This modular approach allows easy adaptation of their generic designs to meet the specific requirements of each programme.

The SVM OBC provide a redundant MIL 1553 bus to connect the payload computer, the SVM mass memory, the PCDU and a number of the individual AOCS equipments like thrusters, gyros and the fine guidance sensor equipment.

The OBC includes a telecommand decoder with both the packet telecommand decoder function and the Command Pulse Distribution Unit (CPDU) function. The CPDU is hard-wired and issues direct commands without any software involvement as part of the autonomous recovery sequences. The CPDU receives packets either from the telecommand decoder, the Reconfiguration Module (RM) or the active processor. The packet telecommand decoder receives data from the transponders, which are organised according to the ESA Packet Utilisation Standard (PUS).

The OBC also provides a direct telecommand function, which allows high priority commands to be received, interpreted and distributed by the OBC via purely hardware means without the needs for processor intervention. These direct telecommands are available internally for OBC configuration switching and externally for direct control of the principal WFI spacecraft equipments.

The telemetry encoder function is built according to the ESA Packet Telemetry Standard. TM data is packetized according to the ESA Packet Utilisation Standard (PUS). Usually the capability is implemented to transmit a group of selected housekeeping parameters also in case of unavailability of all on-board computers to allow ground control to assess the status of essential spacecraft items.

The OBC is equipped with nominal and redundant microprocessors; these are typically the ERC32 (SPARC RISC) single chip processor or the LEON2 processor. Performances are at least 15MIPS for the ERC32 and 86 MIPS for LEON2. All OBC suppliers are slowly upgrading their ERC32 based OBC to LEON processor. It is probable that at the time of WFI, all suppliers will offer both options.

The watchdog supervises the processor and the software. It has to be refreshed within a programmable time window to prevent from expiring and alarm triggering.

The timing and synchronisation function include the Local On-board Time (OBT) based on a hardware counter and the generation of a spacecraft synchronisation clock.

The reconfiguration function is handled by two hot redundant Reconfiguration Modules (RM) that process incoming alarms and generate CPDU packets for execution by the CPDU. Different packets can be generated for different alarm situations and for different hardware configurations. Each RM provides both internal and external alarm inputs. Typical internal alarms could be initiated by the software, processor module hardware alarms or power converter undervoltage detection.

A Safe Guard Memory (SGM) is normally provided as part of RM and operated in hot redundancy. The software reads from and writes into the SGM via the RM/Processor communication interface. Writing can be done in parallel such that the data are stored simultaneously in both SGMs.

8.6.5 List of Equipment and Budgets

Element 1	WFI Spacecraft		MASS [kg]			
Unit	Unit Name Click on button above to insert new unit	Quantity	Mass per quantity excl. margin	Maturity Level	Margin	Total Mass incl. margin
1	SVM computer	1	19.1	To be modified	10	21.0
2	SVM Mass Memory	1	18.6	To be modified	10	20.5
SUBSYSTEM TOTAL		2	37.7		10.0	41.5

Table 8-24: SVM Data handling mass budget

Element 1	WFI Spacecraft		
Unit	Unit Name Click on button above to insert new unit	Quantity	Ppeak
1	SVM computer	1	35.0
2	SVM Mass Memory	1	52.0
SUBSYSTEM TOTAL		2	87.0

Table 8-25: SVM Data handling power consumption

Element 1	WFI Spacecraft		DIMENSIONS [m]		
Unit	Unit Name Click on button above to insert new unit	Quantity	Dim1 Length	Dim2 Width or D	Dim3 Height
1	SVM computer	1	480.0	240.0	302.0
2	SVM Mass Memory	1	440.0	302.0	240.0
SUBSYSTEM TOTAL		2			

Table 8-26: SVM Data handling unit dimensions

8.7 AOCS

8.7.1 Requirements and Design Drivers

8.7.1.1 Functional requirements

The AOCS shall be capable of performing the following attitude and orbital control manoeuvres as a result of the observation strategy and the selected orbit and orbit injection:

- Accurate scan of the telescope line of sight (LOS) with a step of 300 arcsec
- Dithering of the telescope LOS with a step of 10 – 15 arcsec
- Slew manoeuvre of the telescope LOS at steps of 2, 5, 10, & 180 degrees, the exact slew steps could vary between 0 and 10 degree according to the actual spectrometer requirements and task scheduling
- Roll manoeuvre of the telescope around its LOS at a step of 90 degree
- Launcher and cruise dispersion correction in 3 axes
- Orbital maintenance during the whole mission life.

8.7.1.2 Performance requirements

To achieve the science observation target, the AOCS is required to have the following pointing performance during the science operation periods:

- **Absolute Pointing Error (APE)** is driven by the re-pointing capability of the spectrometer to a specified supernova, after scanning the sky. It is chosen as a fraction (1/3) of the field of view of the spectrometer. Thus the APE in line of sight is required to be below 1 arcsec (3σ).
- **Relative Pointing Error (RPE)** is driven by the fine pointing mode, where imaging is performed. To guarantee an acceptable blurring or smearing level of the imagine, the attitude movement is limited to be within 10% of one pixel (1σ) during the imaging process, thus the RPE requirement in LOS is set as:
  - 10 mas over 4000 second (1σ)
  - 30 mas over 4000 second (3σ)
- The RPE requirement around LOS is set as:
  - 1 arcsec over 4000 second (1σ)
  - 3 arcsec over 4000 second (3σ)

8.7.1.3 Design drivers

Clearly the RPE is the major design driver for the AOCS sizing. Meanwhile, the time-line allocation for each science operation, including scan, dithering, slew, etc, plays an important role in sizing the thrust levels. In summary, the following factors drive the AOCS design and sizing:

- The challenging RPE requirement drives the need for a dedicated Fine Guidance Sensor (FGS) to achieve such a high pointing accuracy, which is beyond the capability of available autonomous star tracker.

- The RPE requirement also drives the need for a micro-thrust propulsion system (at the level of a few hundred micro Newton) with an appropriate thrust resolution, to meet the pointing stability requirement.
- The orbital correction and maintenance requirement, on the other side, drives the need for a mini-thrust propulsion system, at the level of a few Newton, which unfortunately falls out of the scope of the micro-thrust system configured for the RPE accuracy, thus a hydrazine reaction control system (RCS) is configured as well, in parallel to the micro-thrust propulsion system.

8.7.2 Assumptions and Trade-Offs

The main assumptions are as follows:

- The service module / telescope can be treated as a single rigid body, that is, no flexibility effects are considered between and among the two parts of the spacecraft
- The optical system from the telescope is available for the fine guidance sensor, that is, FGS will share the same optical system with the telescope to achieve a high pointing accuracy
- The only external disturbance is a constant solar pressure
- Solar panel is fixed on the body of the service module, no appendages are applied on the spacecraft at all, that is, no flexible effects are considered for AOCS design
- There are no eclipses during the science operation period
- The pointing stability, not the pointing measurement accuracy or absolute pointing accuracy, is the primary driver.

8.7.3 Baseline Design

Two aspects dominate the AOCS design, one is the preliminary design of a dedicated FGS to provide the required high attitude pointing accuracy, the other is the definition of the specifications of a micro-thrust propulsion system to guarantee the continuous stability of the fine pointing during imaging process while meeting the requirement of operation time scheduling in term of thrust levels.

8.7.3.1 Fine Guidance Sensor (FGS)

The basic requirements and performance specifications are as follows:

- Use the same telescope optics, which provides a 2.15m aperture for light capture with a focal length of 20m
- The sensor head shall be placed on the same science instrument focal plane, to avoid extra optics and thermal design
- Only used for fine pointing during science operation (imaging, dithering, & spectrometering)
- It will be an ESA (customer) provided item with dual redundancy
- Pointing accuracy: < 5 mas (1σ) across boresight, 0.7 arcsec (1σ) around boresight Wavelength: Visible (350 to 1000 nm)
- FOV: 3.3x3.3 arcmin^2, driven by high probability of having at least 1 guide star in the FOV

- Readout: at ca. 20 Hz, to be decided by AOCS design
- Detector: proposed 2048x2048 pixel of 10 µm

To derive a baseline design of FGS, the following basic assumptions are made:

- No stray light is considered
- The temperature of the focal plane will be stable at 140 K, provided by the telescope thermal design
- There is zero contribution from structure, thermal and calibration residual effects
- S curve characterisation is avoided by over-dimensioning
- Identification of stars will be done on ground
- Angular rate is assumed to be less than 0.1 arcsec/sec to keep continuous FGS measurement accuracy
- PSF is between 20 and 50 microns diameter in focal plane – this is within the range needed by the FGS but limits the useable pixel size to 8 to 17 microns.
- Primary AOCS and initial calibration accuracies are sufficient to place the target stars in FoV of FGS.

With the above assumptions, the following baseline design is proposed:

- FGS consists of two independent systems. Each system consists of three measurement heads (MH) and one processing electronics.
- Each measurement head consists of a 1024x1024 pixel frame transfer CCD with the storage area covered from incident light, a Correlated Double Sampling Circuit and a 14 or 16 bit ADC. Estimated total size is 3cm x 3cm, estimated total power dissipation is 0.3 to 0.4 watts, and estimated total mass is 50g.
- Each processing electronics controls 3 MH. They perform a FoV search for star objects and report X, Y positions and total signal to ground. They will also perform single star tracking per MH, reporting X, Y and total signal. Measurements will be checked for disturbances due to SEU and will be flagged accordingly. Each processing electronics is expected to require 10 watts and have a mass of 2 Kg. Maximum separation between MH and processing electronics is expected to be 3 metres.
- The two FGS systems will both have the MH distributed around the edge of the payload FoV and may be operated in cold redundancy (for reliability) or together (hot redundancy - for increased sky coverage). The MH layout on the focal plane is illustrated in Figure 8-36.

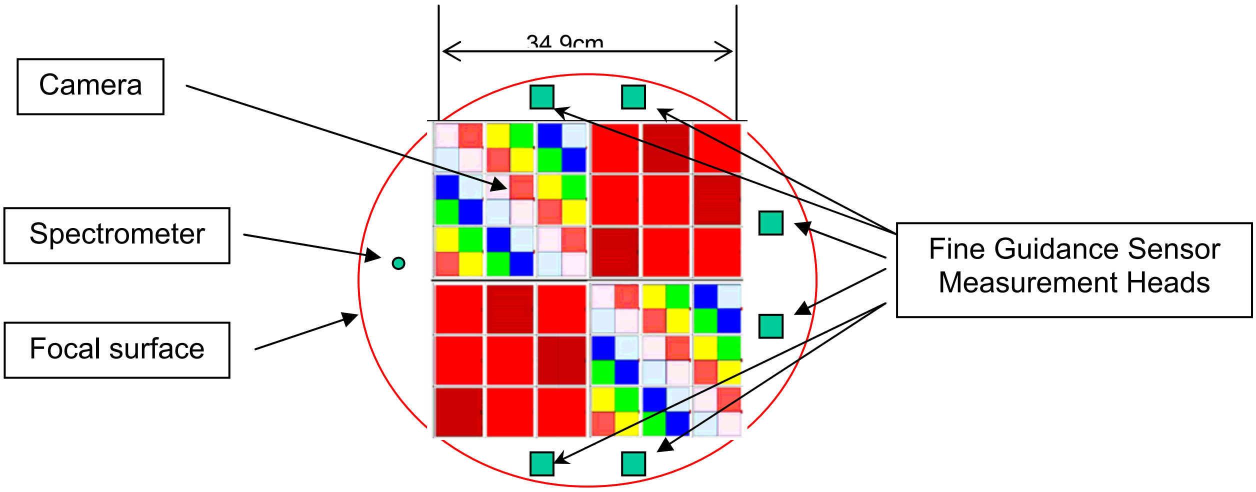

Figure 8-36: FGS MH layout in the focal plane

- As a baseline, each MH will be a 1024*1024 pixel CCD with 13 micron pixels. The FoV will be 0.13" per pixel giving a total FoV of 2.2 arcminutes per detector. A benefit would be gained in going to a smaller pixel size – 8 to 10 microns. Smaller than 8 should be avoided due to problems with the FoV size and accommodating the required small slews.
- Telescope distortion will be handled by calibration, while correction can be made in FGS electronics
- Sensitivity calculations are required in the next phase. Estimation of magnitude star that would give sufficient SNR in order to assess sky coverage
- The baseline integration time will be 100ms. This gives a limiting magnitude close to Mi 18. However, to obtain the required accuracy a brighter star, of magnitude 16.5 to 17 is required. The MH will be able to use stars between Mi 14 and Mi 18. Full sky coverage should be obtainable with Mi 16.5 to 17 for a system of three 2.2 arcminute sensors. A centroiding accuracy of between 20 and 25 is required for this system; a smaller FoV (i.e. smaller pixels) could reduce this to around 10 which eases the design and validation. Any increase in FoV requiring a factor greater than 25 can significantly increase the complexity and risk.
- Baseline operational concept shall be to filter 10 measurements to provide an effective measurement at 1Hz. This is expected to be a better approach than using a 1second integration time for the following reasons (though this should be traded off further in a later stage):
  - With use of low signal level stars at very low temperatures the readout and ADC noise are expected to be dominant, such an approach reduces these whereas increased integration time does not.
  - The scheme provides a robustness against SEU effects on the detector

The following areas require further investigation in next phase:

- Confirmation of sky coverage

- Production of detailed error budget and inclusion of PSF shape and distortion effects
- How the distortion effects will be calibrated on ground
- How the accuracy of the units will be tested on ground
- The calibration and operational procedure in orbit (current philosophy requires a high level of ground interaction)
- Iteration, with a wider base search, of the CCD choice.

The FGS concept presented above appears feasible without undue risk at this stage of the development. With the above baseline design, the pointing accuracy of 5 mas in LOS of below 0.7 arcsec, meeting the requirement, shall be achievable.

Moreover, rough calculation reveals that with the 3 MH being distributed around the edge of the focal plane, as in Figure 8-36, the FGS shall be able to provide roll attitude information (around LOS) of down to 0.7 arcsec, meeting the requirement of 1 arcsec around LOS.

The mass and power budget with the above baseline design is summarized in Table 8-27.

Items	No.	Mass [g]	Power [W]
CCD Head	6	50	0.4
Electronics	2	2000	10
Cables (6x3m)		1000	
Total w/o margin		5300	22.4*

* If cold-redundancy is used, the power consumption shall be 11.2W

Table 8-27: FGS mass and power budget

8.7.3.2 Coarse and fine control strategy

During the science operation mode, the telescope is required to repeat the scan step of 300 arcsec every 4000 sec, following by two continuous dithering of 10 arcsec along X and Y direction. Combining these two dithering steps, equals approximately one dithering step of 14.12 arcsec. These two fine attitude control manoeuvres require high pointing accuracy, especially for the dithering process, the RPE of 10 mas / 4000 sec is strictly required.

To keep continuous FGS pointing accuracy, the angular rate is limited to 0.1 arcsec/sec, therefore a 15 arcsec dithering needs at least 150 sec to perform, which puts a high pressure on the time-line task scheduling.

To have a quick dithering manoeuvre, an open-loop control scheme is proposed for the fine control operation, based on the available performance from the FGS baseline design. Before defining the control scheme, two control concepts are defined here:

- **Coarse control:** the attitude control manoeuvre based on the attitude measurement information from the on-board autonomous star tracker. No FGS measurements are used during this attitude manoeuvre. This control shall bring the attitude to be within 3 arcsec of the required pointing.

- **Fine control:** the attitude control manoeuvre based on the attitude measurement information from the FGS. This control shall be able to bring the attitude along LOS to be within 1 arcsec in absolute pointing error. With continuous FGS operation, this control shall be able to keep the attitude RPE to be within 10 mas.

8.7.3.3 Micro-thrust propulsion system

The RPE requirements drives a need for micro thrust propulsion system to compensate the solar radiation pressure and to stabilize the LOS pointing within its specification during imaging process. An analysis has been carried out to determine what thrust level and resolution is required, and what thruster layout can be configured. For the calculation, the assumptions listed in Table 8-28 were applied.

TERM	VALUE
S/C Mass [kg]	M = 1800
S/C Moment of Inertia [kg·m^2]	I_{XX} = 9000 I_{YY} = 9000 I_{ZZ} = 1500
S/C reflectance surface [m^2]	A_c = 17.58
S/C reflectance factor	k = 0.6
Solar Constant at L2 [W/ m^2]	Φ = 1340
Moment arm of SRP torque [m]	L_{SRP} = 0.53
Moment arm of micro-thrusters [m]	L_X = 2.26 L_Y = 2.26 L_Z = 1.0

Table 8-28: Assumptions for micro thrust specifications

The SRP force can be estimated with the following formula

$$F_{SRP} = (1+k)\frac{\Phi}{c}A_c \cos i = 1.26\times 10^{-4}\cos i \quad [\text{N}]$$

Where c is the speed of light in vacuum, *i* is solar incidence angle. For thruster sizing and total impulse estimation, the max SRP force at 0 incidence angle is applied, that is, 126 μN.

Since the RPE performance requirement on Z axis (around LOS) is 100 times less stringent than the X and Y axes (LOS direction), thus the sizing analysis is carried out on X and Y axes.

The rigid body angular kinematics is expressed by:

$$\Delta\theta = \frac{1}{2}\ddot{\theta}\Delta t^2 = \frac{\Delta F \cdot L_X}{2I_{XX}}\Delta t^2$$

Where $\Delta\theta$ represents the angular changes within a give time period of Δt. To meet the RPE requirement of 10 mas, the telescope LOS angular motion within a control cycle shall be less than half of the error budget, that is:

$$\frac{\Delta F \cdot L_X}{2I_{XX}}\Delta t^2 < \frac{1}{2}e_{RPE} = 0.5 * 48.5 \times 10^{-9} \text{ [rad]}$$

From the FGS baseline design, the attitude control bandwidth is set at 0.5 Hz, thus the corresponding control cycle will be roughly at Δt = 2 sec. Applied to the above equation, the level requirement on the micro-thrust level is determined as:

$$\Delta F < 0.5 * 48.5 \times 10^{-9} \frac{2I_{XX}}{\mathrm{L_X} \cdot 4} = 48.3 \times 10^{-6} \text{ [N]}$$

Considering a certain margin, the lower thrust level requirement on the micro-thruster system is set as 40 μN.

The upper thrust level is sized by a trade-off between the slew time, total impulse, and maximum angular rate that are all linked to the thrust magnitude by the following relations:

$$t = \sqrt{\frac{4\theta \cdot I_{XX}}{F \cdot L_X}}, \qquad E_{T.I.} = F \cdot t, \qquad \omega_{\max} = \ddot{\theta} \cdot \frac{t}{2} = \sqrt{\frac{F \cdot L_X \cdot \theta}{I_{XX}}}$$

Assuming the thrust varies from 100 μN up to 1200 μN, the corresponding attitude manoeuvre time at different slew steps are plotted in Figure 8-37, the corresponding total impulse are illustrated in Figure 8-38:, and the resultant maximum angular rates are illustrated in Figure 8-39:

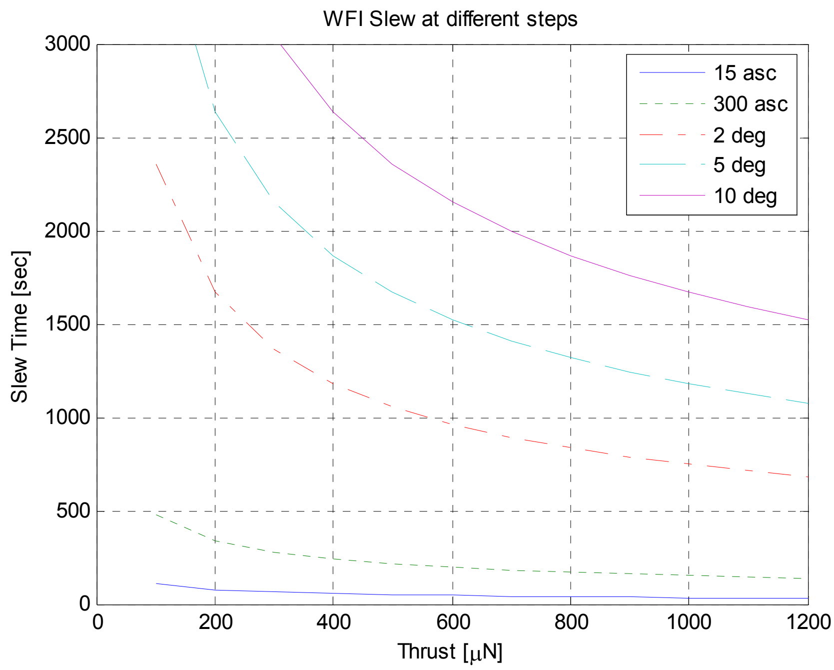

Figure 8-37: Slew time at different steps and thrust levels

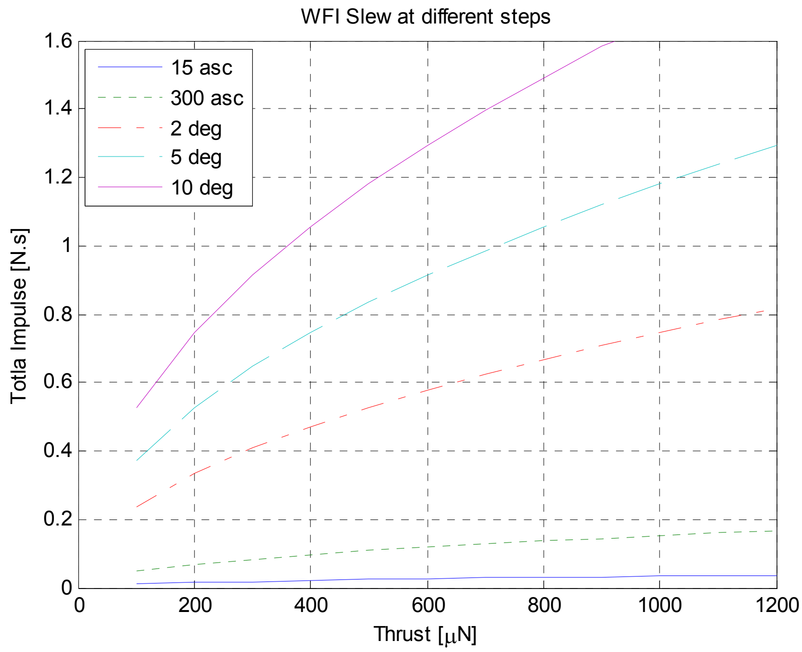

Figure 8-38: Total impulse at different steps and thrust levels

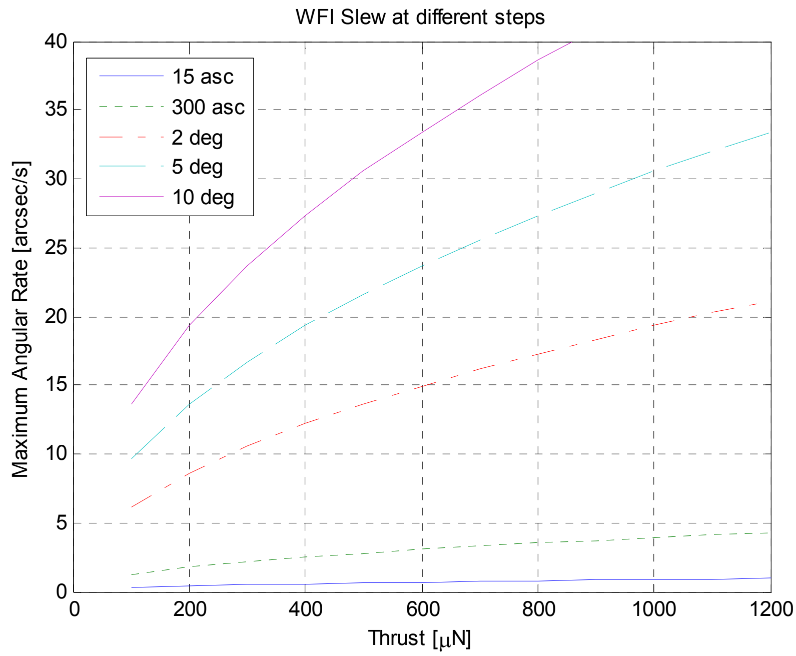

Figure 8-39: Maximum Angular rate at different steps and thrust levels

As it can be seen, the higher the thrust level, the quicker the slew manoeuvre with a higher total impulse requirement. For low thrust, the changing rate is quite high; however, when the thrust level is above 500 μN, the curve flattens out. Bearing in mind the current available magnitude of micro-thrust propulsion system, e.g., FEEP or cold-gas proportional thruster, and the overall operational time budget (Chapter 5), the required micro-thrust level is chosen as 500 μN. At this thrust level, the required time, total impulse and resulted maximum angular rate are listed in Table 8-29. System analysis shows that the required times meet the operational schedule with ample margin.

Step Size	**Slew Time** [sec]	**Total Impulse** [N.s]	**Max. Angular Rate** [arcsec/s]
15 arcsec	48.143	0.024	0.623
300 arcsec	215.250	0.108	2.787
2 degree	1054.508	0.527	13.656
5 degree	1667.323	0.834	21.591
10 degree	2357.951	1.179	30.535
180 degree	10003.938	5.002	129.549

Table 8-29: Attitude slew manoeuvre parameters at 500 μN

Concerning thruster configuration, 12 micro-thrusters are configured with full redundancy, providing 3 axes attitude control capability for both coarse and fine pointing control. Their preliminary layout is illustrated in Figure 8-40: , where F1 – F8 are mounted to provide maximum torques on X and Y axis, that is, the thrust direction shall be perpendicular to the direction of pointing towards the S/C COG, while F9 - F12 are configured to provide torques on Z axis (roll manoeuvre).

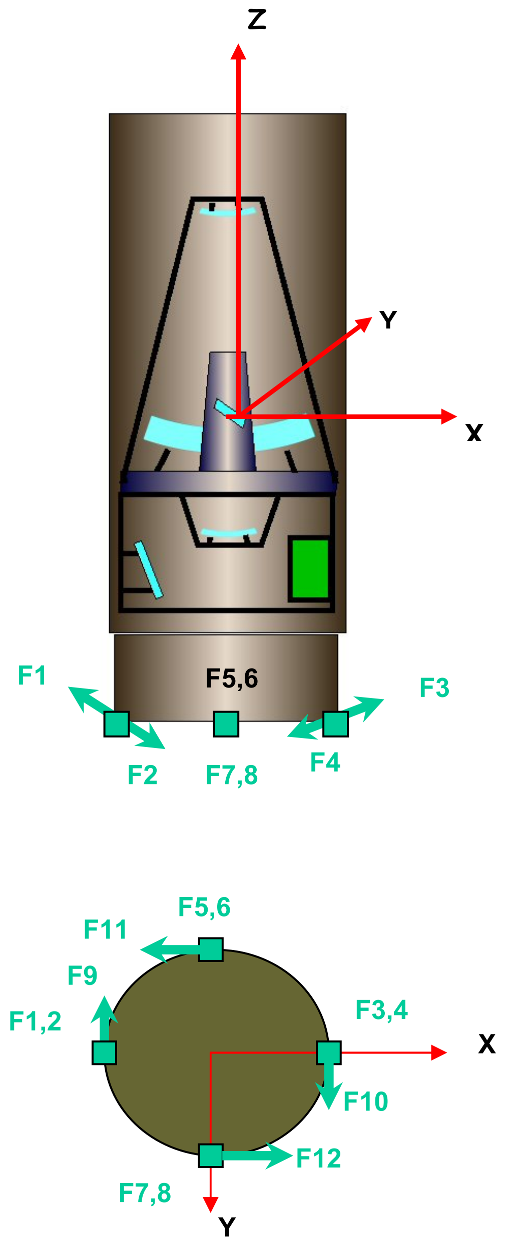

Figure 8-40: Micro-thrust propulsion system configuration layout

The total impulse of the micro-thrust propulsion system is estimated based on the attitude manoeuvre as required for science observation plus the constant compensation for the SRP torques. For coarse control, the total impulses at different slew steps are already estimated in Table 8-29. But for fine control with continuous FGS measurements, the maximum angular rate is limited to 0.1 arcsec/s. After each slew manoeuvre with coarse control, the attitude error will be less than 3 arcsec, then a closed-loop fine control based on FGS shall be used to bring the telescope to its final pointing. For this fine control period, the control scheme will first fire a thruster at 500 µN to accelerate the telescope up to 0.1 arcsec/s, then switch off the thruster to let the telescope slew at this maximum angular rate, and before reaching the final position, fire a thruster in the opposite direction (also at 500 µN) to decelerate the S/C finally, the telescope shall arrive at its final pointing with zero angular rate. The total impulse for this fine control of maximum 3 arcsec consists then only of acceleration deceleration periods.

With 500 µN thrust, the angular acceleration is 0.0259 arcsec/s^2, to reach 0.1 arcsec/s, it takes 3.86 sec, thus the total impulse of micro thrusters for a closed-loop fine control of up to 3 arcsec is:

$$E_{Fine-Control.} = 2 \times 3.86 \times 500 \times 10^{-6} = 0.00386 \ [\text{N.s}]$$

Within an operational cycle of 5 days, the total impulse required for science operation is estimated in Table 8-30.

Activity	**T.I./time [Ns]**	**Times/5 day**	**T.I. [Ns]**
300"scan coarse control	0.10763	144	15.498
300"scan fine control (3")	0.00386	144	0.556
15"dithering open loop	0.02407	144	3.466
Dithering fine control (1.5")	0.00386	144	0.556
Fine ctrl for spectro & cali (3")	0.00386	16	0.062
2 deg slew back and spectro	0.52725	15	7.909
5 deg slew calibration	0.83366	1	0.834
Total			**28.880**

Table 8-30: Attitude slew manoeuvre parameters at 500 µN

Meanwhile, to compensate the SRP induced torque over 5 days, the required micro-thrust total impulse is:

$$E_{SRP/5days} = \frac{F_{SRP} \cdot L_{SRP}}{L_X} \times 5 \times 24 \times 3600 = 12.497 \ [\text{N.s}]$$

Over the total life period of 6 years, the total impulse on the micro-thrust propulsion system is then summarized in Table 8-31,

Activities	**T.I. Per Unit**	**Times of Units**	**T.I. [Ns]**
SRP Torque Compensation	12.497	438	5473.63
Fine Control (imaging)	20.138	438	8820.34
Slew Control (2 deg & 5 deg)	8.742	438	3829.20
Roll Slew of 90 deg	2.171	24	52.10

Activities	T.I. Per Unit	Times of Units	T.I. [Ns]
Half-term slew of 180 deg	5.002	1	5.00
Total Without Margin			**18180.27**
Total With 50% Margin			**27270.41**

Table 8-31: Total Impulse Estimation for mission life

In summary, the performance requirements on the micro-thrust propulsion system are reported in Table 8-32.

Terms	Requirements	Remark
Minimum thrust level	≤ 40 μN	
Resolution/Noise	≤ 4 μN	Taken as 10% of the min level
Magnitude	≥ 500 μN	
Total Impulse	≥ 27270 Ns	For all 12 thrusters
Number of thrusters	12	3 DOF attitude control with full redundancy
Moment arm	As long as possible	To be mounted to provide maximum torques around X and Y axes

Table 8-32: Requirements on micro-thrust propulsion system

8.7.3.4 Mini-Thrust Propulsion System

Orbital maintenance and launcher dispersion correction require a high level thrust capability, e.g., in the order of 10 N. Thus, a mini-thrust propulsion system is required based on a hydrazine monopropellant subsystem.

Due to the requirement of three axes translational orbital correction, the mini-thrust system shall be configured to provide both force and torques on all the 3 axes. Eight mini-thrusters are needed, with the layout illustrated in Figure 8-41: F1 – F4 are placed on the upper edge of the service module, providing force upwards to telescope, while F5 – F8 are placed on the bottom edge of the service module, providing forces downwards the telescope. Meanwhile, all the thrusters are mounted with an appropriate cant angle, e.g., 20 deg, in order to provide the roll torque capability.

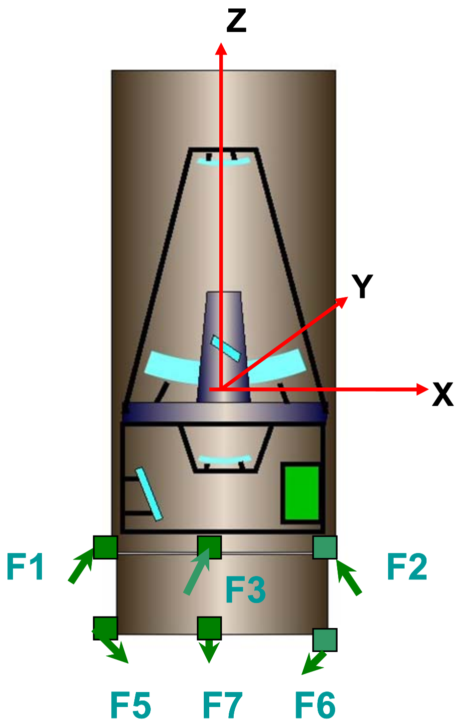

Figure 8-41: Mini-thrust propulsion system configuration layout

8.7.4 List of Equipment & Mass/Power Budgets

The overall AOCS sensors proposed for this WFI mission is summarized in Table 8-33.

Sensors	No.	Scope & Purpose
FGS	**2**	Provide fine pointing RPE of < 10 mas in pitch/yaw axis, of < 1 arcsec in roll axis, used for imaging & spectrometering, with full redundancy
Star Tracker	**3**	Provide 3-axis pointing accuracy of < 3 arcsec, with full redundancy, to be mounted on –X, -Y & -Z direction separately. 2 sensors shall be switched on all time to provide 3 axis accurate measurements.
Sun Sensor	**2**	Used during deployment and cruise phases; used also for FDIR & Safety Monitoring, during science modes, with full redundancy
Gyro	**2**	Used for deployment, cruise & safety modes, with full redundancy

Table 8-33: AOCS Sensors summary

Apart from the FGS, all the other sensors are well developed. Candidates are listed in Table 8-34. The overall mass/power budget of the AOCS subsystem is in Table 8-35.

Sensors	Mass/unit [kg]	Size [cm]	Power [W]	Candidates
Star Tracker	3.0	15.0×15.0×30.0	10	SED16 (Sordern); HE-5AS (Terma), etc
Sun Sensor	0.375	10.8×10.6×4.9	0.2	TPD-TNO Analogue Fine Sun Sensor (NL)
Gyro	1.45	12.5×12.5×12.0	5.5	Laben TRIS (Italy); BAE (MEMS), etc

Table 8-34. Sensor data of baseline candidate

Items	No.	Mass per set [kg]	Power per Set [W]
Star Tracker	3	3.00	20
Gyro Assembly	2	1.45	5.5
Sun Sensor	2	0.4	0.2
Fine Guidance Sensor	2	2.65	11.2
Total without margin		**18.0 (in total)**	**36.9 (per Set)**

Table 8-35 Overall AOCS mass/power budget

8.7.5 FDIR Scheme

The FDIR scheme for AOCS design is based on the full redundancy principle, that is, any one failure in sensors or actuators shall not reduce the mission performance in any sense. Preliminarily, the following measures are taken for FDIR purpose.

- All sensors are configured with full redundancy – any single failure will not reduce the mission performance
- FGS is carrying 3 CCD heads, for more redundancy at component level
- All thrusters are configured with full redundancy to be tolerant to any single failure
- Sun Sensors are mounted facing the Sun during science operation, to prevent any risk of pointing telescope towards Sun
- Mini-Thrusters are configured to provide back-up quick control of the S/C attitude in case of emergency, e.g. safe mode.

8.7.6 Conclusions

With the exception of the FGS, the AOCS sensors and actuators are mostly available off the shelf. The micro-thrust propulsion system shall be available in due time for this mission. The major challenging part for this mission, in term of AOCS aspect, is the design and development of a dedicated FGS to meet the RPE performance requirements. Otherwise, the AOCS units configured in the baseline design of the AOCS satisfy the mission requirements and still leave ample margins.

8.8 Thermal

8.8.1 Requirements and Design Drivers

No specific requirements apply to the SVM units. It has been assumed that all the equipments on the service module should stay within -20/+40 C.

8.8.2 Assumptions and Trade-Offs

The following materials and coatings' thermal properties have been used for the design:

	alpha	epsilon
Goldised Kapton	0.30	0.02
White Paint	0.29	0.90
Black Paint	0.95	0.90
M1/M2	0.49	0.04
CCD&NIR (as Si-cell)	/	0.83

Table 8-36: Thermal properties of TC materials

Solar flux in Halo orbit is: 1300/1340 W/m^2

Values of power dissipations vs. modes were assumed as follows:

Others Power Consumption per Mode	
Others Mode 1 total Pon	45
Others Mode 2 total Pon	50.7
Others Mode 3 total Pon	50.7
Others Mode 4 total Pon	50.7
Others Mode 5 total Pon	133.977
Others Mode 6 total Pon	181.8569619
Others Mode 7 total Pon	155.4201378
Others Mode 8 total Pon	-
Others Mode 9 total Pon	50.7

Table 8-37: Power dissipations vs. modes

8.8.3 Baseline Design

Service Module design is simple and straightforward. It consists of MLI blankets covering the external surface, white painted radiator surfaces for heat dissipation (0.4 m^2) located on the three external panels always opposite to the Sun direction, heat pipes as bridge between the dissipative units and the radiator, heaters to provide heating power when needed and in particular low power dissipation modes.

8.8.4 List of Equipment

8.8.4.1 Mass budget

Table 8-38 shows the thermal units. The ones related to the service module are marked with respect to the ones related to the payload.

Element 1	WFI Spacecraft		MASS [kg]			
Unit	Unit Name	Quantity	Mass per quantity excl. margin	Maturity Level	Margin	Total Mass incl. margin
	Click on button above to insert new unit					
1	Black paint on baffle and top int. surf.	1	4.93	To be modified	10	5.42
2	WP on 1/4 on baffle ext. surf.	1	1.06	To be modified	10	1.17
3	20 layers MLI on 3/4 baffle ext. surf.	1	14.17	To be modified	10	15.59
4	FP Radiator (structure+WP+int. finishing)	1	15.47	To be modified	10	17.02
5	ROE Radiator (structure+WP+int. finishing)	1	2.21	To be modified	10	2.43
6	2 mil Goldised Kapton (HS and FP rear side and top of baffle ext. surf.)	1	0.31	To be modified	10	0.34
7	Graphite Heat Path Bars	1	28.08	To be modified	10	30.89
8	Al ring	1	5.26	To be modified	10	5.78
9	Payload Heaters/Sensors	1	3.15	To be modified	10	3.47
10	SM Radiator (WP+int. finishing)	1	0.05	To be modified	10	0.06
11	20 layers MLI on SM ext. surf.	1	9.77	To be modified	10	10.75
12	Heat pipes	1	3.00	To be modified	10	3.30
13	Miscellaneous	1	1.00	To be modified	10	1.10
14	SM Heaters/Sensors	1	0.49	To be modified	10	0.54
-	Click on button below to insert new unit		0.00	To be developed	20	0.00
SUBSYSTEM TOTAL		14	88.96		10.0	97.86

Table 8-38: Thermal control mass breakdown

8.8.4.2 Power budget

The following tables list the heating power vs. mode (defined in Table 8-11) in the case of Sun at 45 deg. This refers to the total heating power including the one related to the Service Module.

- Sun not entering into the baffle

Heating Power Budget when Sun does't get in the buffle		On SM
Mode 1	0.00 [W]	0.00 [W]
Mode 2	205.44 [W]	35.00 [W]
Mode 3	205.44 [W]	35.00 [W]
Mode 4	260.25 [W]	35.00 [W]
Mode 5	225.25 [W]	0.00 [W]
Mode 6	105.25 [W]	0.00 [W]
Mode 7	175.25 [W]	0.00 [W]
Mode 9	260.25 [W]	35.00 [W]

Table 8-39: Total S/C heating power vs. modes

- Sun entering into the baffle

Heating Power Budget when Sun gets in the buffle		On SM	
Mode 1	0.00 [W]	0.00 [W]	as case 1
Mode 2	205.44 [W]	35.00 [W]	as case 1
Mode 3	205.44 [W]	35.00 [W]	as case 1
Mode 4	200.39 [W]	35.00 [W]	
Mode 5	164.74 [W]	0.00 [W]	
Mode 6	44.24 [W]	0.00 [W]	
Mode 7	114.87 [W]	0.00 [W]	
Mode 9	200.74 [W]	35.00 [W]	

Table 8-40: Total S/C heating power vs. modes

9 GROUND SEGMENT AND OPERATIONS

The ground segment and operations infrastructure for the Mission Operations Centre (MOC) will be set up by ESA/ESOC, and will be based on the extension of the existing ground segment infrastructure, customised to meet the WFI specific requirements. The concept for the establishment of the WFI ground segment will be the maximum sharing and reuse of facilities and tools made available for former Observatory missions, (Herschel/Planck, GAIA) if applicable.

9.1 Requirements and Design Drivers

The design of the Ground Segment and the Operations Concept for the WFI mission are driven by the compliance with the mission requirements and the constrained mission cost envelope. When and where possible the technical facilities and tools and the manpower expertise gained with Herschel/Planck and GAIA will be reused/transferred by/to the WFI mission.

Due to the characteristics of the mission, and the high amount of data generated by the science payload, the satellite will communicate with the ground station in X-band for TT&C up and downlink and in the 26 GHz Ka-band for science data downlink. The ground station chosen in the baseline design for communications with the spacecraft (TT&C and science TM) has been the ESA Deep Space Antenna (DSA) in Cebreros (Spain). The Cebreros Ground Station will have to be upgraded in order to be able to receive the 26 GHz Ka-band signal, which will be a major design/cost. The antenna in Cebreros has already the capability for 32 GHz Ka-band reception, but this is reserved for deep space missions.

Currently ESA is considering the construction of a third DSA at American longitudes, which would represent an option to Cebreros.

The Intermediate Frequency Modem System (IFMS) equipment would also need to be upgraded in order to be able to deal with the high downlink data rate foreseen for WFI, namely 50 Mbps.

Another aspect to be taken into account during the early design phases is the foreseen load of the ESA Deep Space Antennas according to the ESA mission model, such that a correct allocation can be done.

Nominal spacecraft control during most of the cruise and the observation phase will be “off-line”. Only one ground station will be allocated for communications with the spacecraft during these phases. The required daily visibility duration is about 4 hours. This implies that WFI is assumed to provide on-board capabilities (enough degree of spacecraft autonomy required) such that the satellite is able to perform corrective actions in case of on-board anomalies and the ground segment does not need to monitor the spacecraft in real time. Consequently, anomalies will be detected on ground with a typical delay of approximately 1 day.

9.2 Assumptions and Trade-Offs

The main assumptions considered for the definition of the ground segment for WFI are the following:

- It is assumed that other Observatory missions will be flying or in preparation, sharing the Observatory missions facilities (mainly software as MCS, Simulator, and the dedicated control room) and manpower (mainly in the areas of Quality Assurance, Project Control, Ground Segment Management, Operations Management). However WFI will have separate core teams for Flight Control and Flight Dynamics. SPACONS sharing will be considered if possible.

- A close link of the GAIA and the WFI Project team is assumed.
- It is assumed that the WFI operations can be performed by a team that is organisationally as close as possible/practical to the GAIA Mission Operations and Satellite Control team.
- A launch date in the interval 2015-2020 is required.
- The following durations for the different mission phases have been considered:
  - LEOP: 1 week.
  - Transfer to L2 operational orbit: approximately 3 months.
  - Commissioning and Verification Phase: 2 months.
  - Nominal routine operations: 3 years.
  - Extended operations: 3 years.
- The spacecraft will be launched by a Soyuz rocket with a Fregat upper stage from Kourou.
- No dedicated backup station will be considered for the routine mission. (S/C emergency cases will be supported by the network as per priority rules).
- The minimum HKTM data rate will be 4 kbps.
- It is assumed that payload HKTM is included in the same virtual channel as the satellite HKTM and is therefore directly available to ESOC.
- Science data acquisition from Cebreros (26 GHz Ka-band) is the baseline.
- The composition of the Flight Control Team during mission preparations and mission operations will be determined by the criticality of the operations and the possibilities of sharing the team with other Observatory missions.
- The provision, installation and validation of a mini-Mission Control System (mini-MCS) in the main ground station is part of the baseline.
- Use of the corresponding version of the SCOS2000 Mission Control System is assumed. The cost for the MCS development will include the Mission Planning System.
  It is assumed that some automation will be available including: Initial Pass Operations/Establishing of Ground Station Link and some limited reporting capabilities.
- Hardware usage will be shared with GAIA where possible (e.g. back-up system for the DDS).
- Always in routine phases under ground station visibility (approximately 8 hrs/day maximum) operations will be performed in Near Real Time.
- Off-line operations are performed during the periods when no ground station visibility is available.
- SPACON positions will be manned one 8 hours shift per day (7 days/week)
- Half of the duration of a ground station pass has been dedicated to science downlink.
- Spacecraft TM and TC service will be compliant with the ECSS Standards.

9.3 Baseline Design

The ESA/ESOC ground segment will consists of:

- The Ground Stations and the Communications Network
- The Mission Control Centre (infrastructure and computer hardware)
- The Flight Control System (data processing and Flight Dynamics Software)
- Infrastructure (Mission Control System, Simulator, etc).

The WFI ground segment will provide:

- A satellite monitoring and control chain, which includes:
  - A X-band Housekeeping TM acquisition and processing functional chain
  - A X-band TC generation and uplink functional chain
  - Offline performance analysis functions.
- An orbit and attitude monitoring and control functional chain.
- An overall Mission Planning function
- A OBSM facility
- Data archiving

9.3.1 Ground Station and Communications Network

The ground station network to be used for WFI during LEOP will be composed by the 15 metres antenna in Kourou, Villafranca and Perth (these two last antennas could be substituted by the 35 metres antennas in Cebreros and New Norcia). This network almost guarantees 24 hours coverage of the spacecraft during this critical period.

For the transfer phase and the nominal observation and extended phases the 35 metres antenna in Cebreros is the baseline. In order to receive 26 GHz Ka-band science telemetry, the antenna has to be upgraded. The possible third ESA Deep Space Antenna will be located at American longitudes (either in Chile, Argentina or Canada) and will be operative by 2012, and could be considered as an option for the WFI mission design. As for Cebreros, 26 GHz Ka-band reception would be required and it would be optimal to include this capability in the initial ground station design.

A preliminary analysis of the ESA Deep Space Network load has been performed in order to assess the ground station availability.

New Norcia:

Rosetta. Long daily passes needed during 2015, due to near comet operations. This activity would be compatible with a 4 hours daily visibility window for a spacecraft in L2, as Rosetta will be approaching the perihelion of its trajectory.

Herschel/Planck. No interference with WFI, although they will have Lissajous orbits around L2, the end of both missions is foreseen by 2012. Each mission needs a 3 hours daily visibility window and communicates with the ground station in X-band.

Solar Orbiter. SolO requires the upgrade of the New Norcia ground station to 32 GHz Ka-band reception, making the Rx 26 GHz upgrade technically very challenging (although not impossible). Launch of SolO is foreseen during the first trimester 2017.

SolO would be compatible with WFI in the same ground station if the installation of the Rx 26 GHz band would be feasible on top of the Rx 32 GHz as the missions take place in opposite hemispheres of the Earth with respect to the Sun.

Cebreros:

GAIA. The spacecraft will be in a Lissajous Orbit around L2. The nominal mission end is during the second half of 2017.GAIA will need the complete duration of the daily visibility window for science data downlink. Seasonally, daily visibility has to be even completed with New Norcia. In order to minimise the conflict with WFI, the daily coverage of GAIA could be split between Cebreros and New Norcia, although this is not foreseen in the ESA mission model. The conflict disappears if WFI is launched after GAIA end of mission. This is the baseline that has been assumed for this study.

Bepi Colombo. The launch of Bepi Colombo is planned during the first quarter 2013. The projected extended end of mission occurs during the second quarter 2021. Daily passes are required, but Bepi Colombo is an inner solar system mission and will not conflict with WFI.

Third DSA:

Exomars. This mission will need daily passes from June 2011 to June 2015 (extended mission). No conflict is foreseen with WFI as missions do not coincide in time.

Mars Sample Return. The launch will take place after 2015, with an expected mission duration of 4 years. A detailed visibility study should be performed during the overlapping periods, as the visibility patterns of an L2 and a Mars mission coincide seasonally. A shared visibility slot will be most probably possible.

LISA. This mission will be launched after 2017. A detailed visibility study has to be carried out yet.

The Ground Facilities Control Centre monitors and remotely controls all the ESTRACK ground tracking stations, using information provided by Flight Dynamics and the scheduling office. They are also responsible for the TM/TC links to and from the ground stations and any data retrieval of stored science from the TMPs or the ranging IFMS, CORTEX and MPTS equipment.

A station computer monitors and controls (locally, automatically or remotely from the MOC) all equipment on the station. It provides different backup modes (TM quicklook, backup commanding). A Front-End controller unit controls the antenna subsystem.

All ESA stations interface to the MOC at ESOC in Darmstadt via the OPSNET communications network. OPSNET is a closed Wide Area Network for data (telecommand, telemetry, tracking data, station monitoring and control data) and voice.

It is assumed that the communication system will support the LEOP and routine data exchanges between the Control Centre in Darmstadt and the Ground Stations identified in this section.

9.3.2 The Mission Control Centre

The WFI mission will be operated from ESA/ESOC and it will be controlled from the Mission Operations Centre (MOC), which consists of the Main Control Room (MCR) augmented by the Flight Dynamics Room (FDR) and Dedicated Control Rooms (DCR's) and Project Support Rooms (PSR's). The MCR will be used for mission control during LEOP and possibly the

Commissioning Phase in case of serious anomaly. During transfer to L2, and the observation phase the mission control will be conducted from a Dedicated Control Room possibly shared with other Observatory missions.

The control centre is equipped with workstations giving access to the different computer systems used for different tasks of operational data processing. The control centre will be staffed by SPACONS possibly shared with other observatory missions with support from operations engineering staff, experts in S/C control, flight dynamics and network control, available on a part time basis for the full mission duration. Space and equipment for scientists, project and industry experts and public relations will be provided close to the MOC as required, during the critical phases of the mission.

9.3.3 Computer Facilities

The computer configuration used in the MOC for the WFI mission will be derived from existing structures. The computer system basically consists of:

- A computer system used for the Flight Operations Plan generation in a form directly usable by the mission-dedicated computer.
- A mission dedicated computer system (including workstations hosting SCOS2000) used for real time telemetry processing and for command preparation and telemetry and command log archiving, and also for non real time mission planning and mission evaluation.
- Workstations hosting the Flight Dynamics System.
- The simulation computer, providing an image of the S/C system during ground segment verification, for staff training and during operations.

All computer systems in the control centre will be redundant with common access to data storage facilities and peripherals. Preferably workstations of a similar type will be used for all related computing, to maximise flexibility and to minimise maintenance costs. The workstations allowing privileged user access to the Flight Control System will be located in the different control rooms as necessary.

9.3.4 The Flight Control Software System

The Flight Control System will be based in infrastructure development (SCOS2000), using a distributed architecture for all spacecraft monitoring and control activities. The Flight Control System includes the following facilities:

- Telemetry reception facilities for acquisition, quality checking, filing and distribution.
- Telemetry analysis facilities for status/limit checking, trend evaluation.
- Telecommand processing facilities for the generation of commands for control, master schedule updates, and on-board software maintenance. The facilities will provide also uplink and verification capabilities.
- Monitoring of instrument housekeeping telemetry for certain parameters which affect spacecraft safety and command acceptance and execution verification.
- Separation and forwarding of payload telemetry to Science Data Processing Centres.
- Checking, reformatting, scheduling command request for payload.

Within the SCOS2000 system, mission specific software will be developed wherever necessary.

9.4 Mission Operations Concept

9.4.1 Overview

The operations support activities for WFI will be conducted according to the following general concept:

- All operations will be conducted by ESOC according to procedures laid down in the Flight Operations Plan (FOP).
- The WFI mission operations will be conducted with one shift of spacecraft controllers, with analysts and engineers working nominal hours. Except for the first period after launch (LEOP duration 1 week), where 24 hours operations per day will be conducted.
- All WFI operations will be conducted by uplink of a master schedule of commands for later execution on the spacecraft. This schedule will contain all commands necessary to undertake the spacecraft and instruments operations in a predictable fashion. A limited number of time tagged commands will be used for spacecraft safety operations. The master schedule will be prepared by a Mission Planning System.

9.4.2 Spacecraft Monitoring and Control

The WFI spacecraft subsystems performance will be monitored in near real time following each used contact period. All housekeeping data, as recorded in the spacecraft memory, will be processed and analysed for exceptional events and trends (e.g. power, temperatures, etc.). The following assumptions have been made:

- Near real time housekeeping telemetry will be processed in the MOC in real time as it arrives from the ground stations.
- All playback telemetry is assumed to pass through the on-board memory and to be dumped in the same time sequence in which it has been recorded; HK data shall be available to the operator in real time as it is dumped during the pass.
- All real-time TM will be downlinked directly during coverage.
- Auxiliary data (attitude and orbit history and derived parameters) will be made available to authorised personnel via the DDS from the MCS.
- Data structures will comply with CCSDS recommendations.
- Level 1a and 1b processing of science telemetry packets will not be performed at ESOC, but by the Science Teams.

In addition to near real time HK data processing for spacecraft monitoring, standard facilities will be used for long term performance evaluation and HKTM, TC history and system message archiving.

The command activity comprises the following:

- One command queue will be provided in the MOC: for uplink of the master schedule, integrating the instruments and platform commands. In addition there will be a facility for (manual) uplink of real time commands.

- Off-line requests for changing science operations will be submitted by the Science Teams as a complete and consistent input to the MPS. The response time to such changes will nominally be TBD.
- The MOC will be the only source of commands to the WFI spacecraft.
- The MOC will provide pre-transmission validation and verification of correct command uplink by the ground station, and verification of correct execution of command in the master schedule, using verification TM packets.
- A history of all commands submitted for uplink will be available in the MOC (and made available to the Science/Project Teams on the data server).

It will be possible to manipulate the master schedule using the standard PUS services.

9.4.3 Orbit and Attitude Control

Orbit and attitude determination and control will be performed by the team of specialists, which has prepared the related software facilities.

The operational support to be provided by Flight Dynamics to the WFI mission will consist of the following major items:

- Launch and Early Orbit Phase LEOP support. This will include LEOP set-up and testing, ground station predictions; early orbit assessment; preparation of manoeuvres if necessary; monitoring of attitude acquisition.
- Orbit determination and auxiliary data product generation. A forward propagation of the orbit will be used to obtain antenna pointing information for the ground stations (in the form of Spacecraft Trajectory Data Messages STDM's), and other auxiliary data such as station pass profiles, eclipse times, prediction of maintenance manoeuvre times, input to MPS, etc. Orbit determination will be performed during all mission phases using coherent Doppler tracking data from up to three ground stations (depending on the mission phase). Orbit determination includes tracking data pre-processing, the calibration of all engines and thrusters used for orbit correction and ground controlled attitude manoeuvres that are not pure torques.
- Transfer Orbit manoeuvre optimisation consisting of the preparation and maintenance of high precision orbit prediction software with and without future planned manoeuvres. The complete sequence of manoeuvres from the rocket separation until insertion into the Lissajous orbit will be optimised to minimise propellant consumption and taking into account all operational conditions. Following each manoeuvre, the remaining sequence will be re-optimised on the basis of the current manoeuvre performance.
- Preparation and evaluation of Lissajous orbit maintenance manoeuvres. The time sizes and directions of the orbit maintenance manoeuvres will be optimised to guarantee payload operations for up to 6 years with a minimum of interruption.
- Periodic monitoring of telemetered positions, velocities and attitudes and their rates. This will be largely automated.
- Periodic monitoring of sensor outputs (FGS, star tracker, sun sensor, gyros), also largely automated.
- Generation of the values of any onboard parameters that need routinely updating onboard, related to attitude and orbit.

- The payload pointing will be pre-programmed according to the scanning law with the exception of spectrometer whose measurements will be commanded by input from the SOC every 5 days.
- Manoeuvre monitoring in near real time of all manoeuvres performed in the presence of an Earth communications link. Deviation from expected performance might cause a long manoeuvre to be terminated by ground command.
- Calibration of thrusters and sensors by comparing planned and achieved results. The output of the calibration process will be used for planning of subsequent manoeuvres. All sensor data will be calibrated on ground and the related parameters in the on-board attitude system will be updated.

Auxiliary data as orbit, attitude, spin rate, manoeuvre histories, will be provided to the scientists. Flight Dynamics data needed for mission planning purposes, such as ground station visibility times, will also be provided by the FD team.

10 TECHNICAL RISK ASSESSMENT

10.1 WFI Risk Management

The risk management implementation for WFI has been done according to the steps depicted in Figure 10-1: . This figure is based on the ECSS-M-00-03B Risk Management for information.

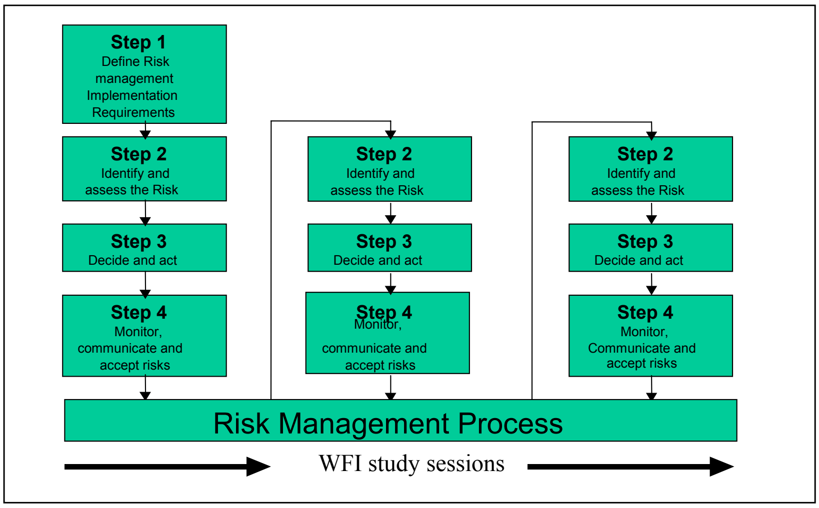

Figure 10-1: Risk management process

The following actions have been carried out as basis for the implementation of the risk management for the study:

- Identification of the set of resources with impact on risks
- Identification of the goals and resource constraints
- Definition of scheme for ranking the risk goals according to the requirements
- Establishment of scoring schemes for the severity of consequences and likelihood of occurrence for the relevant resources
- Establishment of a risk index scheme to denote the magnitudes of the risks of the various risks scenario.
- Establishment of criteria to determine the actions to be taken on risks
- Definition of risk acceptance criteria for individual risks
- Establishment of a method for the ranking and comparison of the risks

10.2 Set of Resources with Impact On Risks

The following sources of risks are identified as potential areas of concern for the mission.

Sources	Description
Space Segment – Service Module	Issues related to the subsystems of the service module be it a whole subsystem or parts of subsystem having an impact on the mission.
Space Segment - Payload	Issues related to the Payload be it a whole subsystem or parts of subsystems of the Payload having an impact on the mission.
Launch Services	Issues related to the constraints on the mission derived by the selected launcher.
Ground Segment- Operations	Issues related to the Ground Station system, Ground communication subnet, and Mission Control system such as aspects of development of required infrastructure.
Managerial External	All issues related to contractual, procedural aspects or collaboration with other space agency.

Table 10-1: Sources of risk for WFI

10.3 WFI Risk Scoring Scheme

The risk scenarios are classified according to their domains of impact. The consequence severity level of the risks scenarios is defined according to the worst case potential effect with respect to cost, schedule, technical issues and science value.

Identified risks that may jeopardize the mission are ranked in terms of likelihood of occurrence and severity of consequence using the tables below.

The scoring scheme with respect to the severity of consequence is on a scale of 1 to 5 as established in **Table 10-2** and the likelihood of occurrence is normalized on a scale of A to E as per **Table 10-3**.

Score	Severity	Cost	Schedule	Technical	Science
5	Maximum	*Cost increase beyond estimated CaC.*	2017-2020 Launch opportunity lost	Loss of system/mission with impact on Safety;	None of top level scientific goals are achieved. No scientific data return.
4	Critical	*No increase on the estimated CaC, however contingency margin lost.*	Delay >TBD 1 months	Loss of capability to perform the mission.	Major reduction (50-90%) of the science return.
3	Major	*No increase on the estimated CaC, however major part of the*	Delay > TBD 2 months.	Major degradation of the system/ mission.	20-50% reduction of the science return.

Score	Severity	Cost	Schedule	Technical	Science
		contingency margin lost.			
2	Significant	*No increase on the estimated CaC, however significant part of the contingency margin lost.*	Delay > TBD 3 months	Degradation of system/mission (e.g: system is still able to control the consequences)	Significant reduction (10-20%) of the science return.
1	Minimum	*No/ minimal consequences.*	No/ minimal consequences.	No/ minimal consequences.	No/ minimal consequences.

Table 10-2: Severity of consequence - scoring scheme concept.

Score	Likelihood	Definition
E	Maximum	Certain to occur, will occur once or more times per project.
D	High	Will occur frequently, about 1 in 10 projects
C	Medium	Will occur sometimes, about 1 in 100 projects
B	Low	Will occur seldom, about 1 in 1000 projects
A	Minimum	Will almost never occur, 1 in 10000 projects

Table 10-3: Likelihood scoring scheme

10.4 Risk Index

A Risk Index is given as a combination of the likelihood of occurrence and the severity of consequences for a given risk item.

Risk ratings of low, medium, high are assigned based on the criteria of the Risk Index Scheme shown in Table 10-4.

The level of criticality for a risk item is denoted by the analysis of the risk index. Following the scheme below the highest possible Risk Index will therefore be 5E, and the lowest possible Index, 1A.

Severity					Risk Index: Severity & Likelihood	
5	5A	5B	5C	5D	5E	
4	4A	4B	4C	4D	4E	
3	3A	3B	3C	3D	3E	
2	2A	2B	2C	2D	2E	
1	1A	1B	1C	1D	1E	
	A	B	C	D	E	Likelihood
		high		medium		low

Table 10-4: Risk index scheme

10.5 Identified Risks and Areas of Potential Risk Reduction

During the course of the study there were identified some critical areas, which, because of their contribution to the risk of the mission, had a higher potential for risk reduction. The risk scenarios were assessed with respect to their risk magnitude and the suitable risk reduction actions were suggested. The same risk scenarios, together with others that were identified along the study sessions, were assessed at the end of the study, showing therefore an evolution which was recorded via a trend indicator.

10.5.1 Payload

- Large size SiC Mirrors

<u>Unavailability of dedicated manufacturing facilities for large size SiC mirrors</u>

Manufacturing a monolithic SiC mirror of these dimensions is not possible at the present. This is the highest risk to overcome for the achievement of the goals of the mission. Some risk elimination means have been assessed such as: large investment in mirror material alternative (i.e.: Zerodur) or mirror segmentation.

The Zerodur option as material alternative has been discarded since it would imply an increase of approximately 400kg on the total WFI spacecraft mass.

Concerning the other solutions, it cannot be guaranteed that they will effectively mitigate the risk. An early investment in technology development should allow an understanding what the best option is.

The range of suppliers of SiC is very limited at the moment. It would be recommendable to widen their search to avoid cost and programmatic risks.

- Curved Focal Plane Assembly

<u>Limitation on the testing facilities for the mirrors (FPA)</u>

The fact that the FPA is curved implies uncertainties in the existing testing procedures and means.

It is therefore recommended as a mitigation risk, to take the necessary managerial and engineering actions as early as possible in the life of the project so that the uncertainties in terms of test complexities and facilities are lowered to an acceptable level.

- Alignment stability

<u>The stringent requirements on alignment stability are crucial to the achievement of the goals of the mission</u>

It is, therefore, of extreme importance to reduce any uncertainty about changes due to temperature variation, mechanisms operations, structures, etc. All these parameters are already being considered in the design so that the issue is tracked and kept under control.

Early mitigation means the avoidance of deployable, rotating or vibration inducing elements as much as possible, as well as modelling the behaviour of the system, and the establishment of the relevant stringent stability requirements on every subsystem. This is an activity that will evolve during all the phases of the mission until the risk is lowered to an acceptable level.

- Radiation hazard

<u>The Detectors are identified as potentially sensitive to the radiation environment</u>

Some risk mitigation methods are identified such as using p-channel CCDs instead of n-channel ones, establishing requirements on radiation hardening and shielding and making use of the heritage of similar environment missions like GAIA (that have a large focal plane array similar to WFI).

In Hubble, longer exposures are built up by adding together shorter exposures, in order to discriminate real targets from cosmic ray hits. It is recommended to optimise the exposure times taking into account this factor.

- Contamination

<u>The cleanliness requirements for missions involving optics are very strict</u>

Usually they apply inside the telescope tube, which is a Class 100 environment, and to the mirrors. In the design phase these requirements are taken into account by making the mirror modules, and the telescope tube separately closed units with their own doors and purging devices. The telescope tube is sealed from CFRP outgassing towards the inside by a continuous aluminium foil.

The XMM lessons learnt (RD[57]) regarding cleanliness are recorded here as a recommendation for risk mitigation purposes:

- Keep all sensitive surfaces closed and enclosed volumes purged as long as possible.
- Use all existing techniques for measuring particulate and molecular contamination extensively throughout the programme and take immediate action if cleanliness deteriorates.
- Test contamination-control procedures during the structural and thermal model programme.

  - Perform regular cleanliness inspections involving the materials laboratory.
  - Coat or passivate vulnerable surfaces.
  - Material selection.

- Spectrometer

<u>The Spectrometer is crucial to the achievement of the goals of the mission</u>
Without the spectrometer the photometry can still be done but not the analysis of supernovae. It is therefore recommended to implement the fault tolerance requirements and have a redundant spectrometer. Therefore the impact on mass and eventual added mechanisms and complexity need to be assessed.

10.5.2 Payload Data Handling Electronic Critical Aspects

- Technology/supplier

<u>The choice of microprocessor and related architecture</u>
The initial selection of the GINA processors was found to be critical because of its technology readiness status conflicting with the WFI schedule. The design was then re-oriented to the use of the SCS750 board from Maxwell (PPC750 FX microprocessor from IBM, 1800 MIPS). The present baseline is the SCS750, which is subject to ITAR export control. It has been selected for GAIA; this fact is expected to reduce the export control derived programmatic risk.

<u>The meeting of the required FGS performance</u>
The FGS development needs to provide stringent performance (accuracy, sensitivity, FoV, etc.) that is mission enabling.

10.5.3 Communications

<u>Baseline new technology 26GHz transmitter + Amplifier for science telemetry</u>

Some alternatives have been discussed to reduce the associated risk such as the use of X-Band transponders (GAIA/Herschel) but the impact on the science value and on the cost needs to be assessed (i.e.: the transmission would go from 576Gbits/day during 4h/day to 99Gbit/day during 8h/day).

10.5.4 Ground Segment

<u>Unavailability of DSN Ground Station for 26Ghz</u>

To mitigate this risk it is proposed to invest Cebreros with 26GHz capability. X-Band is discarded as a back up solution given the high data volume required by WFI. Also, the 32 GHz Ka- Band is discarded because the required Earth trailing orbit is not achievable.

10.5.5 Propulsion/ AOCS Critical Aspects:

- Technology

The thrusters selected are a key element of the mission. The eventual risk to the WFI mission posed by the micro propulsion technologies come from the fact that both options considered have not reached full qualification yet. Although the system design is presently compatible with both alternatives, their availability for WFI relies on their selection and performance from either the GAIA mission or LISA Pathfinder.

10.5.6 Mechanisms

The lid and the focusing mechanisms are considered crucial for the achievement of the goals of the mission. Requirements on fault tolerance are in place as risk mitigation means, so there is no single failure which can prevent the mechanisms from performing their tasks.

10.6 Results: Ranked Risks Log Trend

The identified risks are ranked with respect to their risk magnitude and categorised by the relevant factors:

- Technology
- Facilities
- Supplier
- System engineering/ AIT aspects
- Design maturity

In the next sub-sections of this paragraph, the tables with the ranked risks are shown as well as their trend indicator, which shows in a graphic manner how the associated risk magnitude (RM) evolved during the study from the initial assessment to the “end of study” assessment.

No evolution from the beginning of the study is represented with ↔

Reduced risk as a consequence of CDF design actions is represented with ↘

10.6.1 Technology Risks

Risk Scenario	Impact	Initial RM	End of study	Trend Indicator	Risk reduction Actions	Remarks
Unavailability of dedicated manufacturing facilities for large coated SiC mirrors.	All	5E	5E	↔	• Invest in technology for large mirrors. • M1 mirror segmentation. • Margin on the schedule for development (1 year)	Risk reduction feasibility cannot currently be confirmed. No design backup found (i.e. reduction of mirror size to current technological capability has very large impact on science objectives).
Unavailability of presently assumed detectors.		5E	5E	↔	• Invest in technology development. • Manufacturing & inspection requirements to minimize the gap between detectors. • Exposure time optimization analysis.	

Risk Scenario	Impact	Initial RM	End of study	Trend Indicator	Risk reduction Actions	Remarks
Unavailability of Fine Guidance Sensors.		5E	5E	↔	• Invest in technology development.	Performances are within present technology capabilities.
Inadequacy of the AOCS thruster technology to the mission	All	5C	5B	↘	• Micro propulsion alternative technologies available. • Investigate potential spacecraft contamination	Lisa PF, Microscope & GAIA will be using these technologies first.
Unavailability of the 26GHz transmitter+ amplifier for high data rate	All	5C	5B	↘	• Development of new transmitter+ amplifier.	Use of X-band would give a large reduction of the science data. GMES likely to use same technology.
Inadequacy of the Detectors to the mission environment.	All	4D	4C	↘	• Characterize alternative P & N-channel CCD's adequacy to the WFI radiation environment.	
Degradation of payload data handling capability.	All	4C	4B	↘	• Maxwell SCS750 selected as baseline. Therefore, initiate ITAR process early in the project. • GINA's processor as a back up solution. Invest in new technology.	GAIA heritage wrt ITAR issues.

Table 10-5: Technology related risks trend

10.6.2 Infrastructure Risks

Risk Scenario	Impact	Initial RM	End of Study RM	Trend Indicator	Risk reduction Actions	Remarks
Unavailability of DSN station for 26GHz.	All	5D	5D	↔	• Invest in Cebreros with 26GHz capability, or a 3rd ESA DSN.	X-Band discarded as a back up solution. 32Ghz Ka-Band is discarded since the Earth trailing orbit is not achievable.
Soyuz unavailability from Kourou	All	4B	4A	↘	Early involvement of ESA managers.	The infrastructure is foreseen to be ready by 2008.
Inadequacy of the optics testing facilities.	All	3E	3E	↔	• Managers take the necessary actions/margins early enough in the project.	Complexity derived from the FPA curved nature.

Table 10-6: Infrastructure related risks trend

10.6.3 Suppliers Related Risks

Risk Scenario	Impact	Initial RM	End of Study RM	Trend Indicator	Risk reduction Actions	Remarks
Single source supplier for SiC mirrors.	All	5E	5E	↔	• Invest in SiC industrial capabilities so there are alternative suitable suppliers.	The Zerodur alternative was discarded since it would imply an increase of more than 400kg.

Table 10-7: Suppliers related risks trend

10.6.4 System Engineering / AIT Related Risks

Risk Scenario	Impact	Initial RM	End of Study RM	Trend Indicator	Risk reduction Actions	Remarks
Optics contamination during on ground operations.	All	5D	5B	↘	• Cleanliness requirements specification. • XMM, Herschel experience and lessons learnt will be used.	Cleanliness requirements will cover material selection. AIT facilities and handling, shipping and transportation procedures.
Optics contamination during flight operations.	S	5D	4C	↘	• Cleanliness requirements specification. • Configuration layout such that the sources of contamination cannot impact on sensitive surfaces. • Allocation for purging devices. • Cover lid for the telescope.	Contamination would only be partial.
Loss of focusing capability	S	5D	5B	↘	• Mechanism Fault tolerant design. • Testing.	
Lid mechanism fails to open.	S	5D	5B	↘	• Fault tolerant design. • Testing.	
Mirrors misalignment during flight operations.	S	5C	5B	↘	• Stability requirements in place. • Refocusing mechanism. • Avoidance of noise sources.	The margins for changes due to T variation, mechanisms operations, etc are considered in the design. Thermal Analysis shows feasibility of stability requirements.

Risk Scenario	Impact	Initial RM	End of Study RM	Trend Indicator	Risk reduction Actions	Remarks
Mirrors aberration	S	5C	4C	↘	• Manufacturing and Testing reqs in place. • Product Assurance Plan.	It can be partially compensated by image processing.
Calibration inaccuracy	S	4D	4D	↔	• Establishment of a Calibration Plan.	
On board data processing inadequacy	S	4C	4C	↔	• Dedicated SW PA programme.	No heritage.
Loss of Integral Field Spectrometry.	S	5C	5B	↘	• Slicer design and manufacturing effort. • Redundant read out electronics in the Spectrometer.	
Wrong launcher correction manoeuvre	S	3C	3C	↔	• Improve operation reliability & implement fault tolerance requirements for thrusters.	

Table 10-8: System engineering / AIT related risk trend

10.6.5 Design Maturity Related Risks

Risk Scenario	Impact	Initial RM	End of Study RM	Trend Indicator	Risk reduction Actions	Remarks
AOCS loss of fine pointing capability.	S	5D	4B	↘	• Design is fault tolerant. • Cold gas thrusters' reliability. • Potential problems with gas leakage to be investigated.	Full redundancy is envisaged for the thrusters and the sensors involved in this function.
Loss of camera read out electronics due to the Sun in the FOV.	S	5C	5B	↘	• AOCS fault tolerance and Safe Mode.	
Loss of Thermal Control cooling capability.	S	4C	4B	↘	• Passive design. • Fault tolerant heaters.	
Solar array capacity degradation due to radiation exposure.	S	4C	4B	↘	• Design margins in place.	Herschel radiation environment taken as reference.
Loss of AOCS sun pointing capability	S	4C	4B	↘	• Safe Mode implemented.	
Loss of Comms	S	4C	4B	↘	• HGA design for minimum risks • Mechanisms design for minimum risk • Fault tolerance.	
Loss of Propulsion	S	4C	4B	↘	• Safety margins, design for minimum risk. • Fault tolerance.	

Table 10-9: Design maturity related risks trend

10.7 Conclusions

Experience shows that it is mandatory for all risk items with a critical risk index (red area 5C-4D-3E) to be analysed and proposals for risk treatment actions elaborated.

Therefore, at the end of the study the top nine risk index scenarios are highlighted to the management so the relevant actions can be taken in due time.

For the risks in yellow there should be an alert with respect to a possible increase of the Risk Index. These risks should be taken care of during next design phases.

Risk Scenario	Category	Risk reduction Actions	Priority
Unavailability of dedicated manufacturing facilities for large coated SiC mirrors.	Technology development	• Invest in dedicated facilities. • Invest in technology for large mirrors. • M1 mirror segmentation. • Margin on the schedule (1 year) • Flexibility on the launch window.	Urgent. Risk reduction actions should start as early as possible.
Unavailability of presently assumed detectors.	Technology development	• Invest in technology development. • Manufacturing & inspection requirements to minimize the gap between detectors. • Exposure time optimization analysis.	
Unavailability of Fine Guidance Sensors.	Technology development	• Invest in technology development.	
Single source supplier for SiC mirrors.	Technology development/ Procurement policy	• Invest in SiC industrial capabilities so there are alternative suppliers.	
Unavailability of DSN station for 26GHz.	Infrastructure Development	• Invest in a 3rd ESA DSN or Cebreros with 26GHz capability.	
Calibration inaccuracy.	System Engineering / AIT	• Establishment of a Calibration Plan.	Phase A/B issues to be considered in next industrial design phases.

Risk Scenario	Category	Risk reduction Actions	Priority
Optics contamination during flight operations.	System Engineering / AIT	• Cleanliness requirements specification. • Configuration layout such that the sources of contamination cannot impact on sensitive surfaces. • Allocation for purging devices. • Cover lid for the telescope	
Mirror aberration.	System Engineering / AIT	• Manufacturing and Testing requirements in place. • Product Assurance plan.	
On board data processing inadequacy.	System Engineering / AIT	• Dedicated SW PA programme.	

Table 10-10: Ranked risks log

11 CONCLUSIONS

The study has shown that the technical implementation of the WFI science objectives results in a medium-class mission, compatible with the Soyuz Fregat 2.1b launcher.

The orbit that best satisfies science requirements and provides sufficient mass performance with Soyuz (so reduced cost) is a Halo orbit around the Lagrangian point L2. All other alternative architectures studied, including a dual Ariane 5 launch together with a GTO passenger and later transfer to L2 by own propulsion, show a lower performance over cost ratio. Therefore, the Soyuz mass capability to L2 is a hard limit for the mission and mass budget control is a driver.

The proposed design includes a Service Module and a Payload Module that, in turns, contains a large aperture Telescope, two Instruments (Camera and Spectrometer) with their associated electronics, data handling and thermal control and a Fine Guidance Sensor used by the Service Module attitude control system.

The design encompasses sufficient margins and has been performed taking into account flexibility in the choice of the optical configuration (e.g. 4-mirror versus 5-mirror design) and in the technology for the micro-thrusters for fine pointing. Presently, the mission can accommodate the worst cases among the above options; so that the final choice can be left to future phases of the project when more consolidated performance data will be available.

Several options also exists to reduce spacecraft mass or increase launch capacity if this becomes necessary at the cost of limited science performance reduction and/or mission risk increase.

The Service Module design is straightforward and comparable to the Gaia or Herschel/Planck ones, though re-use of GAIA platform might be possible although modifications are necessary due to differences in attitude and mission strategy.

The Payload Module, if benefiting from the Gaia experience, will require dedicated technology developments, in particular, in the area of lightweight SiC mirrors of 2-m range size and low read-out noise, rad-hard detectors.

The capability of manufacturing large mirrors in SiC is enabling for the mission, as any back-up (e.g. the use of Zerodur) will imply unacceptable mass penalty within a Soyuz mission. Technology development in this area shall therefore be initiated as early as possible to confirm the assumptions of the study.

An important mission driver is the very large amount of data generated by the payload. This imposes the use of high speed on-board data processing and the need of a 26 GHz Ka band communication system.

This latter requires only limited spacecraft technology development and it is in line with future trends in Earth Observation missions. However, upgrade of the ESA Deep Space Ground Station to cope with this frequency band is required. In the cost assessment for the mission, as a worst case, the cost of this upgrade has been considered to be on the WFI project, though in reality, only a fraction of it will probably need to be contributed.

A mission mass driver is the diameter of the main mirror that sizes the telescope dimensions and the associated baffle mass and optical support structure mass. Diameter reduction of about 10% leads to about 5% decrease on the total launch mass. However, at this stage, this does not seem to justify the associated science performance degradation.

11.1 Compliance Matrix

Compliance of the design proposed with the given requirements is shown in summary in the following Figure 11-1 to Figure 11-3.

	Compliance (Y/N)	Comment
Two survey fields shall be covered, one close to each ecliptic pole within ± 20 deg of pole	Y	Compliant
Perform Wide Field Imaging in multiple filter bands over a wavelength range of 0.3 to 1.8 microns with I-band diffraction-limited optics	Y	Compliant
Measure supernovae spectra near peak luminosity with a resolution of 100 ($\lambda/\delta\lambda$) over 0.30 to 1.8 microns.	Y	Compliant
The observation strategy shall cover a 10 sq degree scan strip with a revisit rate of 5 days.	Y	Time budget and data budget fit mission design
Photometric observations will be taken over the scan strip during the first 4 days of the 5 day period with step size 300 arcsec, and 2 dither frames of 1000s per step.	Y	Observation strategy incl AOCS design, DHS, comms and GS & Ops meets this requirement
Photometric observations shall be taken for at least 10 (peak and off-peak) points along the SN light curve with first detection at average 2.2 magnitudes below peak with S/N>5 (worst case is for z = 1.7)	TBD	S/N for NIR wavelengths not yet simulated, for visible only to z = 1 verified so far
Spectrometry measurements will be scheduled according to SN peak luminosity times during day 5 of the 5 day observation cadence as the telescope slews back to starting position of the scan.	Y	In worst case, spectro of SN target is taken ± 2 days from peak luminosity

Figure 11-1: Compliance to Science Requirements

	Compliance (Y/N)	Comment
WFI shall be launched between 2015 and 2020.	Y	Schedule assessment and Ground Station availability show 2017 is feasible
Only technologies with a TRL of 5 by 2009 (start ph-B) shall be used for the SVM.	Y	Expect cold gas/FEEP to be flight qualified on GAIA and LISA respectively by that date. High data rate 26 GHz transponder likely available. FGS will require immediate start of development
The mission shall be compatible with the ESA DSN	N	Upgrade to 26 GHz required
The launch vehicle shall be Soyuz-Fregat giving an available payload volume of 3800 diam x 5070 height cylindrical (more if cone is considered) and a launch capacity of 2000 kg for direct injection into selected L2 orbit	Y	Configuration, baffle design fit requirement

Figure 11-2: Compliance to Programmatic requirements

	Compliance (Y/N)	Comment
Straylight contribution to noise shall be at least a factor of 10 less than the zodiacal light contribution	Y	L2 Halo orbit minimises Earth contribution (4 orders of magnitude less than zodiacal light)
The WFI RPE shall be 10 milliarcsec in LOS over 2000s (1 sigma) and 1 arcsec around LOS over 2000s	Y	FGS design and RCS thruster selection and arrangement compliant
The baseline comms frequency band for science data shall be 26GHz Ka-band using Cebreros	Y	26GHz link budget, visibility, comms s/s design adequate to downlink all science data
GOAL: X-band option using ESA DSN shall be considered	N	Not possiible given other requirements/constraints such as compression rate, comms window availability, data rate
The wavefront error shall be kept below 71.4 nm RMS, and the delta wavefront error shall be kept below 49.4 RMS	Y	WFE 70.9nm RMS, delta-WFE 48.9nm RMS by allocation of misalignment and stability requirements
The OTA shall be kept at 290K during science measurements	Y	Thermal design consistent
The delta-T between M1 and M2 shall be lower than 0.6K	Y	Achieved by heater design
The SVM shall be capable of accomodating the worst case in terms of resources between cold gas and FEEP propulsion systems	Y	Mass budget consistent with cold gas thrusters and power budget consistent with FEEP thrusters
The spacecraft design shall be capable of accommodating both optical configurations analysed (5-mirror or 4-mirror)	Y	5-mirror configuration more demanding for mass, 4-mirror more demanding for volume
The payload DHS shall be capable of handling an input data rate of 29 Tbytes raw data in 1000s	Y	Maxwell SCS750 processor compliant

Figure 11-3: Compliance to mission/spacecraft requirements

In general, the main mission science requirements have been verified with the notable exception of the signal over noise ratio requirements for the high red shift supernovae. Modelisation of near IR wavelengths could not be performed within the short study time frame and with the available resources. Priority shall be given to this activity in the following project phases.

Concerning programmatics, the earliest recommended launch date is 2017 to allow timely payload technology development, upgrade and off-loading of ESA Ground Stations.

This Page Intentionally Blank

12 REFERENCES

RD[1] Hechler, M.: GAIA Consolidated Report on Mission Analysis Issue 2.0, GAIA-ESC-RP-0001, ESA/ESOC/OPS/GFA, March 2006

RD[2] Hechler, M.:GAIA/FIRST Mission Analysis: Ariane and the Orbits Around L2, Mission Analysis Working Paper 393, ESA/ESOC/OPS/GFA, November 1997

RD[3] WFI Preliminary SRD Issue 0, SCI/AM/WFI-SRD/05, P. Gondoin, Issue 0, 24 Nov. 2005

RD[4] A new design for integral field spectroscopy with 8-m telescopes, Content R.,SPIE proceedings vol.2871, pp.1295-1305,1997

RD[5] Encyclopaedia of Astronomy and Astrophysics

RD[6] Integral field spectrometer and multi-object spectrometry with MEMS, A.Wuttig, R.Riesenberg, G.Nitzsche, Imaging Spectrometry VII, Proc.SPIE vol.4480, pp.367-376, 2002

RD[7] Realising Integral Field Spectroscopy in the Far-Infrared, L.W.Looney, W.Raab, A.Poglitsch, N.Geis, The Astrophysical Journal, 597:628–643, 2003 November 1

RD[8] An integral field spectrograph for SNAP supernova studies, SNAP-TECH-02014

RD[9] Opto-mechanical design of the Near Infrared Spectrograph NIRSpec*,* Maurice te Plate, Wolfgang Holota, Winfried Posselt, Jess Köhler, Markus Melf, Giorgio Bagnasco, Pierangelo Marenaci, Proc. SPIE Vol. 5904

RD[10] Asiago database on photometric systems, http://ulisse.pd.astro.it/Astro/ADPS/ReadMe/

RD[11] SNAP satellite focal plane development, Proc. SPIE Int. Soc. Opt. Eng. 5164, 74 (2003)

RD[12] Anastigmatic three-mirror telescope, D.Korsch, Applied Optics, vol.16 No.8, August 1977

RD[13] Design of the high resolution optical instrument for the PLEIADES HR earth observation satellites, J.L.Lamard,C.Gaudin-Delrieu, D.Valentini,C.Renard, T.Tournier, J.M.Laherrere,Proceedings of ICSO 2004, pp.149-156

RD[14] SNAP Telescope Metering Structure Analysis, SNAP-TEC-05008

RD[15] SOFIA Primary Mirror Assembly: Structural properties and optical performances, Airborne Telescope Systems II, Hermann Bittner, Matthias Erdmann, Peter Haberler, Karl-Heinz Zuknik,, Proceedings of SPIE Vol. 4857, p.266-273

RD[16] Lectures on optical systems, Mr.Ruch, Ecole Supérieure d'Optique, 1996

RD[17] Optical Coating Technology, P.W.Baumeister, SPIE Press Editor

RD[18] Challenges in optics for Extremely Large Telescope Instrumentation, P. Spano, F.M. Zerbi, C.J. Norrie, C.R. Cunningham, K.G. Strassmeier, A. Bianco, P.A. Blanche, M. Bougoin, M. Ghigo, P. Hartmann, L. Zago, E. Atad-Ettedgui, B. Delabre, H. Dekker, M. Melozzi, B. Snyders, R. Takke, and D.D. Walker, Astron.Nachr, n.88,789-811 (2006)

RD[19] Calibrating SNAP, article, S. Deustua, and al, SPIE 2003
http://snap.lbl.gov/pubdocs/SPIECalibration.pdf

RD[20] SNAP Instrument R&D, presentation, C. Bebek, Nov. 2003, internal review

RD[21] SCI/AM/WFI-OBSDM/05, On-board Science Data Management Requirements, Issue 1, Revision 2, 13 February 2006

RD[22] CCSDS 121.0-B-1, Lossless Data Compression, Issue 1, 1997

RD[23] TSIM LEON3 simulator, Gaisler Research,
http://www.gaisler.com/cms4_5_3/index.php?option=com_content&task=view&id=38&Itemid=56

RD[24] AT697E Rad-hard SPARC V8 embedded processor,
http://www.atmel.com/dyn/products/product_card.asp?part_id=3178

RD[25] A Giga INstruction Architecture (GINA) for the future ESA microprocessor based on the LEON3 IP Core, DASIA2006, A.L.R. Pouponnot - ESA/ESTEC, The Netherlands

RD[26] Super Nova-Acc. Probe (SNAP), Andy Gerber, October/November 2002.

RD[27] SNAP Systems Engineering WBS 1.3, ppt presentation, David Pankow, University of California Berkeley, November 2003.

RD[28] SNAP Electrical/Mechanical/Thermal, ppt presentation, Michael Sholl, University of California Berkeley, November 2003.

RD[29] XMM Executive Summary, XM-RP-DOR-0088, XMM Team Dornier GmbH, Issue 1, August 1999.

RD[30] XMM-UMTC TCS Design Description, XM-HD-OCW-5002, E. Tennant oerlikon-contraves space, Issue 1 rev. B, January 1997.

RD[31] Thrust Verification Tests of the Goce Cold Gas Thruster, TEC-MPE/2004/45/AB, A. Bulit, Issue1, 20 August 2004

RD[32] Cold Gas: Technology Status and Plan, PowerPoint Presentation, C. Hunter, 22 June 2005

RD[33] Darwin Payload Definition Document, SCI-A/2005/301/DARWIN/DMS/Lda, L. d'Arcio, Issue 1 rev2, 31 August 2005

RD[34] Endurance Tests of 150 µN FEEP Microthrusters, IEPC-2005-183, M. Andrenucci, L. Biagioni, F. Ceccanti, M. Saviozzi, D. Nicolini, November 2005

RD[35] IN-FEEP Characterisation of Microthruster Model, TRP Final Presentation, M.Tajmar, October 2005

RD[36] Technical note on µNRIT predevelopment, Technical Note, UNI-GI-DOC-200503, D.Feili, Issue1, 21 February 2005

RD[37] A Miniaturized HET System on board of VEGA-1 P/L, Technical Note, TEC-MP/2005/165/DDC, D. Di Cara, Issue1, 11 September 2005

RD[38] ECSS-E-50-05A, *Radio Frequency And Modulation Standard*, published 24 Jan 2003

RD[39] CCSDS 101.0-B-6. *Telemetry Channel Coding Standard*. Blue Book. Issue 6. October 2002.

RD[40] PSS-04-104, *Ranging Standard*, March 1991

RD[41] CCSDS 102.0-B-5. *Packet Telemetry Standard*. Blue Book. Issue 5. November 2000.

RD[42] CCSDS 201.0-B-3. *Telecommand Part 1—Channel Service*. Blue Book. Issue 3. June 2000.

RD[43] CCSDS 202.1-B-2. *Telecommand Part 2.1—Command Operation Procedures*. Blue Book. Issue 2. June 2001.

RD[44] CCSDS 203.0-B-2. *Telecommand Part 3—Data Management Service*. Blue Book. Issue 2. June 2001.

RD[45] ECSS-E-70-41A, *Telemetry And Telecommand Packet Utilization*, published 30 January 2003

RD[46] CCSDS 211.0-B-2. *Proximity-1 Space Link Protocol*—Data Link Layer. Blue Book. Issue 2. April 2003

RD[47] CCSDS 211.1-B-1. *Proximity-1 Space Link Protocol*—Physical Layer. Blue Book. Issue 1. April 2003

RD[48] CCSDS 211.2-B-1. *Proximity-1 Space Link Protocol*—Coding and Synchronization Sublayer. Blue Book. Issue 1. April 2003.

RD[49] SCI-A/2006-XXX/WFI/AJ, WFI Mission Requirements Document, 30 January 2006, Issue 1, draft

RD[50] Performance of the onboard compression algorithm for ACS, Instrument Science Report ACS-98-04, F.R. Boffi & M. Stiavelli January 28, 1999

RD[51] WFI Science Operations Concept Document, SCI/AM/WFI-OPS/06, P. Gondoin, Issue 1.1, February 2006.

RD[52] GAIA Mission Assumptions Document, GAIA-GS-1001-OPS-OSA, J.L. Pellón-Bailón, Issue 2.0, February 2005.

RD[53] WFI Internal Final Presentations, CDF Team, Drafts, April 2006.

RD[54] Risk Management Policy ESA Scientific Programme, M.G. Sarah, Issue 1, 08-07-2003

RD[55] Micro propulsion technology assessment for Darwin, Evaluation of existing and emerging Micro propulsion Technologies for the DARWIN Attitude and Position Control System, SCI-A/2003/296/DARWIN/MK1, March 2004.

RD[56] Space system failures, David M. Harland and Ralph D Lorenz, 2005 Praxis publishing.

RD[57] Product assurance on the XMM Project. J.P. van Dooren ESA Bulletin 100- December 1999.

This Page Intentionally Blank

13 ACRONYMS

Acronym	**Definition**
AIT	Assembly, Integration and Test
AIV	Assembly, Integration and Verification
AOCS	Attitude and Orbit Control System
APE	Absolute Pointing Error
ASM	Attached Synchronisation Marker
AU	Astronomical Unit
BB	Breadboard Model
BCR	Battery Charge Regulator
BDR	Battery Discharge Regulator
BER	Bit Error Rate
CBS	Cost Breakdown Structure
CCD	Charge Coupled Device
CCSDS	Consultative Committee for Space Data Systems
CDF	Concurrent Design Facility
CDR	Critical Design Review
CEB	Cebreros Ground Station
CFRP	Carbon Fibre Reinforced Polymer/Plastic
CORTEX	Command Ranging and Telemetry Unit
CPDU	Command Pulse Distribution Unit
CTE	Coefficient of Thermal Expansion
CVP	Commissioning and Verification Phase
DCR	Dedicated Control Room
DDS	Data Distribution System
DHS	Data Handling System
DM	Design Model
DOD	Depth Of Discharge
DoF	Degree of Freedom
DSA	Deep Space Antenna
DSM	Deep Space Manoeuvre

Acronym	**Definition**
DSN	Deep Space Network
ECA	Etage Cryogénique A
ECSS	European Cooperation for Space Standardization
EIRP	Effective isotropically-radiated power
EM	Engineering Model
EMC	Electromagnetic Compatibility
EMI	Electromagnetic Interference
EPS	Electrical Power System
EPSA	Electric Propulsion System Assembly
EQM	Electrical Qualification Model
ESOC	European Space Operations Centre
ESTRACK	ESA Tracking Stations Network
FCT	Flight Control Team
FCU	Flow Control Unit
FD/FDS	Flight Dynamics/Flight Dynamics System
FDR	Flight Dynamics Room
FEEP	Field Emission Electric Propulsion
FEM	Finite Element Model
FER	Frame Error Rate
FGS	Fine Guidance Sensor
FOP	Flight Operation Plan
FOV	Field of View
FP	Focal Plane
FSA	Focal Surface Assembly
G/S	Ground Station
GIE	Grid Ion Engine
GMES	Global Monitoring
GMSK	Gaussian Minimum Shift Keying
GTO	Geostationary Transfer Orbit
H/W	Hardware
HEO	Highly Eccentric Orbit

Acronym	Definition
HET	Hall Effect Thruster
HGA	High Gain Antenna
HK	House Keeping
ICVI	Isothermal Chemical Vapour Infiltration
I/F	Interface
IFMS	Intermediate Frequency and Modem System
IFS	Integral field spectrometer
IFU	Integral Field Unit
IM	Interface Module
IMG	Imaging/Image
IR	Infrared
ISL	Inter-satellite link
L2	Second Lagrangian Equilibrium Point (Sun-Earth System)
LAN	Local Area Network
LCC	Life Cycle Cost
LEO	Low Earth Orbit
LEOP	Launch and Early Operations
LGA	Low Gain Antenna
LOS	Line of Sight
LV	Launch Vehicle
M1	Primary Mirror
M2	Secondary Mirror (similarly M3-M5 are the 3rd-5th mirrors)
Mbps	Mega bits per second
MCR	Main Control Room
MCS	Mission Control System
MGA	Medium Gain Antenna
MH	Measurement Head
MLI	Multi Layer Insulation
MOC	Mission Operations Centre
MOI	Moment of Inertia
MOPS	Millions of Operations per Second

Acronym	Definition
MPPT	Maximum Power Point Tracker
MPS	Mission Planning Centre
MPTS	Multipurpose Tracking System
NA	Neutralizer
NIR	Near-infrared (light wavelength range)
NNO	New Norcia Ground Station
NRT	Near Real Time
OBC	On Board Computer
OBSM	On-Board Software Maintenance
OBT	On Board Time
OGSE	Optical Ground
OPSNET	Operational Network
OTA	Optical Telescope Assembly
P/L	Payload
PA	Product Assurance
PCB	Printed Circuit Board
PCDU	Power and Conversion Distribution Unit
PDM	Power Distribution Module
PDR	Preliminary Design Re view
PF	Pathfinder
PFM	Proto-flight Model
PLM	Payload Module
PM	Processor Module
PPCU	Power Processing and Control Unit
PSR	Project Support Room
PUS	Packet Utilisation Standard
RBE2	Rigid Body Element Form 2
RCS	Reaction Control System
RF	Radio Frequency
RFDU	Radio Frequency Distribution Unit
RFG	Radio Frequency Generator

Acronym	Definition
RITA	Radiofrequency Ion Thruster Assembly
RM	Risk Magnitude
RMS	Root Mean Square
ROE	Read-Out Electronics
RPE	Relative Pointing Error
S	Science
S/C	Spacecraft
S/N, SNR	Signal to Noise Ratio
S/W	Software
S3R	Sequential Switching Shunt Regulator
S4R	Sequential Switching Shunt and Series Regulator
SA	Solar Array
SADM	Solar Array Drive Mechanism
SCOS	Spacecraft Control System
SDR	System Design Review
SGM	Safe Guard Memory
SiC	Silicon Carbide
SMA	Shape Memory Alloy
SN	Supernova
SPACON	SPAcecraft CONtroller
SRR	System Requirement Review
SRRC-OQPSK	Square-Root Raised Cosine Offset Quadrature Phase Shift Keying
SSEA	Sun-Spacecraft-Earth Angle
SSPA	Solid State Power Amplifier
STDM	Spacecraft Trajectory Data Messages
STM	Structural Model
SVM	Service Module
TA	Thruster Assembly
TC	Telecommand
TC	Thermal Control
TM	Telemetry

Acronym	Definition
TRL	Technology Readiness Level
TT&C	Tracking, Telemetry and Command
TV/TB	Thermal Vacuum/Thermal Balance
TWTA	Travelling Wave Tube Amplifier
VIS	Visible (light wavelength range)
WAN	Wide Area Network
WFE	Wave Front Error
WFI	Wide Field Imager
WSB	Weak Stability Boundary
XFCU	Xenon Flow Control System
z	Redshift